



# Automatic Control of a Parabolic Trough Solar Thermal Power Plant

**Adham Alsharkawi**

A thesis submitted in partial fulfillment  
of the requirements for the degree of  
Doctor of Philosophy

Automatic Control and Systems Engineering  
University of Sheffield  
July 2017



*Dedicated to my parents for their unconditional love, endless support and  
encouragement*



# ABSTRACT

This thesis is interested in improving the operation of a parabolic trough technology based solar thermal power plant by means of automatic control. One of the challenging issues in a solar thermal power plant, from the control point of view, is to maintain the thermal process variables close to their desired levels. In contrast to a conventional power plant where fuel is used as the manipulated variable, in a solar thermal power plant, solar radiation cannot be manipulated and in fact it ironically acts as a disturbance due to its change on a daily and seasonal basis.

The research facility ACUREX is used as a test bed in this thesis. ACUREX is a typical parabolic trough technology based solar thermal power plant and belongs to the largest research centre in Europe for concentrating solar technologies, namely the Plataforma Solar de Almería (PSA) in south-east Spain. The plant exhibits nonlinearities as well as resonance characteristics that lie well within the desired control bandwidth. Failure to adequately capture the resonance characteristics of the plant results in an undesired oscillatory control performance. Moreover, measured disturbances are an integral part of the plant and while some of the measured disturbances do not have a significant impact on the operation of the plant, others do.

Hence, with the aim of handling the plant nonlinearities and capturing the plant resonance characteristics, while taking explicit account of the measured disturbances, in this thesis a gain scheduling feedforward predictive control strategy is proposed. The control strategy is based upon a family of local linear time-invariant state space models that are estimated around a number of operating points. The locally estimated linear time-invariant state space models have the key novelty of being able to capture the resonance characteristics of the plant with the minimal number of states and hence, simple analysis and control design.



Moreover, while simple classical, series and parallel, feedforward configurations have been proposed and used extensively in the literature to mitigate the impact of the measured disturbances of the ACUREX plant, the proposed control strategy incorporates a feedforward systematically by including the effects of the measured disturbances of the ACUREX plant into the predictions of future outputs.

In addition, a target (set point) for a control strategy is normally set at the ACUREX plant by the plant operator. However, in this thesis it is argued that, in parallel, the operator must choose between potentially ambitious and perhaps unreachable targets and safer targets. Ambitious targets can lead to actuator saturation and safer targets imply electricity production losses.

Hence, in this thesis a novel two-layer hierarchical control structure is proposed with the gain scheduling feedforward predictive control strategy being deployed in a lower layer and an adequate reachable reference temperature being generated from an upper layer. The generated reference temperature drives the plant near optimal operating conditions, while satisfying the plant safety constraints, without any help from the plant operator and without adding cost.

The proposed two-layer hierarchical control strategy has the potential benefits of: (i) maximising electricity production; (ii) reducing the risk of actuator saturation; (iii) extending the life span of various elements of the plant (e.g. synthetic oil, pump and valves) and (iv) limiting the role of the plant operator.

The efficacy of the proposed two-layer hierarchical control strategy is evaluated using a nonlinear simulation model that approximates the dynamic behaviour of the ACUREX plant. The nonlinear simulation model is constructed in this thesis and validated in the time and frequency domain.



# ACKNOWLEDGMENTS

First and foremost, I would like to express my sincere sense of gratitude to my supervisor, Dr J. Anthony Rossiter for his encouragement and continuous support. I would like also to thank him for the invaluable learning experience and giving me the opportunity to grow as a researcher.

Many thanks to my colleagues: Evans Ejegi, Shukri Dughman, Yahya Al-naumani, Wai Hou (Alan) Lio, Muhammad Abdullah and Hassrizal B Hassan Basri.

To my family and friends, thank you for always being there.

Finally, I would like to extend a special thanks to the University of Jordan, Jordan for funding my PhD studies.

Adham Yaseen Mohammad Alsharkawi  
aalsharkawi1@sheffield.ac.uk

July 2017

# STATEMENT OF ORIGINALITY

Unless otherwise stated in the text, the work described in this thesis was carried out solely by the candidate. None of this work has already been accepted for any degree, nor is it concurrently submitted in candidature for any degree.

Candidate: \_\_\_\_\_

Adham Alsharkawi

Supervisor: \_\_\_\_\_

Dr. J. Anthony Rossiter

# CONTENTS

<b>List of Figures</b>	<b>xiii</b>
<b>List of Tables</b>	<b>xvii</b>
<b>Acronyms and abbreviations</b>	<b>xviii</b>
<b>I Overview</b>	<b>1</b>
<b>Chapter 1: Introduction</b>	<b>2</b>
1.1 An Overview . . . . .	2
1.2 Challenges . . . . .	4
1.3 Motivation . . . . .	4
1.4 Aims and Objectives . . . . .	5
1.5 An Overview of the Main Contributions . . . . .	6
1.6 Thesis Layout . . . . .	7
<b>Chapter 2: Background: Plant Description, Modelling and Fundamental Control Strategy</b>	<b>9</b>
2.1 Chapter Overview . . . . .	9
2.2 Plant Description . . . . .	9
2.3 Nonlinear Simulation Model . . . . .	14
2.4 Fundamental Control Strategy . . . . .	20
2.5 Summary . . . . .	30
<b>Chapter 3: Summary of Contributions</b>	<b>32</b>
3.1 Chapter Overview . . . . .	32

3.2	Unifying Review . . . . .	32
3.3	Simulation Model . . . . .	35
3.4	Gain Scheduling Design . . . . .	38
3.5	Feedforward Design . . . . .	47
3.6	Hierarchical Control . . . . .	53
3.7	Summary . . . . .	62
<b>Chapter 4: Conclusions and Future Perspectives</b>		<b>65</b>
4.1	Final Conclusions . . . . .	65
4.2	Recommendations for Future Research . . . . .	68
<b>II Contributions</b>		<b>77</b>
<b>Appendix A: Distributed Collector System: Modelling, Control and Optimal Performance</b>		<b>78</b>
A.1	Introduction . . . . .	79
A.2	CSP Technologies . . . . .	81
A.3	Modelling Approaches . . . . .	88
A.4	Control Approaches . . . . .	90
A.5	Opportunities . . . . .	95
A.6	Conclusion and Future Directions . . . . .	96
<b>Appendix B: Modelling Analysis of a Solar Thermal Power Plant</b>		<b>103</b>
B.1	Introduction . . . . .	104
B.2	Nonlinear Models of the ACUREX Plant . . . . .	106
B.3	Construction of a Nonlinear Simulation Model . . . . .	108
B.4	Open-Loop Analysis . . . . .	108
B.5	Closed-Loop Analysis . . . . .	109
B.6	Discussion and Concluding Remarks . . . . .	115

---

<b>Appendix C: Dual Mode MPC for a Concentrated Solar Thermal</b>	
<b>Power Plant</b>	<b>121</b>
C.1 Introduction . . . . .	122
C.2 Plant Description and Control Problem . . . . .	125
C.3 Mathematical Model . . . . .	126
C.4 Resonant Modes and System Identification . . . . .	130
C.5 Dual Mode MPC . . . . .	133
C.6 Simulation Results . . . . .	133
C.7 Conclusion . . . . .	136
<b>Appendix D: Gain Scheduling Dual Mode MPC for a Solar Thermal</b>	
<b>Power Plant</b>	<b>140</b>
D.1 Introduction . . . . .	141
D.2 Mathematical Models . . . . .	144
D.3 Resonant Modes and System Identification . . . . .	146
D.4 Control Design . . . . .	150
D.5 Simulation Results . . . . .	154
D.6 Conclusion . . . . .	156
<b>Appendix E: Towards an Improved Gain Scheduling Predictive Con-</b>	
<b>trol Strategy for a Solar Thermal Power Plant</b>	<b>162</b>
E.1 Introduction . . . . .	163
E.2 Nonlinear Dynamic Models of ACUREX . . . . .	167
E.3 System Identification and Models of the Measured Disturbances . . .	171
E.4 Control Design . . . . .	176
E.5 Simulation Results . . . . .	187
E.6 Conclusion . . . . .	193
<b>Appendix F: Hierarchical Control Strategy for a Solar Thermal Power</b>	
<b>Plant: A Pragmatic Approach</b>	<b>203</b>

F.1	Introduction . . . . .	204
F.2	Plant Description and the Phenomena of Resonant Modes . . . . .	207
F.3	Nonlinear Dynamic Models of the Plant . . . . .	209
F.4	Two-Layer Hierarchical Control Structure . . . . .	211
F.5	Simulation Scenarios . . . . .	220
F.6	Conclusions . . . . .	224

**Appendix G: Towards an Improved Hierarchical Control Strategy for  
a Solar Thermal Power Plant** **229**

G.1	Introduction . . . . .	230
G.2	Plant Description . . . . .	232
G.3	Nonlinear Simulation Model of the Plant . . . . .	232
G.4	Two-Layer Hierarchical Control Structure . . . . .	235
G.5	Proposals for Improved Algorithms . . . . .	237
G.6	Evaluation . . . . .	241
G.7	Conclusions . . . . .	246

# LIST OF FIGURES

1.1	World energy consumption between 1971 and 2014. Adapted from IEA (2016). . . . .	2
2.1	ACUREX distributed solar collector field. . . . .	10
2.2	Cross-section of the ACUREX collector (Dudley and Workhoven, 1982). . . . .	11
2.3	ACUREX: Principle of operation. Adapted from Camacho et al. (2012). . . . .	12
2.4	Frequency response of the field outlet temperature around a volumetric flow rate of $0.010 \text{ m}^3/\text{s}$ . . . . .	13
2.5	Construction of a nonlinear simulation model. . . . .	17
2.6	Measured inputs. . . . .	21
2.7	Measured output, model output and time-varying variables. . . . .	22
3.1	Concentrating solar technologies (Philibert, 2010). . . . .	34
3.2	Frequency responses of an estimated local models. . . . .	37
3.3	Input-output data. . . . .	43
3.4	Bode plot of the local LTI state space models. . . . .	46
3.5	Gain scheduling control strategy. . . . .	46
3.6	First scenario: Control performance on a clear day. . . . .	48
3.7	Bode plot: Estimated models of solar radiation. . . . .	50
3.8	Bode plot: Estimated models of the field inlet temperature. . . . .	51
3.9	Frequency responses of the field outlet temperature for changes in solar radiation and the field inlet temperature obtained through two different approaches around a given operating point. . . . .	52
3.10	A performance comparison: GSMPC against GSFFMPC. . . . .	54
3.11	Two-layer hierarchical control structure. . . . .	56

3.12	Generation of a reference temperature using measurements from the ACUREX plant collected on 18 July 2003. . . . .	59
3.13	Generation of a reference temperature using measurements from the ACUREX plant collected on 28 July 2003. . . . .	60
3.14	An improved two-layer hierarchical control structure. . . . .	61
3.15	Control signals of the GSMPC and the GSFFMPC given some measured data from the ACUREX plant and a generated reference temperature. . . . .	62
A.1	CSP technologies (Philibert, 2010). . . . .	82
B.1	Measured inputs. . . . .	110
B.2	Simulation models against the measured output. . . . .	111
B.3	Frequency responses of the estimated local models. . . . .	113
B.4	Solar radiation and flow rate of the HTF. . . . .	114
B.5	Closed-loop performance. . . . .	114
B.6	Model validation around operating point 1. . . . .	116
B.7	Model validation around operating point 2. . . . .	117
B.8	Model validation around operating point 3. . . . .	118
C.1	ACUREX schematic diagram. Figure adapted from Álvarez et al. (2008). . . . .	126
C.2	Schematic for the nonlinear distributed parameter model. . . . .	128
C.3	Input-output data. . . . .	131
C.4	Bode plot of the estimated LTI state space model. . . . .	132
C.5	First scenario: simulation results for a clear day. . . . .	135
C.6	Second scenario: simulation results for a passing cloud. . . . .	137
D.1	Bode plot of the local LTI state space models. . . . .	149
D.2	GS control strategy. . . . .	153
D.3	First scenario: Control performance on a clear day. . . . .	155

---

D.4	Second scenario: control performance on a cloudy day. . . . .	158
E.1	Measured inputs to the ACUREX plant. . . . .	171
E.2	Measured output against model output. . . . .	172
E.3	Bode plot: Estimated models of solar radiation. . . . .	175
E.4	Bode plot: Estimated models of the field inlet temperature. . . . .	176
E.5	Frequency responses of the field outlet temperature for changes in the volumetric flow rate of the HTF (Model $\alpha$ ) and solar radiation (Model $\beta$ ) around a given operating point. . . . .	177
E.6	Frequency responses of the field outlet temperature for changes in solar radiation and the field inlet temperature obtained through two different approaches around a given operating point. . . . .	178
E.7	A performance comparison: GSMPC against GSFFMPC. . . . .	196
E.8	A local performance comparison. . . . .	197
E.9	A performance comparison: LFFMPC1 against LFFMPC1-23-step ahead. . . . .	198
E.10	Deviation of solar radiation from an estimated steady-state value. . .	199
F.1	ACUREX distributed solar collector field. . . . .	208
F.2	Bode plot: Estimated models of solar radiation. . . . .	216
F.3	Bode plot: Estimated models of the field inlet temperature. . . . .	217
F.4	Two-layer hierarchical control structure. . . . .	219
F.5	First scenario: Reference temperature at normal operating conditions.	221
F.6	Second scenario: Reference temperature against a measured field outlet temperature. . . . .	222
F.7	Third scenario: Generation of a reference temperature using measurements from the ACUREX plant collected on 18 July 2003. . . . .	224
F.8	Fourth scenario: Generation of a reference temperature using measurements from the ACUREX plant collected on 28 July 2003. . . . .	225
G.1	ACUREX distributed solar collector field. . . . .	233

G.2 Two-layer hierarchical control structure. . . . .	242
G.3 First scenario: Control performance of GSMPC against Algorithm 1. . . . .	244
G.4 Second scenario: Control performance of Algorithm 1 against Algorithm 2. . . . .	245

# LIST OF TABLES

2.1	Variables and Parameters. . . . .	16
2.2	Parameters of the Nonlinear Simulation Model . . . . .	18
3.1	Summary of Contributions . . . . .	63
B.1	Variables and Parameters. . . . .	107
B.2	Assessment of the Simulation Models . . . . .	109
B.3	Summary of the Estimated Local Models . . . . .	112
B.4	Assessment of the Local Controllers . . . . .	115
C.1	Variables and Parameters. . . . .	127
D.1	Variables and Parameters. . . . .	145
D.2	Model Order and Best Fit Criterion . . . . .	148
D.3	Model Order and Best Fit Criterion . . . . .	150
E.1	Variables and Parameters . . . . .	168
E.2	Model Order and Best Fit Criterion ( $I$ ) . . . . .	174
E.3	Model Order and Best Fit Criterion ( $T_{f,inlet}$ ) . . . . .	174
E.4	Dual Mode MPC Algorithms . . . . .	188
E.5	Set Point Tracking Performance (GS Case) . . . . .	191
E.6	Set Point Tracking Performance (Local Case) . . . . .	192
F.1	Variables and Parameters. . . . .	210
F.2	Model Order and Best Fit Criterion ( $I$ ) . . . . .	215
F.3	Model Order and Best Fit Criterion ( $T_{f,inlet}$ ) . . . . .	215
G.1	Variables and Parameters. . . . .	234

# ACRONYMS AND ABBREVIATIONS

**AIC** Akaike's Information Criterion.

**ARMAX** Auto-Regressive Moving Average with eXogenous inputs.

**ARX** Auto-Regressive with eXogenous inputs.

**CARIMA** Controlled Auto-Regressive Integrated Moving Average.

**CSP** Concentrated Solar Power.

**CVA** Canonical Variable Algorithm.

**d.o.f** Degrees of Freedom.

**DSG** Direct Steam Generation.

**GS** Gain Scheduling.

**GSFFMPC** Gain Scheduling Feedforward dual mode MPC

**GSMPC** Gain Scheduling MPC.

**HTF** Heat Transfer Fluid.

**IEA** International Energy Agency.

**LFFMPC1** Local Feedforward dual mode MPC 1.

**LFFMPC2** Local Feedforward dual mode MPC 2.

**LFFMPC3** Local Feedforward dual mode MPC 3.

**LFFMPC1- $n_a$ -step ahead** Local Feedforward dual mode MPC 1- $n_a$ -step ahead.

**LMPC** Local dual mode MPC.

**LTI** Linear Time-Invariant.

**MPC** Model-based Predictive Control.

**MSE** Mean Squared Error.

**ODEs** Ordinary Differential Equations.

**PDES** Partial Differential Equations.

**PI** Proportional-Integral.

**PID** Proportional-Integral-Derivative.

**PRBS** Pseudo-Random Binary Sequence.

**PSA** Plataforma Solar de Almería.

**PV** Photovoltaic.

**QFT** Quantitative Feedback Theory.

**QP** Quadratic Programming.

**RMSE** Root Mean Square Error.

**SEGS** Solar Electricity Generating Systems.

**SMC** Sliding Mode Control.

**s.t.** Subject to.



# Part I

## Overview

# Chapter 1

## INTRODUCTION

### 1.1 An Overview

World energy consumption has increased rapidly since the early seventies of the last century. This is illustrated in Fig. 1.1. Moreover, energy consumption is expected to continue to increase over the next fifty years. Hence, given the current impact of fossil fuels on climate change and the expected depletion of fossil fuels in the near future (Goswami et al., 2015), there is an urgent need for clean and sustainable energy resources.

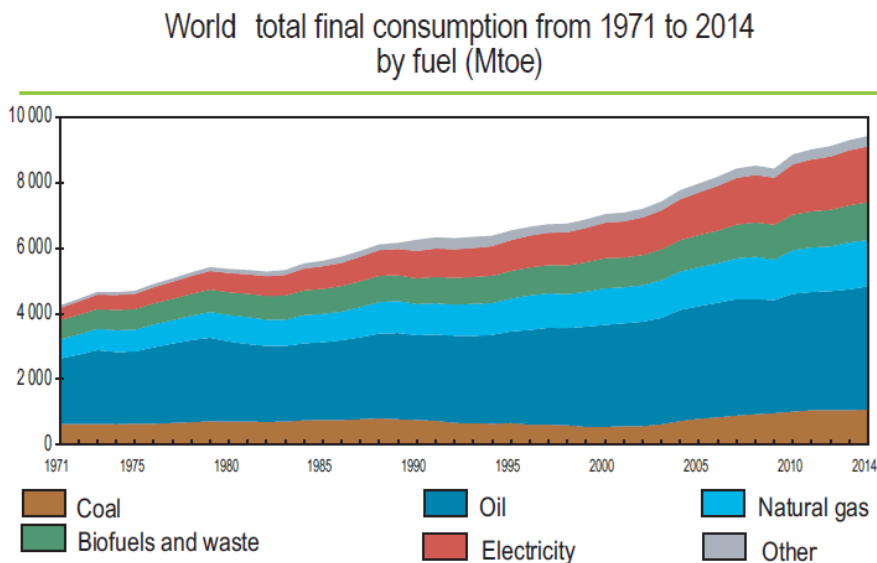


Figure 1.1: World energy consumption between 1971 and 2014.

Adapted from IEA (2016).

Solar energy technologies are promising energy resources. In 2011, the International Energy Agency (IEA) stated that “*The development of affordable, inexhaustible and clean solar energy technologies will have huge longer-term benefits. It will increase countries energy security through reliance on an indigenous, inexhaustible and mostly import-independent resource, enhance sustainability, reduce pollution, lower the costs of mitigating climate change, and keep fossil fuel prices lower than otherwise. These advantages are global*” (IEA, 2011).

Solar energy is converted into electrical energy by two main technologies, photovoltaic and thermal technology. While the current commercial efficiency of photovoltaic technology has reached more than 20 %, thermal technology has achieved efficiencies of 40-60 % (Goswami et al., 2015). Furthermore, according to Teske et al. (2016), solar thermal technology is expected to meet up to 6 % of the world’s power needs by 2030 and 12 % by 2050, given the advanced industry development and high levels of energy efficiency. Hence, solar thermal technology would play a significant role in the reduction of CO<sub>2</sub> globally.

Solar thermal technology is becoming competitive on price with conventional fossil fuels due to technological developments, mass power production, economies of scale and improved operation (Teske et al., 2016). This thesis is interested in improving the operation of a solar thermal power plant by means of automatic control.

Solar thermal technology utilising concentrating parabolic trough collectors was the first solar technology to demonstrate its grid power potential. A 354 MW parabolic trough technology-based solar thermal power plant has been running continuously in California since 1988 (Goswami et al., 2015). This thesis looks into a similar solar thermal power plant, namely ACUREX (Camacho et al., 2012).

ACUREX is a research facility in Spain that has helped researchers across academia and industry to gain an insight into its main dynamics and inherent characteristics, and thus develop various model forms and control strategies with the aim of improving the operation of the plant, as well as others similar to ACUREX.

## **1.2 Challenges**

One of the challenging issues in a solar thermal power plant, from the control point of view, is to maintain the thermal process variables close to their desired levels. In contrast to a conventional power plant, where fuel is used as the manipulated variable, in a solar thermal power plant, solar radiation cannot be manipulated and in fact it ironically acts as a disturbance due to its change on a daily and seasonal basis.

Moreover, the ACUREX plant exhibits some nonlinearities and studies (Meaburn and Hughes, 1993, 1994) have also revealed that the plant exhibits some resonance characteristics that lie well within the desired control bandwidth. Failure to adequately capture the resonance characteristics of the plant results in an undesired oscillatory control performance.

In summary, changes in solar radiation, nonlinearities and the plant resonance characteristics constitute a real challenge to the control at the ACUREX plant.

## **1.3 Motivation**

During the normal operation of the ACUREX plant, parabolic trough collectors concentrate the incident solar radiation onto a receiver tube that is positioned along its focal line. A thermal oil passes through the receiver tube and circulates in a distributed solar collector field. The thermal oil then gets heated and, when a desired field outlet temperature is reached, the heated oil finally passes through a series of heat exchangers to produce steam, which in turn is used to drive a steam turbine to generate electricity.

Hence, the control problem at the ACUREX plant is to maintain the field outlet temperature at a desired level (reference temperature) by suitably adjusting the oil flow rate within a safety limits. This can be handled efficiently by a well designed tailored control strategy that appreciates the nonlinearities and resonance characteristics of the plant.

However, the ACUREX plant is constantly subject to changes in solar radiation and the field inlet temperature (measured disturbances) and thus the plant requires the full attention of an experienced plant operator, whose job is to set an adequate reachable reference temperature that takes into account the status of the measured disturbances and the plant safety constraints. In parallel, the operator must choose between potentially ambitious and perhaps unreachable targets and safer targets. Ambitious targets can lead to actuator saturation and safer targets imply electricity production losses.

#### ***1.4 Aims and Objectives***

The main aim of this thesis is to design and evaluate a pragmatic control strategy that ensures an automatic operation of a parabolic trough technology-based solar thermal power plant with minimal intervention from the plant operator. The control strategy should be feasible over a wide range of operation and drive the plant near optimal operating conditions.

Hence, to achieve these aims, a number of objectives can be listed as follows.

- Construct a simulation environment that approximates the dynamic behaviour of the plant.
- Control the main thermal variable of the plant, namely the field outlet temperature.
- Handle the nonlinear characteristics of the plant.
- Capture the resonance characteristics of the plant.
- Take systematic account of the plant safety constraints.
- Make an effective use of available information on the measured disturbances.

### ***1.5 An Overview of the Main Contributions***

The main contributions of this thesis can be outlined as follows:

1. Conducting a review on concentrating solar technologies with an emphasis placed on parabolic trough technology and its utilisation in the ACUREX plant. Moreover, the review has identified avenues for future research in the area of control of solar energy systems.
2. Construction and validation of a nonlinear simulation model that approximates the dynamic behaviour of the ACUREX plant. The nonlinear simulation model takes into account the resonance phenomena of the plant and is validated in the time and frequency domain.
3. A gain scheduling predictive control strategy has been formulated. The control strategy is based upon a local linear time-invariant state space models that have been estimated around a number of operating points, while taking into account the frequency response of the plant. Moreover, the gain scheduling predictive control strategy ensures a feasible operation over a wide range of operation while taking a systematic account of the plant safety constraints.
4. The gain scheduling predictive control strategy is improved by incorporating a systematic feedforward to compensate for the measured disturbances, solar radiation and the field inlet temperature. This has resulted in formulating a gain scheduling feedforward predictive control strategy. Local linear time-invariant state space models of solar radiation and the field inlet temperature have been estimated over a wide range of operation, while taking into account the frequency of the plant.
5. Given a set of complete one-step ahead prediction models that relate the field outlet temperature (reference temperature) to solar radiation and the field

inlet temperature, a reference temperature is generated automatically from an upper layer in a two-layer hierarchical control structure. The generated reference temperature is adequate reachable and smoothly adapted to changes in solar radiation and the field inlet temperature while satisfying the plant safety constraints.

## **1.6 Thesis Layout**

This thesis consists mainly of seven different papers that discuss original contributions to the automatic control of a parabolic trough solar thermal power plant.

The thesis is divided into two parts. Part I sets the scene for Part II by providing an essential background information in Chapter 2, a summary of contributions in Chapter 3 and some conclusions and future perspectives in Chapter 4. Part II presents the papers as appendices in the following order:

### *Appendix A*

**Alsharkawi, A.** and Rossiter, J. A. (2015). Distributed collector system: Modelling, control and optimal performance. In *Proceedings of the International Conference on Renewable Energy and Power Quality 2015, La Coruna, Spain*.

### *Appendix B*

**Alsharkawi, A.** and Rossiter, J. A. (2017). Modelling analysis of a solar thermal power plant. In *Proceedings of the 6th International Conference on Clean Electrical Power*, Liguria, Italy.

### *Appendix C*

**Alsharkawi, A.** and Rossiter, J. A. (2016). Dual mode MPC for a concentrated solar thermal power plant. In *Proceedings of the 11th IFAC Symposium on Dynamics*

*and Control of Process Systems, including Biosystems, Trondheim, Norway*, volume 49(7), pages 260–265. Elsevier.

#### *Appendix D*

**Alsharkawi, A.** and Rossiter, J. A. (2016). Gain scheduling dual mode MPC for a solar thermal power plant. In *Proceedings of the 10th IFAC Symposium on Nonlinear Control Systems, California, USA*, volume 49(18), pages 128–133. Elsevier.

#### *Appendix E*

**Alsharkawi, A.** and Rossiter, J. A. (2017). Towards an improved gain scheduling predictive control strategy for a solar thermal power plant. *IET Control Theory & Applications*, DOI: 10.1049/iet-cta.2016.1319.

#### *Appendix F*

**Alsharkawi, A.** and Rossiter, J. A. (2017). Hierarchical control strategy for a solar thermal power plant: A pragmatic approach. Submitted to *Journal of Process Control*.

#### *Appendix G*

**Alsharkawi, A.** and Rossiter, J. A. (2017). Towards an improved hierarchical control strategy for a solar thermal power plant. To be submitted.

## Chapter 2

# BACKGROUND: PLANT DESCRIPTION, MODELLING AND FUNDAMENTAL CONTROL STRATEGY

### *2.1 Chapter Overview*

The purpose of this chapter is to give background information on the solar thermal power plant considered in this thesis, construction of a nonlinear simulation model of the plant and finally a fundamental control strategy that forms the cornerstone of the control strategies developed in this thesis. A plant description is given in Section 2.2, a nonlinear simulation model of the plant is discussed in Section 2.3, the fundamental control strategy is outlined in Section 2.4 and finally a summary of the chapter is given in Section 2.5.

### *2.2 Plant Description*

The solar thermal power plant ACUREX is considered in this thesis. The plant is one of the research facilities at the Plataforma Solar de Almería (PSA) owned and operated by the Spanish public research institution CIEMAT. The PSA is located in south-east Spain and is considered the largest research centre in Europe for concentrating solar technologies.

The solar thermal power plant ACUREX is best described in Camacho et al.

(2012) and hence background information in this section and the next is from Camacho et al. (2012), unless stated otherwise.

ACUREX is a parabolic trough technology-based solar thermal power plant. The main part of the plant is the distributed solar collector field which consists of 480 east-west oriented parabolic trough collectors. The parabolic trough collector is ACUREX model 3001 (Camacho et al., 1997). It is line focus and single axis tracking. Fig. 2.1 shows the installation of the distributed solar collector field at the PSA and Fig. 2.2 shows a cross-section of the ACUREX collector.



Figure 2.1: ACUREX distributed solar collector field.

The ACUREX collectors are arranged in 10 parallel loops with 48 collectors in each loop suitably connected in series. The heat transfer fluid (HTF) running through the receiver tube of each of the ACUREX collectors is the synthetic thermal oil Therminol<sup>®</sup> 55, capable of efficiently delivering temperatures up to 300 °C. A peak thermal power of 1.2 MW can be achieved by the ACUREX plant with solar radiation of 900 W/m<sup>2</sup> (Camacho et al., 1997).

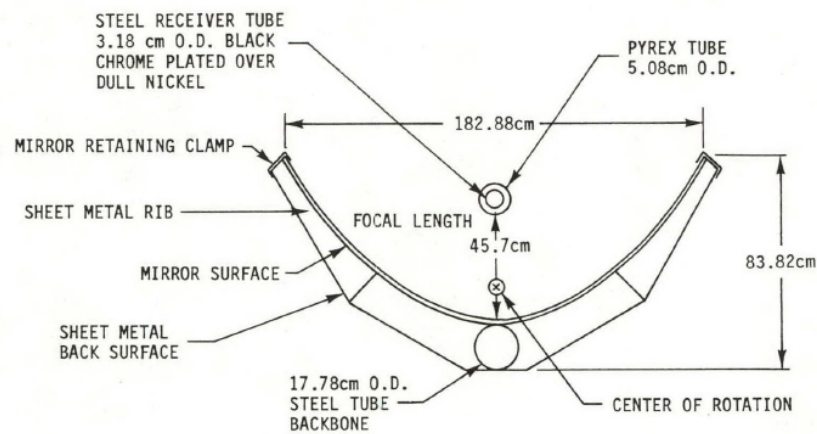


Figure 2.2: Cross-section of the ACUREX collector (Dudley and Workhoven, 1982).

### 2.2.1 Principle of operation

The ACUREX collector concentrates the incident solar radiation onto the receiver tube that is positioned along its focal line. Once the thermal oil is pumped from the bottom of a thermal storage tank, it then passes through the receiver tube and circulates in the distributed solar collector field. The thermal oil gets heated and when a certain field outlet temperature is reached, the heated oil is returned to the top of the storage tank by means of a three-way valve. The heated oil finally passes through a series of heat exchangers to produce steam which in turn is used to drive a steam turbine to generate electricity.

Note that the thermal storage tank is providing a degree of independence from the intermittency of solar energy and hence ensures a continuous operation of the plant. Fig. 2.3 gives an illustration of the principle of operation at the ACUREX plant.

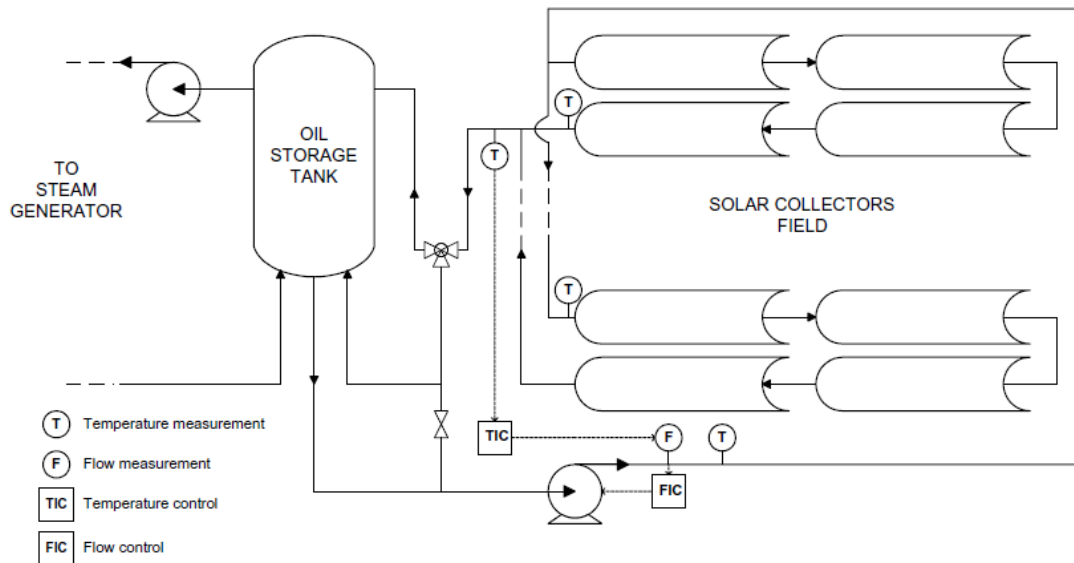


Figure 2.3: ACUREX: Principle of operation. Adapted from Camacho et al. (2012).

### 2.2.2 Control problem

One of the biggest control challenges at the ACUREX plant, is to maintain the field outlet temperature at a desired level despite changes, mainly in solar radiation and the field inlet temperature. This can be handled efficiently by manipulating the volumetric flow rate of the HTF within a certain range during the normal operation of the plant.

The operating volumetric flow rate of the HTF is normally between  $0.002 \text{ m}^3/\text{s}$  and  $0.012 \text{ m}^3/\text{s}$ . The minimum limit helps to maintain the field outlet temperature below  $305^\circ\text{C}$ . Exceeding this temperature puts the thermal oil at the risk of being decomposed. Another important restriction is to keep the difference between the field outlet and inlet temperature less than  $80^\circ\text{C}$ . Exceeding a temperature difference of  $100^\circ\text{C}$  gives a significant risk of oil leakage due to high oil pressure in the piping system.

### 2.2.3 Resonant modes

The ACUREX plant possesses resonance characteristics, namely resonant modes that lie well within the desired control bandwidth. The resonance phenomena arise due to the relatively slow flow rate of the HTF and the length of the receiver tube (Meaburn and Hughes, 1993).

To give an insight into this resonance phenomena, Fig. 2.4 shows the frequency response of the field outlet temperature. The frequency response is obtained from a nonlinear simulation model of the ACUREX plant and after some variations in the volumetric flow rate of the HTF around  $0.010 \text{ m}^3/\text{s}$ . The resonance characteristics are quite apparent and indeed lie within the Nyquist bandwidth.

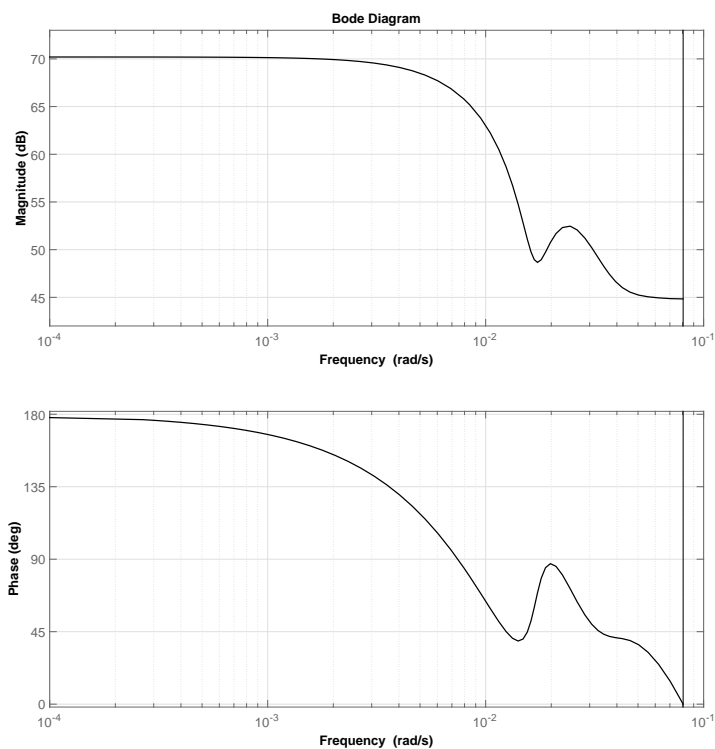


Figure 2.4: Frequency response of the field outlet temperature around a volumetric flow rate of  $0.010 \text{ m}^3/\text{s}$ .

It has been found in Meaburn and Hughes (1993) that the phenomena have a significant impact on the control performance. Hence, modelling the resonant modes sufficiently accurately is crucial to ensure high control performance with adequate robustness.

As will be seen in the next chapter, the resonance phenomena and its control implications have received a considerable amount of attention in this thesis.

### **2.3 *Nonlinear Simulation Model***

In this thesis, the successful development of a nonlinear simulation model that describes the main dynamics of the ACUREX plant has played a key role in:

- Gaining valuable information about the dynamic characteristics of the plant under many different and commonplace operating conditions.
- Obtaining direct, linear and dynamic relationships between the manipulated variable (volumetric flow rate of the HTF) and the controlled variable (field outlet temperature). This has led to the development of various model-based control strategies tailored to the ACUREX plant.
- Obtaining direct, linear and dynamic relationships between the measured disturbances (solar radiation and the field inlet temperature) and the field outlet temperature. This has led to the development of a systematic feedforward design and hierarchical control strategies.

The development of an accurate nonlinear simulation model of the ACUREX plant is motivated by first, the lack of access to the actual plant; and second, the many problems encountered with the currently available simulation software packages. For example, the simulation software package of the ACUREX plant described in Camacho et al. (1993) has been widely used by early researchers in the field, however, it has been over 25 years since the simulation software package was devel-

oped and hence, in addition to the limited access to some of the key source files, the software package suffers from major compatibility issues.

### 2.3.1 Dynamic behaviour

The dynamic behaviour of a single loop at the ACUREX distributed solar collector field is governed by a set of energy balance partial differential equations (PDEs) developed in Carmona (1985) and reported in Camacho et al. (2012). The energy balance PDEs are developed under the following assumptions:

- Properties of the HTF are a function of the working field outlet temperature.
- In each section of the receiver tube, the flow rate of the HTF is circumferentially uniform and equal to an average value.
- The receiver tube has a thin wall and fine thermal conductivity and hence variation in the radial temperature is neglected.
- Axial heat conduction in the receiver tube wall and HTF is negligible.
- The HTF is incompressible.

Hence, the set of PDEs is given as:

$$\rho_m C_m A_m \frac{\partial T_m}{\partial t} = n_o G I - D_o \pi H_l (T_m - T_a) - D_i \pi H_t (T_m - T_f), \quad (2.1a)$$

$$\rho_f C_f A_f \frac{\partial T_f}{\partial t} + \rho_f C_f q \frac{\partial T_f}{\partial x} = D_i \pi H_t (T_m - T_f), \quad (2.1b)$$

where the subindex  $m$  refers to the metal of the receiver tube and  $f$  to the HTF. Table 2.1 gives a description of all the variables and parameters and lists their SI units.

Note that the temperature of the HTF ( $T_f$ ) and the receiver tube ( $T_m$ ) in (2.1) are a function of time and position. Next the set of PDEs in (2.1) is approximated by a set of nonlinear first order ordinary differential equations (ODEs).

Table 2.1: Variables and Parameters.

Symbol	Description	SI unit
$\rho$	Density	kg/m <sup>3</sup>
$C$	Specific heat capacity	J/kg°C
$A$	Cross-sectional area	m <sup>2</sup>
$T$	Temperature	°C
$t$	Time	s
$I$	Solar radiation	W/m <sup>2</sup>
$n_o$	Mirror optical efficiency	–
$G$	Mirror optical aperture	m
$D_o$	Outer diameter of the receiver tube	m
$H_l$	Global coefficient of thermal losses	W/m°C
$T_a$	Ambient temperature	°C
$D_i$	Inner diameter of the receiver tube	m
$H_t$	Metal-fluid heat transfer coefficient	W/m <sup>2</sup> °C
$q$	HTF volumetric flow rate	m <sup>3</sup> /s
$x$	Space	m

### 2.3.2 Model construction

A nonlinear simulation model of the plant can be constructed by dividing the receiver tube into  $N$  segments each of length  $\Delta x$ . This is illustrated in Fig. 2.5 .

Hence, the nonlinear distributed parameter model in (2.1) is approximated, for  $n = 1, \dots, N$ , by the following set of ODEs with the boundary condition  $T_{f,0} = T_{f,inlet}$  (field inlet temperature) and  $H_{l,n}, H_{t,n}, \rho_{f,n}$  and  $C_{f,n}$  being time-varying:

$$\rho_m C_m A_m \frac{dT_{m,n}}{dt} = n_o G I - D_o \pi H_l (T_{m,n} - T_a) - D_i \pi H_t (T_{m,n} - T_{f,n}), \quad (2.2a)$$

$$\rho_f C_f A_f \frac{dT_{f,n}}{dt} + \rho_f C_f q \frac{T_{f,n} - T_{f,n-1}}{\Delta x} = D_i \pi H_t (T_{m,n} - T_{f,n}). \quad (2.2b)$$

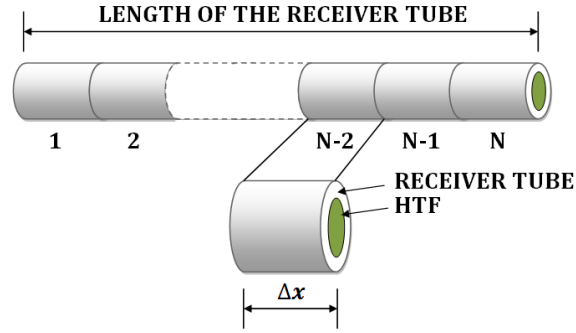


Figure 2.5: Construction of a nonlinear simulation model.

The set of ODEs in (2.2) is implemented and solved using the MATLAB<sup>®</sup> solver ODE45 (an explicit Runge-Kutta method) where the temperature distribution in the receiver tube and HTF can be accessed at any point in time and for any segment  $n$ . The number of ODEs solved at each sampling instant  $k$  for  $N$  segments is  $2 \times N$ .

Note that the approximation  $\frac{T_{f,n} - T_{f,n-1}}{\Delta x}$  in (2.2b) is known as a backward finite difference approximation since it uses backward differencing. An alternative would be to use a forward or central differencing. However, both approximations, forward and central differences, require the availability of  $T_{f,n+1}$ . For more details on discrete approximation of derivatives, see Ozisik (1994).

A detailed modelling analysis of the ACUREX plant in Alsharkawi and Rossiter (2017b) has revealed that dividing the receiver tube into a large number of segments captures the dynamics of the plant at high frequencies, while dividing the receiver tube into a small number of segments captures the dynamics of the plant at low frequencies.

In addition to some time-based measurements from the ACUREX plant, this dilemma has been resolved by relating to the frequency response of the ACUREX plant around a number of operating points. It has been found that dividing the receiver tube into 7 segments gives a reasonable trade-off between prediction accuracy and computational burden while still adequate enough to capture the resonance characteristics of the plant.

Although the set of PDEs in (2.1), that describes the main dynamics of the plant, has been developed in Carmona (1985) from first principles of thermodynamics, some of the variables have been determined using measured data from the ACUREX plant. Table 2.2 gives values <sup>1</sup> to the parameters in (2.1) and this is then followed by a brief description of some of the properties of the HTF and the rest of the variables.

Table 2.2: Parameters of the Nonlinear Simulation Model

Symbol	Value in SI unit
$\rho_m$	7800 kg/m <sup>3</sup>
$C_m$	550 J/kg°C
$A_m$	$8 \times 10^{-4}$ m <sup>2</sup>
$G$	1.82 m
$D_o$	$3.180 \times 10^{-2}$ m
$D_i$	$2.758 \times 10^{-2}$ m
$A_f$	$6 \times 10^{-4}$ m <sup>2</sup>

#### *Properties of the HTF ( $\rho_f$ and $C_f$ )*

It has been mentioned before that the HTF at the ACUREX plant is the synthetic thermal oil Therminol<sup>®</sup> 55. One of its main characteristics is that its density is highly dependent on its working temperature and this is in fact the main cause of the phenomenon of thermal stratification at the thermal storage tank. The phenomenon here simply means that the hot oil is stored at the top of the storage tank and the cold oil at the bottom.

Following a technical data sheet of the Therminol<sup>®</sup> 55, density and specific heat

---

<sup>1</sup>These values have been obtained from different literature sources.  $\rho_m$ ,  $C_m$  and  $G$  have been obtained from Camacho et al. (1993) and  $A_m$ ,  $D_o$ ,  $D_i$  and  $A_f$  have been obtained from Gálvez-Carrillo et al. (2009).

capacity are reported in Camacho et al. (2012) as:

$$\rho_f = 903 - 0.672 T_f, \quad (2.3)$$

$$C_f = 1820 + 3.478 T_f. \quad (2.4)$$

*Metal-fluid heat transfer coefficient ( $H_t$ )*

This coefficient has been determined experimentally in Carmona (1985). It is a function of the working field outlet temperature ( $T_f$ ) and the volumetric flow rate of the HTF ( $q$ ). The coefficient is given as:

$$H_t = H_v q^{0.8}, \quad (2.5)$$

where

$$H_v = 2.17 \times 10^6 - 5.01 \times 10^4 T_f + 4.53 \times 10^2 T_f^2 - 1.64 T_f^3 + 2.10 \times 10^{-3} T_f^4. \quad (2.6)$$

*Global coefficient of thermal losses ( $H_l$ )*

Similar to the metal-fluid heat transfer coefficient  $H_t$ , the global coefficient of thermal losses  $H_l$  has been determined experimentally in Carmona (1985) and it is a function of the working field outlet temperature  $T_f$  and the ambient temperature  $T_a$ . The coefficient is given as:

$$H_l = 0.00249 (T_f - T_a) - 0.06133. \quad (2.7)$$

**Remark 2.1.** *Properties of the HTF ( $\rho_f$  and  $C_f$ ), metal-fluid heat transfer coefficient ( $H_t$ ) and global coefficient of thermal losses ( $H_l$ ) are solved at each sampling instant  $k$  and for each segment  $n$ .*

*An illustrative example*

The nonlinear simulation model represented by the set of ODEs in (2.2) has been properly validated in Alsharkawi and Rossiter (2017b,c) using measured data from

the ACUREX plant and hence the aim of this section is not to validate the nonlinear simulation model, but rather to illustrate the dynamic behaviour of the different time-varying variables discussed earlier. Using some measured data from the ACUREX plant collected <sup>2</sup> on 15 July 2003 after a series of step changes in the volumetric flow rate of the HTF, the dynamic behaviour of the nonlinear simulation model along with its time-varying variables have been obtained. Fig. 2.6 shows the measured inputs and Fig. 2.7 shows the measured output, model output and time-varying variables.

It can be clearly seen from Fig. 2.7 that indeed the variables  $\rho_f$ ,  $C_f$ ,  $H_t$  and  $H_l$  are all time-varying and influenced by the field outlet temperature. It is worth noting that to ensure safe plant operation, the controlled variable at the ACUREX plant is the highest outlet temperature of the 10 collector loops (Camacho et al., 1997). Hence, the model output here is compared with the outlet temperature of collector loop 5 which is located at the middle of the distributed solar collector field and has the highest outlet temperature.

## **2.4 Fundamental Control Strategy**

It has been mentioned before that the measured disturbances, solar radiation and the field inlet temperature, are an integral part of the ACUREX plant and it has been mentioned also that constraints are imposed on the manipulated variable, volumetric flow rate of the HTF, to ensure safe plant operation. Hence, one of the aims of this thesis is to make an effective use of available information on the measured disturbances of the ACUREX plant while taking into account the plant safety constraints. Model-based predictive control (MPC) enables systematic feedforward design and takes systematic account of constraints.

---

<sup>2</sup>During the data collection, the number of active loops was 9 and mirror optical efficiency ( $n_o$ ) was 56 %.

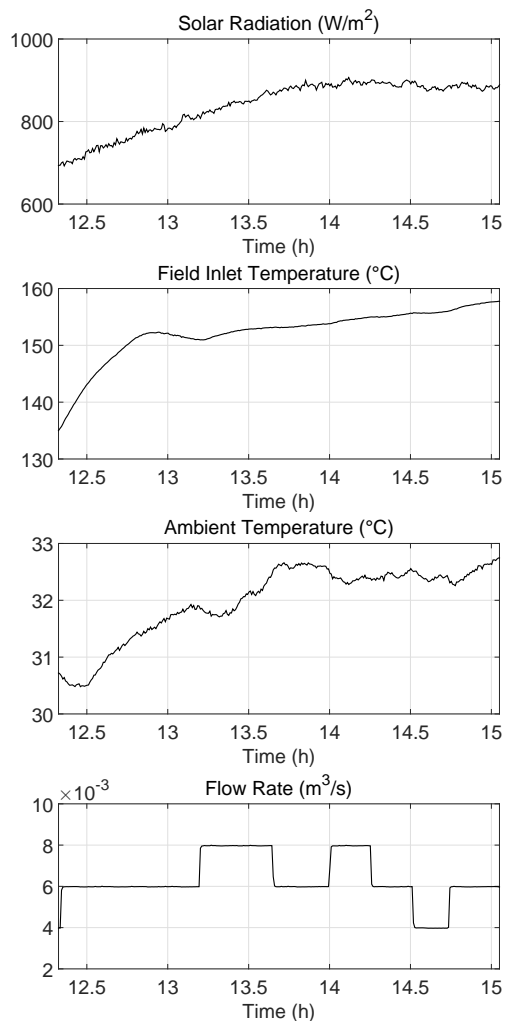


Figure 2.6: Measured inputs.

### 2.4.1 An overview

MPC is broadly referred to as that family of controllers in which there is a direct use of an explicit process model (Garcia et al., 1989). However, unlike conventional control, which makes use of a pre-computed control law, MPC solves optimal control problems on-line and at each sampling instant.

More specifically, MPC can be referred to as the form of control that utilises an explicit process model to predict the future response of a plant. At each sampling instant, MPC attempts to optimise the future response of the plant by computing

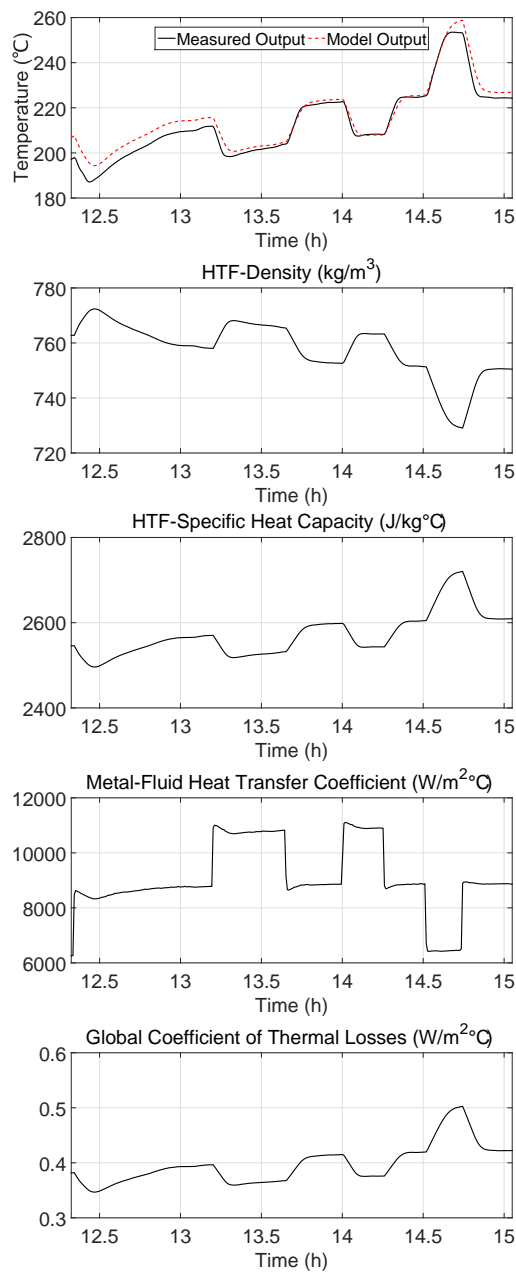


Figure 2.7: Measured output, model output and time-varying variables.

on-line an optimal sequence of future control actions and applies only the first control action in that sequence to the plant (receding horizon).

Although the idea of receding horizon was first proposed back in the early sixties of the last century (Propoi, 1963), which forms the core of all MPC algorithms

(Garcia et al., 1989), interest in the field of MPC only started to emerge over a decade later after the successful applications of two variants of MPC, IDCOM and DMC described in Richalet et al. (1978) and Cutler and Ramaker (1980) respectively, and since then its popularity in the process industries has increased steadily (Garcia et al., 1989).

Over 4600 MPC applications are reported in a survey paper conducted in the year 2003 (Qin and Badgwell, 2003) which is over twice the number reported five years earlier in Qin and Badgwell (1997). Despite the capability of MPC for controlling multivariable plants, the primary reason for this success in the process industries is indeed the capability of MPC to handle process constraints on-line and in a systematic manner (Garcia et al., 1989).

More recently, however, it is argued in Yu-Geng et al. (2013) that the current MPC is faced with great challenges due to the increasing requirements on the constrained optimisation control arising from the rapid development of economy and society. These challenges can be briefly summarised by the following. Many of the currently available industrial MPC algorithms are mainly suitable for processes with slow dynamics and restricted to linear or quasi-linear processes. Moreover, from an application point of view, these algorithms mainly rely on experience and require an ad hoc design.

After investigating the current research status on MPC, the survey (Yu-Geng et al., 2013) highlights some key issues like bridging the gap between existing MPC theory and practical applications, developing efficient industrial MPC algorithms and exploring new application areas. These in fact have been acknowledged recently by many researchers from different disciplines. For example, in Kufoalor et al. (2017), with the aim of filling the gap between fast quadratic programming solver developments and industrial MPC implementations based on step response models, a new formulation for step response MPC is proposed. In Neunert et al. (2016), a highly efficient iterative optimal control algorithm is used in an MPC setting to solve a nonlinear optimal control problem in a receding horizon fashion for simultaneously

trajectory optimisation and tracking control. Away from oil refining, petrochemical and chemical industry, MPC has found new applications ranging from micro-aerial vehicles (Kumar and Michael, 2012; Turpin et al., 2012), a fast growing field in robotics, to marine electric power plants (Bø and Johansen, 2013, 2017).

MPC is a generic acronym that is widely used to denote the whole area of predictive control (Maciejowski, 2002) and in spite of the slight differences due to modelling or prediction assumptions, the different variants of MPC share the following essential components (Rossiter, 2003):

- Output predictions based on an explicit process model.
- Some performance criteria mathematically represented by a cost function.
- An optimisation algorithm to minimise the cost function.
- Receding horizon, where the control input is updated at each sampling instant.

One variant of MPC, namely dual mode MPC, lays the foundation for the control strategies developed in this thesis and hence the remainder of this section discusses the idea of dual mode MPC and its principal components.

The fundamental dual mode strategy considered in this thesis is best described in Rossiter (2003) and hence for the remainder of this section, background information on dual mode MPC is from Rossiter (2003), unless stated otherwise.

#### *2.4.2 Dual mode MPC*

For a desired operating point, the notation dual mode refers to the predictions of process behaviour being separated into two modes, a transient and terminal mode. As the process converges to the desired operating point; that is, moving from the transient mode to the terminal mode,  $n_c$  degrees of freedom (d.o.f) are utilised within the transient mode and normally a fixed feedback law is utilised within the terminal mode. The details are given next.

*Dual mode predictions and the cost function*

A typical discrete-time linear time-invariant (LTI) state space model takes the form:

$$\begin{aligned} x_{k+1} &= Ax_k + Bu_k, \\ y_k &= Cx_k, \end{aligned} \quad (2.8)$$

where  $x_k \in \mathbb{R}^{n \times 1}$ ,  $u_k \in \mathbb{R}^{m \times 1}$  and  $y_k \in \mathbb{R}^{l \times 1}$  are the state vector, input vector and output vector respectively at sampling instant  $k$ .  $A \in \mathbb{R}^{n \times n}$ ,  $B \in \mathbb{R}^{n \times m}$  and  $C \in \mathbb{R}^{l \times n}$  are the coefficient matrices. The system in (2.8) is assumed to be controllable and observable.

Hence, under the assumption that the first  $n_c$  control moves are free and the remaining moves are given by a state feedback  $K$ , input and state predictions could be given by:

$$u_{k+i} = \begin{cases} u_{k+i}, & \forall i < n_c, \\ -Kx_{k+i}, & \forall i \geq n_c, \end{cases} \quad (2.9a)$$

$$x_{k+i+1} = \begin{cases} Ax_{k+i} + Bu_{k+i}, & \forall i < n_c, \\ \phi x_{k+i}, & \forall i \geq n_c, \end{cases} \quad (2.9b)$$

where  $\phi = A - BK$ . Thus, it is convenient to separate a quadratic cost function of the form:

$$J_k = \sum_{i=0}^{\infty} x_{k+i+1}^T Q x_{k+i+1} + u_{k+i}^T R u_{k+i}, \quad (2.10)$$

into two modes, transient and terminal mode as follows:

$$J_k = \underbrace{\sum_{i=0}^{n_c-1} x_{k+i+1}^T Q x_{k+i+1} + u_{k+i}^T R u_{k+i}}_{\text{Transient mode}} + \underbrace{\sum_{i=n_c}^{\infty} x_{k+i+1}^T Q x_{k+i+1} + u_{k+i}^T R u_{k+i}}_{\text{Terminal mode}}. \quad (2.11)$$

Note that one can form the whole vector of state predictions  $\underset{\rightarrow k}{x}$  up to a horizon  $n_c$

as follows:

$$\underbrace{\begin{bmatrix} x_{k+1} \\ x_{k+2} \\ \vdots \\ x_{k+n_c} \end{bmatrix}}_{\substack{x \\ \rightarrow k}} = \underbrace{\begin{bmatrix} A \\ A^2 \\ \vdots \\ A^{n_c} \end{bmatrix}}_{W_x} x_k + \underbrace{\begin{bmatrix} B & 0 & \cdots \\ AB & B & \cdots \\ \vdots & \vdots & \vdots \\ A^{n_c-1}B & A^{n_c-2}B & \cdots \end{bmatrix}}_{H_x} \underbrace{\begin{bmatrix} u_k \\ u_{k+1} \\ \vdots \\ u_{k+n_c-1} \end{bmatrix}}_{\substack{u \\ \rightarrow k-1}}, \quad (2.12)$$

where  $\underset{\rightarrow k-1}{u}$  is the future input sequence. Hence, the cost function in the transient mode can be presented as:

$$\underbrace{[W_x x_k + H_x \underset{\rightarrow k-1}{u}]^T \bar{Q} [W_x x_k + H_x \underset{\rightarrow k-1}{u}] + \underset{\rightarrow k-1}{u}^T \bar{R} \underset{\rightarrow k-1}{u}}_{\text{Transient mode}}, \quad (2.13)$$

where  $\bar{Q} \in \mathbb{R}^{n_c n \times n_c n}$  and  $\bar{R} \in \mathbb{R}^{n_c m \times n_c m}$  are diagonal matrices of the form:

$$\bar{Q} = \begin{bmatrix} Q & & \\ & \ddots & \\ & & Q \end{bmatrix}; \quad \bar{R} = \begin{bmatrix} R & & \\ & \ddots & \\ & & R \end{bmatrix}. \quad (2.14)$$

The cost function in the terminal mode, on the other hand, can be evaluated using a Lyapunov equation. From the input and state predictions in (2.9), assume  $\forall i \geq n_c$ :

$$x_{k+i+1} = \phi x_{k+i} = \phi^{i+1} x_k, \quad u_{k+i} = -K x_{k+i} = -K \phi^i x_k, \quad (2.15)$$

then the cost function in the terminal mode takes the form:

$$\underbrace{\sum_{i=0}^{\infty} [\phi^{i+1} x_{k+n_c}]^T Q [\phi^{i+1} x_{k+n_c}] + [-K \phi^i x_{k+n_c}]^T R [-K \phi^i x_{k+n_c}]},_{\text{Terminal mode}} \quad (2.16)$$

which can be simplified to:

$$\underbrace{x_{k+n_c}^T P x_{k+n_c}}_{\text{Terminal mode}}, \quad (2.17)$$

where  $P$  is simply:

$$P = \sum_{i=0}^{\infty} (\phi^{i+1})^T Q \phi^{i+1} + (\phi^i)^T K^T R K \phi^i, \quad (2.18)$$

and is the solution to a Lyapunov equation:

$$\phi^T P \phi = P - \phi^T Q \phi - K^T R K, \quad (2.19)$$

which can be easily solved using `dlyap.m` in MATLAB<sup>®</sup>.

Before combining the transient cost in (2.13) and the terminal cost in (2.17), one can find a prediction for  $x_{k+n_c}$  in (2.17) using the last block rows of the state predictions in (2.12) as follows:

$$x_{k+n_c} = W_{n_c} x_k + H_{n_c} \underset{\rightarrow k-1}{u}, \quad (2.20)$$

where  $W_{n_c}$  and  $H_{n_c}$  are the  $n_c^{\text{th}}$  block rows of  $W_x$  and  $H_x$  respectively. Hence, the terminal cost function in (2.17) becomes:

$$\underbrace{[W_{n_c} x_k + H_{n_c} \underset{\rightarrow k-1}{u}]^T P [W_{n_c} x_k + H_{n_c} \underset{\rightarrow k-1}{u}]}_{\text{Terminal mode}}, \quad (2.21)$$

and finally, after bringing the cost in (2.13) and (2.21) together, the cost function in (2.11) takes the following form:

$$\begin{aligned} J_k = & [W_x x_k + H_x \underset{\rightarrow k-1}{u}]^T \bar{Q} [W_x x_k + H_x \underset{\rightarrow k-1}{u}] + \underset{\rightarrow k-1}{u}^T \bar{R} \underset{\rightarrow k-1}{u} \\ & + [W_{n_c} x_k + H_{n_c} \underset{\rightarrow k-1}{u}]^T P [W_{n_c} x_k + H_{n_c} \underset{\rightarrow k-1}{u}], \end{aligned} \quad (2.22)$$

which can be further simplified to a simple quadratic form with  $n_c$  block d.o.f:

$$J_k = \underset{\rightarrow k-1}{u}^T S \underset{\rightarrow k-1}{u} + \underset{\rightarrow k-1}{u}^T L x_k + e, \quad (2.23)$$

where  $S = H_x^T \bar{Q} H_x + \bar{R} + H_{n_c}^T P H_{n_c}$ ,  $L = 2[H_x^T \bar{Q} W_x + H_{n_c}^T P W_{n_c}]$  and  $e$  does not depend on the future input sequence  $\underset{\rightarrow k-1}{u}$ .

### *Constraint handling and the dual mode MPC algorithm*

It has been mentioned earlier in this section that MPC handles process constraints on-line and in a systematic manner. Constraints may occur on any of the process variables. However, common constrained variables are on input rate, input and

output. These operational constraints can be presented as linear inequalities over a horizon  $n_c$  as follows:

$$\Delta u_{min} \leq \Delta u_{k+i} \leq \Delta u_{max}, \quad i = 0, \dots, n_c - 1, \quad (2.24a)$$

$$u_{min} \leq u_{k+i} \leq u_{max}, \quad i = 0, \dots, n_c - 1, \quad (2.24b)$$

$$y_{min} \leq y_{k+i} \leq y_{max}, \quad i = 0, \dots, n_c - 1, \quad (2.24c)$$

where  $\Delta u_k$  is the input rate at sampling instant  $k$ .  $\Delta u_{min}$ ,  $u_{min}$  and  $y_{min}$  are the lower limits on the input rate, input and output respectively and similarly,  $\Delta u_{max}$ ,  $u_{max}$  and  $y_{max}$  are the upper limits on the input rate, input and output respectively.

In this thesis, safety constraints are imposed on the volumetric flow rate of the HTF and hence from the constrained variables in (2.24), only the input constraints (2.24b) are considered.

Hence, input constraints in (2.24b) can be rewritten as:

$$\underbrace{\begin{bmatrix} u_{min} \\ u_{min} \\ \vdots \\ u_{min} \end{bmatrix}}_{U_{min}} \leq \underbrace{\begin{bmatrix} u_k \\ u_{k+1} \\ \vdots \\ u_{k+n_c-1} \end{bmatrix}}_{\substack{u \\ \rightarrow k-1}} \leq \underbrace{\begin{bmatrix} u_{max} \\ u_{max} \\ \vdots \\ u_{max} \end{bmatrix}}_{U_{max}}, \quad (2.25)$$

which is conventionally represented in terms of a single linear inequalities as follows:

$$\begin{bmatrix} I \\ -I \end{bmatrix} \substack{u \\ \rightarrow k-1} \leq \begin{bmatrix} U_{max} \\ -U_{min} \end{bmatrix}, \quad (2.26)$$

where  $I \in \mathbb{R}^{n_c \times n_c}$  is an identity matrix.

The input constraints in (2.26) together with the cost function in (2.23) are the required components to define a practical dual mode MPC algorithm.

---



---

Dual mode MPC

---



---

1: At each sampling instant  $k$ , perform the optimisation

$$\min_{\underline{u}_{\rightarrow k-1}} \underline{u}_{\rightarrow k-1}^T S \underline{u}_{\rightarrow k-1} + \underline{u}_{\rightarrow k-1}^T Lx_k, \quad \text{s.t.} \quad (2.26). \quad (2.27)$$

2: Solve for the first element of  $\underline{u}_{\rightarrow}$  and implement on process.

---

The optimisation in (2.27) is a typical quadratic programming (QP) problem with input constraints and finite number of d.o.f. which can be easily solved using `quadprog.m` in MATLAB<sup>®</sup>.

### 2.4.3 Offset-free tracking

Due to the nonlinearity of the ACUREX plant, a model-plant mismatch is likely to happen (Camacho et al., 2012). That is, in a particular tracking scenario a plant reaches an inaccurate final value because simply the steady state gain of a model of the plant is not accurately captured (Maciejowski, 2002). Hence, to ensure offset-free tracking, slight modifications to the cost function in (2.23) and input constraints in (2.25) and (2.26) are necessary.

The cost function in (2.23) and input constraints in (2.25) and (2.26) are modified as follows:

$$J_k = \underline{\bar{u}}_{\rightarrow k-1}^T S \underline{\bar{u}}_{\rightarrow k-1} + \underline{\bar{u}}_{\rightarrow k-1}^T L\bar{x}_k + e, \quad (2.28)$$

$$\underbrace{\begin{bmatrix} \bar{u}_{min} \\ \bar{u}_{min} \\ \vdots \\ \bar{u}_{min} \end{bmatrix}}_{\bar{U}_{min}} \leq \underbrace{\begin{bmatrix} \bar{u}_k \\ \bar{u}_{k+1} \\ \vdots \\ \bar{u}_{k+nc-1} \end{bmatrix}}_{\underline{\bar{u}}_{\rightarrow k-1}} \leq \underbrace{\begin{bmatrix} \bar{u}_{max} \\ \bar{u}_{max} \\ \vdots \\ \bar{u}_{max} \end{bmatrix}}_{\bar{U}_{max}}, \quad (2.29)$$

$$\begin{bmatrix} I \\ -I \end{bmatrix} \underline{\bar{u}}_{\rightarrow k-1} \leq \begin{bmatrix} \bar{U}_{max} \\ -\bar{U}_{min} \end{bmatrix}, \quad (2.30)$$

where a  $\bar{x}$  and  $\bar{u}$  refer to a deviation from some steady state estimates  $x_{ss}$  and  $u_{ss}$  respectively.

Hence, the optimisation problem in (2.27) becomes:

$$\min_{\substack{\bar{u} \\ \rightarrow}} \bar{u}_{\rightarrow k-1}^T S \bar{u}_{\rightarrow k-1} + \bar{u}_{\rightarrow k-1}^T L \bar{x}_k, \quad \text{s.t.} \quad (2.30). \quad (2.31)$$

Given the desired output  $r_k$  and the current measured output  $y_k^m$ , one can consistently estimate the required steady state values of the state  $x_{ss}$  and the input  $u_{ss}$  as follows:

$$d_k = y_k^m - y_k, \quad (2.32)$$

where  $d_k$  is a bias term that compares the current measured output  $y_k^m$  with the current predicted output  $y_k$ . This is a form of feedback equivalent to assuming that a step disturbance enters the system and remains constant in the future (Qin and Badgwell, 2003). Hence, under the assumption that:

$$d_{k+1} = d_k, \quad (2.33)$$

one can get the following simultaneous equations:

$$\begin{aligned} x_{ss} &= Ax_{ss} + Bu_{ss}, \\ r_k &= Cx_{ss} + d_k, \end{aligned} \quad (2.34)$$

which give a solution of the form (Muske and Rawlings, 1993):

$$\begin{bmatrix} x_{ss} \\ u_{ss} \end{bmatrix} = \begin{bmatrix} I - A & -B \\ C & 0 \end{bmatrix}^{-1} \begin{bmatrix} 0 \\ r_k - d_k \end{bmatrix}. \quad (2.35)$$

## 2.5 Summary

This chapter has presented background information on the ACUREX plant considered in this thesis, construction of a nonlinear simulation model of the plant as well as a dual mode MPC strategy. Section 2.2 mainly described the installation of the ACUREX parabolic trough collectors, principle of operation and the control problem

---

at the ACUREX plant. Dynamic behaviour and detailed construction of a nonlinear simulation model of the plant have been discussed in Section 2.3. This section has also given some special consideration to some of the time-varying variables in the constructed nonlinear simulation model. An overview of MPC, the idea of dual mode MPC and the principal components of the strategy have been discussed in Section 2.4. This section has also highlighted the issue of offset-free tracking.

## Chapter 3

# SUMMARY OF CONTRIBUTIONS

### ***3.1 Chapter Overview***

Original contributions of this thesis to the automatic control of a parabolic trough technology-based solar thermal power plant are in seven different papers and therefore the purpose of this chapter is to give a brief summary of these contributions and show how the research in this thesis has developed from a review paper to an advanced hierarchical control. The main contributions are discussed here under five main topics and with respect to the existing literature, though the way these topics are arranged does not necessarily imply that the papers in this thesis are arranged in a chronological order.

A review on concentrating solar technologies with an emphasis placed on parabolic trough technology and its utilisation in the ACUREX plant is discussed in Section 3.2. Original contributions on constructing a nonlinear simulation model of the ACUREX plant are discussed in Section 3.3. Original contributions on a tailored gain scheduling design is discussed in Section 3.4. Section 3.5 and Section 3.6 discuss original contributions on a systematic feedforward design and pragmatic hierarchical control respectively. Section 3.7 concludes the chapter with a summary.

### ***3.2 Unifying Review***

A review on concentrating solar technologies with an emphasis placed on parabolic trough technology and its utilisation in the ACUREX plant was conducted in Alsharkawi and Rossiter (2015). The review was meant to complement comprehensive

reviews already existing in the literature, namely the reviews in Camacho et al. (2007a,b).

There is a general agreement in the literature that the main concentrating solar technologies are parabolic trough, linear Fresnel reflector, central receiver and parabolic dish technology; see Fig. 3.1. While the reviews in Camacho et al. (2007a,b) cover a large body of research on the modelling and control of the parabolic trough technology-based ACUREX plant, they fail to provide some answers to questions like: *Why has the utilisation of parabolic trough technology in a solar thermal power plant received this considerable amount of attention? Why has the utilisation of a linear Fresnel reflector, central receiver and parabolic dish technology in solar thermal power plants not received similar attention?* Moreover, the reviews in Camacho et al. (2007a,b) were conducted in the year 2007 and when this research has started in 2014, it had been noticed that the literature had developed and research in a particular area has taken shape.

Hence, with an attempt to provide some answers to the earlier posed questions, the review in Alsharkawi and Rossiter (2015) took a step back and looked at the concentrating solar technologies from the different aspects of basic concepts, advantages, disadvantages and successful commercial applications and came to the conclusion that parabolic trough technology is commercially considered the most economic and reliable technology. In fact, it has been reported in Alsharkawi and Rossiter (2015) that over 90% of the currently installed solar power capacity is accounted for by parabolic trough technology-based solar thermal power plants. Therefore, the mainstream mature established parabolic trough technology has left researchers with the impression that any further improvements in plant performance are likely to be gained through the design and implementation of an advanced control strategies.

The review in Alsharkawi and Rossiter (2015) then focused on some modelling and control approaches of the ACUREX plant and highlighted that semi-empirical models are preferable in general and, despite various control efforts, an effective comparison seems to be lacking. The substantial interest in the benefits of applying MPC

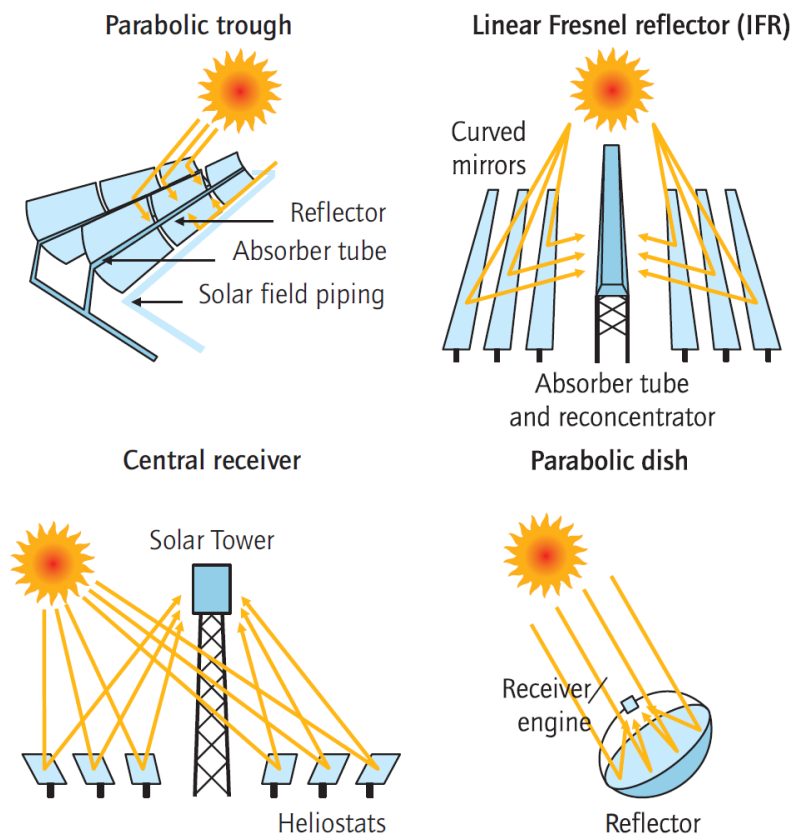


Figure 3.1: Concentrating solar technologies (Philibert, 2010).

has been also appreciated. The review finally underlined some recent developments in hierarchical control and emphasised the point that the adoption of hierarchical control structures is likely to be the future of controlling solar thermal power plants, which moreover allow for effects such as weather prediction and variation in electricity demands.

In summary, the review in Alsharkawi and Rossiter (2015) has indeed laid the foundation for this research by appreciating:

- The fundamental role of the energy balance PDEs (2.1) in constructing a non-linear simulation model of the ACUREX plant.
- The significance of the resonance characteristics of the ACUREX plant and

how such a phenomena can be tackled by the development of high order linear models of the plant within a gain scheduling framework.

- The prime need for a feedforward design to mitigate the effects of the measured disturbances of the ACUREX plant.
- The economic potential of hierarchical control structures.

### **3.3 Simulation Model**

It has been discussed in Chapter 2 that the ACUREX plant possesses resonance characteristics that lie well within the desired control bandwidth and the resonance phenomena have a significant impact on the control performance. Hence, modelling the resonant modes sufficiently accurately is crucial to ensure high control performance with adequate robustness.

It has been also shown in Chapter 2 that a nonlinear simulation model of the plant can be constructed by dividing the receiver tube into a number of segments, each of length  $\Delta x$ , and hence the set of PDEs in (2.1) can be approximated by the set of ODEs in (2.2). Yet, selecting a particular number of segments is not as intuitive as one might expect.

#### *3.3.1 An overview on the literature*

In Alsharkawi and Rossiter (2017b) it has been found that the number of segments used to construct a nonlinear simulation and prediction models of the ACUREX plant has varied significantly in the literature. In one of the early constructed nonlinear simulation models of the ACUREX plant (Camacho et al., 1993), the set of ODEs (2.2) has been obtained after dividing the receiver tube into 100 segments.

More recently and after simplifying the PDEs (2.1) by neglecting the dynamics of the metal of the receiver tube, a set of ODEs has been obtained in Gálvez-Carrillo et al. (2009) for simulation and prediction purposes. For simulation purposes, the re-

ceiver tube was divided into 10 segments and for prediction purposes, after neglecting the heat losses, the receiver tube was divided into 5 segments.

In an attempt to obtain a linearised state space model of the plant in Gallego and Camacho (2012), an ODE was obtained from a simplified version of the PDEs (2.1) and the receiver tube was divided into 8 segments whereas in Gallego et al. (2013) and for the same exact reason, the set of PDEs (2.1) was converted into a set of ODEs by dividing the receiver tube into 15 segments.

### 3.3.2 Discussion and main contributions

The significant variation (from 5 to 100) in the number of segments used to construct nonlinear simulation and prediction models of the plant is apparent and hence in Alsharkawi and Rossiter (2017b) the following question was posed: *How many segments are actually needed to adequately model the resonance characteristics of the plant?*

With the aim of finding an answer to the question, a number of nonlinear simulation models of the ACUREX plant have been constructed for a different number of segments followed by a thorough open-loop and closed-loop analysis. The analysis has led to the following interesting finding. Constructing a nonlinear simulation model using a large number of segments captures the dynamics of the plant at high frequencies, while constructing a nonlinear simulation model using a small number of segments captures the dynamics of the plant at low frequencies.

Obviously this is a dilemma that calls for something beyond the traditional time-based measurements to validate a nonlinear simulation model. The dilemma has been resolved by relating to the frequency response of the ACUREX plant and it has been found that a nonlinear simulation model when 7 segments are considered gives a reasonable approximation to the resonance characteristics of the plant.

In summary, the main contributions in Alsharkawi and Rossiter (2017b) can be summarised as follows.

- Establishing a relationship between the resonance phenomena of the ACUREX

plant and the number of segments needed to construct a nonlinear simulation and prediction models of the plant.

- Showing that inspecting the performance of a constructed model of the plant traditionally in the time-domain and an in open-loop manner gives little information about the resonance phenomena of the plant.
- Showing that as the number of segments is increased, the resonance phenomena captured by a constructed model become more pronounced. This is apparent in Fig. 3.2 where local models 1, 2, 3, 4, and 5 are LTI state space models around an operating point and correspond to nonlinear simulation models constructed with 15, 13, 10, 7, and 4 segments respectively.

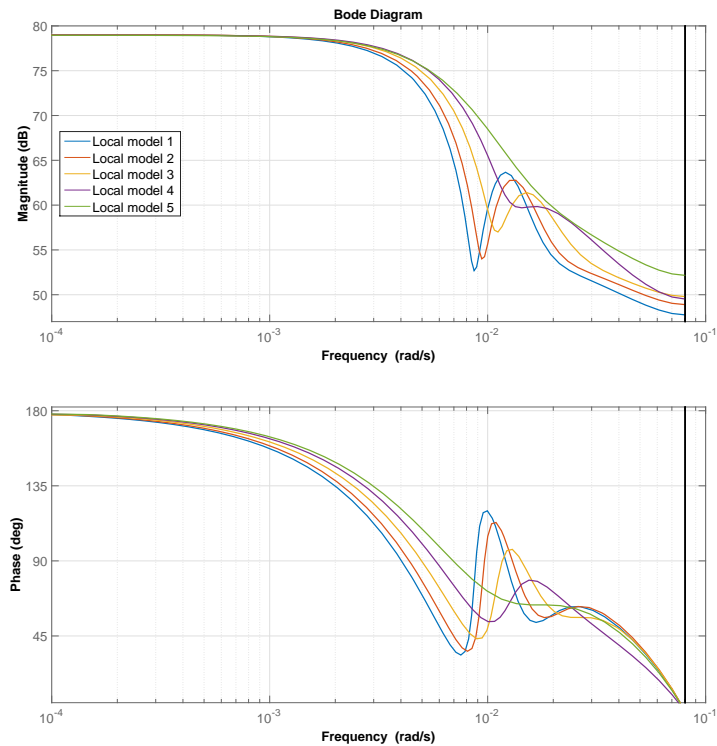


Figure 3.2: Frequency responses of an estimated local models.

- Showing that inspecting the frequency response of a constructed model around

a number of operating points with respect to the frequency response of the plant can be a helpful practice in dividing the receiver tube into a reasonable number of segments.

### **3.4 Gain Scheduling Design**

During the normal operation of the plant, changes in solar radiation and the field inlet temperature lead to substantial changes in the volumetric flow rate of the HTF which implies significant variations in the dynamic characteristics of the plant (e.g. response rate and dead-time) (Camacho et al., 2012). Hence, obtaining an adequate control performance over a wide range of operation is a challenging problem and calls for advanced control approaches. One approach to this highly nonlinear control problem is a gain scheduling design.

Gain scheduling is one of the most accepted nonlinear control design approaches (Leith and Leithead, 2000) which has found applications in many areas, e.g. position control (Mademlis and Kioskeridis, 2010), voltage control (Kakigano et al., 2013) and wind turbine (Bagherieh and Nagamune, 2015) to name just a few. It is usually seen as a way of thinking rather than a fixed design process and well-known for applying powerful linear design tools to challenging nonlinear problems (Rugh and Shamma, 2000). Moreover, implementation of MPC within a gain scheduling framework overcomes the major computational drawbacks of using a direct nonlinear MPC which arise due to the non-convexity of the associated nonlinear optimization problem (Chisci et al., 2003).

#### *3.4.1 An overview on the literature*

In an attempt to tackle the challenging nonlinear control problem at the ACUREX plant, different variants of gain scheduling have been designed (Rato et al., 1997; Pickhardt, 1998; Henriques et al., 1999, 2002; Gil et al., 2002). However, while these variants have appreciated the nonlinearity of the ACUREX plant, they have failed to appreciate its resonance phenomena.

On the other hand, in an attempt to address the nonlinear control problem at the ACUREX plant while explicitly counteracting its resonance phenomena, a variant of gain scheduling has been proposed in Meaburn and Hughes (1994). The control design is based upon a simplified transfer function of the plant that takes the form:

$$G(s) = P(s) \underbrace{(1 - e^{-a(s)L/v})}_{R(s)}, \quad (3.1)$$

where  $P(s)$  is a low order transfer function,  $a(s)$  is a complex function of  $s$ ,  $L$  is the length of the receiver tube,  $v$  is the velocity of the HTF and  $R(s)$  is the portion of  $G(s)$  that represents the resonance characteristics.

Hence, the idea of the control strategy is to design a precompensator  $[R(s)]^{-1}$  to counteract the resonance characteristics at low frequency and handle the plant nonlinearities based solely upon  $P(s)$  by typical gain scheduling with a lookup table and a form of interpolation to obtain a controller parameter. However, due to the complex nature of  $a(s)$ , a direct use of  $R(s)$  was not possible and a simplified alternative  $R^*(s)$  had to be found.

Yet, when  $R^*(s)$  was found and transformed into a discrete Z-transform  $R^*(z)$ , for discrete control compensation purposes, the resulting coefficients of  $R^*(z)$  were overly complicated and moreover a function of two unknowns.

The two unknowns vary with the volumetric flow rate of the HTF and thus with the aim of determining a relationship that relates the coefficients of the precompensator  $[R^*(z)]^{-1}$  to the steady state of the volumetric flow rate, a nonlinear simulation model of the plant had to be excited by a set of sinusoidal signals.

While simulation studies have shown fast and well damped temperature responses, it is fairly obvious that the control design is somewhat ad hoc and far from being practical.

It has been argued in Camacho et al. (1997) that the resonance characteristics of the ACUREX plant can be adequately captured by a nonlinear model of the plant or a family of sufficiently high order linear models around a number of operating points. Hence, convenient and practical gain scheduling strategies based upon a

family of estimated high order ARX models have been proposed in Camacho et al. (1997); Johansen et al. (2000). In Camacho et al. (1997) and after perturbing the ACUREX plant with a Pseudo-Random Binary Sequence (PRBS) signal, obtained input-output data has been used to construct an ARX model of the form:

$$a(z)y_k = b(z)u_k, \quad (3.2)$$

where  $a(z) = 1 + a_1z^{-1} + \dots + a_nz^{-n}$  and  $b(z) = b_0z^{-1} + \dots + b_mz^{-m}$ . Then, using a nonlinear simulation model of the plant, input-output data has been obtained after perturbations with PRBS signals around a number of operating points. Based on the obtained input-output data and a least squares estimation algorithm, local high order ARX models have been estimated using the model structure in (3.2).

At each operating point, local controller parameters have been obtained from a corresponding local ARX model. However, to ensure a smooth transition as the plant dynamics change with time or operating conditions, controller parameters have been adjusted using a linear interpolation in combination with a first order filter.

Using a fairly similar approach, in Johansen et al. (2000) the ACUREX plant has been perturbed with a set of PRBS signals around a number of operating points and using the obtained input-output data, local ARX models of a structure similar to the one in (3.2) have been estimated.

Corresponding local linear controllers have been designed and based on the volumetric flow rate of the HTF and solar radiation, the normal operating range of the plant has been decomposed into a set of neighbouring regions. To ensure a smooth transition between adjacent regions, weighting functions have been designed and used in the interpolation.

### 3.4.2 Discussion

Simulation studies and practical implementations of the two gain scheduling variants (Camacho et al., 1997; Johansen et al., 2000) have shown a fair control performance, yet some comments are given next.

- One of the early steps towards an effective modelling of the resonant modes of the plant is a proper choice and design of an excitation signal. A PRBS is a deterministic binary signal with white noise like properties and ideally suited for linear identification.

However, the white noise like properties are only valid for full-length PRBS signals with a clock period approximately equal to the process sampling time (Zhu, 2001). While the frequency band has not been reported in Camacho et al. (1997), the process sampling time has not been considered in Johansen et al. (2000).

- Resonant modes are more pronounced at high flow rate and less pronounced at low flow rate. Hence, as the model order in Camacho et al. (1997); Johansen et al. (2000) was assumed to be fixed for all the estimated ARX models, one might expect that either the model order at high flow rate is not high enough to capture the resonance phenomena of the plant, or the model order at low flow rate is unnecessarily high.
- Local ARX models in Johansen et al. (2000) have been estimated using input-output data obtained from the ACUREX plant and hence an optimal model accuracy will never be achieved, simply, due to the slow dynamics of the plant and the fast changes in operating conditions (e.g. solar radiation). Indeed this was evident when the gains of the locally estimated ARX models had to be corrected around a nominal solar radiation value.

Moreover, one might also question the accuracy of the decomposition in Johansen et al. (2000), as it is based on the assumption that the locally estimated ARX models are exactly correct at the centre point of their corresponding regions. This in fact has been also questioned in Stirrup et al. (2001) after observing the poor control performance at low flow rate where nonlinearities are more pronounced.

- While plant safety constraints are not reported in Johansen et al. (2000), they were poorly investigated in Camacho et al. (1997), when the field outlet temperature was restricted to not exceed a desired reference under any circumstances; this resulted in a severe performance degradation in the presence of disturbances.

### 3.4.3 Main contributions

Aiming to improve on the gain scheduling variants in Camacho et al. (1997); Johansen et al. (2000), the first few steps towards a gain scheduling dual mode MPC have been carried out in Alsharkawi and Rossiter (2016a) and the main contributions can be summarised as follows.

- A proper design of a full-length PRBS signal that takes into account the prior knowledge of the plant (process time constant). This is shown in Fig. 3.3 along with a corresponding output.
- Assuming steady state operating conditions and using the constructed nonlinear simulation model of the plant discussed in Chapter 2, an LTI state space model has been estimated locally around a nominal operating point directly from the input-output data shown in Fig. 3.3 using the noniterative subspace method N4SID (Van Overschee and De Moor, 1996). Moreover, the estimated model takes into account the frequency response of the plant.
- Based on the locally estimated LTI state space model, a local linear dual mode MPC controller that takes systematic account of the plant safety constraints has been formulated and its efficacy in set point tracking and disturbance rejection around an operating point has been clearly shown in a nonlinear simulation environment.

It is worth noting that an alternative approach of obtaining locally a LTI state space model would be by linearising the nonlinear simulation model in (2.2) around a

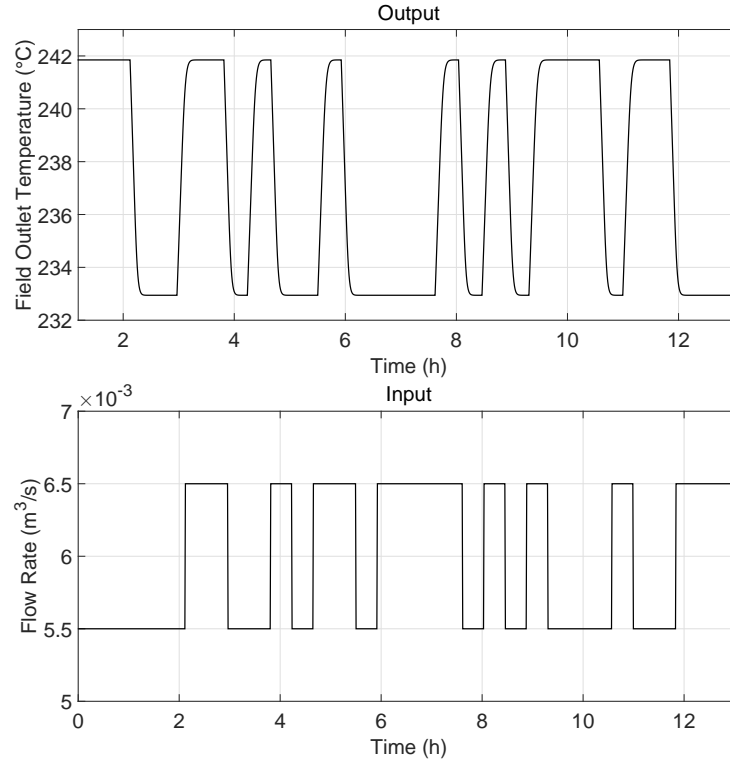


Figure 3.3: Input-output data.

nominal operating point. However, while the resulting linearised state space model might have the potential of providing physical insight into the process behaviour (Seborg et al., 2010), inevitably the model order will be significantly high. Hence, high computational burden.

A prime example of this is the  $30^{\text{th}}$ -order linearised state space model in Gallego et al. (2013). Meanwhile, the locally estimated LTI state space model here, has the key novelty of being able to capture the resonance characteristics of the plant with the minimal number of states (4 states) and hence, simple analysis and control design.

The local linear dual mode MPC controller in Alsharkawi and Rossiter (2016a) has been designed at medium flow rate around  $0.006 \text{ m}^3/\text{s}$  and it has been noticed that, when the local controller is performing at low and high flow rate, its robustness is affected by the new operating conditions which is consistent with Camacho et al.

(1997); Johansen et al. (2000). Hence, in Alsharkawi and Rossiter (2016b) a family of local LTI state space models have been estimated around a number of operating points and a corresponding local linear dual mode MPC controllers has been designed within a gain scheduling framework. The main contributions in Alsharkawi and Rossiter (2016b) are discussed as follows.

- Following the same PRBS design in Alsharkawi and Rossiter (2016a) as well as the estimation process of the local LTI state space model, a family of local LTI state space models have been estimated around a number of operating points. With the aim of adequately capturing the resonance characteristics of the plant while at the same time not using a model order higher than necessary, model orders of the locally estimated state space models have been selected after a careful inspection of a Hankel singular value plot along with a best fit criterion. As expected and in contrast to Camacho et al. (1997); Johansen et al. (2000), this has resulted in a slight variation in the selected model orders. For example, at low flow rate around  $0.004 \text{ m}^3/\text{s}$  the estimated model is of  $4^{\text{th}}$ -order whereas at high flow rate around  $0.01 \text{ m}^3/\text{s}$  the estimated model is of  $5^{\text{th}}$ -order.

Moreover, when model orders of the locally estimated state space models have been compared with the model orders of the ARX models in Camacho et al. (1997); Johansen et al. (2000), a significant model order reduction has been noticed. Yet, for a fair comparison and using the same input-output data sets that have been used for estimating the family of state space models, a family of ARX models of a structure similar to the one in (3.2) have been estimated.

The structure minimises Akaike's Information Criterion (AIC) and when model orders have been compared with the model orders of the estimated state space models it has been noticed that model orders of the estimated ARX models are significantly higher and yet without having any serious impact on the prediction accuracy. For example, at medium flow rate around  $0.006 \text{ m}^3/\text{s}$ , a prediction accuracy of 97.16 % has been achieved by a  $4^{\text{th}}$ -order state space

model, whereas the exact same prediction accuracy has been achieved by an 11<sup>th</sup>-order ARX model.

By inspecting the pole-zero plots of some of the ARX models in Camacho et al. (1997); Johansen et al. (2000) one might explain the unnecessarily high model orders by the existence of some pole-zero pairs which are likely to cancel each other out, and hence may not be required to capture the essential dynamics of the plant.

In summary, the locally estimated LTI state space models are adequate to capture the resonance characteristics of the plant with the minimal number of states and hence, simple analysis and control design. Frequency responses of the locally estimated LTI state space models are shown in Fig. 3.4 and one can clearly identify the resonant modes of the plant, especially at high flow rate, and observe the dependence of their frequencies on the flow rate of the HTF. Local models 1, 2, 3, and 4 refer to nominal operating points around 0.004, 0.006, 0.008 and 0.010 m<sup>3</sup>/s respectively.

- Having a scheduling variable to switch among the locally designed linear dual mode MPC controllers as the plant dynamics change with time or operating conditions is an intrinsic part of the gain scheduling control strategy. Hence, as the plant dynamics are mainly characterised by the volumetric flow rate of the HTF (Camacho et al., 2012), a scheduling variable has been derived from a nonlinear lumped parameter model of the ACUREX plant.

The scheduling variable is an external variable that gives an approximate representation of the volumetric flow rate of the HTF. It takes into account variations in solar radiation, the field inlet temperature and the desired reference temperature. This is shown in Fig. 3.5 where  $Q$  is the scheduling variable and  $T_{f,ref}$  is the desired reference temperature.

- After a thorough simulation analysis, the normal operating range of the plant

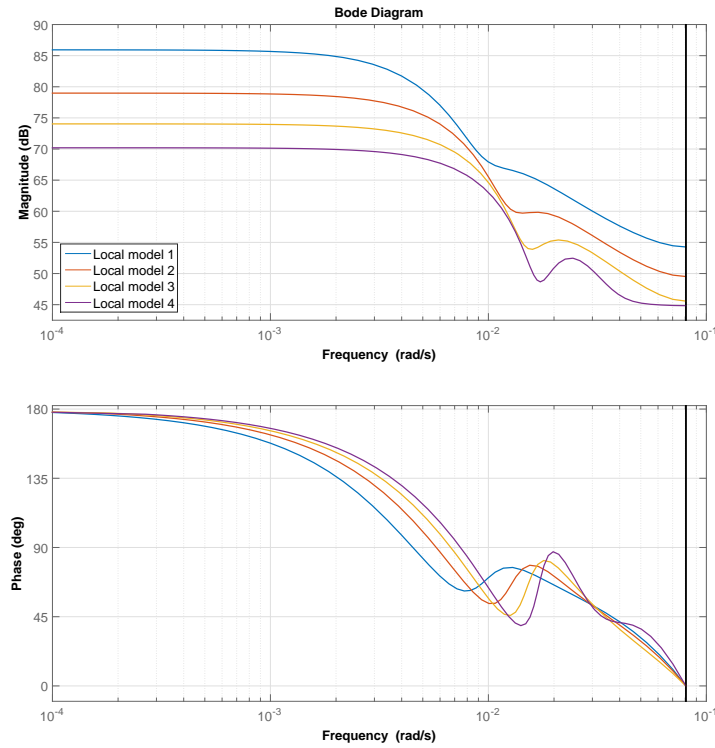


Figure 3.4: Bode plot of the local LTI state space models.

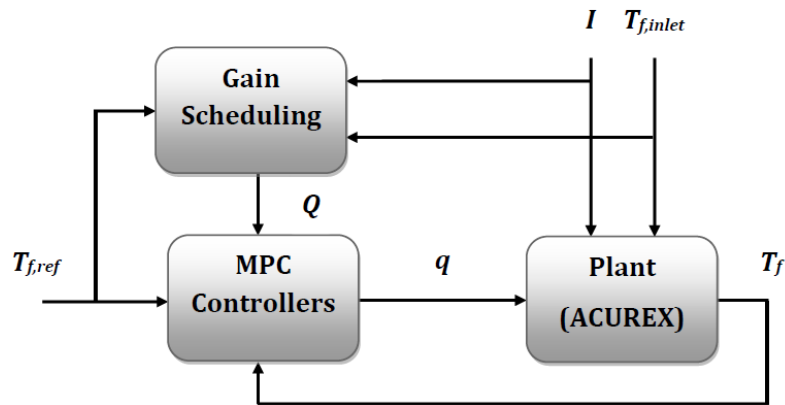


Figure 3.5: Gain scheduling control strategy.

has been decomposed into a set of neighbouring regions. A threshold between any two adjacent regions has an uncertainty factor of less than  $0.00025 \text{ m}^3/\text{s}$ .

- Formulating a gain scheduling dual mode MPC (GSMPC). The efficacy of the GSMPC in set point tracking and disturbance rejection, while satisfying the plant safety constraints, has been clearly shown over a wide range of operation in a nonlinear simulation environment.

It has been also shown that the GSMPC outperforms a single local dual mode MPC controller over a wide range of operation. This is illustrated in Fig. 3.6 where the local controller corresponds to medium flow rate around  $0.006 \text{ m}^3/\text{s}$ .

One can clearly see that when the local controller is performing at low and high flow rate its robustness is affected by the new operating conditions. On the other hand, the GSMPC is showing an excellent control performance over the wide range of operation with fast transients and no overshoot while satisfying the flow rate constraints.

### **3.5 Feedforward Design**

It has already been established in Chapter 2 that the control problem at the ACUREX plant is to maintain the field outlet temperature at a desired level despite any changes, mainly in solar radiation and the field inlet temperature.

Solar radiation and the field inlet temperature act as measured disturbances to the plant and thus, taking a corrective action before they disturb the process, through an effective feedforward design, can significantly improve the overall control performance.

The feedforward design is of a particular importance to the ACUREX plant due to the process large time constant (around 6 min) and the relatively large and frequent changes in solar radiation and the field inlet temperature, i.e. the process may operate constantly in a transient state and never reach a desired steady state.

In Alsharkawi and Rossiter (2017c) the main feedforward approaches that have been proposed over the years to mitigate the impact of the measured disturbances of the ACUREX plant have been discussed and it can be summarised that the vast

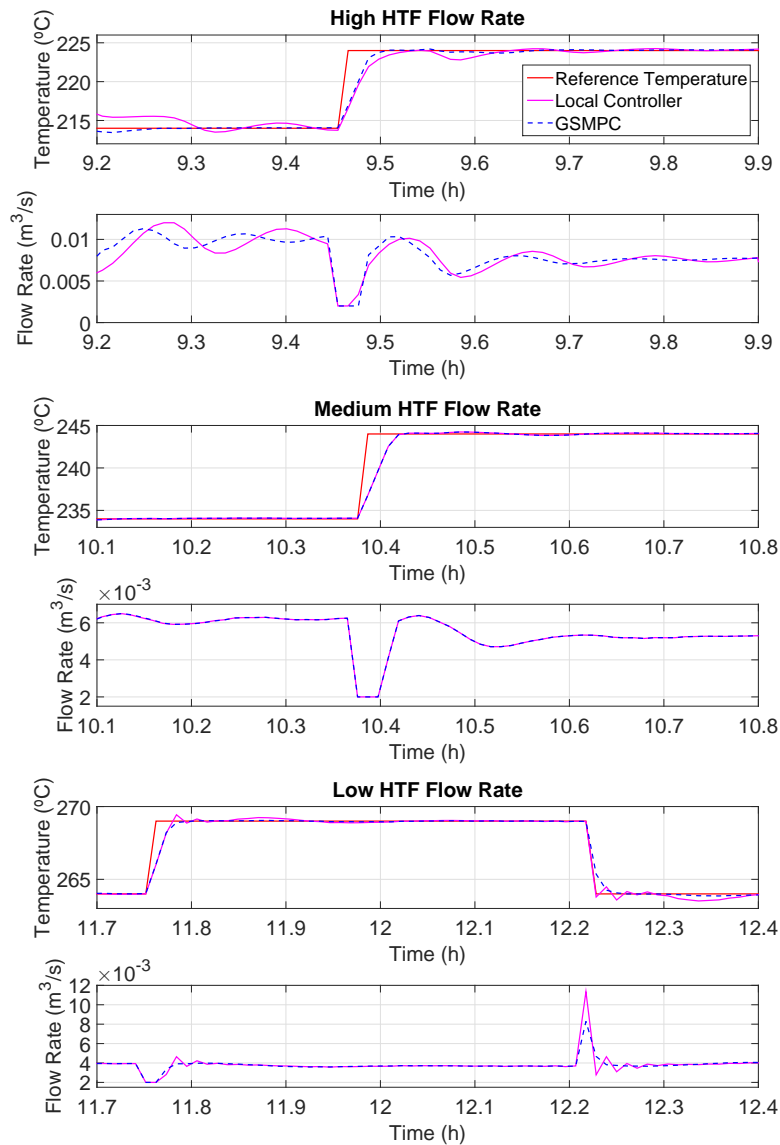


Figure 3.6: First scenario: Control performance on a clear day.

majority of these proposed approaches use, in one form or another, simple classical series or parallel feedforward configuration.

As has been discussed in Chapter 2, the ACUREX plant possesses resonant modes that lie well within the desired control bandwidth and the resonance phenomena have a significant impact on the control performance and hence modelling the resonant modes sufficiently accurately is crucial to ensure high control performance with ad-

equate robustness. More importantly however, in Meaburn and Hughes (1993) and based on experimental data from the ACUREX plant, it has been noticed that the dynamics relating the field outlet temperature to changes in solar radiation are similar to the dynamics relating the field outlet temperature to changes in the volumetric flow rate of the HTF, i.e. fast and abrupt changes in solar radiation excite the resonance characteristics of the plant. Yet, none of the feedforward approaches discussed in Alsharkawi and Rossiter (2017c) have explicitly appreciated this fact and utilised its potential for control implications.

Taking into account the resonance characteristics of the ACUREX plant, the GSMPC in Alsharkawi and Rossiter (2016b) has been improved in Alsharkawi and Rossiter (2017c) by incorporating a systematic feedforward to compensate for the measured disturbances, solar radiation and the field inlet temperature. The main contributions in Alsharkawi and Rossiter (2017c) can be summarised as follows.

- A full-length PRBS signals of solar radiation and the field inlet temperature have been properly designed by taking into account the prior knowledge of the plant and a careful selection of the amplitude range.
- Following the estimation process in Alsharkawi and Rossiter (2016b), compact LTI state space models of solar radiation and the field inlet temperature have been estimated around a number of operating points.
- Showing that the estimated state space models of solar radiation indeed capture the resonance phenomena of the plant which confirms the experimental findings in Meaburn and Hughes (1993) and moreover, showing that also fast and abrupt changes in the field inlet temperature excite the resonance dynamics of the plant, especially at low flow rate. The dynamics of solar radiation and the field inlet temperature are illustrated in Fig. 3.7 and Fig. 3.8 respectively. Models 1, 2, 3, and 4 refer to nominal operating points around 0.004, 0.006, 0.008 and 0.010 m<sup>3</sup>/s respectively.

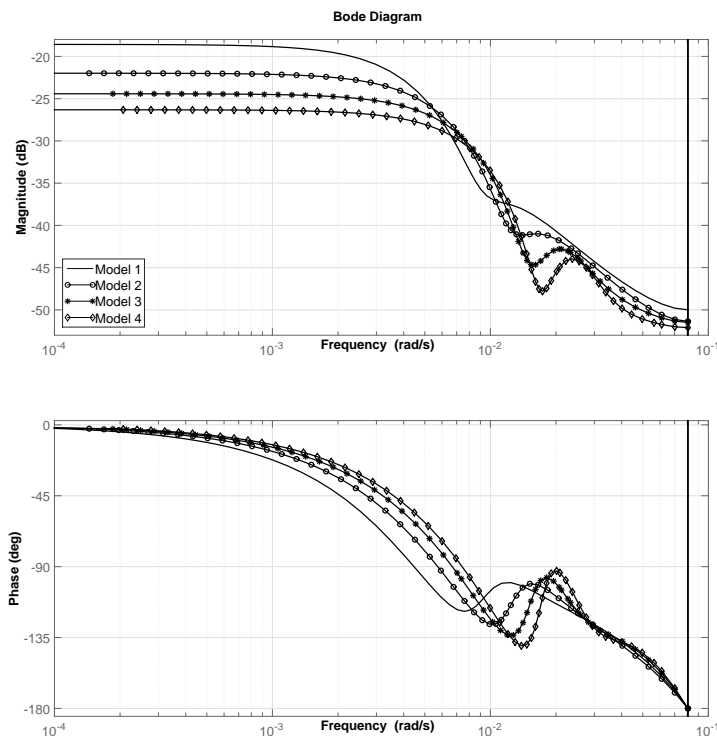


Figure 3.7: Bode plot: Estimated models of solar radiation.

- Showing that the dynamics of the measured disturbances have been underestimated in the literature and simple dynamic models of solar radiation and the field inlet temperature derived from first principles and based on steady state condition are not adequate enough to capture the resonance phenomena of the plant. Frequency responses of the field outlet temperature for changes in solar radiation and the field inlet temperature around an operating point are illustrated in Fig. 3.9. Model  $\gamma$  in Fig. 3.9 is derived from first principles and based on steady state condition and Model  $\omega$  is an augmented model of solar radiation and the field inlet temperature obtained through system identification. The simplistic dynamics of Model  $\gamma$  are quite apparent and hence an undesirable impact on the control performance is rather expected.

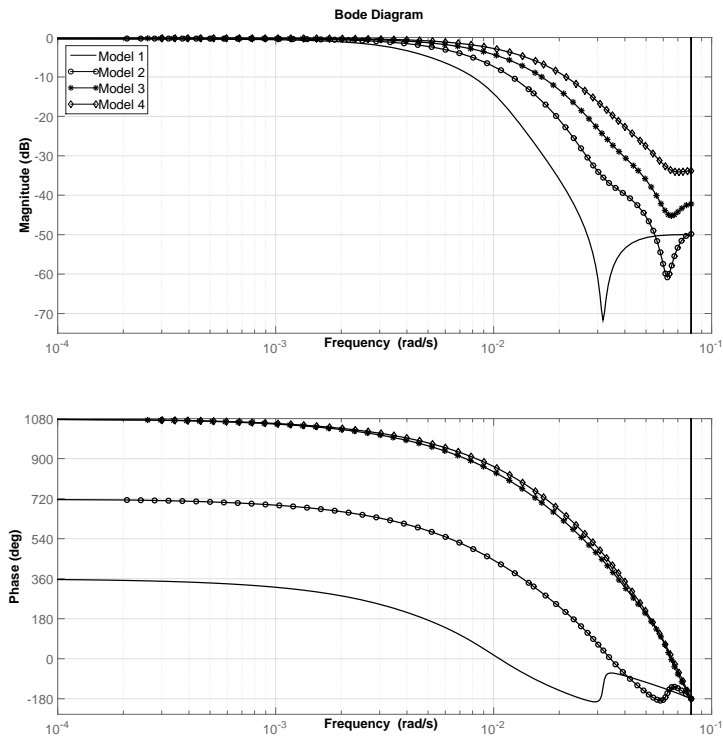


Figure 3.8: Bode plot: Estimated models of the field inlet temperature.

- When compared with local models that take explicit account of the resonance phenomena of the plant, it has been shown that incorporating simple dynamic model of solar radiation and the field inlet temperature, which is derived from first principles and based on steady state condition, results in a poor control performance during the transient phase, set point tracking and disturbance rejection.
- Investigating the impact of not considering the dynamics of the field inlet temperature in the control design. It has been found that the transient phase is affected the most with a large overshoot and quite oscillatory control signal.
- Investigating locally the impact of considering the expected future behaviour

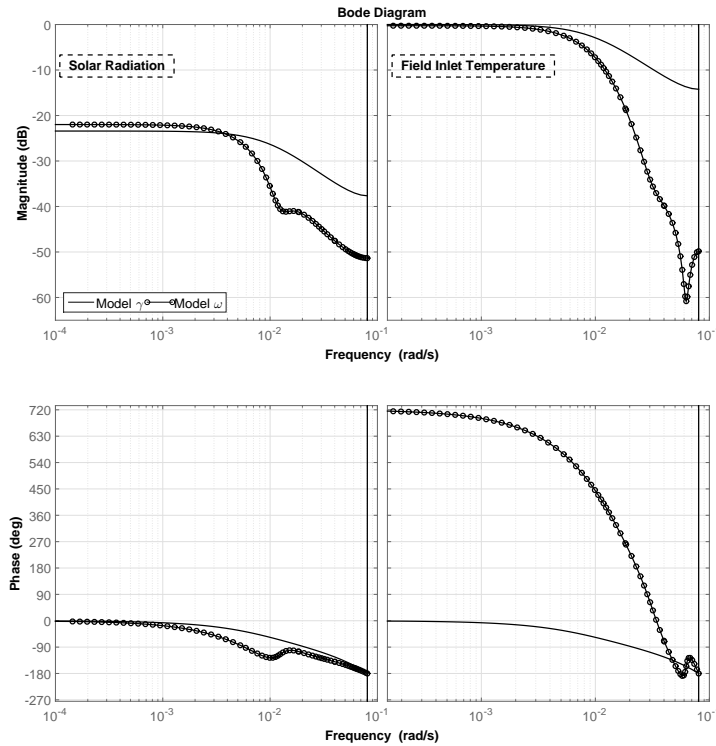


Figure 3.9: Frequency responses of the field outlet temperature for changes in solar radiation and the field inlet temperature obtained through two different approaches around a given operating point.

of solar radiation along a given prediction horizon. This is an area that has received little or no attention in the literature. It has been found that this has the potential of improving the control performance, especially in the presence of strong and large changes in solar radiation.

- Improving the GSMPC in Alsharkawi and Rossiter (2016b) by including the effects of solar radiation and the field inlet temperature in the predictions of future outputs (systematic feedforward design). This has resulted in formulating a gain scheduling feedforward dual mode MPC (GSFFMPC). The efficacy of the GSFFMPC has been evaluated and it has been shown that incorporating sufficient dynamic models of solar radiation and the field inlet temperature,

that take explicit account of the resonance phenomena of the plant, can significantly improve the control performance during the transient phase, set point tracking and disturbance rejection.

Fig. 3.10 illustrates a commonplace scenario at the ACUREX plant. The benefits of the GSFFMPC over the GSMPC are fairly obvious, especially during the transient phase and sudden drop in solar radiation.

### **3.6 Hierarchical Control**

The idea of hierarchical control involves all aspects of automation of the decision making process (measurement, control, optimisation and logistics) and is believed to be an effective way of responding to a dynamic and unpredictable marketplace conditions with minimal capital investment (Prett and Garcia, 1988).

More specifically, the general objective of an industrial process control is to maximise economical efficiency over a long time horizon and for large-scale processes this is not an easy task. Yet, the application of a hierarchical control structure has been proven to be an effective approach, where the original control task is decomposed into a sequence of simpler and hierarchical structured subtasks (Tan et al., 2005).

The idea of hierarchical control structure is well established in the literature (Findeisen et al., 1980) and has found applications in many fields, e.g. activated sludge processes (Piotrowski et al., 2008), integrated wastewater treatment systems (Brdys et al., 2008) and a two-step solar hydrogen production plant (Roca et al., 2013) to name just a few.

#### *3.6.1 An overview on the literature*

The application of hierarchical control to the solar thermal power plant ACUREX was first discussed in Berenguel et al. (2005) and later on a two-layer hierarchical control strategy was first implemented (Cirre et al., 2009). A few years later, this was followed by the design of a three-layer hierarchical control strategy (Camacho

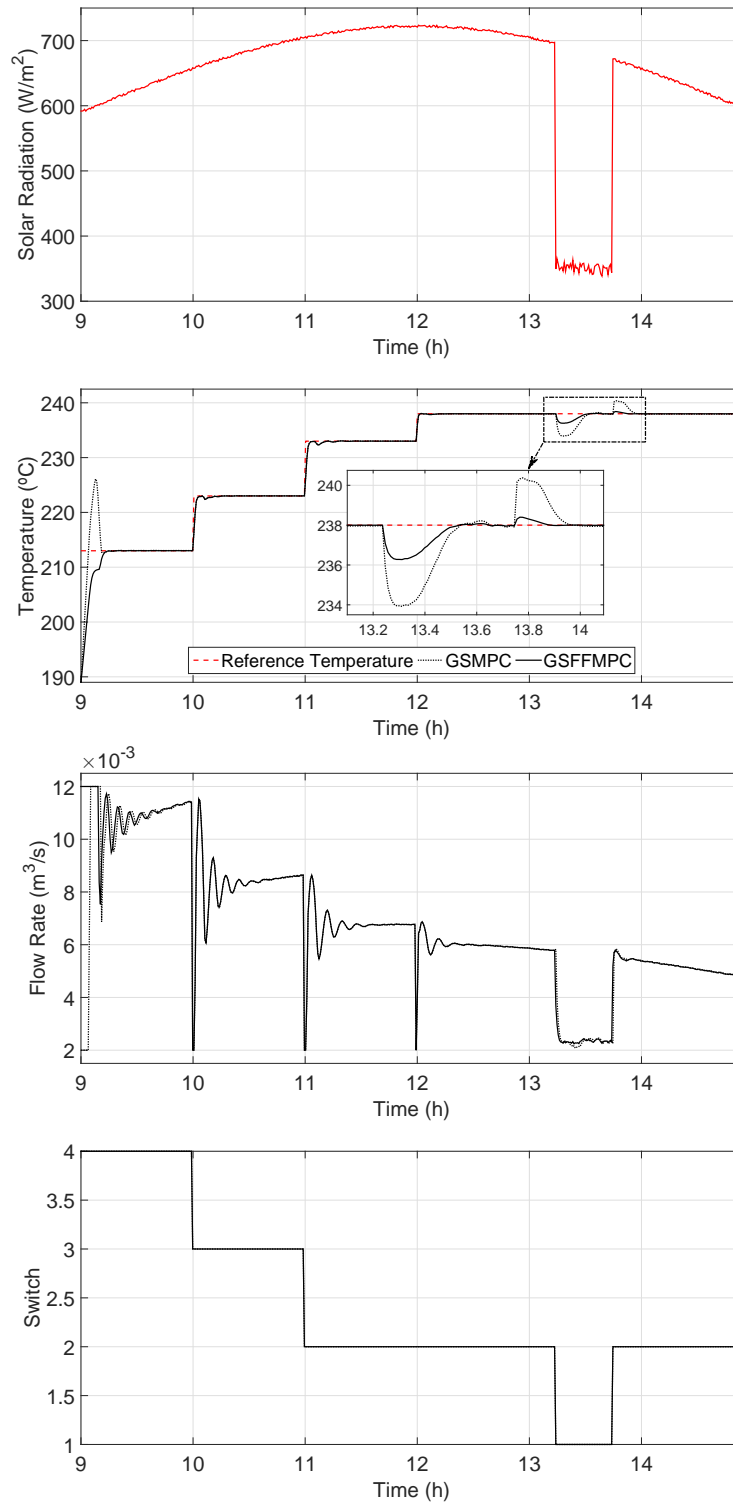


Figure 3.10: A performance comparison: GSMPC against GSFFMPC.

and Gallego, 2013). Apart from these control strategies (Cirre et al., 2009; Camacho and Gallego, 2013), this is an area that has received little attention in the literature.

The main argument in Cirre et al. (2009); Camacho and Gallego (2013) is that the ACUREX plant is constantly subject to changes in solar radiation and the field inlet temperature and hence the plant requires the full attention of an experienced plant operator, whose job is to set an adequate reachable reference temperature that takes into account the status of the measured disturbances and the plant safety constraints. Moreover, the narrow temperature operating range of the plant steam turbine has to be maintained. In parallel, the operator must choose between potentially ambitious and perhaps unreachable targets and safer targets. Ambitious targets can lead to actuator saturation and safer targets imply electricity production losses.

With the aim of resolving this dilemma, a fuzzy logic approach along with an optimisation-based approach performed in the steady state have been proposed in Cirre et al. (2009). The optimisation-based approach has been improved later on in Camacho and Gallego (2013) by taking into account the nonlinear dynamic behaviour of the plant. Yet, the fuzzy logic approach is rather ad hoc and requires years of experience in operating the plant and the optimisation-based approaches are overly complicated and, at some point, even unrealistic due to the non-convexity associated with the nonlinear optimisation problem and high computational burden. Hence, there has been a need for an alternative.

### *3.6.2 Proposal of a two-layer hierarchical control structure*

In Alsharkawi and Rossiter (2017a) a novel pragmatic approach has been proposed. Taking into account the status of the measured disturbances, an adequate reachable reference temperature is generated conceptually from an upper layer while satisfying the plant safety constraints. The approach of generating the reference temperature makes use of system identification and takes into account the frequency response of the plant. Due to the nature of the hierarchy, the GSMPC proposed in Alsharkawi and Rossiter (2016b) is adopted in a lower layer for set point tracking and coping

with the plant nonlinear dynamics. A schematic diagram of the two-layer hierarchical control structure is shown in Fig. 3.11.

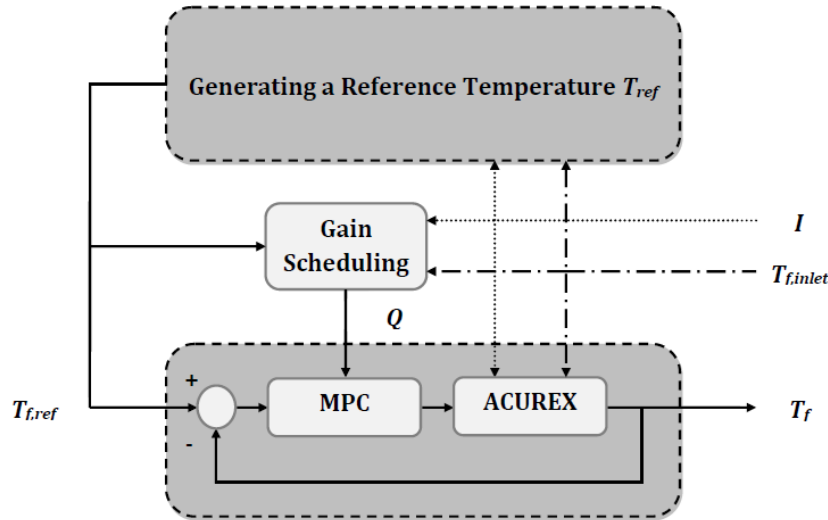


Figure 3.11: Two-layer hierarchical control structure.

It has been established in Alsharkawi and Rossiter (2017c) that modelling solar radiation and the field inlet temperature while taking into account the frequency response of the plant is essential to ensure high prediction accuracy. While this issue has been ignored in Cirre et al. (2009); Camacho and Gallego (2013), it has been given a special attention in Alsharkawi and Rossiter (2017a). Following the estimation process in Alsharkawi and Rossiter (2017c) compact LTI state space models of solar radiation and the field inlet temperature have been estimated around a number of operating points while taking into account the frequency response of the plant. The estimated models establish clear, direct and dynamic relationships with the field outlet temperature (reference temperature).

In particular, at each operating point, a complete one-step ahead prediction model predicts the *best* reference temperature given the measurements of solar radiation and the field inlet temperature. Due to the nonlinear dynamic behaviour of the plant, a mean value of the generated reference temperatures is considered. The

main contributions in Alsharkawi and Rossiter (2017a) are discussed next.

- The proposed two-layer hierarchical control structure operates the ACUREX plant automatically without an intervention from the plant operator and without adding cost.
- The proposed approach is quite simple and intuitive. In contrast to the fuzzy logic approach in Cirre et al. (2009), it requires little knowledge of the plant (process time constant) and in contrast to the optimisation-based approaches in Cirre et al. (2009); Camacho and Gallego (2013), it drives the plant near optimal operating conditions rather than solving a direct nonlinear optimisation problem.
- The mean reference temperature ensures that the reference temperature is within a reachable limit at all times and it corresponds to a medium flow rate around  $0.006 \text{ m}^3/\text{s}$ . Hence, the risk of saturation is reduced.
- The reference temperature serves indirectly as a feedforward for the lower layer, thus enables better feedback control action.
- The generated reference temperature is adequate and smoothly adapted to changes in solar radiation and the field inlet temperature while at the same time satisfying the plant safety constraints. While constraints imposed on the volumetric flow rate of the HTF are explicitly being accounted for by the GSMPC at the lower layer, the generated reference temperature at the upper layer ensures elegantly that the difference between the inlet and outlet temperature is not exceeded.
- Under the normal operating conditions of the plant, the generated reference temperature satisfies the narrow operating range of the plant steam turbine.

- The control design at the lower layer goes hand in hand with the reference temperature design at the upper layer. In essence, as the generated reference temperature at the upper layer is being smoothly adapted to changes in solar radiation and the field inlet temperature, the scheduling variable of the GSMPC at the lower layer is simultaneously being adapted to changes in solar radiation and the field inlet temperature, as well as the generated reference temperature.
- Using some measured data from the ACUREX plant, the efficacy of the proposed two-layer hierarchical control structure in coping with typical changes in solar radiation and the field inlet temperature has been evaluated. Fig. 3.12 and Fig. 3.13 illustrate the results and one can easily notice how the generated reference temperature is being elegantly adapted to changes in solar radiation and the field inlet temperature while satisfying the plant safety constraints.

### *3.6.3 Proposal of an improved two-layer hierarchical control structure*

It may have been noticed that the lower layer of the proposed two-layer hierarchical control structure has adopted the GSMPC and not the improved GSFFMPC, even though the feedforward capability of the latter has been clearly illustrated in Alsharkawi and Rossiter (2017c). The reason for this is simply, as it has already been mentioned, the generated reference temperature at the upper layer serves indirectly as a feedforward for the lower layer and hence to investigate the sole impact of this on the overall control performance, the GSMPC had to be adopted.

However, after the benefits of the two-layer hierarchical control structure have been clearly illustrated in Alsharkawi and Rossiter (2017a), the GSMPC at the lower layer has been replaced in Alsharkawi and Rossiter (2017d) by the GSFFMPC with the aim of improving the overall control performance. Moreover, it has been shown in Alsharkawi and Rossiter (2017c) that considering locally the expected future behaviour of solar radiation along a given prediction horizon has some potential benefits

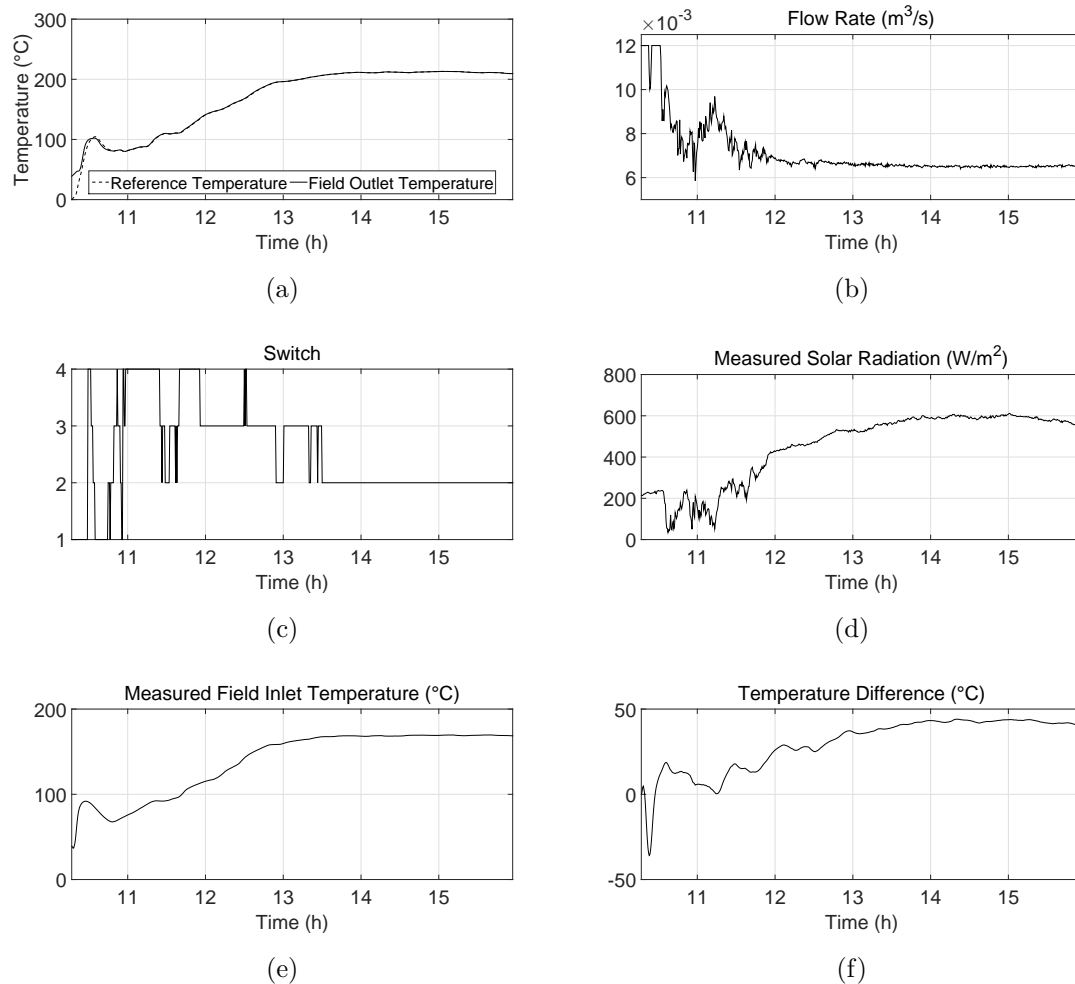


Figure 3.12: Generation of a reference temperature using measurements from the ACUREX plant collected on 18 July 2003.

and hence, the concept has been extended in Alsharkawi and Rossiter (2017d) and a variant of the GSFFMPC has been designed. This variant of the GSFFMPC incorporates systematically, along a given prediction horizon, the expected future behaviour of solar radiation as well as the field inlet temperature. A schematic diagram of the improved two-layer hierarchical control structure is shown in Fig. 3.14.

As it has been mentioned earlier, apart from the strategies in Cirre et al. (2009);

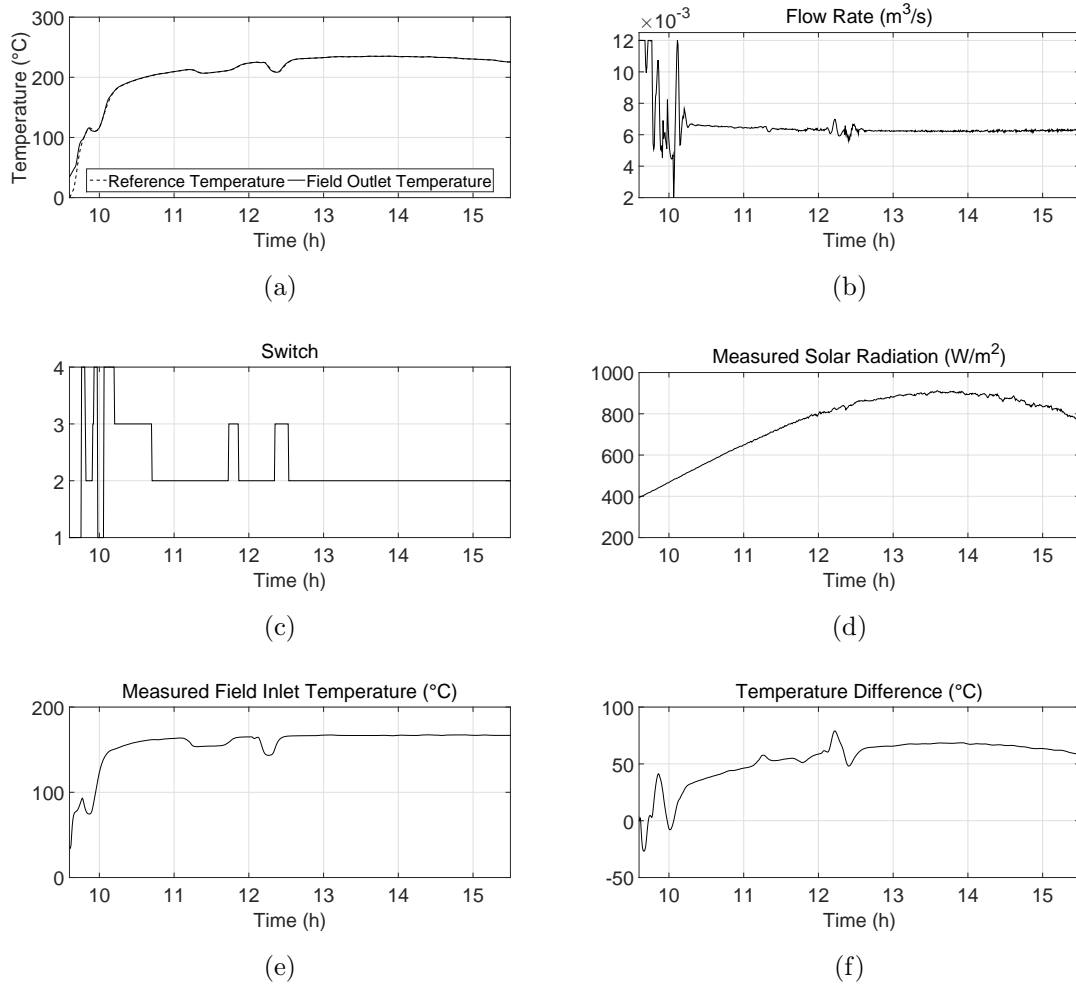


Figure 3.13: Generation of a reference temperature using measurements from the ACUREX plant collected on 28 July 2003.

Camacho and Gallego (2013), hierarchical control for the ACUREX plant is an area that has received little attention. While no feedforward to account for the measured disturbances has been reported in Camacho and Gallego (2013) and a rather simple classical parallel feedforward based on steady state energy balance has been designed for the lower layer in Cirre et al. (2009), the GSFFMPC and its variant incorporate feedforward systematically by including the dynamic effects of solar radiation and the

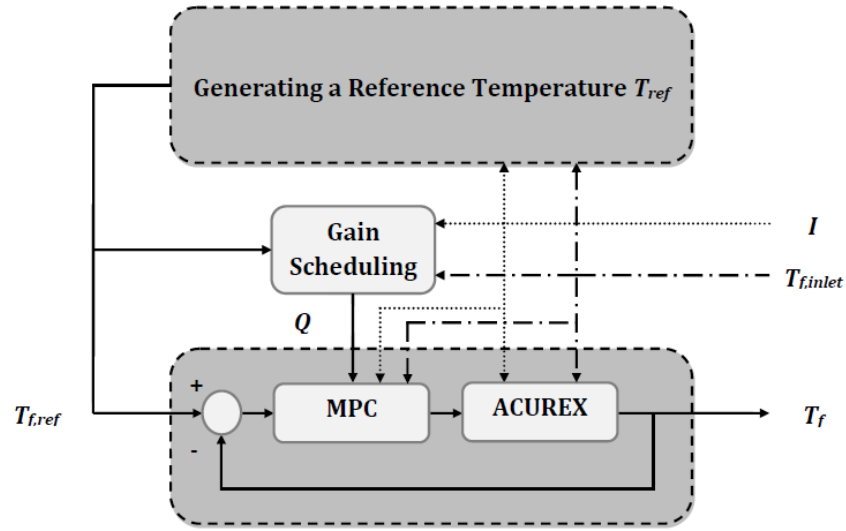


Figure 3.14: An improved two-layer hierarchical control structure.

field inlet temperature into the predictions of future outputs. The main contributions in Alsharkawi and Rossiter (2017d) are summarised next.

- Using some measured data from the ACUREX plant and a generated reference temperature, the control performance of the GSFFMPC has been compared with the control performance of the GSMPC and it has been found that the GSFFMPC has the potential of significantly improving the actuator dynamics. This is illustrated in Fig. 3.15.
- In the presence of strong and large changes in solar radiation, it has been found that a variant of the GSFFMPC, that takes explicit account of the expected future behaviour of solar radiation and the field inlet temperature along a given prediction horizon, has the potential of slightly improving the set point tracking performance and reducing the risk of actuator saturation. For a particular simulation scenario, the set point tracking performance and cost of regulation have been improved by 9.2% and 2.6% respectively.

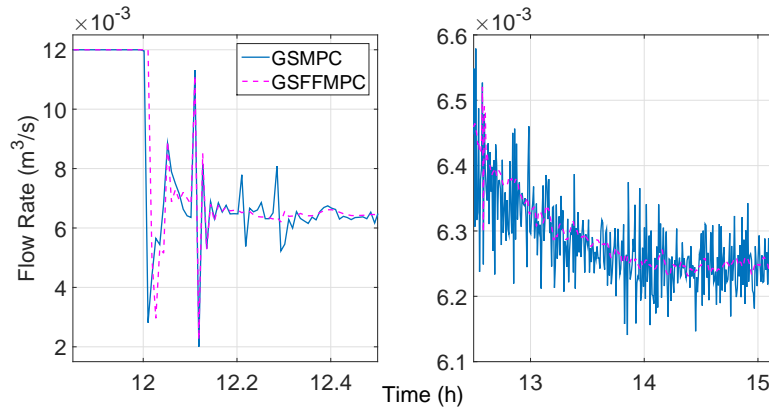


Figure 3.15: Control signals of the GSMPC and the GSFFMPC given some measured data from the ACUREX plant and a generated reference temperature.

### 3.7 Summary

This chapter has discussed original contributions to the automatic control of a parabolic trough technology-based solar thermal power plant. The contributions have been summarised under five main topics: unifying review, simulation model, gain scheduling design, feedforward design and hierarchical control.

The seven papers discussed in this chapter are listed in Table 3.1. The main topic of each paper is highlighted with an overview of general contributions. The appearance of each paper in the next part of the thesis is also highlighted.

Table 3.1: Summary of Contributions

Paper: Topic	Overview	Appendix
(Alsharkawi and Rossiter, 2015): unifying review	A review on concentrating solar technologies with an emphasis placed on parabolic trough technology and its utilisation in the ACUREX plant	A
(Alsharkawi and Rossiter, 2017b): simulation model	Construction and validation of a non-linear simulation model taking into account the resonance phenomena of the ACUREX plant	B
(Alsharkawi and Rossiter, 2016a): gain scheduling design	A proper design of a full-length PRBS signal, estimating a local LTI state space model around an operating point and formulating a corresponding local linear dual mode MPC controller	C
(Alsharkawi and Rossiter, 2016b): gain scheduling design	Local LTI state space models have been estimated over a wide range of operation and corresponding local dual mode MPC controllers have been formulated within a gain scheduling framework	D

- 
- (Alsharkawi and Rossiter, 2017c): feedforward design
- Local LTI state space models of solar radiation and the field inlet temperature have been estimated over a wide range of operation and a gain scheduling predictive control strategy that incorporates a systematic feedforward has been formulated
- E
- (Alsharkawi and Rossiter, 2017a): hierarchical control
- A reference temperature has been generated automatically from an upper layer in a two-layer hierarchical control structure. The generated reference temperature is adequate reachable and smoothly adapted to changes in solar radiation and the field inlet temperature while satisfying the plant safety constraints
- F
- (Alsharkawi and Rossiter, 2017d): hierarchical control
- Improving the actuator dynamics by utilising available information on solar radiation and the field inlet temperature systematically in the lower layer of a two-layer hierarchical control structure
- G
-

## Chapter 4

# CONCLUSIONS AND FUTURE PERSPECTIVES

This final chapter is divided into two sections, Section 4.1 and 4.2. Section 4.1 gives final conclusions and Section 4.2 presents avenues for future research.

### **4.1 *Final Conclusions***

The main aim of this thesis was to design and evaluate a pragmatic control strategy that ensures an automatic operation of a parabolic trough technology-based solar thermal power plant with minimal intervention from the plant operator. The control strategy was required to be feasible over a wide range of operation and drive the plant near optimal operating conditions.

Moreover, the control strategy was required to handle the nonlinear characteristics of the plant, capture the plant resonance characteristics, take a systematic account of the plant safety constraints, make an effective use of available information on the measured disturbances and be evaluated in a nonlinear simulation environment that approximates the dynamic behaviour of the plant.

The research facility ACUREX was used as a test bed for the control strategy. ACUREX is a typical parabolic trough technology-based solar thermal power plant that has helped researchers across academia and industry to gain an insight into its main dynamics and inherent characteristics.

The main aims of this thesis and corresponding objectives have been achieved as follows. Taking into account the resonance phenomena of the plant and after a

thorough open-loop and closed-loop analysis, a nonlinear simulation model of the ACUREX plant has been constructed and validated in the time and frequency domain (Alsharkawi and Rossiter, 2017b).

Regarding the nonlinear characteristics of the plant, this has been handled in two stages. The first stage has been carried out in Alsharkawi and Rossiter (2016a) and it can be summarised by the following. An LTI state space model has been estimated locally around a nominal operating point, while taking into account the frequency response of the plant, and a corresponding local linear dual mode MPC controller has been designed. At this stage, it has been noticed that when the local controller is performing around a new operating point its robustness is affected by the new operating conditions and hence the second stage has been carried out in Alsharkawi and Rossiter (2016b).

In this second stage, a gain scheduling dual mode MPC (GSMPC) has been formulated. Local LTI state space models have been estimated around a number of operating points, while taking into account the frequency response of the plant, and corresponding local linear dual mode MPC controllers have been designed. The GSMPC ensures a feasible operation over a wide range of operation while taking a systematic account of the plant safety constraints.

Available information on solar radiation and the field inlet temperature on the other hand, has been used effectively in a systematic feedforward design and hierarchical control. In Alsharkawi and Rossiter (2017c), the GSMPC has been improved by incorporating a systematic feedforward to compensate for the measured disturbances, solar radiation and the field inlet temperature which has resulted in formulating the gain scheduling feedforward dual mode MPC (GSFFMPC).

Building on Alsharkawi and Rossiter (2016b), compact LTI state space models of solar radiation and the field inlet temperature have been estimated around a number of operating points and it has been shown that the estimated state space models of solar radiation indeed capture the resonance phenomena of the plant which confirms the experimental findings in Meaburn and Hughes (1993). Moreover, it has

been found that fast and abrupt changes in the field inlet temperature excite the resonance dynamics of the plant, especially at low flow rate.

The use of available information on solar radiation and the field inlet temperature in hierarchical control has been carried out in Alsharkawi and Rossiter (2017a,d). Given a set of complete one-step ahead prediction models that relate the field outlet temperature (reference temperature) to solar radiation and the field inlet temperature, a reference temperature is generated from an upper layer in a two-layer hierarchical control structure. The generated reference temperature ensures driving the plant near optimal operating conditions without any help from the plant operator and without adding cost.

In summary, after evaluating the two-layer hierarchical control strategy in Alsharkawi and Rossiter (2017d), with the GSFFMPC being deployed in the lower layer and using the nonlinear simulation model constructed in Alsharkawi and Rossiter (2017b), one can conclude that the control strategy has indeed all the required ingredients to ensure an automatic operation of the ACUREX plant with minimal intervention from the plant operator. Hence, the main aims of this thesis and corresponding objectives have been successfully achieved.

Nonetheless, it is fair to say that this thesis suffers from some limitations. For example, the nonlinear simulation model in Alsharkawi and Rossiter (2017b) has been constructed under the assumption that the dynamics of the ACUREX plant are mainly characterised by the distributed solar collector field and thus dynamics of other plant components such as the thermal storage tank and heat exchanger have not been considered.

As a final remark, although the modelling and control approaches discussed in this thesis have been tailored to the ACUREX plant, there is no apparent reason why these approaches cannot be used in other similar parabolic trough technology-based solar thermal power plants. In essence, once the main dynamics of a plant are clearly defined by a set of energy balance partial differential equations similar to the one in (2.1) and with little knowledge of the plant, the modelling and control

approaches discussed in this thesis can be easily used.

## 4.2 Recommendations for Future Research

Insights and recommendations for a future research are discussed as follows:

1. A variant of the GSFFMPC (Alsharkawi and Rossiter, 2017d) has incorporated systematically, along a given prediction horizon, the expected future behaviour of solar radiation and the field inlet temperature. Although simulation results have shown the potential of slightly improving set point tracking and cost of regulation, it is worth noting that the choice of the prediction horizon was not optimal and hence future research might consider investigating questions like: *How far ahead should one predict?* and accordingly *How significant can the improvements be?* Obviously, this has to be in accordance with the forecasting models available in the existing literature.

While in Chu and Coimbra (2017) it has been shown that accurate forecasting of solar radiation is achievable for up to 20 *min* horizon, forecasting the field inlet temperature is indeed an area that has not been looked at. Forecasting the field inlet temperature could be of a particular importance during the transient (start-up) phase of the plant where changes are mostly noticed.

2. Given the expected future behaviour of solar radiation and the field inlet temperature along a given prediction horizon and with slight modifications to the complete one-step ahead prediction model in Alsharkawi and Rossiter (2017a), one could in fact obtain an advance information on the reference temperature. Hence, it might be worth investigating how much advance information is useful. But first a variant of the GSFFMPC must be formulated. The variant should ensure effective embedding of the advance information. One could get some insights from the discussions in Dughman and Rossiter (2017).
3. Neither stability nor robustness of the gain scheduling design has been analysed

in this thesis. While it is well accepted in the literature (Shamma and Athans, 1990) that such properties are inferred from extensive simulations, developing some sound theoretical analysis in a future research might provide some insights for a better design.

4. Due to the process relatively slow sampling time, it might be worth formulating a nonlinear MPC using a nonlinear process model in the prediction. A comparison with the gain scheduling design might also be carried out in terms of convergence and computational time.
5. An improvement to the proposed two-layer hierarchical control structure might include; first, an efficient optimisation algorithm that minimises a prescribed cost function in the upper layer and second, a systematic account of the temperature difference.
6. It would be interesting in the future to see a practical implementation of the proposed two-layer hierarchical control structure. Moreover, for a particular scenario the performance of the control strategy could possibly be compared with that of the plant operator.

# BIBLIOGRAPHY

- Alsharkawi, A. and Rossiter, J. A. (2015). Distributed collector system: Modelling, control and optimal performance. In *Proceedings of the International Conference on Renewable Energy and Power Quality 2015, La Coruna, Spain*.
- Alsharkawi, A. and Rossiter, J. A. (2016a). Dual mode mpc for a concentrated solar thermal power plant. In *Proceedings of the 11th IFAC Symposium on Dynamics and Control of Process Systems, including Biosystems, Trondheim, Norway*, volume 49, pages 260–265. Elsevier.
- Alsharkawi, A. and Rossiter, J. A. (2016b). Gain scheduling dual mode mpc for a solar thermal power plant. In *Proceedings of the 10th IFAC Symposium on Nonlinear Control Systems, California, USA*, volume 49, pages 128–133. Elsevier.
- Alsharkawi, A. and Rossiter, J. A. (2017a). Hierarchical control strategy for a solar thermal power plant: A pragmatic approach. *Submitted to Journal of Process Control*.
- Alsharkawi, A. and Rossiter, J. A. (2017b). Modelling analysis of a solar thermal power plant. In *Proceedings of the 6th International Conference on Clean Electrical Power, Liguria, Italy*.
- Alsharkawi, A. and Rossiter, J. A. (2017c). Towards an improved gain scheduling predictive control strategy for a solar thermal power plant. *IET Control Theory & Applications*, DOI: 10.1049/iet-cta.2016.1319.
- Alsharkawi, A. and Rossiter, J. A. (2017d). Towards an improved hierarchical control strategy for a solar thermal power plant. *To be submitted*.

- Bagherieh, O. and Nagamune, R. (2015). Gain-scheduling control of a floating offshore wind turbine above rated wind speed. *Control Theory and Technology*, 13(2):160–172.
- Berenguel, M., Cirre, C. M., Klempous, R., Maciejewski, H., Nikodem, M., Nikodem, J., Rudas, I., and Valenzuela, L. (2005). Hierarchical control of a distributed solar collector field. In *Proceedings of the International Conference on Computer Aided Systems Theory*, volume 3643, pages 614–620. Springer.
- Bø, T. I. and Johansen, T. A. (2013). Scenario-based fault-tolerant model predictive control for diesel-electric marine power plant. In *Proceedings of the 2013 MTS/IEEE OCEANS-Bergen*, pages 1–5. IEEE.
- Bø, T. I. and Johansen, T. A. (2017). Dynamic safety constraints by scenario-based economic model predictive control of marine electric power plants. *IEEE Transactions on Transportation Electrification*, 3(1):13–21.
- Brdys, M., Grochowski, M., Gminski, T., Konarczak, K., and Drewa, M. (2008). Hierarchical predictive control of integrated wastewater treatment systems. *Control Engineering Practice*, 16(6):751–767.
- Camacho, E., Berenguel, M., and Rubio, F. (1993). Simulation software package of the acurex field. *Sevilla: ESI of Sevilla, Internal Report*.
- Camacho, E. and Gallego, A. (2013). Optimal operation in solar trough plants: A case study. *Solar Energy*, 95:106–117.
- Camacho, E., Rubio, F., Berenguel, M., and Valenzuela, L. (2007a). A survey on control schemes for distributed solar collector fields. part I: Modeling and basic control approaches. *Solar Energy*, 81(10):1240–1251.
- Camacho, E., Rubio, F., Berenguel, M., and Valenzuela, L. (2007b). A survey on control schemes for distributed solar collector fields. part II: Advanced control approaches. *Solar Energy*, 81(10):1252–1272.

- Camacho, E. F., Berenguel, M., and Rubio, F. R. (1997). *Advanced control of solar plants*. Springer-Verlag.
- Camacho, E. F., Berenguel, M., Rubio, F. R., and Martínez, D. (2012). *Control of solar energy systems*. Springer-Verlag.
- Carmona, R. (1985). Analysis, modeling and control of a distributed solar collector field with a one-axis tracking system. *PhD thesis. University of Seville, Spain*.
- Chisci, L., Falugi, P., and Zappa, G. (2003). Gain-scheduling mpc of nonlinear systems. *International Journal of Robust and Nonlinear Control*, 13(3-4):295–308.
- Chu, Y. and Coimbra, C. F. (2017). Short-term probabilistic forecasts for direct normal irradiance. *Renewable Energy*, 101:526–536.
- Cirre, C. M., Berenguel, M., Valenzuela, L., and Klempous, R. (2009). Reference governor optimization and control of a distributed solar collector field. *European Journal of Operational Research*, 193(3):709–717.
- Cutler, C. R. and Ramaker, B. L. (1980). Dynamic matrix control—a computer control algorithm. In *Proceedings of the Joint Automatic Control Conference*, number 17, page 72.
- Dudley, V. and Workhoven, R. (1982). Performance testing of the acurex solar-collector model 3001-03. Technical report, Sandia National Labs., NM, USA.
- Dughman, S. and Rossiter, J. (2017). Systematic and effective embedding of feed-forward of target information into mpc. *International Journal of Control*, pages 1–15.
- Findeisen, W., Bailey, F. N., Brdys, M., Malinowski, K., Tatjewski, P., and Wozniak, A. (1980). *Control and coordination in hierarchical systems*. John Wiley & Sons.
- Gallego, A. and Camacho, E. (2012). Adaptive state-space model predictive control of a parabolic-trough field. *Control Engineering Practice*, 20(9):904–911.

- Gallego, A., Fele, F., Camacho, E., and Yebra, L. (2013). Observer-based model predictive control of a parabolic-trough field. *Solar Energy*, 97:426–435.
- Gálvez-Carrillo, M., De Keyser, R., and Ionescu, C. (2009). Nonlinear predictive control with dead-time compensator: Application to a solar power plant. *Solar Energy*, 83(5):743–752.
- Garcia, C. E., Prett, D. M., and Morari, M. (1989). Model predictive control: theory and practice—a survey. *Automatica*, 25(3):335–348.
- Gil, P., Henriques, J., Cardoso, A., and Dourado, A. (2002). Neural network in scheduling linear controllers with application to a solar power plant. In *Proceedings of the International Conference on Control and Applications, Cancun, Mexico*.
- Goswami, D. Y., Kreith, F., and Kreider, J. F. (2015). *Principles of solar engineering*. CRC Press.
- Henriques, J., Cardoso, A., and Dourado, A. (1999). Supervision and c-means clustering of pid controllers for a solar power plant. *International Journal of Approximate Reasoning*, 22(1-2):73–91.
- Henriques, J., Gil, P., Cardoso, A., and Dourado, A. (2002). Scheduling of pid controllers by means of a neural network with application to a solar power plant. In *Proceedings of the International Joint Conference on Neural Networks*, volume 1, pages 311–316. IEEE.
- IEA (2011). *Solar energy perspectives*. International Energy Agency.
- IEA (2016). *Key world energy statistics*. International Energy Agency.
- Johansen, T. A., Hunt, K. J., and Petersen, I. (2000). Gain-scheduled control of a solar power plant. *Control Engineering Practice*, 8(9):1011–1022.

- Kakigano, H., Miura, Y., and Ise, T. (2013). Distribution voltage control for dc microgrids using fuzzy control and gain-scheduling technique. *IEEE Transactions on Power Electronics*, 28(5):2246–2258.
- Kufoalor, D., Frison, G., Imsland, L., Johansen, T., and Jørgensen, J. (2017). Block factorization of step response model predictive control problems. *Journal of Process Control*, 53:1–14.
- Kumar, V. and Michael, N. (2012). Opportunities and challenges with autonomous micro aerial vehicles. *The International Journal of Robotics Research*, 31(11):1279–1291.
- Leith, D. J. and Leithead, W. E. (2000). Survey of gain-scheduling analysis and design. *International Journal of Control*, 73(11):1001–1025.
- Maciejowski, J. M. (2002). *Predictive control: with constraints*. Pearson Education.
- Mademlis, C. and Kioskeridis, I. (2010). Gain-scheduling regulator for high-performance position control of switched reluctance motor drives. *IEEE Transactions on Industrial Electronics*, 57(9):2922–2931.
- Meaburn, A. and Hughes, F. (1993). Resonance characteristics of distributed solar collector fields. *Solar Energy*, 51(3):215–221.
- Meaburn, A. and Hughes, F. (1994). Prescheduled adaptive control scheme for resonance cancellation of a distributed solar collector field. *Solar Energy*, 52(2):155–166.
- Muske, K. R. and Rawlings, J. B. (1993). Model predictive control with linear models. *AIChE Journal*, 39(2):262–287.
- Neunert, M., de Crousaz, C., Furrer, F., Kamel, M., Farshidian, F., Siegwart, R., and Buchli, J. (2016). Fast nonlinear model predictive control for unified trajectory optimization and tracking. In *Proceedings of the 2016 IEEE International Conference on Robotics and Automation*, pages 1398–1404. IEEE.

- Ozisik, N. (1994). *Finite difference methods in heat transfer*. CRC press.
- Philibert, C. (2010). *Technology roadmap: concentrating solar power*. OECD/IEA.
- Pickhardt, R. (1998). Application of adaptive controllers to a solar power plant using a multi-model description. In *Proceedings of the American Control Conference*, volume 5, pages 2895–2899. IEEE.
- Piotrowski, R., Brdys, M., Konarczak, K., Duzinkiewicz, K., and Chotkowski, W. (2008). Hierarchical dissolved oxygen control for activated sludge processes. *Control Engineering Practice*, 16(1):114–131.
- Prett, D. and Garcia, C. (1988). *Fundamental Process Control*. Butterworths.
- Propoi, A. (1963). Use of lp methods for synthesizing sampled-data automatic systems. *Automation and Remote Control*, 24:837–844.
- Qin, S. J. and Badgwell, T. A. (1997). An overview of industrial model predictive control technology. In *Proceedings of the AIChE Symposium Series*, volume 93, pages 232–256. New York, NY: American Institute of Chemical Engineers, 1971-c2002.
- Qin, S. J. and Badgwell, T. A. (2003). A survey of industrial model predictive control technology. *Control Engineering Practice*, 11(7):733–764.
- Rato, L., Borrelli, D., Mosca, E., Lemos, J., and Balsa, P. (1997). Musmar based switching control of a solar collector field. In *Proceedings of the European Control Conference*, volume 5, pages 991–996. IEEE.
- Richalet, J., Rault, A., Testud, J., and Papon, J. (1978). Model predictive heuristic control: Applications to industrial processes. *Automatica*, 14(5):413–428.
- Roca, L., de la Calle, A., and Yebra, L. J. (2013). Heliostat-field gain-scheduling control applied to a two-step solar hydrogen production plant. *Applied Energy*, 103:298–305.

- Rossiter, J. A. (2003). *Model-based predictive control: a practical approach*. CRC press.
- Rugh, W. J. and Shamma, J. S. (2000). Research on gain scheduling. *Automatica*, 36(10):1401–1425.
- Seborg, D. E., Mellichamp, D. A., Edgar, T. F., and Doyle III, F. J. (2010). *Process dynamics and control*. John Wiley & Sons.
- Shamma, J. S. and Athans, M. (1990). Analysis of gain scheduled control for non-linear plants. *IEEE Transactions on Automatic Control*, 35(8):898–907.
- Stirrup, R., Loebis, D., Chipperfield, A., Tang, K., Kwong, S., and Man, K. (2001). Gain-scheduled control of a solar power plant using a hierarchical moga-tuned fuzzy pi-controller. In *Proceedings of the IEEE International Symposium on Industrial Electronics*, volume 1, pages 25–29. IEEE.
- Tan, K. G., Yoong, S. W. C., Gopalan, S., et al. (2005). *Iterative algorithms for multilayer optimizing control*. World Scientific.
- Teske, S., Leung, J., Crespo, L., Bial, M., Dufour, E., and Richter, C. (2016). Solar thermal electricity: Global outlook 2016. *Jointly prepared by European Solar Thermal Electricity Association, Greenpeace International and SolarPACES*.
- Turpin, M., Michael, N., and Kumar, V. (2012). Trajectory design and control for aggressive formation flight with quadrotors. *Autonomous Robots*, 33(1-2):143–156.
- Van Overschee, P. and De Moor, B. (2012). *Subspace identification for linear systems: Theory-Implementation-Applications*. Springer Science & Business Media.
- Yu-Geng, X., De-Wei, L., and Shu, L. (2013). Model predictive control-status and challenges. *Acta Automatica Sinica*, 39(3):222–236.
- Zhu, Y. (2001). *Multivariable system identification for process control*. Elsevier.

**Part II**

**Contributions**

## Appendix A

# **DISTRIBUTED COLLECTOR SYSTEM: MODELLING, CONTROL AND OPTIMAL PERFORMANCE**

**Adham Alsharkawi and J. Anthony Rossiter**

This paper has been published in:  
Proceedings of the International Conference on Renewable Energy and Power  
Quality 2015.

*The layout has been revised.*

### **Abstract**

Continual increases in electricity demand, the global rise in oil consumption and prices, the contribution of oil consumption to greenhouse gases emissions and the fact that the supply of fossil fuels will eventually run out are all driving factors in the need for renewable energy solutions. This paper gives an overview of the main concentrated solar thermal power technologies with an emphasis on the modelling and control of conventional parabolic trough technology. Specific focus is given to the benefits of model-based predictive control in a distributed solar collector field of a parabolic trough plant.

### **Keywords**

CSP technologies; Parabolic trough plant; Model-based predictive control; Hierarchical control structure.

### **A.1 Introduction**

In 1972 the US National Science Foundation stated that “*Solar energy is an essentially inexhaustible source potentially capable of meeting a significant portion of the nation’s future energy needs with a minimum of adverse environmental consequences ... The indications are that solar energy is the most promising of the unconventional energy sources*”. In fact all forms of existing energy are solar in origin. Solar energy is converted into electrical energy by two main approaches; a direct approach using photovoltaic (PV) technology and an indirect approach using concentrated solar power (CSP) technology, where the electricity is produced by thermal means (Goswami et al., 2000). In the long-term CSP technology will represent the most reliable energy source with a large installed capacity and thus a key role in grid stabilisation and power security, while the application of PV technology will be limited to decentralised and remote applications (Aringhoff et al., 2005).

CSP plants generate electricity by converting the solar energy into stored heat

energy. The heat energy is then used to drive a power cycle, for instance a steam turbine or a heat engine (Aringhoff et al., 2005; Salazar, 2008). Yet, CSP implementation is faced with the drawbacks of high investment cost and the intermittency of solar energy (Trieb et al., 1997). Technological developments targeting the main elements of a CSP plant and large-scale power production are the only way to overcome these drawbacks (Trieb et al., 1997; Salazar, 2008). Advances in CSP technologies can be found in Mills (2004). Mass power production can be achieved by either having a hybrid operation that combines a CSP plant with a conventional fossil fuel power plant or by having a CSP plant backed up with an efficient heat storage system. Both solutions will allow a compensation for any short time fluctuations in the solar energy and increase the annual operating hours (Trieb et al., 1997).

From a control point of view, one of the challenging issues in a CSP plant is to maintain the thermal process variables close to their desired levels. In contrast to conventional power plant where fuel is used as the manipulated variable, in a CSP plant, solar energy cannot be manipulated. In fact, solar energy acts as a disturbance due to its change on a daily and seasonal basis. The development of efficient control techniques able to cope with this issue will benefit in longer operating hours and electricity cost reductions (Camacho et al., 2012).

Parabolic trough technology is one of the CSP technologies that has received a great deal of attention in terms of modelling and control and indeed a special interest in applying Model-based Predictive Control (MPC) techniques to address the earlier mentioned control problem is also evident. However, the reasons behind the interest in this type of technology is not clearly stated and nor is the motivation to utilize such an advanced control technique. Hence, this paper aims to show the potential benefits of parabolic trough technology compared with the other CSP technologies and moreover to highlight the benefits of applying MPC techniques. The paper also refers to some of the key and recent work in modelling and control of parabolic trough plants and points out where future research is likely to be focused.

This paper is organized as follows: The next section gives an overview of the main

CSP technologies from the aspects of basic concepts, advantages, disadvantages and applications. This is then followed by two sections briefly presenting some modelling and control approaches of parabolic trough plants. A section is then devoted to opportunities in the control of solar energy, before the paper ends with a conclusion and some future directions

## **A.2 CSP Technologies**

CSP technologies have four main elements in common; a concentrator, a receiver, a heat transfer fluid (HTF) and a power conversion (Aringhoff et al., 2005). Some researchers tend to classify CSP technologies according to the concentrator sun tracking mechanism into a single and two axis tracking technologies (Mills, 2004), while others prefer to classify them according to the distribution of the focused solar radiation on an observer into line and point focus technologies (Klaiß et al., 1995). The category of the single axis tracking technologies or the line focus technologies mainly comprises the parabolic trough and linear Fresnel reflector technologies. The category of the two axis tracking technologies or the point focus technologies mainly comprises the central receiver and parabolic dish technologies (Mills, 2004; Aringhoff et al., 2005).

### *A.2.1 Parabolic trough technology*

Concentrators of this technology are sheets of reflective material which are parabolic in shape. Incident solar radiation is concentrated by the parabolic concentrator onto a receiver tube placed at its focal line (Fig. A.1 (a)). Because the parabolic trough collector can only make use of direct solar radiation, it is provided with a single axis tracking mechanism (Fernandez-Garcia et al., 2010). The collector can either track the sun from north to south or from east to west (Kalogirou, 2004).

The receiver tube contains thermal oil that circulates through the solar field and is heated to a temperature of approximately 400 °C. The heated oil passes through a series of heat exchangers to produce steam that is used to drive a conventional steam

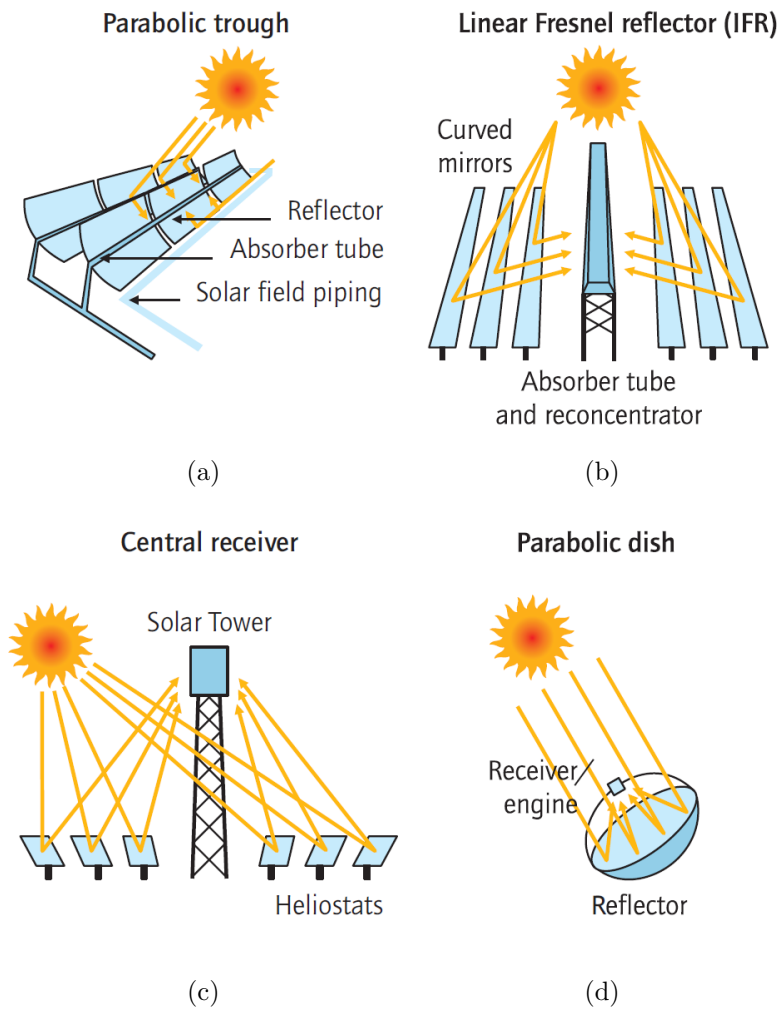


Figure A.1: CSP technologies (Philibert, 2010).

turbine to generate electricity (Aringhoff et al., 2005). Direct Steam Generation (DSG) technology can also be used by having water in the receiver tube (Fernandez-Garcia et al., 2010).

### *Advantages*

- Reliable and mature technology with years of operating experience (Trieb et al., 1997; Aringhoff et al., 2005).

- Concept of hybrid operation has been commercially proven (Trieb et al., 1997).
- Modular and scalable which allows a large-scale power production (Trieb et al., 1997; Aringhoff et al., 2005).
- Storage systems capability (Aringhoff et al., 2005).
- Compared with central receiver and parabolic dish technologies it has shown an efficient land usage and required less materials (Aringhoff et al., 2005).

#### *Disadvantages*

- High investments costs (Mills, 2004).
- Operating temperature is limited to a certain level (Aringhoff et al., 2005).
- Requirements of a stable support structure (Trieb et al., 1997).

#### *Applications*

Parabolic trough technology is best suited for centralized power production (Klaiß et al., 1995; Aringhoff et al., 2005). The U.S. grid-connected Solar Electricity Generating Systems (SEGS) power plants in California represent the most successful parabolic trough plants with a total installed capacity of 354 MW (Fernandez-Garcia et al., 2010).

#### *A.2.2 Linear Fresnel reflector technology*

This is an attempt to enhance and simplify the traditional parabolic trough technology by flattening or nearly flattening the parabolic trough reflectors into a set of rows capable of tracking the sun about one axis and concentrate the solar radiation onto a fixed downward facing receiver parallel to the reflector's rotational axis (Fig. A.1 (b)) (Kalogirou, 2004; Mills, 2004). DSG is well suited for this type of technology (Philibert, 2010; Simbolotti, 2013).

*Advantages*

- Requires less support structure as reflectors positioned close to the ground (Kalogirou, 2004; Simbolotti, 2013).
- Having a stationary receiver eliminates the need for ball joints (Aringhoff et al., 2005; Giostri et al., 2013).
- The flat reflectors are less expensive compared to parabolic trough reflectors (Aringhoff et al., 2005; Simbolotti, 2013).
- Requires less land usage (Giostri et al., 2013; Philibert, 2010).
- Reflectors are easier to clean (Giostri et al., 2013).

*Disadvantages*

- Lower thermal performance is the price of the lower investments and operation and maintenance costs (Philibert, 2010; Simbolotti, 2013).
- Incorporating a storage capacity is challenging (Philibert, 2010; Simbolotti, 2013).
- More complex tracking mechanism (Camacho et al., 2011).

*Applications*

Similar to parabolic trough technology, linear Fresnel technology is suited for centralized power production. One of the recent implementations of this technology is the grid-connected Puerto Errado 2 in Spain with a total installed capacity of 30 MW (Simbolotti, 2013).

### *A.2.3 Central receiver technology*

A large number of heliostats (reflectors) grouped together with a two axis sun tracking mechanism for each one of them. Reflectors are used to concentrate the solar radiation onto a central receiver placed on top of a tower (Fig. A.1 (c)). Solar energy is absorbed at the central receiver by a HTF to be used in a conventional power cycle (Kalogirou, 2004).

#### *Advantages*

- Able to reach an operating temperature over 1000 °C. (Aringhoff et al., 2005).
- Capability of hybrid operation (Trieb et al., 1997; Aringhoff et al., 2005).
- Modular and scalable which allows a large-scale power production (Trieb et al., 1997).
- High storage temperatures (Aringhoff et al., 2005).

#### *Disadvantages*

- Requirements of a stable support structure (Trieb et al., 1997).
- Long-term commercial performance still need to be proven (Simbolotti, 2013).

#### *Applications*

Appropriate technology for centralized power production as discussed in Klaiß et al. (1995); Aringhoff et al. (2005). The commercial PS10 in Spain demonstrates a grid-connected central receiver solar power plant with a total installed capacity in the range of 10 MW (Gil et al., 2010).

#### *A.2.4 Parabolic dish technology*

Concentrator of a parabolic dish technology is dish-shaped reflector that focuses the incident solar radiation at its focal point where a receiver is positioned (Fig. A.1 (d)). HTF running through the receiver is heated up and used by a heat engine for electricity production (Kalogirou, 2004).

#### *Advantages*

- Exhibits the highest energy conversion efficiency (Philibert, 2010; Simbolotti, 2013).
- Can achieve temperatures beyond 1500 °C (Kalogirou, 2004).
- Capability of hybrid operation (Aringhoff et al., 2005; Trieb et al., 1997).
- Modular and scalable which allows a large-scale power production (Aringhoff et al., 2005; Kalogirou, 2004).
- Some operational experience gained from research projects and prototypes (Trieb et al., 1997; Aringhoff et al., 2005).
- Cooling systems for the exhaust heat are not required (Simbolotti, 2013).

#### *Disadvantages*

- Commercial performance and operation is still yet to be proven (Aringhoff et al., 2005).
- Concept of hybrid operation is not proven yet (Trieb et al., 1997).
- Benefits of large-scale power production still need to be proven (Aringhoff et al., 2005).

- High investment cost due to the requirements for a solid and reliable support structure and the dual axis tracking mechanism (Trieb et al., 1997; Simbolotti, 2013).

### *Applications*

Parabolic dish technology is believed to be suitable for distributed power production as a stand-alone units in remote areas and small communities (Klaiß et al., 1995; Simbolotti, 2013). Technology implementation is restricted to prototypes operated successfully over the past decade with installed capacities in the range of 10-100 kW (Simbolotti, 2013). The Boeing SES dish is a U.S. prototype which uses Stirling cycle motors and has delivered over 10,000 h of operation (Mills, 2004).

#### *A.2.5 Discussion*

Although over the past years CSP plants showed a rapid growth in the global market, it is not yet competitive economically with conventional power plants (Simbolotti, 2013). Labour and land cost, incorporation of a storage system, plant size (Philibert, 2010; Simbolotti, 2013), technologies used (Philibert, 2010) and plant maturity (Simbolotti, 2013) have a significant impact on the investment and electricity generating costs for any CSP plant (Philibert, 2010; Simbolotti, 2013). Despite the enhancements that could be done to achieve a reduction in investment and electricity generating costs, parabolic trough technology is commercially considered to be the most economic and reliable technology available (Aringhoff et al., 2005). Over 90% of the currently installed CSP capacity is accounted for by parabolic trough plants (Simbolotti, 2013).

In a parabolic trough plant, a highly skilled and trained operator with a very good knowledge of the sun's daily and seasonal path, observations of changing weather and years of experience is responsible for maintaining the outlet fluid temperature at a desired level regardless of any changes in the sun intensity, the collector inlet temperature and the ambient temperature, by adjusting the flow rate of the HTF

circulating through the collectors within given upper and lower limits. However, the limited performance of a human controller implies the importance of developing effective automatic control (Stuetzle et al., 2004). Automatic control plays a crucial role in the improvement of the efficiency, performance and associated running costs of a parabolic trough plant (Cirre et al., 2009).

As parabolic trough technology represents the most wide spread CSP technology and due to the high influence of automatic control on the overall plant performance, it is not surprising that the literature is rich with work devoted to modelling and control of parabolic trough plants. The next two sections discuss briefly some modelling and control approaches of parabolic trough plants.

### **A.3 Modelling Approaches**

Models can be classified into three main categories; theoretical models, empirical models and semi-empirical models (Seborg et al., 2010).

#### *A.3.1 Theoretical models*

Theoretical models are developed based on first principles and describe the physical behaviour of a process (Seborg et al., 2010). Since the early attempts to control the temperature of the HTF in a parabolic trough plant, the energy balance relations for the receiver tube in (A.1) and the fluid in (A.2) describing the collector dynamics, have established a fundamental role of developing models used in the design of numerous control techniques (Camacho et al., 2012). Both lumped and distributed parameter models can be obtained from (A.1) and (A.2) (Gálvez-Carrillo et al., 2009).

$$\rho_m C_m A_m \frac{\partial T_m}{\partial t} = n_o G I - G H_l (T_m - T_a) - D H_t (T_m - T_f), \quad (\text{A.1})$$

$$\rho_f C_f A_f \frac{\partial T_f}{\partial t} + \rho_f C_f q \frac{\partial T_f}{\partial x} = D H_t (T_m - T_f). \quad (\text{A.2})$$

The subindex  $m$  refers to the receiver tube metal and  $f$  to the fluid,  $\rho$ : density ( $\text{kg}/\text{m}^3$ ),  $C$ : specific heat ( $\text{J}/\text{kg}^\circ\text{C}$ ),  $A$ : cross-sectional area ( $\text{m}^2$ ),  $T$ : temperature ( $^\circ\text{C}$ ),  $n_o$ : optical efficiency,  $I$ : solar radiation ( $\text{W}/\text{m}^2$ ),  $G$ : optical aperture (m),  $H_l$ : global coefficient of thermal losses ( $\text{W}/\text{m}^\circ\text{C}$ ),  $T_a$ : ambient temperature ( $^\circ\text{C}$ ),  $D$ : inner diameter of the receiver tube (m),  $H_t$ : coefficient of metal-fluid transmission ( $\text{W}/\text{m}^2^\circ\text{C}$ ),  $q$ : oil flow ( $\text{m}^3/\text{s}$ ),  $x$ : length (m).

### A.3.2 Empirical models

Empirical models are obtained by the use of experimental data related to specific operating conditions (Seborg et al., 2010). The collector dynamics have been modelled empirically by observing a step response in an open-loop fashion. The response can be approximated by a simple first order system, as shown in (A.3), with a time delay relatively small compared to the system time constant.

$$g(z^{-1}) = z^{-k} \frac{bz^{-1}}{1 - az^{-1}}. \quad (\text{A.3})$$

The model in (A.3) is still an approximation and not adequate enough to capture an important dynamic phenomena of the plant known as anti-resonant modes (Camacho et al., 2012). The phenomena are described in Meaburn and Hughes (1993) as resonance characteristics of the collector dynamics that lie within the desired control bandwidth. Failure to accurately model these resonance characteristics will result in a poor oscillatory performance and low stability margins. Hence, a nonlinear model or several high order linear models for different operating points are required (Camacho et al., 1994b). In Arahall et al. (1998), for instance, the free response of a plant is modelled by a nonlinear version of the AutoRegressive with eXogenous inputs (ARX) model by the application of neural identification using a static (non-recurrent) neural network and the forced response of the plant is modelled by linear Controlled AutoRegressive Integrated Moving Average (CARIMA) models obtained from the Pseudo Random Binary Sequence (PRBS) identification technique.

### *A.3.3 Semi-empirical models*

Semi-empirical models are a combination of theoretical and empirical models in such a way that experimental data is used to calculate the numerical value(s) of the physical parameter(s) in a theoretical model (Seborg et al., 2010). The trade-off between the model simplicity and the ability to describe the dynamics of a plant sufficiently motivated the author in Pickhardt (2000) to develop two slightly different nonlinear models from the basic physical relations. The models are linear in the parameters, thus can be easily estimated on-line and compensate for any time-varying effects or modelling errors. Under the assumption that the system is composed of three main parts: the supply tube, the receiver tube (heated part) and the return tube, a nonlinear grey-box model based on first principles and tuned using real experimental data is presented in Gálvez-Carrillo et al. (2009).

Semi-empirical models receive more interest in the process industry. Although theoretical models provide a physical insight into the process and cover a wide range of operation, their development is quite expensive and time consuming. In addition, some model parameters are not easily obtained. Empirical models are still easier to develop than theoretical models, however, they cover only a limited range of operation. Semi-empirical models on the other hand incorporate conceptual understanding, cover a wider range of operation than empirical models and require less effort to develop than theoretical models (Seborg et al., 2010).

## **A.4 Control Approaches**

Adjusting the flow rate of the HTF in a distributed collector field in order to maintain a desired outlet fluid temperature will result in a significant variations in the collector dynamics (e.g. the response rate and the time delay) which in turn will make the job of a controller with fixed parameters a real challenge (Pickhardt and Da Silva, 1998; Camacho and Berenguel, 1994). Tuning a fixed (proportional-integral-derivative) PID controller with low gain will lead to a poor performance and a tightly tuned

controller might lead to high oscillations (Camacho et al., 2012). Furthermore, such a system imposes constraints on the fluid flow rate, outlet fluid temperature and the difference between outlet and inlet fluid temperatures for safety and energy efficiency (Berenguel et al., 2005). Such issues necessitate the use of more advanced control techniques. The next sub-section presents an overview of the state-of-the-art in controlling the outlet fluid temperature in parabolic trough plants.

#### *A.4.1 State-of-the-art*

Numerous control techniques have been proposed in the literature to address the control challenges of the outlet fluid temperature in a parabolic trough plant. Some of these control techniques are in the form of: i) an adaptive (proportional-integral) PI controller based on a pole assignment approach (Camacho et al., 1992); ii) a robust PI controller with reset action on its integral term (Vidal et al., 2008); iii) a PID controller complemented with a filter to counteract the resonance dynamics effects (Alvarez et al., 2012); iv) a nonlinear PID controller with time varying gain (Neves-Silva, 2013); v) a robust PID controller with fixed parameters based on the quantitative feedback theory (QFT) (Cirre et al., 2010); vi) a feedback linearization (Cirre et al., 2007); vii) an adaptive nonlinear control using feedback exact linearization together with a lyapunov's approach (Barao et al., 2002); viii) an indirect adaptive nonlinear control based on a recurrent neural network and the output regulation theory (Henriques et al., 2010); ix) an internal model control (Álvarez et al., 2010), and x) a fuzzy logic control (Rubio et al., 1995). A feedforward term is a fundamental element in most of these control frameworks in order to mitigate the effect of the measured disturbances on the plant dynamics. Different forms of MPC have been also proposed by many researchers (Camacho and Bordons, 2004). MPC and its implementation to a parabolic trough plant is presented next in more detail.

It should be pointed out that the aim of this sub-section is not to compare the different proposed control techniques, but rather to provide references to some of the key and recent work and give a general idea of some of the various types

that have been proposed. The performance of each of these control techniques was validated with different design assumptions and at different operating conditions so inappropriate for a fair comparison.

#### *A.4.2 Model-based predictive control*

The design concept underpinning MPC is to imitate human behaviour. In a particular situation and based on past information and internal model, a set of control actions are selected and expected to lead to the best predicted outcome over a limited horizon. The planned control actions/strategy are updated continually as more information becomes available. Thus the main components of a predictive control law can be summarized by the following (Rossiter, 2003):

- Output predictions based on a process model.
- Some performance measure to define the optimal future control actions.
- Receding horizon: control actions are updated and modified at every sampling instant.

Applying MPC to address the outlet oil temperature control problems in a parabolic trough plant can be beneficial for several reasons; time delays are implicitly considered due to the predictive nature of MPC; the predicted behaviour gives the chance to avoid any undesired dynamics by selecting the appropriate set of control actions; the system constraints are handled on-line in a systematic fashion and the feedforward term is taken into account automatically (Rossiter, 2003; Camacho and Bordons, 2004). Most of the proposed MPC algorithms can be found in the adaptive, robust, gain scheduling and nonlinear form (Camacho et al., 2012).

#### *Adaptive MPC*

The idea of adaptive control is to tune the controller parameters on-line in a process where the dynamics change frequently in an unpredictable manner. This can be

approached by describing the control law in terms of the on-line estimated process model parameters (Seborg et al., 2010). One of the early applications of adaptive MPC to a solar power plant is presented in Camacho et al. (1994a). The adaptive MPC is developed based on a simple linear model of the process and the resulting control law is linear and can be described by a few parameters. In order to obtain an approximation of the true controller parameters, a set of Ziegler-Nichols-type functions were considered to relate the control law parameters to the process model parameters. More recently, a constrained nonlinear adaptive model-based predictive control based on an affine state-space three layered neural network was developed (Gil et al., 2014). A dual unscented Kalman filter is considered for the on-line recursive updating of the neural network weights and state estimation.

### *Robust MPC*

In contrast to adaptive control, a robust control scheme can cope with changes to process model parameters using a suitable constant gain feedback controller as long as the parameter changes are within certain bounds (Ioannou and Sun, 2012). A robust MPC based on a simple linear model of a plant with bounded errors is proposed in Camacho and Berenguel (1997). Model parameters were allowed to vary within a certain range in order to cope with the changing dynamics and the parameters uncertainty level is determined by a robust identification technique. A hybrid approach that combines the strengths of MPC and sliding mode control (SMC) is presented in de la Parte et al. (2008). The resulting controllers are believed to present a high degree of robustness when they are appropriately tuned. Lately, robustness of stability against parameters uncertainty and measurement errors in a nonlinear MPC has been taken care of by simply including a candidate Lyapunov function in the objective function and the constraints of the controller (Andrade et al., 2013).

### *Gain Scheduling MPC*

The performance requirements in a gain scheduling approach can be met by designing several feedback controllers with constant gains that correspond to a number of operating points. Hence, the implementation requires a look-up table to store the values of the controller gains and a criteria to relate the changes in a process dynamics to the appropriate controller gain (Ioannou and Sun, 2012). High order CARIMA type models obtained from input-output data of a plant were used for different operating points in a gain scheduling MPC approach (Camacho et al., 1994b). As the plant dynamics are mainly affected by the changes in the fluid flow, two tables of the process and the controller parameters were obtained for different fluid flow values. An alternative gain scheduling MPC approach, but also based on the fluid flow value, is proposed in Pickhardt (1998) where linear ARMAX models were identified on-line for different operating points and used for an indirect adaptive MPC controller.

### *Nonlinear MPC*

Linear control techniques can be effective in physical processes, which exhibit nonlinear behaviour to a small degree, for example where one is limited to a narrow range of operation. Otherwise, traditional linear control techniques may not be adequate and nonlinear control techniques can be an option to enable performance improvements (Seborg et al., 2010). For an MPC control scheme presented in Arahall et al. (1998), the response of a plant is divided into a forced and free terms. A linear model is used for the forced response to obtain a set of control actions, while a nonlinear model of the free response is used to handle the effect of the disturbances. A recent application of a nonlinear MPC is presented in Andrade et al. (2013). A distributed parameter model is used for the simulated process and a lumped parameter model with time delay is used for prediction. The main contribution of this work is that the parameters of the prediction model do not require any identification or adaptation in order to meet the expected results, which implies a reduction in the computational

cost when computing the control algorithm.

Once again, this section has demonstrated a large body of research focussed on applying differing forms of MPC, but as yet a useful and insightful comparison seems to be lacking.

### **A.5 Opportunities**

Reduction in investment and operating costs and an increase in solar plant performance can make solar energy more economical (Camacho et al., 2011). Advanced control techniques can reduce operating costs and increase plant performance (Camacho and Gallego, 2013). However, most of the control techniques focus on a certain level of automatic control and neglect other levels of process automation, which results in a poor performance at some operating points, particularly during the start up and shut down of the plant. During the start up, the plant is controlled in manual mode by the plant operator until conditions to change to automatic control mode are reached, which is inefficient and time consuming (Cirre et al., 2009). In order to extend the automation of the process to other levels and improve the final plant performance, hierarchical control approaches are proposed in Berenguel et al. (2005); Cirre et al. (2009); Camacho and Gallego (2013).

The idea of a hierarchical control structure was first presented in Berenguel et al. (2005) to optimize the electricity production process in solar power plants with distributed collectors. The use of a multilayer hierarchical control structure is coming from the fact that the problem involves systems with different dynamical behaviour and time scales. The generic control structure is composed of the following four main layers:

- The regulation layer is concerned with typical set point temperature tracking and disturbance rejection where simply any control technique can be used.
- The set point optimization layer is concerned with obtaining the most adequate set points considering the actual operating conditions and plant constraints.

- The daily optimization layer is concerned with the determination of the daily operating hours of the plant.
- The weekly optimization layer is concerned with the operational scheduling of the plant within a weekly planning period.

Applying a hierarchical control approach to a solar power plant can benefit in maximizing the electricity production, extend the lifetime of the various elements of the plant, reduce the risk of controller saturation and limit the tasks of the plant operator. In Cirre et al. (2009), a two-layer hierarchical control strategy is described. The upper layer is implemented using two different approaches for set point optimization in the steady state and the lower layer is a combination of a simple feedforward and feedback controllers for reference tracking and disturbance rejection. The hierarchical structure is extended in Camacho and Gallego (2013) to include a third layer for operational scheduling and the set point optimization layer is computed taking into account the dynamic behaviour of the plant while the regulation layer is controlled by an adaptive PI controller.

### ***A.6 Conclusion and Future Directions***

Features of the main CSP technologies have been presented and it has been discussed that parabolic trough technology is widely accepted and has shown excellent performance in the commercial power industry. Moreover, due to the important part of automatic control in the overall plant performance, some of the key and recent efforts in modelling and control of parabolic trough plants are also presented. Notably conclusions and avenues for future study are:

- For accurate modelling of the plant the dynamic phenomena of anti-resonant modes must be taken care of but as yet there is no convergence in the literature on whether nonlinear models or gain scheduling of high order linear models are to be preferred.

- There is some consensus that semi-empirical models are preferable in general.
- Many control techniques have been used, but an effective comparison seems to be lacking.
- There has been substantial interest in the benefits of applying MPC but as yet a reliable comparison and consensus is lacking.
- The adoption of hierarchical control structures is likely to be the future of controlling parabolic trough plants which moreover allow for effects such as weather prediction and variation in electricity demands.

# BIBLIOGRAPHY

- Álvarez, J., Normey-Rico, J., and Berenguel, M. (2012). Design of PID controller with filter for distributed parameter systems. *IFAC Proceedings Volumes*, volume 45(3), 495–500.
- Álvarez, J.D., Costa-Castelló, R., Berenguel, M., and Yebra, L.J. (2010). A repetitive control scheme for distributed solar collector field. *International journal of control*, volume 83(5), 970–982.
- Andrade, G., Pagano, D., Álvarez, J., and Berenguel, M. (2013). A practical NMPC with robustness of stability applied to distributed solar power plants. *Solar Energy*, volume 92, 106–122.
- Arahal, M., Berenguel, M., and Camacho, E. (1998). Neural identification applied to predictive control of a solar plant. *Control Engineering Practice*, volume 6(3), 333–344.
- Aringhoff, R., Brakmann, G., Geyer, M., and Teske, S. (2005). Concentrated solar thermal power-now. *Greenpeace, Amsterdam, ESTIA, Brussels and SolarPACES, Agudulce, Spain*.
- Barao, M., Lemos, J., and Silva, R. (2002). Reduced complexity adaptive nonlinear control of a distributed collector solar field. *Journal of Process Control*, volume 12(1), 131–141.
- Berenguel, M., Cirre, C.M., Klempous, R., Maciejewski, H., Nikodem, M., Nikodem, J., Rudas, I., and Valenzuela, L. (2005). Hierarchical control of a distributed solar collector field. In *Proceedings of the International Conference on Computer Aided Systems Theory*, volume 3643, 614–620. Springer.

- Camacho, E.F. and Berenguel, M. (1994). Application of generalized predictive control to a solar power plant. In *Proceedings of the 1994 IEEE Conference on Control Applications*, volume 3, 1657–1662. IEEE.
- Camacho, E.F. and Berenguel, M. (1997). Robust adaptive model predictive control of a solar plant with bounded uncertainties. *International Journal of Adaptive Control and Signal Processing*, volume 11(4), 311–325.
- Camacho, E.F., Berenguel, M., Rubio, F.R., and Martínez, D. (2012). *Control of solar energy systems*. Springer-Verlag.
- Camacho, E.F., Samad, T., Garcia-Sanz, M., and Hiskens, I. (2011). Control for renewable energy and smart grids. *The Impact of Control Technology, Control Systems Society*, 69–88.
- Camacho, E.F., Berenguel, M., and Bordons, C. (1994a). Adaptive generalized predictive control of a distributed collector field. *IEEE Transactions on Control Systems Technology*, volume 2(4), 462–467.
- Camacho, E., Berenguel, M., and Rubio, F. (1994b). Application of a gain scheduling generalized predictive controller to a solar power plant. *Control Engineering Practice*, volume 2(2), 227–238.
- Camacho, E. and Bordons, C. (2004). Model predictive control. *Advanced Textbooks in Control and Signal Processing* (.).
- Camacho, E. and Gallego, A. (2013). Optimal operation in solar trough plants: A case study. *Solar Energy*, volume 95, 106–117.
- Camacho, E., Rubio, F., and Hughes, F. (1992). Self-tuning control of a solar power plant with a distributed collector field. *IEEE Control Systems*, volume 12(2), 72–78.

- Cirre, C.M., Berenguel, M., Valenzuela, L., and Camacho, E.F. (2007). Feedback linearization control for a distributed solar collector field. *Control Engineering Practice*, volume 15(12), 1533–1544.
- Cirre, C.M., Berenguel, M., Valenzuela, L., and Klempous, R. (2009). Reference governor optimization and control of a distributed solar collector field. *European Journal of Operational Research*, volume 193(3), 709–717.
- Cirre, C.M., Moreno, J.C., Berenguel, M., and Guzmán, J.L. (2010). Robust control of solar plants with distributed collectors. *IFAC Proceedings Volumes*, volume 43(5), 823–828.
- de la Parte, M.P., Cirre, C.M., Camacho, E.F., and Berenguel, M. (2008). Application of predictive sliding mode controllers to a solar plant. *IEEE Transactions on Control Systems Technology*, volume 16(4), 819–825.
- Fernandez-Garcia, A., Zarza, E., Valenzuela, L., and Pérez, M. (2010). Parabolic-trough solar collectors and their applications. *Renewable and Sustainable Energy Reviews*, volume 14(7), 1695–1721.
- Gálvez-Carrillo, M., De Keyser, R., and Ionescu, C. (2009). Nonlinear predictive control with dead-time compensator: Application to a solar power plant. *Solar Energy*, volume 83(5), 743–752.
- Gil, A., Medrano, M., Martorell, I., Lázaro, A., Dolado, P., Zalba, B., and Cabeza, L.F. (2010). State of the art on high temperature thermal energy storage for power generation. part 1-concepts, materials and modellization. *Renewable and Sustainable Energy Reviews*, volume 14(1), 31–55.
- Gil, P., Henriques, J., Cardoso, A., Carvalho, P., and Dourado, A. (2014). Affine neural network-based predictive control applied to a distributed solar collector field. *IEEE Transactions on Control Systems Technology*, volume 22(2), 585–596.

- Giostri, A., Binotti, M., Silva, P., Macchi, E., and Manzolini, G. (2013). Comparison of two linear collectors in solar thermal plants: parabolic trough versus Fresnel. *Journal of Solar Energy Engineering*, volume 135(1), 011001.
- Goswami, D.Y., Kreith, F., and Kreider, J.F. (2000). *Principles of solar engineering*. CRC Press.
- Henriques, J., Gil, P., Cardoso, A., Carvalho, P., and Dourado, A. (2010). Adaptive neural output regulation control of a solar power plant. *Control Engineering Practice*, volume 18(10), 1183–1196.
- Ioannou, P.A. and Sun, J. (2012). *Robust adaptive control*. Courier Corporation.
- Kalogirou, S.A. (2004). Solar thermal collectors and applications. *Progress in Energy and Combustion Science*, volume 30(3), 231–295.
- Klaiß, H., Köhne, R., Nitsch, J., and Sprengel, U. (1995). Solar thermal power plants for solar countries-technology, economics and market potential. *Applied Energy*, volume 52(2), 165–183.
- Meaburn, A. and Hughes, F. (1993). Resonance characteristics of distributed solar collector fields. *Solar Energy*, volume 51(3), 215–221.
- Mills, D. (2004). Advances in solar thermal electricity technology. *Solar Energy*, volume 76(1), 19–31.
- Neves-Silva, R. (2013). Non linear control of a distributed solar field. In *Proceedings of the 2013 International Conference on Renewable Energy Research and Applications*, 1096–1101. IEEE.
- Philibert, C. (2010). *Technology roadmap: concentrating solar power*. OECD/IEA.
- Pickhardt, R. (1998). Application of adaptive controllers to a solar power plant using a multi-model description. In *Proceedings of the American Control Conference*, volume 5, 2895–2899. IEEE.

- Pickhardt, R. (2000). Nonlinear modelling and adaptive predictive control of a solar power plant. *Control Engineering Practice*, volume 8(8), 937–947.
- Pickhardt, R. and Da Silva, R.N. (1998). Application of a nonlinear predictive controller to a solar power plant. In *Proceedings of the 1998 IEEE International Conference on Control Applications*, volume 1, 6–10. IEEE.
- Rossiter, J.A. (2003). *Model-based predictive control: a practical approach*. CRC press.
- Rubio, F.R., Berenguel, M., and Camacho, E.F. (1995). Fuzzy logic control of a solar power plant. *IEEE Transactions on Fuzzy Systems*, volume 3(4), 459–468.
- Salazar, C.M. (2008). An overview of CSP in Europe, north Africa and the middle east. *CSP Today*.
- Seborg, D.E., Mellichamp, D.A., Edgar, T.F., and Doyle III, F.J. (2010). *Process dynamics and control*. John Wiley & Sons.
- Simbolotti, G. (2013). Concentrating solar power technology brief. *IEA-ETSAP and IRENA*.
- Stuetzle, T., Blair, N., Mitchell, J.W., and Beckman, W.A. (2004). Automatic control of a 30 MWe SEGS VI parabolic trough plant. *Solar Energy*, volume 76(1), 187–193.
- Trieb, F., Langniß, O., and Klaiß, H. (1997). Solar electricity generation—a comparative view of technologies, costs and environmental impact. *Solar Energy*, volume 59(1-3), 89–99.
- Vidal, A., Banos, A., Moreno, J.C., and Berenguel, M. (2008). PI+CI compensation with variable reset: application on solar collector fields. In *Proceedings of the 34th Annual Conference of IEEE Industrial Electronics*, 321–326. IEEE.

Appendix B

**MODELLING ANALYSIS OF A SOLAR  
THERMAL POWER PLANT**

**Adham Alsharkawi and J. Anthony Rossiter**

This paper has been accepted for publication in:  
Proceedings of the 6th International Conference on Clean Electrical Power.

*The layout has been revised.*

### **Abstract**

This paper looks into the modelling of the ACUREX distributed solar collector field at the Plataforma Solar de Almería (PSA). ACUREX possesses resonance characteristics that lie well within the desired control bandwidth and quite commonly is modelled by dividing the receiver tube in the solar collector field into a number of segments. However, the number of segments has varied significantly in the literature. This paper provides an open-loop and closed-loop analysis with the aim of finding the number of segments needed to adequately model the resonance characteristics.

### **Keywords**

Nonlinear systems; Parabolic trough; Resonant modes; Solar thermal power plant.

## **B.1 Introduction**

### *B.1.1 Background and problem statement*

The latest world energy statistics (IEA, 2016) illustrate the need to produce marketable electricity from clean and sustainable alternatives to fossil fuels. The steady increase in the consumption of fossil fuels (coal, oil and natural gas) and their contribution to  $CO_2$  emissions are the driving factors behind this need. Solar energy is a highly appealing alternative.

In 2011, the International Energy Agency (IEA) stated that “*The development of affordable, inexhaustible and clean solar energy technologies will have huge longer-term benefits. It will increase countries’ energy security through reliance on an indigenous, inexhaustible and mostly import-independent resource, enhance sustainability, reduce pollution, ...*” (IEA, 2011).

Solar energy is converted into electrical energy by two main approaches; a direct approach using photovoltaic (PV) technology and an indirect approach using concentrated solar power (CSP) technology, where electricity is produced by ther-

mal means (Goswami et al., 2000). The scope of this paper will be limited to the application of the most developed CSP technology, namely parabolic trough.

ACUREX is a parabolic trough technology-based solar thermal power plant. It is one of the research facilities of the Plataforma Solar de Almería (PSA) in south-east Spain and has served as a benchmark for many researchers across academia and industry. Collectors of the ACUREX plant are parabolic in shape and concentrate the incident solar radiation onto a receiver tube that is placed at its focal line. A heat transfer fluid (HTF) is heated as it flows through the receiver tube and circulates through a distributed solar collector field. The heated HTF then passes through a series of heat exchangers to produce steam which in turn is used to drive a steam turbine to generate electricity.

From a control point of view, one of the biggest challenges is to maintain the field outlet temperature at a desired level despite changes, mostly in solar radiation, field inlet temperature, or ambient temperature. This can be handled by manipulating the volumetric flow rate of the HTF. A detailed description of the plant and control problem can be found in Camacho et al. (2012).

It was argued in Meaburn and Hughes (1993) that the ACUREX distributed solar collector field possesses resonance characteristics, namely resonant modes that lie well within the desired control bandwidth. These phenomena arise due to the relatively slow flow rate of the HTF and the length of the receiver tube. It was also found that the phenomena have a significant impact on the control performance and hence modelling the resonant modes sufficiently accurately is crucial to ensure high control performance with adequate robustness.

A common approach for constructing nonlinear models of the ACUREX plant is to divide the receiver tube in the solar collector field into a number of segments as will be discussed later on in the paper. However, the literature has witnessed a significant variation in the number of segments used and hence it makes one wonder how many segments are actually needed to adequately model the resonant modes of the plant. Surprisingly, this has received little attention in the literature.

### B.1.2 Paper contribution and organisation

The paper draws attention to a practice that can be helpful in deciding on the number of segments needed and hence begins by constructing a number of nonlinear simulation models of the plant for a different number of segments and investigating their performance in an open-loop and closed-loop fashion.

For the open-loop analysis, the performance of each model will be analysed against a measured output from the ACUREX plant. The closed-loop analysis requires the estimation of a linear time-invariant (LTI) state space model from each and every constructed nonlinear simulation model and hence the estimation process and some frequency-domain analysis will be discussed first.

A brief literature review of the available nonlinear models of the ACUREX plant is presented in Section B.2 and then a general procedure for constructing a nonlinear simulation model for any number of segments is discussed in Section B.3. This is followed by an open-loop analysis in Section B.4 and a closed-loop analysis in Section B.5. Finally, Section B.6 is devoted to a discussion of the overall results and some concluding remarks.

## B.2 Nonlinear Models of the ACUREX Plant

The dominant dynamics of the ACUREX plant are captured by a set of energy balance partial differential eqns. (PDEs):

$$\begin{aligned}\rho_m C_m A_m \frac{\partial T_m}{\partial t} &= n_o G I - D_o \pi H_l (T_m - T_a) - D_i \pi H_t (T_m - T_f), \\ \rho_f C_f A_f \frac{\partial T_f}{\partial t} + \rho_f C_f q \frac{\partial T_f}{\partial x} &= D_i \pi H_t (T_m - T_f),\end{aligned}\tag{B.1}$$

where the subindex  $m$  refers to the metal of the receiver tube and  $f$  to the HTF (Carmona, 1985; Camacho et al., 2012). See Table B.1 for variables and parameters.

It is a common practice in the literature to construct nonlinear simulation and prediction models based on these PDEs by dividing the receiver tube into  $N$  segments each of length  $\Delta x$  and then converting the set of PDEs (B.1) into a set of ordinary differential equations (ODEs) or simply a set of difference equations. One of the

Table B.1: Variables and Parameters.

Symbol	Description	SI unit
$\rho$	Density	kg/m <sup>3</sup>
$C$	Specific heat capacity	J/kg°C
$A$	Cross-sectional area	m <sup>2</sup>
$T$	Temperature	°C
$t$	Time	s
$I$	Solar radiation	W/m <sup>2</sup>
$n_o$	Mirror optical efficiency	–
$G$	Mirror optical aperture	m
$D_o$	Outer diameter of the receiver tube	m
$H_l$	Global coefficient of thermal losses	W/m°C
$T_a$	Ambient temperature	°C
$D_i$	Inner diameter of the receiver tube	m
$H_t$	Metal-fluid heat transfer coefficient	W/m <sup>2</sup> °C
$q$	HTF volumetric flow rate	m <sup>3</sup> /s
$x$	Space	m

early constructed nonlinear simulation models is reported in Camacho et al. (2012), where the receiver tube was divided into 100 segments each of length  $1m$ . The PDEs (B.1) were solved using a two-stage algorithm of three difference equations.

More recently and after simplifying the PDEs by neglecting the dynamics of the metal of the receiver tube, a set of ODEs has been obtained for simulation and prediction purposes. For simulation purposes, the receiver tube was divided into 10 segments and for prediction purposes and after neglecting the heat losses, the receiver tube was divided into 5 segments (Gálvez-Carrillo et al., 2009). In Gallego and Camacho (2012), in an attempt to obtain a linearised state space model of the plant, an ODE is obtained from a simplified version of the PDEs and the receiver

tube has been divided into 8 segments whereas in Gallego et al. (2013) and for the same exact reason, the PDEs were converted into a set of ODEs by dividing the receiver tube into 15 segments.

Clearly, the number of segments used to construct nonlinear simulation and prediction models has varied significantly (from 5 to 100) in the literature and these are examples where the number of segments was stated explicitly.

### B.3 Construction of a Nonlinear Simulation Model

The set of PDEs (B.1) can be approximated by a set of ODEs by dividing the receiver tube into  $N$  segments each of length  $\Delta x$  with the boundary condition  $T_{f,0} = T_{f,inlet}$  (field inlet temperature) and  $H_l, H_t, \rho_f$  and  $C_f$  being time-varying (Alsharkawi and Rossiter, 2016a).

$$\begin{aligned} \rho_m C_m A_m \frac{dT_{m,n}}{dt} &= n_o G I - D_o \pi H_l (T_{m,n} - T_a) - D_i \pi H_t (T_{m,n} - T_{f,n}) \\ \rho_f C_f A_f \frac{dT_{f,n}}{dt} + \rho_f C_f q \frac{T_{f,n} - T_{f,n-1}}{\Delta x} &= D_i \pi H_t (T_{m,n} - T_{f,n}) \end{aligned}, \quad n = 1, \dots, N. \quad (\text{B.2})$$

The set of ODEs (B.2) is transparent and can be simply implemented for any number of segments. In order to meet the first aim of this paper, five nonlinear simulation models have been constructed for  $N = 15, 13, 10, 7,$  and  $4$ .

**Remark B.1.** *The set of ODEs (B.2) is implemented and solved for the five nonlinear simulation models using the MATLAB<sup>®</sup> solver ODE45 (an explicit Runge-Kutta method) where the temperature distribution in the receiver tube and HTF can be accessed at any point in time and for any segment  $n$ . The number of ODEs solved at each sample time  $k$  for a nonlinear simulation model of  $N$  segments is  $2 \times N$ .*

### B.4 Open-Loop Analysis

In this section and using some measured data <sup>1</sup> from the ACUREX plant, the performance of the five nonlinear simulation models is assessed in the time-domain and

---

<sup>1</sup>The measured data was collected on 15 July 2003 and after a series of step changes in the volumetric flow rate of the HTF.

in an open-loop manner. Fig. B.1 shows the measured inputs and Fig. B.2 shows the performance of the five nonlinear simulation models against the measured output. Note that models 1, 2, 3, 4 and 5 refer to the nonlinear simulation models with 15, 13, 10, 7 and 4 segments respectively.

Inspection of Fig. B.2 indicates that the variation in the number of segments is only affecting the transients, i.e., the larger the number of segments the slower the response. To gain better insight into the respective performance, Table B.2 gives a numerical comparison of the five non-linear models.

Table B.2: Assessment of the Simulation Models

Simulation model	RMSE ( $^{\circ}\text{C}$ )
1	14.4859
2	14.2301
3	13.8792
4	13.5739
5	13.3112

Table B.2 shows that a small number of segments gives lower root mean square error (RMSE), but the impact on RMSE of the variation in the number of segments is not significant. The similarity in accuracy of these models could be an explanation for the notable variation in the number of segments used in the literature; the next section delves deeper into the problem.

## ***B.5 Closed-Loop Analysis***

### *B.5.1 Control objective and strategy*

It has been mentioned earlier that in a solar thermal power plant a core control objective is to keep the field outlet temperature at a specific target in spite of any changes in solar radiation, the field inlet temperature, or ambient temperature by

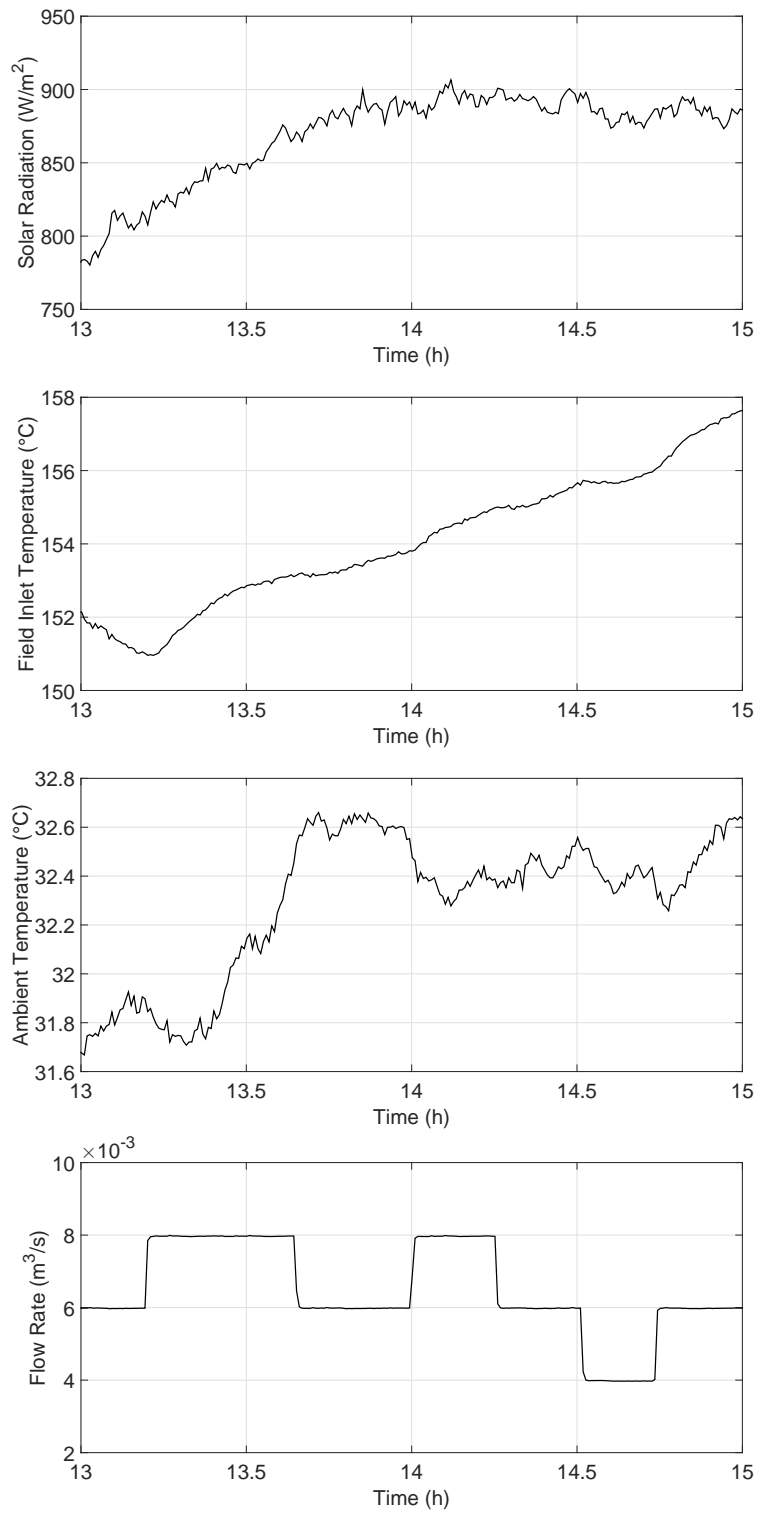


Figure B.1: Measured inputs.

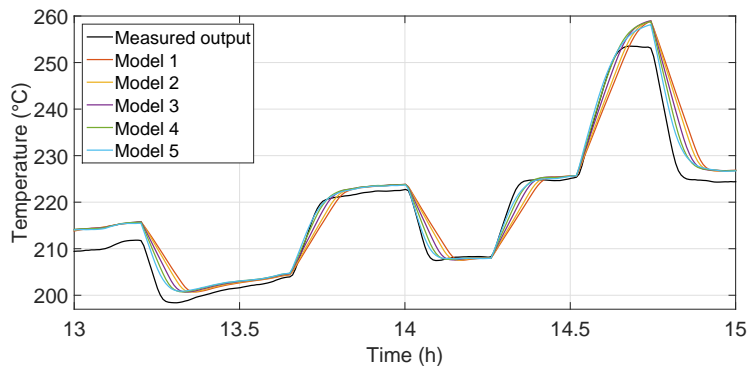


Figure B.2: Simulation models against the measured output.

suitably adjusting the volumetric flow rate of the HTF. In order to meet this aim, researchers have proposed many different control strategies (e.g. see comprehensive surveys on control strategies Camacho et al. (2007a,b)).

In Alsharkawi and Rossiter (2016a), and due to the nonlinearity of the ACUREX plant, a predictive control strategy has been designed locally around a single operating point. That control strategy is adopted here and used to investigate the performance of the five nonlinear simulation models. The control strategy is model-based and hence a local LTI state space model needs to be estimated from each of the five nonlinear simulation models.

### *B.5.2 System identification and frequency-domain analysis*

Following the same identification process in Alsharkawi and Rossiter (2016a), LTI state space models are estimated directly from input-output data using the subspace identification method N4SID (Van Overschee and De Moor, 1996). Table B.3 gives a summary of the results. Local models 1, 2, 3, 4 and 5 have been estimated from the constructed nonlinear simulation models with 15, 13, 10, 7 and 4 segments respectively.

One way of describing Table B.3 is to say that as the number of segments is increased, the model order of the estimated state space models is increased as well

Table B.3: Summary of the Estimated Local Models

Local model	Model order	Best fit (%)	CT (s)	MSE
1	5 <sup>th</sup>	97.17	125.835	0.2854
2	5 <sup>th</sup>	97.21	106.471	0.2649
3	5 <sup>th</sup>	97.21	79.556	0.2373
4	4 <sup>th</sup>	97.16	53.797	0.212
5	3 <sup>rd</sup>	97.10	30.443	0.1909

as the computational time (CT) required to obtain the input-output data. The best fit and mean squared error (MSE) are quantitative assessments of the estimation process and one can notice slight variation to their values. Further details on model order selection and best fit criterion can be found in Alsharkawi and Rossiter (2016a).

The fact that the time-domain analysis gives little information about the resonant modes of the plant necessitated an alternative approach. Fig. B.3 shows the frequency response of the locally estimated LTI state space models. The Bode plot clearly shows that the resonant modes indeed lie within the Nyquist bandwidth and more importantly, as the number of segments is increased they become more obvious and indeed the resonance characteristics are not quite captured by local model 5.

### B.5.3 Simulation results

The estimated local LTI state space models are used for the design of corresponding local predictive controllers. The performance of the estimated models in capturing locally the behaviour of the plant is put to the test using the simulation scenario illustrated in Fig. B.4 and Fig. B.5. The scenario assumes a fixed field inlet and ambient temperature and each time a local controller is applied the plant is represented by the corresponding nonlinear simulation model. The scenario starts with a clear day and slowly time-varying solar radiation, but adds a sudden drop in solar radiation at 12.45 h to simulate a passing cloud.

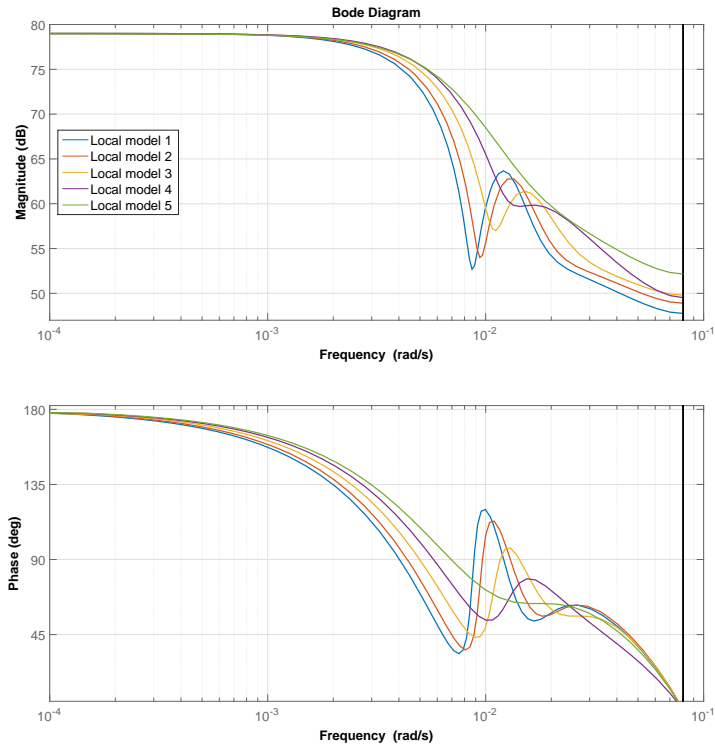


Figure B.3: Frequency responses of the estimated local models.

The closed-loop performance of the five local controllers can be summarised by the following interesting observations. During set point tracking, the local controllers that have been designed based on a small number of segments show less oscillatory tracking performance than the ones that have been designed based on a large number of segments. Also local controllers designed based on a large number of segments and when operating far from the nominal operating point ( $0.006 \text{ m}^3/\text{s}$ ) give more severe control actions.

Conversely, in terms of the resonant modes of the plant, they have been excited by the sudden drop in the solar radiation. Inspection of Fig. B.5 shows that the local controllers that have been designed based on a large number of segments react to the disturbance in a better way than the ones designed based on a small number of segments.

For a better insight into the set point tracking performance and disturbance

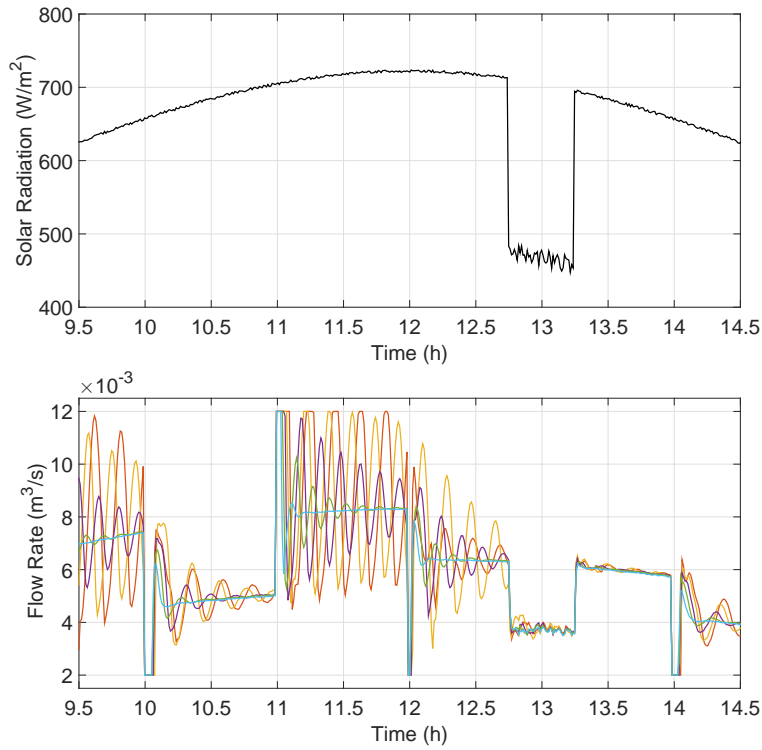


Figure B.4: Solar radiation and flow rate of the HTF.

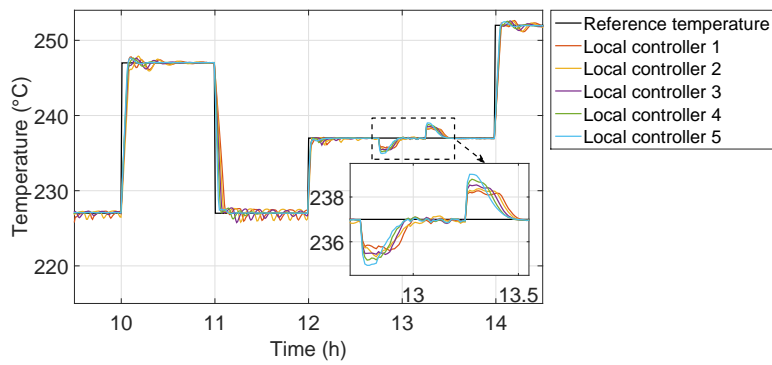


Figure B.5: Closed-loop performance.

rejection, Table B.4 gives an assessment of the five local controllers across the whole range of operation ( $RMSE_w$ ) and the narrow range of the disturbance ( $RMSE_d$ ).

Table B.4: Assessment of the Local Controllers

Local Controller	RMSE <sub>w</sub> (°C)	RMSE <sub>d</sub> (°C)
1	2.3623	0.7753
2	2.4044	0.8047
3	2.1531	0.8385
4	1.9699	0.8725
5	1.8117	0.8943

### ***B.6 Discussion and Concluding Remarks***

This paper investigated the number of segments needed to adequately model the resonance characteristics of the ACUREX plant. A number of nonlinear simulation models were constructed and their performance assessed in open-loop and closed-loop manner.

The open-loop analysis revealed that the variation in the number of segments primarily affects transients and gives little information about the resonant modes. A closed-loop analysis requires the estimation of a LTI state space models; here the resonant modes are more obvious when the models are estimated from a nonlinear simulation model with many segments.

The LTI state space models were evaluated using a nonlinear simulation environment. The state space models estimated based on a large number of segments react to a sudden disturbance in a better way than those based on a small number of segments. On the other hand, the state space models estimated based on a small number of segments have shown better set point tracking performance.

This leads to the following interesting finding. Constructing a nonlinear simulation model using a large number of segments captures the dynamics of the plant at high frequencies and constructing a nonlinear simulation model using a small number of segments captures the dynamics of the plant at low frequencies. Obviously

this is a dilemma that calls for something beyond the time-based measurements to validate a nonlinear simulation model.

One way of resolving the dilemma is to relate to the frequency response of the plant. In Johansen et al. (2000), the frequency response of the plant has been obtained around three different operating points and by inspecting the frequency response of the five nonlinear simulation models around the same operating points, it has been found that a nonlinear simulation model when 7 segments are considered gives a reasonable approximation to the resonance characteristics of the plant. This can be clearly seen in Fig. B.6, Fig. B.7 and Fig. B.8.

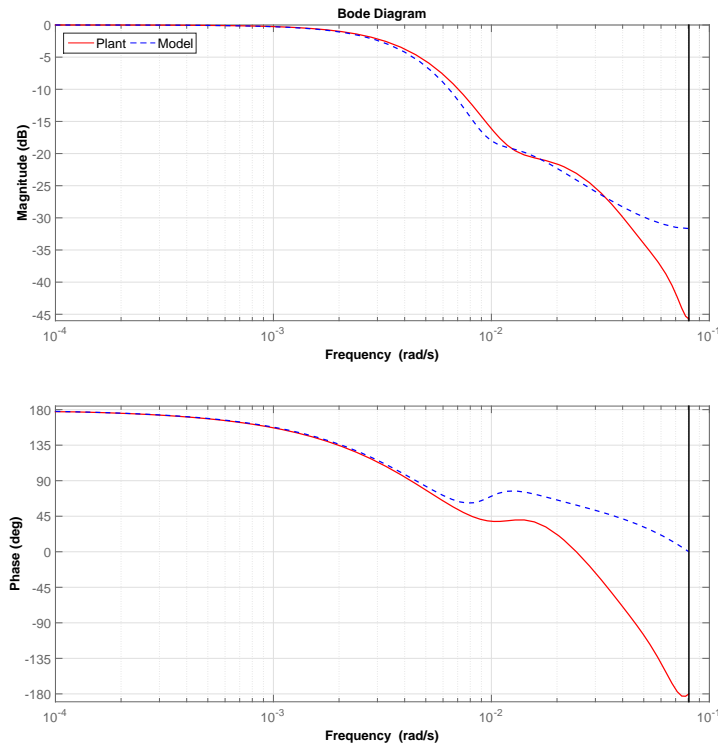


Figure B.6: Model validation around operating point 1.

Note that the linear models that have been used here to generate the frequency response of the plant are quite controversial as discussed in Alsharkawi and Rossiter (2016b) due to the fact that these models were subject to changes in solar radiation

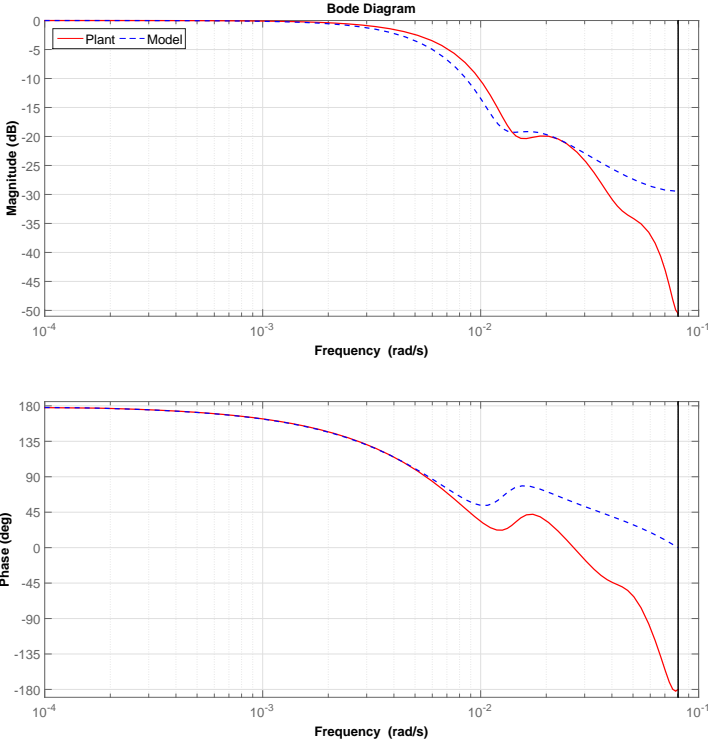


Figure B.7: Model validation around operating point 2.

during the identification process, but this is not an issue here since the normalised steady-state gain has been used for validation.

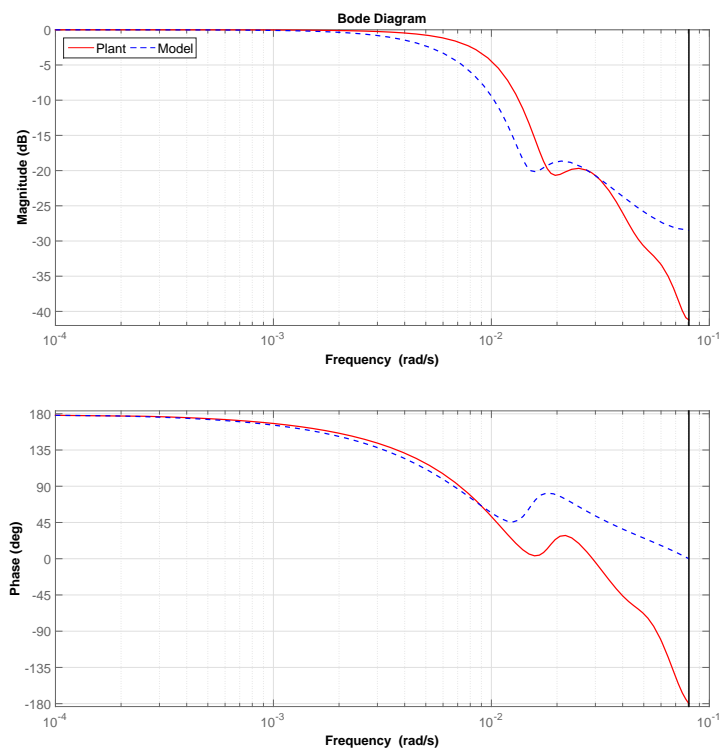


Figure B.8: Model validation around operating point 3.

# BIBLIOGRAPHY

- Alsharkawi, A. and Rossiter, J. A. (2016a). Dual mode MPC for a concentrated solar thermal power plant. In *Proceedings of the 11th IFAC Symposium on Dynamics and Control of Process Systems, including Biosystems, Trondheim, Norway*, volume 49(7), 260–265. Elsevier.
- Alsharkawi, A. and Rossiter, J. A. (2016b). Gain scheduling dual mode MPC for a solar thermal power plant. In *Proceedings of the 10th IFAC Symposium on Nonlinear Control Systems, California, USA*, volume 49(18), 128–133. Elsevier.
- Camacho, E.F., Berenguel, M., Rubio, F.R., and Martínez, D. (2012). *Control of solar energy systems*. Springer-Verlag.
- Camacho, E., Rubio, F., Berenguel, M., and Valenzuela, L. (2007a). A survey on control schemes for distributed solar collector fields. part i: Modeling and basic control approaches. *Solar Energy*, volume 81(10), 1240–1251.
- Camacho, E., Rubio, F., Berenguel, M., and Valenzuela, L. (2007b). A survey on control schemes for distributed solar collector fields. part ii: Advanced control approaches. *Solar Energy*, volume 81(10), 1252–1272.
- Carmona, R. (1985). *Analysis, modeling and control of a distributed solar collector field with a one-axis tracking system*. Ph.D. thesis. University of Seville, Spain.
- Gallego, A. and Camacho, E. (2012). Adaptative state-space model predictive control of a parabolic-trough field. *Control Engineering Practice*, volume 20(9), 904–911.
- Gallego, A., Fele, F., Camacho, E., and Yebra, L. (2013). Observer-based model predictive control of a parabolic-trough field. *Solar Energy*, volume 97, 426–435.

- Gálvez-Carrillo, M., De Keyser, R., and Ionescu, C. (2009). Nonlinear predictive control with dead-time compensator: Application to a solar power plant. *Solar Energy*, volume 83(5), 743–752.
- Goswami, D.Y., Kreith, F., and Kreider, J.F. (2000). *Principles of solar engineering*. CRC Press.
- IEA (2011). *Solar energy perspectives*. International Energy Agency.
- IEA (2016). *Key world energy statistics*. International Energy Agency.
- Johansen, T.A., Hunt, K.J., and Petersen, I. (2000). Gain-scheduled control of a solar power plant. *Control Engineering Practice*, volume 8(9), 1011–1022.
- Meaburn, A. and Hughes, F. (1993). Resonance characteristics of distributed solar collector fields. *Solar Energy*, volume 51(3), 215–221.
- Van Overschee, P. and De Moor, B. (2012). *Subspace identification for linear systems: Theory-Implementation-Applications*. Springer Science & Business Media.

Appendix C

**DUAL MODE MPC FOR A  
CONCENTRATED SOLAR THERMAL  
POWER PLANT**

**Adham Alsharkawi and J. Anthony Rossiter**

This paper has been published in:  
Proceedings of the 11th IFAC Symposium on Dynamics and Control of Process  
Systems, including Biosystems.

*The layout has been revised.*

### ***Abstract***

A model predictive control strategy for a concentrated solar thermal power plant is proposed. Design of the proposed controller is based on an estimated linear time-invariant state space model around a nominal operating point. The model is estimated directly from input-output data using a subspace identification method and taking into account the frequency response of the plant. Input-output data are obtained from a nonlinear distributed parameter model of a plant rather than the plant itself. Effectiveness of the proposed control strategy in terms of tracking and disturbance rejection is evaluated through two different scenarios created in a nonlinear simulation environment.

### ***Keywords***

Concentrated solar thermal power plant; Parabolic trough; Nonlinear distributed parameter model; Resonant modes; Subspace identification; Model predictive control.

### ***C.1 Introduction***

It takes only a quick look at the latest world energy statistics (IEA, 2014) to realise the steady increase in the consumption of fossil fuels (coal, oil and natural gas) and electricity and more importantly the contribution of fossil fuels to the  $CO_2$  emissions over the years. Hence, there is an urgent need to produce marketable electricity from clean and sustainable alternatives to fossil fuels. Solar energy is one of the most promising existing alternatives. It can be converted into electrical energy by two main approaches; a direct approach using photovoltaic (PV) technology and an indirect approach using concentrated solar power (CSP) technology, where electricity is produced by thermal means (Goswami et al., 2000). Future scenarios for some of the promising areas for solar energy applications show that CSP plants will play a major role in the long-term energy supply and thus a key element for grid stabilisation and power security while PV plants will be limited to decentralised

applications.

CSP plants produce electricity by converting the solar energy into stored heat energy and then use this to drive a power cycle, for instance a steam turbine or a heat engine (Aringhoff et al., 2005). Parabolic trough, linear Fresnel reflector, solar tower and parabolic dish are the four main CSP technologies. Of these, parabolic trough stands out among these technologies as the most mature and reliable technology and indeed parabolic trough forms the bulk of the current commercial CSP plants (Philibert, 2010).

From a control point of view, maintaining the thermal variables in a CSP plant close to their desired levels to enable stable power production is far more challenging than in a conventional fossil fuel power plant due to the intermittency of solar energy and therefore efficient and advanced control strategies are required. In addition to Camacho et al. (2012), a comprehensive survey of the modelling and control of parabolic trough CSP plants is presented in Camacho et al. (2007a,b).

The parabolic trough ACUREX plant is considered in this paper. This plant exhibits some important dynamics, namely resonant modes and for a linear control system, high order linear models are required to capture these dynamics and attain a high control performance (Camacho et al., 2012). However, obtaining convenient high order linear models analytically is not an easy task due to the nonlinearities and complexities of the plant (Álvarez et al., 2009).

An empirical approach has been found to be more reasonable as in Camacho et al. (1997); Johansen et al. (2000) where explicit recognition of the plant resonant modes through the estimation of high order linear models for different operating points is reported. High order local linear ARX type models are estimated using experimental data from the plant. These local models formed the basis for the design of gain scheduling control strategies. Both control strategies have a family of local linear controllers that correspond to the different operating points and a scheduling criteria to switch among these controllers as the plant dynamics change with time or operating conditions. As part of their evaluation process, the performance of the

scheduling controller is compared to the performance of a single local linear controller over a wide range of operation. Without a doubt, the gain scheduling controller has been shown to be superior to the single controller.

However, even though the simulation results and the real implementations on the plant have shown good performance of the control strategies, improvements can still be made. For example, safety constraints on the manipulated and controlled variables of the process have been completely ignored in the control system design in Johansen et al. (2000) and poorly investigated in Camacho et al. (1997) when the controlled variable was only restricted to not exceed a desired reference under any circumstances; this resulted in a severe performance degradation in the presence of disturbances. Moreover, since the linear models have been estimated from experimental data of the plant, an optimal model accuracy will never be achieved due to the slow dynamics of the plant and the fast changes in the operating conditions within a limited time frame. That is evident in Johansen et al. (2000) when the plant was perturbed with Pseudo-Random Binary sequence (PRBS) signals without taking into account the prior knowledge of the process. Three local models were estimated for three different operating points. Gains of the three local models had to be corrected around a nominal solar radiation value due to the changes in the solar radiation during the PRBS tests and one of the local models was unable to capture the resonant modes of the plant accurately which was attributed to the poor PRBS design. The PRBS design in terms of frequency band and amplitude is not reported in Camacho et al. (1997).

This paper takes into account the frequency response of the plant and embeds prior knowledge of the process and then estimates a linear time-invariant (LTI) state space model around a nominal operating point using the subspace identification method. Input-output data are obtained from a nonlinear distributed parameter model of the plant rather than the plant itself. The paper also incorporates the plant safety constraints. A final contribution is to implement and demonstrate the efficacy of a dual mode model-based predictive control (MPC) strategy for tracking

and disturbance rejection over a wide range of operation for the nonlinear model. Apart from the plant characteristics that need an advanced control strategy to cope with the changing dynamics, nonlinearities and uncertainties (Camacho et al., 2012), the main motivation for implementing the dual mode MPC strategy is due to its ability to do online constraint handling in a systematic fashion. Specifically, the dual mode MPC gives a handle on the predictions over an infinite horizon while still allowing a sensible limit on the number of control degrees of freedom (d.o.f) and constraints.

This paper is organised as follows: Section C.2 gives a brief description to the plant and control problem; Section C.3 discusses the mathematical modelling of the plant; Section C.4 describes the phenomena of resonant modes and the identification process; Section C.5 outlines the dual mode MPC design. This is then followed by Section C.6 where the simulation results are presented and finally, the main findings and some concluding remarks are presented in Section C.7.

## ***C.2 Plant Description and Control Problem***

ACUREX is a parabolic trough technology-based concentrated solar thermal power plant. Collectors of this type of technology are parabolic in shape and concentrate the incident solar radiation onto a receiver tube that is placed at its focal line. A heat transfer fluid (HTF) is heated as it flows along the receiver tube and then passes through a series of heat exchangers to produce steam that is used to drive a conventional steam turbine to generate electricity (Aringhoff et al., 2005).

The plant is one of the research facilities at the Plataforma Solar de Almería (PSA) in the province of Almeria in south-east Spain and has served as a benchmark for many researchers across academia and industry. ACUREX is mainly composed of a distributed solar collectors field, a thermal storage tank, and a power unit. One of the biggest challenges in such a plant is to maintain the field outlet temperature at a desired level regardless of any changes, mostly in solar radiation, field inlet temperature, or ambient temperature. This is can only be achieved by manipulating

the volumetric flow rate of the HTF. A schematic diagram of the plant is shown in Fig. C.1 and a more detailed description of the plant can be found in Camacho et al. (2012).

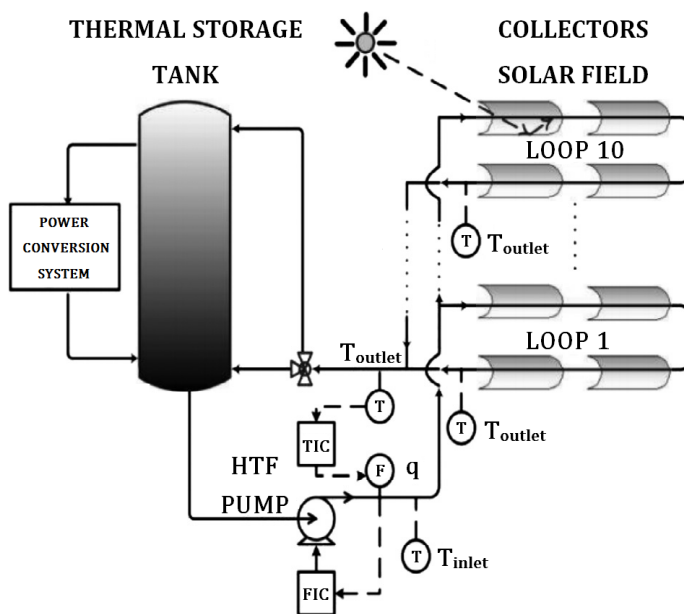


Figure C.1: ACUREX schematic diagram. Figure adapted from Álvarez et al. (2008).

### C.3 Mathematical Model

This section presents a mathematical model of the ACUREX plant. A nonlinear distributed parameter model for simulation purposes is discussed first and this is followed by description of a local LTI state space model to be used for control design purposes.

#### C.3.1 Nonlinear distributed parameter model

The distributed solar collector field comprises 480 single axis parabolic trough collectors arranged in 10 parallel loops with 48 collectors in each loop. The dynamic

behaviour can be described by the following set of energy balance partial differential equations (PDEs):

$$\begin{aligned}\rho_m C_m A_m \frac{\partial T_m}{\partial t} &= n_o G I - D_o \pi H_l (T_m - T_a) - D_i \pi H_t (T_m - T_f), \\ \rho_f C_f A_f \frac{\partial T_f}{\partial t} + \rho_f C_f q \frac{\partial T_f}{\partial x} &= D_i \pi H_t (T_m - T_f),\end{aligned}\quad (\text{C.1})$$

where the subindex  $m$  refers to the metal of the receiver tube and  $f$  to the HTF (Carmacho et al., 2012). Table C.1 gives a description to all the variables and parameters and lists their SI units.

Table C.1: Variables and Parameters.

Symbol	Description	SI unit
$\rho$	Density	kg/m <sup>3</sup>
$C$	Specific heat capacity	J/kg°C
$A$	Cross-sectional area	m <sup>2</sup>
$T$	Temperature	°C
$t$	Time	s
$I$	Solar radiation	W/m <sup>2</sup>
$n_o$	Mirror optical efficiency	—
$G$	Mirror optical aperture	m
$D_o$	Outer diameter of the receiver tube	m
$H_l$	Global coefficient of thermal losses	W/m°C
$T_a$	Ambient temperature	°C
$D_i$	Inner diameter of the receiver tube	m
$H_t$	Metal-fluid heat transfer coefficient	W/m <sup>2</sup> °C
$q$	HTF volumetric flow rate	m <sup>3</sup> /s
$x$	Space	m

The idea of a distributed parameter model is to divide the receiver tube into a set of an active and a passive series of segments based on the direct contact with

the solar radiation (Camacho et al., 2012). By considering only the active segments of the tube the energy balance PDEs can be approximated by a set of ordinary differential equations (ODEs) that correspond to  $N$  ( $n = 1, 2, \dots, N$ ) segments each of length  $\Delta x$  (Fig. C.2):

$$\begin{aligned} \rho_m C_m A_m \frac{dT_{m,n}}{dt} &= n_o G I - D_o \pi H_l (T_{m,n} - T_a) - D_i \pi H_t (T_{m,n} - T_{f,n}), \\ \rho_f C_f A_f \frac{dT_{f,n}}{dt} + \rho_f C_f q \frac{T_{f,n} - T_{f,n-1}}{\Delta x} &= D_i \pi H_t (T_{m,n} - T_{f,n}), \end{aligned} \quad (\text{C.2})$$

with the boundary condition  $T_{f,0} = T_{f,inlet}$  (field inlet temperature) and  $H_l, H_t, \rho_f$  and  $C_f$  being time-varying. The term  $(\rho_f C_f q \frac{T_{f,n} - T_{f,n-1}}{\Delta x})$  in (C.2) is indeed the main source of nonlinearity of the process.

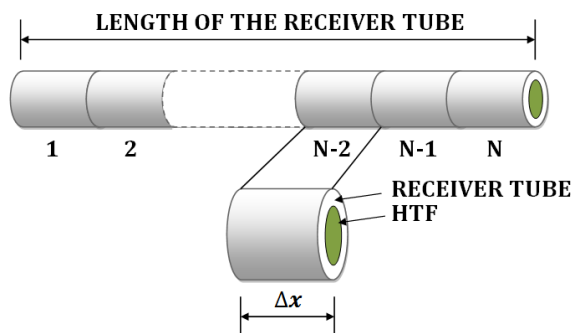


Figure C.2: Schematic for the nonlinear distributed parameter model.

Experiments have revealed that dividing the receiver tube into  $N$  segments is a requirement to capture the main dynamics (resonance characteristics) of the plant. However, it has also been revealed that a lesser number of  $N$  ( $< 3$ ) is unable to capture these dynamics adequately and a greater number of  $N$  ( $> 10$ ) increases the computational burden without adding a significant improvement to the prediction accuracy. Dividing the receiver tube into 7 segments has been found to give a reasonable trade-off as will be demonstrated in a later section.

The system of ODEs in (C.2) is solved numerically and efficiently using the MATLAB<sup>®</sup> solver ODE45 (an explicit Runge-Kutta method).

### C.3.2 Local LTI state space model

Model-based control system design requires suitable mathematical models. Subspace identification is one way of obtaining these models directly from input-output data (Favoreel et al., 2000). Algorithms for subspace identification are computationally simple and effective in identifying dynamic state space linear systems and overcome some of the major problems encountered in the classical identification methods, i.e., parametrization, convergence and model reduction. The general form of an estimated discrete-time LTI state space model is given as:

$$\begin{aligned}x_{k+1} &= Ax_k + Bu_k + \xi_k, \\y_k &= Cx_k + Du_k + \eta_k,\end{aligned}\tag{C.3}$$

$$E \left[ \begin{pmatrix} \xi_p \\ \eta_p \end{pmatrix} \begin{pmatrix} \xi_q^T & \eta_q^T \end{pmatrix} \right] = \begin{pmatrix} Q & S \\ S^T & R \end{pmatrix} \delta_{pq} \leq 0,\tag{C.4}$$

where  $x_k \in \mathbb{R}^{n \times 1}$ ,  $u_k \in \mathbb{R}^{m \times 1}$ ,  $y_k \in \mathbb{R}^{l \times 1}$ ,  $\xi_k \in \mathbb{R}^{n \times 1}$  and  $\eta_k \in \mathbb{R}^{l \times 1}$  are the state vector, input vector, output vector, process noise and measurement noise respectively at discrete time instant  $k$ .  $A, B, C$  and  $D$  are the coefficient matrices of appropriate dimensions.  $\xi_k$  and  $\eta_k$  are assumed to be white noise sequences.  $Q, S$  and  $R$  are the covariance matrices of appropriate dimensions.  $E$  is the expected value operator and  $\delta_{pq}$  is the Kronecker delta.

The system in (C.3) is assumed to be asymptotically stable, the pair  $(A, B)$  is controllable and the pair  $(A, C)$  is observable (Van Overschee and De Moor, 1996). A local LTI state space model similar to the one in (C.3) is estimated from input-output data around a nominal operating point using the N4SID algorithm with the assumptions that there is no direct feedthrough from the input to the output ( $D = 0$ ) and the system is deterministic ( $\xi_k = \eta_k = 0$ ). The N4SID subspace identification method is discussed in Favoreel et al. (2000).

#### C.4 Resonant Modes and System Identification

It was mentioned earlier that the plant exhibits some resonance characteristics. The phenomena of these resonance characteristics are described in Meaburn and Hughes (1993) as resonant modes that lie well within the control bandwidth and are a result of the relatively slow flow rate of the HTF. The phenomena are believed to have a significant impact on the control performance. Hence, modelling these resonance characteristics accurately is crucial to ensure a high control performance with adequate robustness. Resonant modes can be accurately accounted for by a nonlinear distributed parameter model or a relatively high order linear models (Camacho et al., 2012). Here a LTI state space model is considered which is convenient for the control system design.

Taking into account the prior knowledge of the process, the nonlinear distributed parameter model in (C.2) is excited with a PRBS signal which is a deterministic binary signal with white noise like properties and ideally suited for linear identification. The signal is generated using MATLAB<sup>®</sup> with an amplitude of  $0.0005 \text{ m}^3/\text{s}$  and a clock period equals to the process sampling time 39 s (the process time constant is around 6 min). The identification process assumes steady state operating conditions around a nominal operating point ( $q_{nom} = 0.006 \text{ m}^3/\text{s}$ ,  $T_{f,nom} = 237^\circ\text{C}$ ,  $I_{nom} = 674.75 \text{ W}/\text{m}^2$ ,  $T_{f,inlet,nom} = 183^\circ\text{C}$  and  $T_{a,nom} = 28^\circ\text{C}$ ). Since only a full-length PRBS captures the white noise like properties and due to the slow dynamics of the plant, the identification process had to be carried out over a large set of data (1209 samples). However, only 1100 samples have been considered as early samples during the transients have been ignored (Fig. C.3).

Unlike the nonlinear distributed parameter model of the plant, use of a full-length PRBS taking into account the process time constant will be impractical to perform on the plant itself due to the fast changes in the operating conditions and the large data set required and this issue is one for further study. The order of the model is estimated by inspecting the singular values given by the N4SID algorithm.

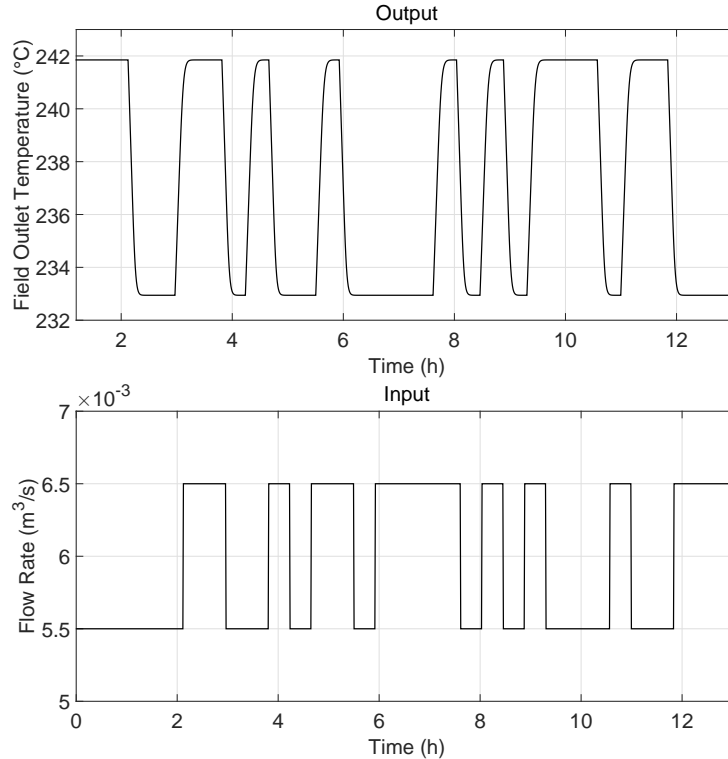


Figure C.3: Input-output data.

The algorithm suggests a local LTI state space model of the  $4^{th}$ -order. In terms of model order, the estimated model is less complex than the models presented in Camacho et al. (1997); Johansen et al. (2000) while still adequate enough to capture the phenomena of resonant modes as illustrated in Fig. C.4.

Fig. C.4 also shows the bode plots of a  $3^{rd}$ -order and  $5^{th}$ -order estimated models. Certainly, a model of the  $4^{th}$ -order is optimal, so to speak, as the  $3^{rd}$ -order model fails to capture the phenomena of resonant modes accurately and the dynamics of the  $5^{th}$ -order model are shown to be almost identical to the dynamics of the  $4^{th}$ -order model.

Since the estimated LTI state space model is mainly used for prediction within the control system design, the simulated model output (infinite-step ahead prediction) is evaluated through a best fit criterion. The criterion used is given in Ljung (1995)

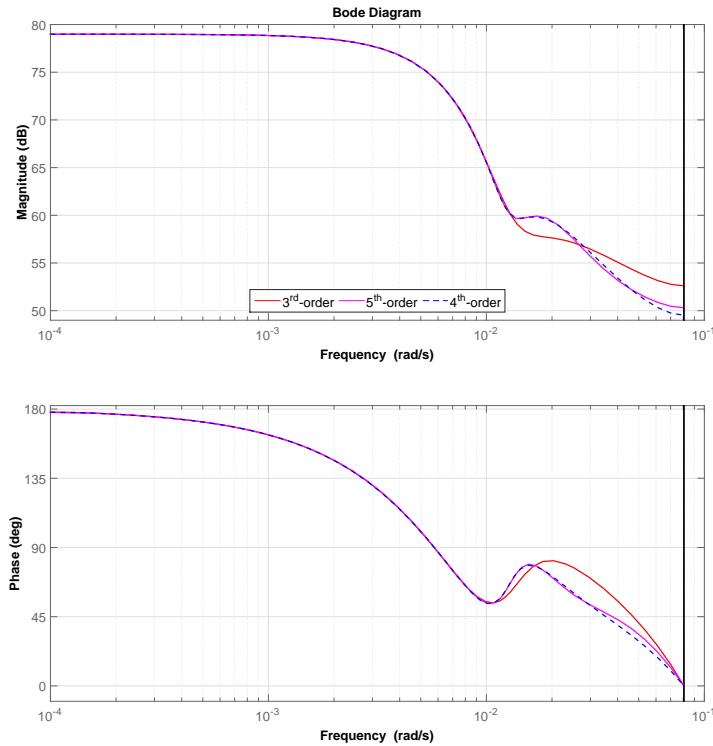


Figure C.4: Bode plot of the estimated LTI state space model.

as:

$$Best\ fit = \left( 1 - \frac{\sum_{i=1}^n |y_i - \hat{y}_i|}{\sum_{i=1}^n |y_i - \bar{y}|} \right) \times 100, \quad (C.5)$$

where  $y$ ,  $\hat{y}$  and  $\bar{y}$  are the measured output, the simulated model output and the mean of the measured output respectively.

The criterion showed a prediction accuracy of 97.16% which confirms that the model is able to reproduce the main dynamic characteristics of the plant at a given operating point and time horizon.

### C.5 Dual Mode MPC

The notation dual mode refers to a separation in the model predictions into transient (mode 1) and asymptotic (mode 2) predictions. The separation gives a handle on the predictions over an infinite horizon, where a standard linear analysis can be applied, while still allowing a reduction in the number of d.o.f. and constraints (Rossiter, 2003). For a deterministic version of the system in (C.3) and assuming no direct feedthrough, the deviation from the estimated steady state values  $x_{ss}$ ,  $u_{ss}$  and  $y_{ss}$  can be expressed as:

$$\begin{aligned}\hat{x}_{k+1} &= A\hat{x}_k + B\hat{u}_k, \\ \hat{y}_k &= C\hat{x}_k.\end{aligned}\tag{C.6}$$

A standard dual mode cost function (online performance measure)  $J$  is given as:

$$J = \sum_{i=0}^{n_c-1} [\hat{x}_{k+1+i}^T Q \hat{x}_{k+1+i} + \hat{u}_{k+i}^T R \hat{u}_{k+i}] + \hat{x}_{k+n_c}^T P \hat{x}_{k+n_c},\tag{C.7}$$

where  $n_c$  is the number of free d.o.f.,  $Q$  and  $R$  are weighting matrices of appropriate dimensions and  $P$  is obtained from a Lyapunov equation of appropriate dimension. The cost function in (C.7) can be simplified to take the form of a standard quadratic programming problem with constraints and solved online as:

$$\min_{\hat{u}_{\rightarrow k-1}} \hat{u}_{\rightarrow k-1}^T S \hat{u}_{\rightarrow k-1} + \hat{u}_{\rightarrow k-1}^T L \hat{x}_k \quad \text{s.t.} \quad M \hat{u}_{\rightarrow} \leq \gamma,\tag{C.8}$$

where  $\hat{u}_{\rightarrow k-1} = [\hat{u}_k \ \hat{u}_{k+1} \ \dots \ \hat{u}_{k+n_c-1}]^T$ ,  $S$  and  $L$  depend upon the matrices  $A$ ,  $B$ ,  $Q$ ,  $R$  and  $P$ ,  $M$  is time-invariant and  $\gamma$  depends upon the system past input-output information. Detailed treatment of the control strategy can be found in Rossiter (2003).

### C.6 Simulation Results

The proposed control strategy is evaluated through two different simulation scenarios. The first scenario assumes a clear day with a mean solar radiation value of

674.75 W/m<sup>2</sup> while the second scenario considers a sudden change in the solar radiation (e.g. passing cloud). For both scenarios the plant is represented by the nonlinear distributed parameter model in (C.2) with a slight increase to thermal losses in order to make the scenarios more realistic. Field inlet temperature ( $T_{in}$ ) and ambient temperature ( $T_a$ ) are kept fixed at 189 °C and 28 °C respectively even though that may not be the case in the normal operation of the plant. The HTF is assumed to be the synthetic oil Therminol<sup>®</sup> 55 and constrained to the range 0.002–0.012 m<sup>3</sup>/s where the minimum limit is normally for a safety reason. Exceeding a temperature of 305 °C puts the synthetic oil at the risk of being decomposed. The difference between the field outlet temperature and the field inlet temperature is also constrained not to exceed 80 °C in order to avoid the risk of oil leakage (Camacho et al., 2012). The latter has been taken care of implicitly when the nominal operating point and the reference temperature were selected. Flow rate constraints are explicitly considered in the control design as will be demonstrated in the following two scenarios.

### C.6.1 First scenario

Fig. C.5 illustrates the simulation results for a clear day where several interesting observations can be made. The time period 12-14 h shows that the dual mode MPC controller works very well (fast transient and no overshoot of the field outlet temperature) near the nominal operating point where the LTI state space model was estimated (0.006 m<sup>3</sup>/s) and moreover copes with the slow variation of the daily cycle of solar radiation even though the local model was estimated based on steady state operating conditions. Furthermore, as the system operates slightly farther away from the nominal operating point, the field outlet temperature is able to track the reference temperature with an acceptable transient and an overshoot of less than 1 °C, although this is rather oscillatory. The control action is also somewhat oscillatory during large transients in reference temperature (this moves from 247 °C to 227 °C in the period 11-12 h). Worse control performance is certainly expected at higher (>0.008 m<sup>3</sup>/s) and lower (<0.004 m<sup>3</sup>/s) flow rates. More importantly however, MPC

handles the flow rate constraints efficiently over the whole range of operation.

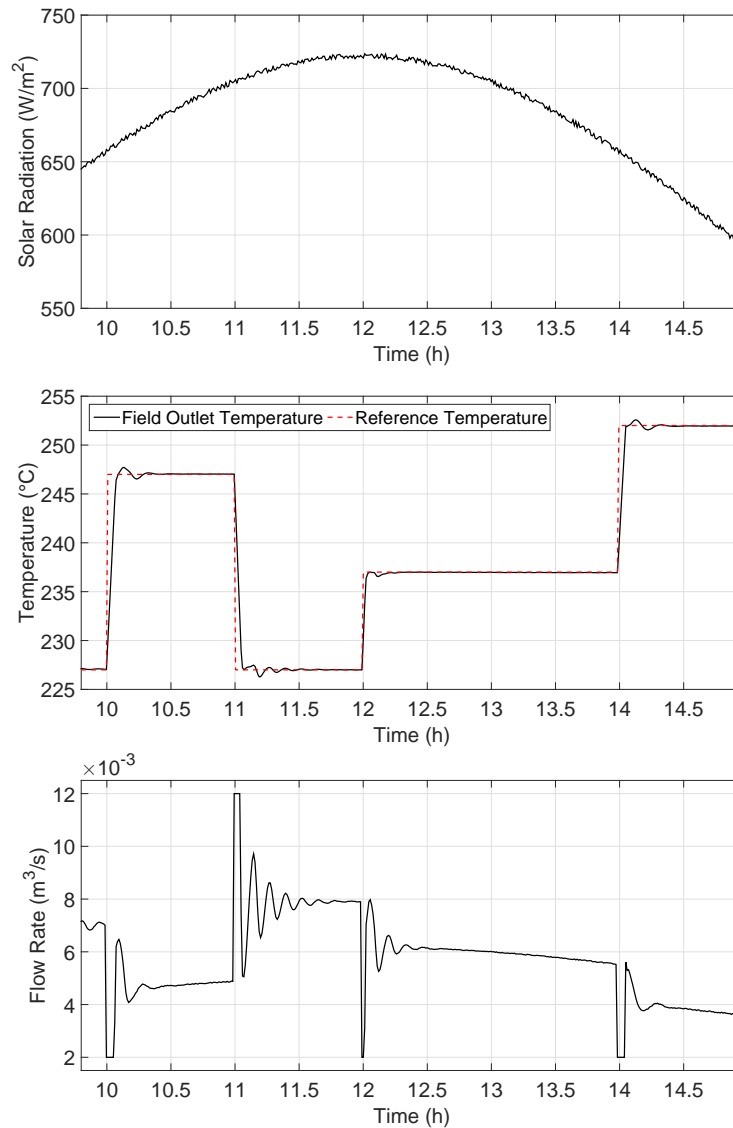


Figure C.5: First scenario: simulation results for a clear day.

### C.6.2 Second scenario

This scenario investigates the effect of a passing cloud on the system. Clouds act as a disturbance to the system and therefore must be properly rejected. Simulation results of a passing cloud near the nominal operating point are illustrated in Fig. C.6.

The cloud is simulated by a sudden drop in the solar radiation with a relatively high level of noise. Clearly, the controller shows a satisfactory performance by rejecting the disturbance with a fair and sensible recovery time and a deviation from the reference temperature of less than  $2^{\circ}\text{C}$ . One potentially interesting question for future study is whether performance could be improved further still with a more effective use of the feedforward term; this is an area which has received relatively little attention in the MPC literature.

### ***C.7 Conclusion***

This paper has extended some of the existing control approaches for solar power plant currently in the literature and demonstrated a clear potential benefits as well as identifying areas of obvious future study. First, a LTI state space model was estimated directly from input-output data around a given operating point using a subspace identification method. Due to the slow dynamics of the plant and the fast changes in the operating conditions, the input-output data were obtained from a distributed parameter model of the ACUREX plant rather than the plant itself. A second key contribution is that the model is estimated taking into account the dynamic phenomena of resonant modes and the prior knowledge of the process. This technique resulted in a model order reduction when compared to the models available in the open literature and hence enabled a less complex control design. Finally, the model served as a platform for a dual mode control strategy for tracking and disturbance rejection and also including plant safety constraints.

The control strategy is shown to have satisfactory performance around a nominal operating point for two different and commonplace scenarios. As expected, when operating far from the nominal operating point a poor performance was observed which is consistent with Camacho et al. (1997); Johansen et al. (2000). Hence, the need to extend the work to cover more operating points is evident.

While this paper as clearly demonstrated that the proposed approach is feasible and effective, obvious avenues for future work, in addition to a comprehensive eval-

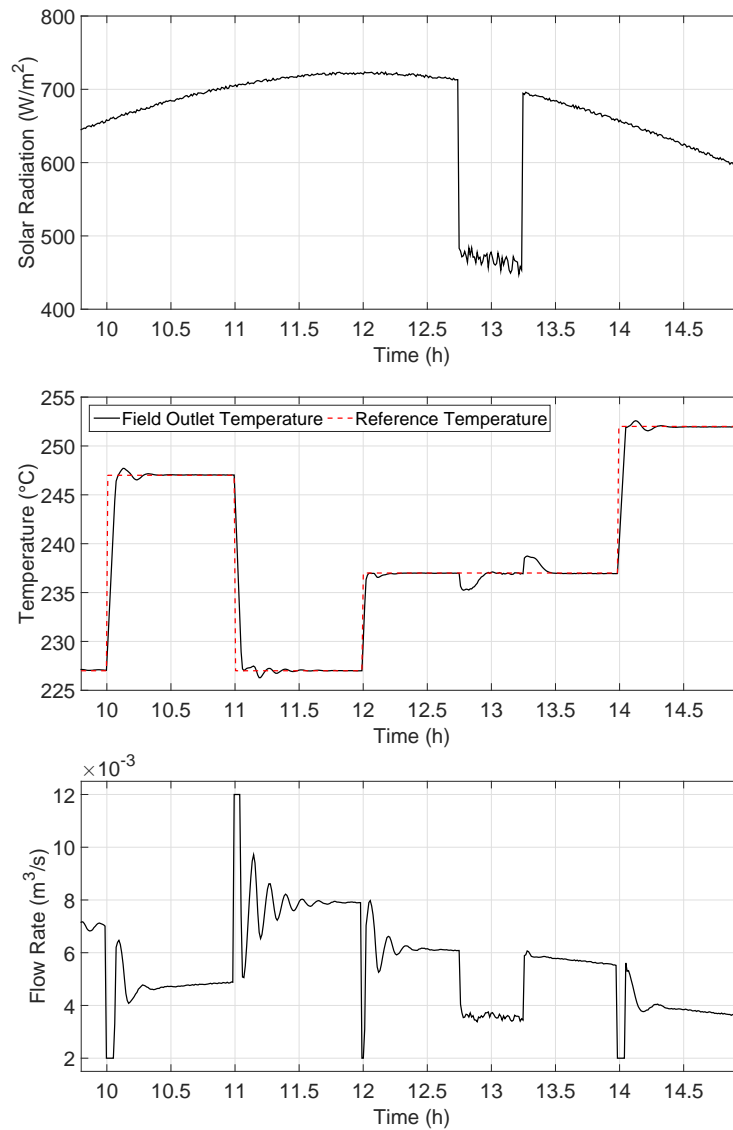


Figure C.6: Second scenario: simulation results for a passing cloud.

uation and comparison with alternatives, include the extension to a gain scheduling control strategy through the estimation of LTI state space models around different operating points and the design of the correspondent dual mode MPC controllers. There is also a need to develop algorithms which can incorporate and exploit feed-forward information in order to improve disturbance rejection.

## BIBLIOGRAPHY

- Álvarez, J., Yebra, L., and Berenguel, M. (2008). *Control strategies for thermal heat exchangers*. Editorial CIEMAT, Madrid, (in Spanish).
- Álvarez, J., Yebra, L., and Berenguel, M. (2009). Adaptive repetitive control for resonance cancellation of a distributed solar collector field. *International Journal of Adaptive Control and Signal Processing*, volume 23(4), 331–352.
- Aringhoff, R., Brakmann, G., Geyer, M., and Teske, S. (2005). Concentrated solar thermal power-now. *Greenpeace, Amsterdam, ESTIA, Brussels and SolarPACES, Aguadulce, Spain*.
- Camacho, E.F., Berenguel, M., and Rubio, F.R. (1997). *Advanced control of solar plants*. Springer-Verlag.
- Camacho, E.F., Berenguel, M., Rubio, F.R., and Martínez, D. (2012). *Control of solar energy systems*. Springer-Verlag.
- Camacho, E., Rubio, F., Berenguel, M., and Valenzuela, L. (2007a). A survey on control schemes for distributed solar collector fields. part i: Modeling and basic control approaches. *Solar Energy*, volume 81(10), 1240–1251.
- Camacho, E., Rubio, F., Berenguel, M., and Valenzuela, L. (2007b). A survey on control schemes for distributed solar collector fields. part ii: Advanced control approaches. *Solar Energy*, volume 81(10), 1252–1272.
- Favoreel, W., De Moor, B., and Van Overschee, P. (2000). Subspace state space system identification for industrial processes. *Journal of Process Control*, volume 10(2), 149–155.

- Goswami, D.Y., Kreith, F., and Kreider, J.F. (2000). *Principles of solar engineering*. CRC Press.
- IEA (2014). *Key world energy statistics*. International Energy Agency.
- Johansen, T.A., Hunt, K.J., and Petersen, I. (2000). Gain-scheduled control of a solar power plant. *Control Engineering Practice*, volume 8(9), 1011–1022.
- Ljung, L. (1995). *System identification toolbox: user's guide*. Citeseer.
- Meaburn, A. and Hughes, F. (1993). Resonance characteristics of distributed solar collector fields. *Solar Energy*, volume 51(3), 215–221.
- Philibert, C. (2010). *Technology roadmap: concentrating solar power*. OECD/IEA.
- Rossiter, J.A. (2003). *Model-based predictive control: a practical approach*. CRC press.
- Van Overschee, P. and De Moor, B. (1996). *Subspace identification for linear systems: Theory-Implementation-Applications*. Springer Science & Business Media.

Appendix D

**GAIN SCHEDULING DUAL MODE  
MPC FOR A SOLAR THERMAL  
POWER PLANT**

**Adham Alsharkawi and J. Anthony Rossiter**

This paper has been published in:  
Proceedings of the 10th IFAC Symposium on Nonlinear Control Systems.

*The layout has been revised.*

### **Abstract**

A nonlinear gain scheduling control strategy is proposed for a concentrated solar thermal power plant. The strategy involves the identification of local linear time-invariant state space models around a family of operating points, the design of corresponding local linear dual mode model-based predictive controllers and the selection of an appropriate scheduling variable to govern the switching. The local models are estimated directly from input-output data using a subspace identification method while taking into account the frequency response of the plant. Input-output data are obtained from a nonlinear simulation model of the plant rather than the plant itself. The effectiveness of the proposed control strategy in terms of tracking and disturbance rejection is evaluated through two different scenarios created in a nonlinear simulation environment.

### **Keywords**

Solar thermal power plant; Subspace identification; Resonant modes; Dual mode model-based predictive control; Nonlinear control; Gain scheduling.

### **D.1 Introduction**

The significant global rise in the consumption of electricity and fossil fuels (coal, oil and natural gas) since the early 1970s and hence the high levels of greenhouse gas emissions and their contribution to climate change (IEA, 2014) are all driving factors in the desire to develop clean and sustainable energy solutions. The US National Science Foundation in 1972 stated that “*Solar Energy is an essentially inexhaustible source potentially capable of meeting a significant portion of the nation’s future energy needs with a minimum of adverse environmental consequences... The indications are that solar energy is the most promising of the unconventional energy sources...*”.

Solar energy can be converted by thermal means into electrical energy using concentrated solar power (CSP) technology (Goswami et al., 2000). The application

of CSP technology is expected to have a major role in long-term energy supply and thus be a key element in power security (Aringhoff et al., 2005). Parabolic trough, linear Fresnel reflector, solar tower and parabolic dish are the most common types of CSP technology. These four share the same principle of operation; electricity is generated by converting solar energy into stored heat energy which in turn is used to drive a power cycle, for example a steam turbine or a heat engine (Philibert, 2010).

The scope of this paper will be limited to the application of parabolic trough technology. Parabolic trough stands out among the rest of the technologies as the most mature and reliable technology and indeed forms the bulk of current commercial CSP plants (Philibert, 2010).

The parabolic trough technology-based ACUREX plant is considered in this paper. ACUREX is one of the research facilities of the Plataforma Solar de Almería (PSA) in the province of Almeria in south-east Spain. The plant has provided opportunities for many researchers across academia and industry to explore the main dynamics of CSP technology and thus to evaluate various model forms and control strategies. A detailed description of the plant can be found in Camacho et al. (2012).

Collectors of parabolic trough technology are parabolic in shape and concentrate the incident solar radiation onto a receiver tube that is placed at its focal line. A heat transfer fluid (HTF) is heated as it flows through the receiver tube and circulates through a distributed solar collector field. The heated HTF then passes through a series of heat exchangers to produce steam which in turn is used to drive a steam turbine to generate electricity (Aringhoff et al., 2005). One of the biggest challenges of the process is to maintain the field outlet temperature at a desired level despite changes, mostly in solar radiation, field inlet temperature, or ambient temperature. This can be handled efficiently by manipulating the volumetric flow rate of the HTF through advanced control strategies (Camacho et al., 2012). A comprehensive survey of the modelling and control approaches for distributed solar collectors fields is presented in Camacho et al. (2007a,b).

In a previous work Alsharkawi and Rossiter (2016), it was argued that the plant

ACUREX possesses resonance characteristics, namely resonant modes and for a linear control system design, high order linear models are required to capture these dynamic characteristics and hence attain a high control performance. There is a need to overcome some of the drawbacks of the gain scheduling (GS) control strategies reported in Camacho et al. (1997); Johansen et al. (2000), where the plant resonant modes had been considered explicitly through the identification of high order linear models around a family of operating points. The drawbacks can be summarized as follows:

- Poor Pseudo-Random Binary Sequence (PRBS) design in Johansen et al. (2000), where the prior knowledge of the plant was not taken into account. The design of the frequency band and amplitude of the PRBS signal is not reported in Camacho et al. (1997).
- Local high order linear models were estimated from experimental data of the plant and hence an optimal model accuracy will never be achieved due to the slow dynamics of the plant and the fast changes in the operating conditions (e.g. solar radiation) within a limited time frame.
- Decomposition of the normal region of operation of the plant is selected in Johansen et al. (2000) such that the gain and time constant of the local models differ by less than a factor of 2 between any neighbouring regions. This relies on the big assumption that the local models are exactly correct at the centre points of their corresponding regions.
- Plant safety constraints were ignored in the control system design in Johansen et al. (2000) and poorly investigated in Camacho et al. (1997) when the field outlet temperature was restricted to not exceed a desired reference under any circumstances.

The first few steps towards an improved GS control strategy were carried out in Alsharkawi and Rossiter (2016), when a linear time-invariant (LTI) state space

model was estimated directly from input-output data around a nominal operating point through a subspace identification method and a corresponding local dual mode model-based predictive control (MPC) strategy was designed for tracking and disturbance rejection. This paper aims to continue the work started in Alsharkawi and Rossiter (2016) by estimating LTI state space models around a family of operating points and designing corresponding dual mode MPC controllers within a GS framework. The region of operation is decomposed in a more sophisticated manner through a best fit criterion and plant safety constraints are incorporated systematically and handled online over a wide range of operation.

This paper is organised as follows: mathematical models of the plant are described in Section D.2; Section D.3 is devoted to the phenomena of resonant modes and system identification; Section D.4 outlines the local dual mode MPC design and discusses the nonlinear GS control strategy. Section D.5 presents the simulation results for two commonplace scenarios and the main findings and some concluding remarks are presented in Section D.6.

## ***D.2 Mathematical Models***

This section gives a brief description of two mathematical models of the ACUREX plant: a nonlinear distributed parameter model for simulation purposes followed by a nonlinear lumped parameter model for control design purposes.

### *D.2.1 Nonlinear distributed parameter model*

The distributed solar collector field of the ACUREX plant consists of 480 single axis parabolic trough collectors which are arranged in 10 parallel loops each of length 172 m. The dynamic behaviour of the plant can be described by the following set of energy balance partial differential equations (PDEs):

$$\begin{aligned} \rho_m C_m A_m \frac{\partial T_m}{\partial t} &= n_o G I - D_o \pi H_l (T_m - T_a) - D_i \pi H_t (T_m - T_f), \\ \rho_f C_f A_f \frac{\partial T_f}{\partial t} + \rho_f C_f q \frac{\partial T_f}{\partial x} &= D_i \pi H_t (T_m - T_f), \end{aligned} \quad (\text{D.1})$$

where the subindex  $m$  refers to the metal of the receiver tube and  $f$  to the HTF (Carmacho et al., 2012). Table D.1 gives a description of all the variables and parameters and lists their SI units.

Table D.1: Variables and Parameters.

Symbol	Description	SI unit
$\rho$	Density	kg/m <sup>3</sup>
$C$	Specific heat capacity	J/kg°C
$A$	Cross-sectional area	m <sup>2</sup>
$T$	Temperature	°C
$t$	Time	s
$I$	Solar radiation	W/m <sup>2</sup>
$n_o$	Mirror optical efficiency	–
$G$	Mirror optical aperture	m
$D_o$	Outer diameter of the receiver tube	m
$H_l$	Global coefficient of thermal losses	W/m°C
$T_a$	Ambient temperature	°C
$D_i$	Inner diameter of the receiver tube	m
$H_t$	Metal-fluid heat transfer coefficient	W/m <sup>2</sup> °C
$q$	HTF volumetric flow rate	m <sup>3</sup> /s
$x$	Space	m

A nonlinear simulation model of the plant can be constructed by dividing the receiver tube into  $n$  ( $n = 1, 2, \dots$ ) segments each of length  $\Delta x$ , and hence the nonlinear distributed parameter model in (D.1) can be approximated by the following set of ordinary differential equations (ODEs):

$$\begin{aligned} \rho_m C_m A_m \frac{dT_{m,n}}{dt} &= n_o G I - D_o \pi H_l (T_{m,n} - T_a) - D_i \pi H_t (T_{m,n} - T_{f,n}), \\ \rho_f C_f A_f \frac{dT_{f,n}}{dt} + \rho_f C_f q \frac{T_{f,n} - T_{f,n-1}}{\Delta x} &= D_i \pi H_t (T_{m,n} - T_{f,n}), \end{aligned} \quad (\text{D.2})$$

with the boundary condition  $T_{f,0} = T_{f,inlet}$  (field inlet temperature) and  $H_l, H_t, \rho_f$  and  $C_f$  being time-varying.

It has been found in Alsharkawi and Rossiter (2016) that dividing the receiver tube into 7 segments is a reasonable trade-off between the prediction accuracy and computational burden while still adequate enough to capture the resonant modes of the plant. The nonlinear lumped parameter submodels in (D.2) are implemented and solved efficiently using the MATLAB<sup>®</sup> solver ODE45 (an explicit Runge-Kutta method) where the temperature distribution in the receiver tube and HTF can be easily accessed at any point in time and for any segment  $n$ .

### D.2.2 Nonlinear lumped parameter model

The dynamic behaviour of the ACUREX plant can also be described by a simple nonlinear lumped parameter model. Variation in the internal energy of the fluid can be described by:

$$C \frac{dT_f}{dt} = n_o S I - Q P_{cp} (T_f - T_{f,inlet}) - H_l (T_{mean} - T_a), \quad (D.3)$$

where  $S$  is the collectors solar field effective surface,  $Q$  is the HTF volumetric flow rate,  $P_{cp}$  is a factor that takes into account some geometrical and thermal properties and  $T_{mean}$  is the mean of  $T_f$  and  $T_{f,inlet}$  (Camacho et al., 2012).

## D.3 Resonant Modes and System Identification

The resonance phenomena of the ACUREX plant are described in Meaburn and Hughes (1993) as resonant modes that lie well within the desired control bandwidth. The phenomena arise due to the relatively slow flow rate of the HTF and the length of the receiver tube involved. It has also been found that the phenomena have a significant impact on the control performance and hence modelling the resonant modes sufficiently is crucial to ensure high control performance with adequate robustness.

One of the first steps towards an effective modelling of the resonant modes is a proper choice and design of excitation signals. Here PRBS-type excitation signals

were chosen. A PRBS is a deterministic binary signal with white noise like properties and ideally suited for linear identification. However, the white noise like properties are only valid for full-length PRBS signals with a clock period approximately equals the process sampling time (Zhu, 2001).

Since the dynamics of the ACUREX plant are mainly characterised by the flow rate of the HTF (Camacho et al., 2012), the nonlinear simulation model of the plant described by the system in (D.2) was excited with a set of full-length PRBS signals with an amplitude of  $0.0005 \text{ m}^3/\text{s}$  and a clock period equal to the process sampling time 39 s (the process time constant is around 6 min) around the operating points 0.004, 0.006, 0.008 and  $0.010 \text{ m}^3/\text{s}$ . The identification process assumed steady state operating conditions ( $I_{nom} = 674.75 \text{ W/m}^2$ ,  $T_{f,inlet,nom} = 183^\circ\text{C}$  and  $T_{a,nom} = 28^\circ\text{C}$ ) and used a data set of 1100 samples for each of the nominal operating points.

Compact local LTI state space models were identified around the nominal operating points using a subspace identification method (N4SID). Subspace identification methods are computationally efficient and overcome some of the major problems encountered in classical identification methods, i.e, parametrization, convergence and model reduction (Van Overschee and De Moor, 1996). The general form of a discrete-time LTI state space model is given as:

$$\begin{aligned} x_{k+1} &= Ax_k + Bu_k + \xi_k, \\ y_k &= Cx_k + Du_k + \eta_k, \end{aligned} \tag{D.4}$$

where  $x_k \in \mathbb{R}^{n \times 1}$ ,  $u_k \in \mathbb{R}^{m \times 1}$ ,  $y_k \in \mathbb{R}^{l \times 1}$ ,  $\xi_k \in \mathbb{R}^{n \times 1}$  and  $\eta_k \in \mathbb{R}^{l \times 1}$  are the state vector, input vector, output vector, process noise and measurement noise respectively at discrete time instant  $k$ .  $A, B, C$  and  $D$  are the coefficient matrices of appropriate dimensions.

The local models were estimated under the assumptions that there is no direct feedthrough from the input to the output ( $D = 0$ ) and the system is deterministic ( $\xi_k = \eta_k = 0$ ). Initial states were set to zero during the estimation process and the weighting scheme canonical variable algorithm (CVA) was used for the singular value decomposition (SVD). The N4SID method and the associated weighting scheme

CVA are discussed in Van Overschee and De Moor (1996) and Larimore (1990) respectively.

Model order was estimated for each of the local models by inspecting the singular values of a certain covariance matrix constructed from the observed data. Model order and best fit criterion are shown in Table D.2. Local models 1, 2, 3, and 4 refer to the nominal operating points around 0.004, 0.006, 0.008 and 0.010 m<sup>3</sup>/s respectively.

Table D.2: Model Order and Best Fit Criterion

Local model	Model order	Best fit criterion (%)
1	4 <sup>th</sup>	95.07
2	4 <sup>th</sup>	97.16
3	4 <sup>th</sup>	98.05
4	5 <sup>th</sup>	98.51

Since the estimated local LTI state space models are mainly used for prediction within the dual mode MPC control design, the simulated model output (infinite-step ahead prediction) is validated through a best fit criterion. The criterion is given in Ljung (1995) as:

$$Best\ fit = \left( 1 - \frac{\sum_{i=1}^n |y_i - \hat{y}_i|}{\sum_{i=1}^n |y_i - \bar{y}|} \right) \times 100, \quad (D.5)$$

where  $y$ ,  $\hat{y}$  and  $\bar{y}$  are the measured output, the simulated model output and the mean of the measured output respectively.

The best fit criterion in (D.5) reflects the ability of the estimated local models to reproduce the main dynamics of the plant at a given operating point and time horizon. From Table D.2, one can observe that the prediction accuracy is improved as the flow rate of the HTF is increased from 0.004 to 0.010 m<sup>3</sup>/s. This can be explained by the high nonlinearities of the plant at low flow rates (long residence

time of the HTF in the collectors solar field), which has been also noticed in Stirrup et al. (2001) when a fuzzy proportional-integral (PI) controller with feedforward term was developed for the highly nonlinear part of the plant whereas a GS control strategy was developed for the more linear part.

The estimated local models capture the phenomena of resonant modes adequately as validated by inspecting the Bode plots shown in Fig. D.1. One can clearly identify the resonant modes of the plant and observe the dependence of their frequencies on the flow rate of the HTF. Another observation is the changes in the steady state gain as the flow rate is increased from 0.004 to 0.010 m<sup>3</sup>/s.

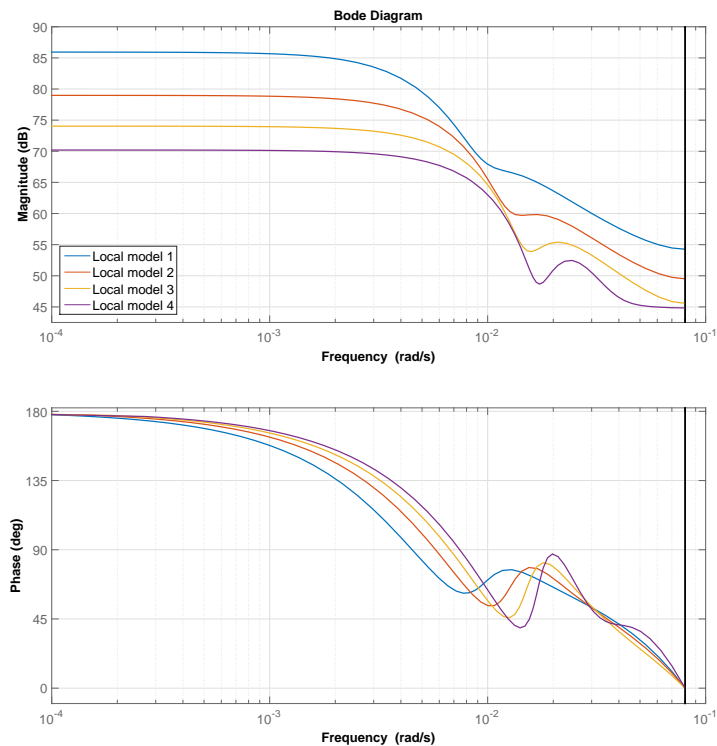


Figure D.1: Bode plot of the local LTI state space models.

In summary it should be emphasised that the estimated local state space models are less complex than the local ARX models presented in Camacho et al. (1997); Johansen et al. (2000) in terms of model order. However, for a fair comparison,

local ARX models similar to the ones used in Camacho et al. (1997); Johansen et al. (2000) were estimated using the same sets of data that had been used earlier to produce Table D.2. Model order was estimated for each of the local models through Akaike's information criterion (AIC). The order of the local ARX models in Table D.3 is significantly higher than the order of the local state space models in Table D.2 without having a serious impact on the prediction accuracy.

Table D.3: Model Order and Best Fit Criterion

Local model	Model order	Best fit criterion (%)
1	7 <sup>th</sup>	94.88
2	11 <sup>th</sup>	97.16
3	12 <sup>th</sup>	98.07
4	12 <sup>th</sup>	98.52

## D.4 Control Design

This section outlines the local dual mode MPC design and the nonlinear GS control strategy.

### D.4.1 Dual mode MPC

The term dual mode refers to a separation in the model predictions into transient (mode 1) and asymptotic (mode 2) predictions. The separation gives a handle on the predictions over an infinite horizon, where a simple linear feedback law can be implemented, thus allowing a reduction in the number of degrees of freedom (d.o.f) and constraints (Rossiter, 2003). For a deterministic version of the system in (D.4) and assuming no direct feedthrough, the deviation from the estimated steady state

values  $x_{ss}$ ,  $u_{ss}$  and  $y_{ss}$  can be expressed as:

$$\begin{aligned}\hat{x}_{k+1} &= A\hat{x}_k + B\hat{u}_k, \\ \hat{y}_k &= C\hat{x}_k.\end{aligned}\tag{D.6}$$

A standard dual mode cost function (online performance measure)  $J$  is given as:

$$J = \sum_{i=0}^{n_c-1} [\hat{x}_{k+1+i}^T \delta \hat{x}_{k+1+i} + \hat{u}_{k+i}^T \lambda \hat{u}_{k+i}] + \hat{x}_{k+n_c}^T P \hat{x}_{k+n_c},\tag{D.7}$$

where  $n_c$  is the number of free d.o.f.,  $\delta$  and  $\lambda$  are weighting matrices of appropriate dimensions and  $P$  is obtained from a Lyapunov equation of appropriate dimension. The cost function in (D.7) can be simplified to take the form of a standard quadratic programming problem with constraints and solved online as:

$$\min_{\hat{u}_{\rightarrow k-1}} \hat{u}_{\rightarrow k-1}^T S \hat{u}_{\rightarrow k-1} + \hat{u}_{\rightarrow k-1}^T L \hat{x}_k \quad \text{s.t.} \quad M \hat{u}_{\rightarrow k-1} \leq \gamma,\tag{D.8}$$

where  $\hat{u}_{\rightarrow k-1} = [\hat{u}_k \ \hat{u}_{k+1} \ \dots \ \hat{u}_{k+n_c-1}]^T$ ,  $S$  and  $L$  depend upon the matrices  $A$ ,  $B$ ,  $\delta$ ,  $\lambda$  and  $P$ ,  $M$  is time-invariant and  $\gamma$  depends upon the system past input-output information. Detailed treatment of the dual mode MPC and proper definitions of the various parameters can be found in Rossiter (2003).

#### D.4.2 Nonlinear GS control

GS is one of the most accepted nonlinear control design approaches which has found applications in many fields ranging from aerospace to process control (Leith and Leithead, 2000). GS control is usually seen as a way of thinking rather than a fixed design process and well-known for applying powerful linear design tools to challenging nonlinear problems (Rugh and Shamma, 2000). Moreover, implementation of MPC within a GS framework overcomes the major computational drawbacks of using nonlinear MPC which arise due to the non-convexity of the associated nonlinear optimization problem (Chisci et al., 2003).

The design workflow of the proposed nonlinear GS control strategy involves the designing and tuning of a nominal linear dual mode MPC controller around medium

operating conditions ( $0.006 \text{ m}^3/\text{s}$ ) and using simulations to determine the operating conditions at which the nominal controller loses robustness. Local LTI state space models around the new operating conditions were estimated and corresponding local linear dual mode MPC controllers were designed.

Having a scheduling variable to switch among the local linear dual mode MPC controllers as the plant dynamics change with time or operating conditions is an intrinsic part of the GS control strategy. Since the plant dynamics are mainly characterised by the flow rate of the HTF,  $Q$  (HTF volumetric flow rate) is used as the scheduling variable and obtained from the nonlinear lumped parameter model in (D.3).

Assuming steady state condition ( $\frac{dT_f}{dt} = 0$ ) and best case scenario ( $T_f = T_{f,ref}$  and  $H_l = 0$ ), where  $T_{f,ref}$  is the desired reference temperature, the model in (D.3) can be given as:

$$0 = n_o SI - Q P_{cp}(T_{f,ref} - T_{f,inlet}), \quad (\text{D.9})$$

which can be rewritten as:

$$Q = \frac{n_o SI}{P_{cp}(T_{f,ref} - T_{f,inlet})}. \quad (\text{D.10})$$

The relationship in (D.10) means that the scheduling variable  $Q$  is proportional to the solar radiation  $I$  and inversely proportional to the desired temperature change ( $T_{f,ref} - T_{f,inlet}$ ). Schematic diagram of the proposed GS control strategy is depicted in Fig. D.2.

Once the scheduling variable is obtained and the distinct nominal operating points are identified, the final step of the design process is to have a fine decomposition of the region of operation. In other words, the scheduling thresholds between the neighbouring local operating regions should be carefully selected so that optimal control performance is achieved. An appropriate local operating regions were identified after performing an extensive simulations, where the ability of each and every one of the local models of representing a potential thresholds was investigated through the best fit criterion in (D.5). Potential thresholds were identified

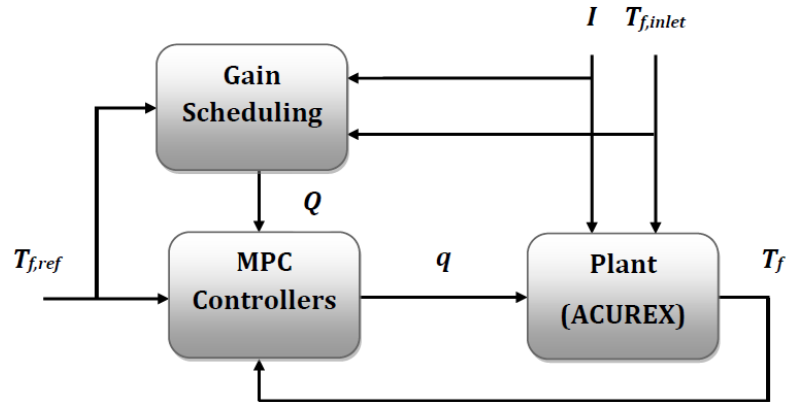


Figure D.2: GS control strategy.

following the same identification process discussed earlier in Section D.3. Scheduling thresholds  $0.00475 - \alpha$ ,  $0.00675 + \alpha$  and  $0.00875 + \alpha \text{ m}^3/\text{s}$  were found, where  $\alpha$  is an uncertainty factor of less than  $0.00025 \text{ m}^3/\text{s}$ . The decomposition that has been selected can be described by the following set of if-then rules:

*if*  $Q < 0.00475$ , *then*  
 $s = 1$ ,  
*if*  $0.00475 \leq Q \leq 0.00675$ , *then*  
 $s = 2$ ,  
*if*  $0.00675 < Q \leq 0.00875$ , *then*  
 $s = 3$ ,  
*if*  $Q > 0.00875$ , *then*  
 $s = 4$ ,

where the variable  $s$  is a switch that specifies when to switch from one local model to another and accordingly from one local controller to another.

## D.5 Simulation Results

The effectiveness of the proposed nonlinear GS control strategy is evaluated through two different simulation scenarios. The first scenario assumes a clear day with a mean solar radiation value of  $674.75 \text{ W/m}^2$ . This scenario intends to evaluate the control performance of the proposed control strategy in terms of tracking and the associated control action. For a meaningful evaluation and interpretation of the control strategy, the control performance is compared to that with a single local dual mode MPC controller. The second scenario on the other hand intends to evaluate the robustness of the proposed control strategy against a sudden change in the solar radiation (e.g. passing cloud). For both scenarios the plant is represented by the nonlinear simulation model described by the system in (D.2) with a slight increase to thermal losses in order to make the scenarios more realistic. Field inlet temperature ( $T_{in}$ ) and ambient temperature ( $T_a$ ) are kept fixed at  $189 \text{ }^\circ\text{C}$  and  $28 \text{ }^\circ\text{C}$  respectively. Even though this may not be the case in the normal operation of the plant, this is still a reasonable assumption during the steady state phase. The HTF is assumed to be the synthetic oil Therminol<sup>®</sup> 55 and constrained to the range  $0.002\text{--}0.012 \text{ m}^3/\text{s}$  where the minimum limit is normally for a safety reason. Exceeding a temperature of  $305 \text{ }^\circ\text{C}$  puts the synthetic oil at the risk of being decomposed. The difference between the field outlet and inlet temperature is also constrained not to exceed  $80 \text{ }^\circ\text{C}$  in order to avoid the risk of oil leakage (Camacho et al., 2012). The latter has been taken care of implicitly when the nominal operating points and the desired reference temperature were selected. The HTF flow rate constraints are considered explicitly in the control design process as will be demonstrated in the following two scenarios.

### D.5.1 First scenario—clear day

Fig. D.3 compares the control performance of the proposed GS control strategy with one of the local dual mode MPC controllers that was designed around the

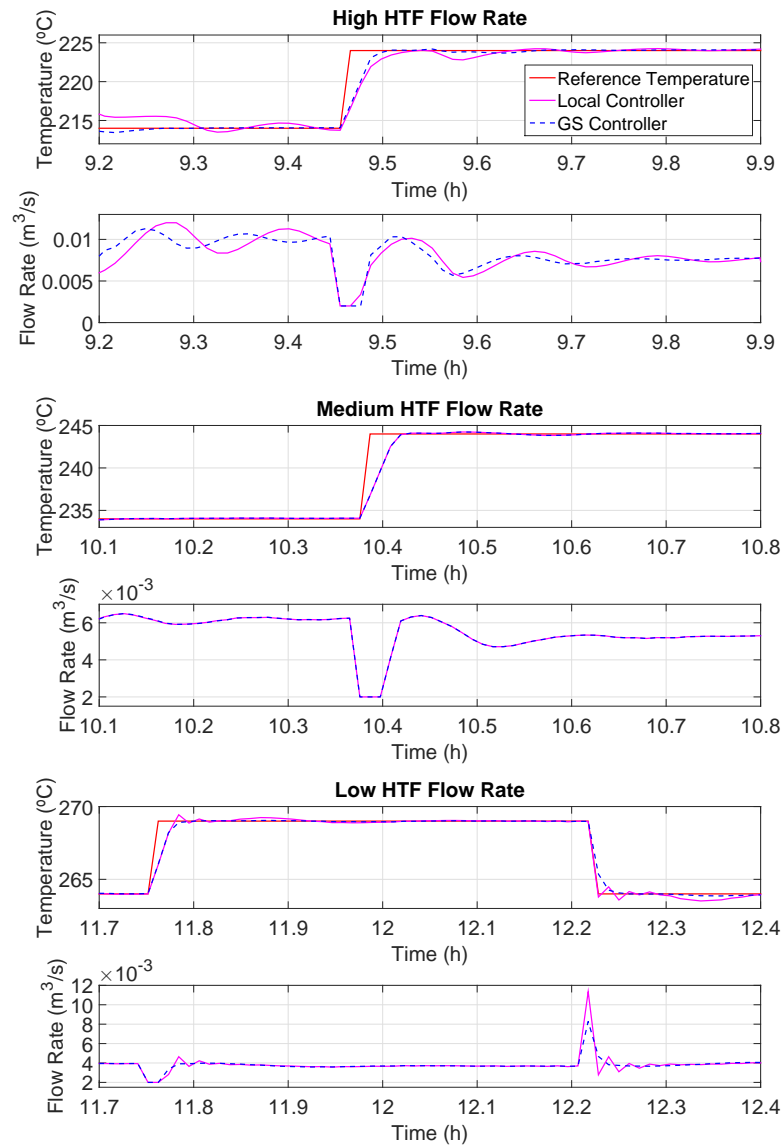


Figure D.3: First scenario: Control performance on a clear day.

nominal operating point  $0.006 \text{ m}^3/\text{s}$ . For a clear day with a slowly time-varying solar radiation, the reference tracking and the associated control action around high, medium and low HTF flow rate are presented.

The GS controller shows excellent performance, coping with the slowly time-varying solar radiation over the whole range of operation with fast transients, with no overshoot and handling the flow rate constraints efficiently. Conversely, the local

dual mode MPC controller performs well only in the region near the operating point where the corresponding linear model was identified (medium HTF flow rate). The oscillatory control performance of the local controller during high flow rates and the poor control performance during low flow rates with overshoot and severe control action can be seen clearly.

#### *D.5.2 Second scenario—cloudy day*

The second scenario investigates the effect of a passing cloud on the GS control performance. Clouds act as a disturbance to the plant and therefore must be properly rejected. For a clear day with a slowly time-varying solar radiation around the mean of  $674.75 \text{ W/m}^2$ , the cloud is simulated by an extreme situation through a sudden drop in radiation with a relatively high level of noise. The scenario as illustrated in Fig. D.4 starts with a typical plant operation where a smooth switching between the local controllers in order to cope with the changing dynamics can be observed clearly. During the steady state operation of the plant around the nominal operating point  $0.006 \text{ m}^3/\text{s}$  a passing and persistent cloud passes by. The cloud drives the HTF to be decreased to around the operating condition  $0.004 \text{ m}^3/\text{s}$  where it gets handled by the corresponding controller sufficiently.

### **D.6 Conclusion**

A GS dual mode MPC was developed in this paper to control the field outlet temperature of the ACUREX plant. The paper has continued the work started in Alsharkawi and Rossiter (2016) and extended some of the control strategies currently available in the literature. Specifically, compact LTI state space models around a family of operating points were estimated using a subspace identification method and corresponding dual mode MPC controllers within GS framework were designed. The estimated models have shown significant model order reduction when compared to the models available in the open literature while adequately capturing the phenomena of resonant modes. A fine decomposition of the plant region of operation

has also been achieved through a best fit criterion as well as a systematic and online handling of the plant safety constraints over a wide range of operation. Feasibility and effectiveness of the proposed control strategy is demonstrated through two different and commonplace scenarios. The control strategy is shown to perform very well for both tracking and disturbance rejection and indeed superior to a single local controller.

As a final remark regarding the resonant modes of the plant, it should be pointed out that low order ARX models are not expected to capture these phenomena. This is evident from the poor control performance in Rato et al. (1997); Pickhardt (1998) when 3<sup>rd</sup>-order ARX models were estimated online in an adaptive control strategy. However, it can also be argued that the inappropriate selection of the scheduling variable is also contributing to the poor control performance as the actual flow rate of the HTF has not been taken into account.

One interesting question for future study is whether performance could be improved with an effective incorporation of feedforward term; this is an area which has received relatively little attention in the MPC literature.

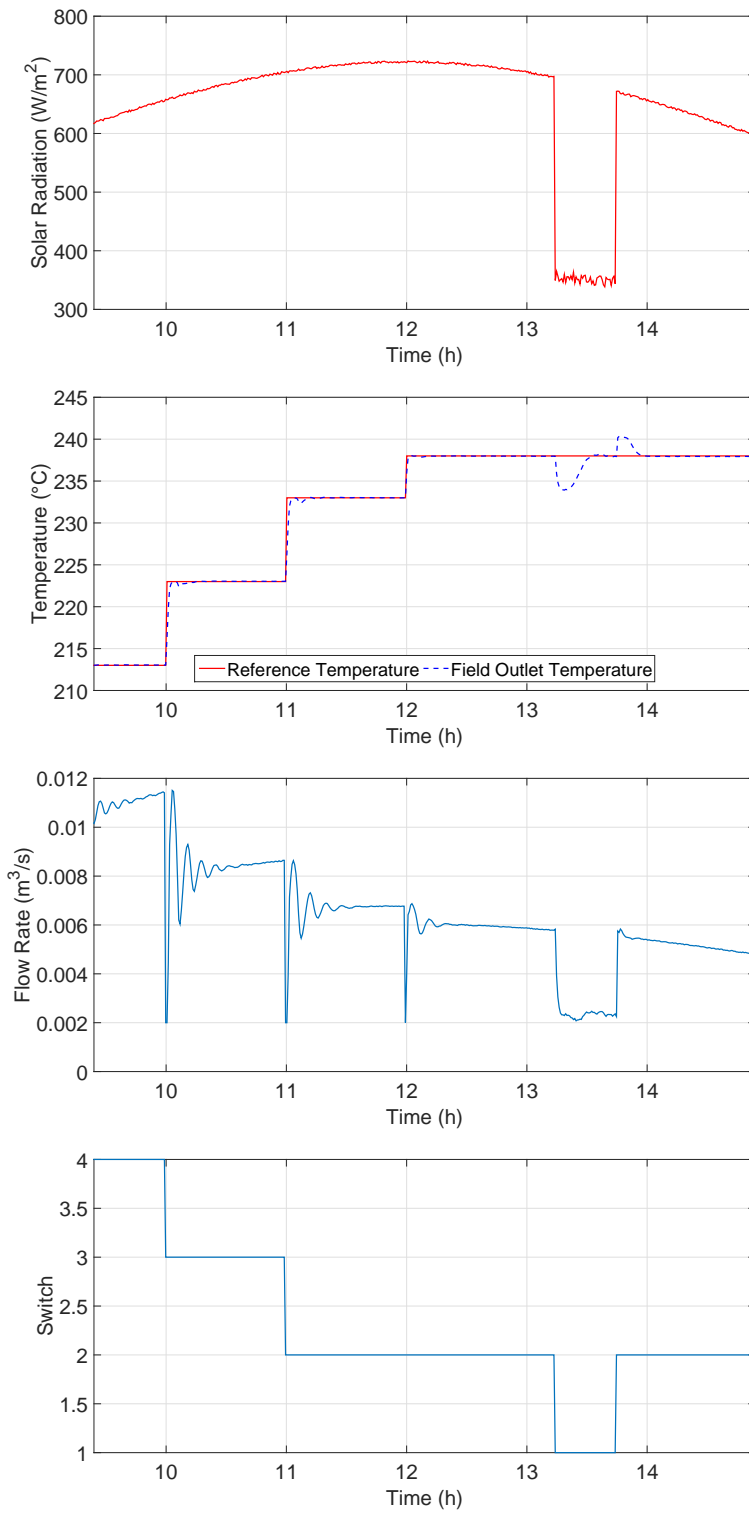


Figure D.4: Second scenario: control performance on a cloudy day.

# BIBLIOGRAPHY

- Alsharkawi, A. and Rossiter, J.A. (2016). Dual mode MPC for a concentrated solar thermal power plant. In *Proceedings of the 11th IFAC Symposium on Dynamics and Control of Process Systems, including Biosystems, Trondheim, Norway*, volume 49(7), 260–265. Elsevier.
- Aringhoff, R., Association, E.S.T.P.I., Agreement, I.S.I., et al. (2005). *Concentrated Solar Thermal Power-Now!* Greenpeace.
- Camacho, E.F., Berenguel, M., and Rubio, F.R. (1997). *Advanced control of solar plants*. Springer-Verlag.
- Camacho, E.F., Berenguel, M., Rubio, F.R., and Martínez, D. (2012). *Control of solar energy systems*. Springer-Verlag.
- Camacho, E., Rubio, F., Berenguel, M., and Valenzuela, L. (2007a). A survey on control schemes for distributed solar collector fields. part i: Modeling and basic control approaches. *Solar Energy*, volume 81(10), 1240–1251.
- Camacho, E., Rubio, F., Berenguel, M., and Valenzuela, L. (2007b). A survey on control schemes for distributed solar collector fields. part ii: Advanced control approaches. *Solar Energy*, volume 81(10), 1252–1272.
- Chisci, L., Falugi, P., and Zappa, G. (2003). Gain-scheduling MPC of nonlinear systems. *International Journal of Robust and Nonlinear Control*, volume 13(3-4), 295–308.
- Goswami, D.Y., Kreith, F., and Kreider, J.F. (2000). *Principles of solar engineering*. CRC Press.

- IEA (2014). *Key world energy statistics*. International Energy Agency.
- Johansen, T.A., Hunt, K.J., and Petersen, I. (2000). Gain-scheduled control of a solar power plant. *Control Engineering Practice*, volume 8(9), 1011–1022.
- Larimore, W.E. (1990). Canonical variate analysis in identification, filtering, and adaptive control. In *Proceedings of the 29th IEEE Conference on Decision and Control*, 596–604. IEEE.
- Leith, D.J. and Leithead, W.E. (2000). Survey of gain-scheduling analysis and design. *International Journal of Control*, volume 73(11), 1001–1025.
- Ljung, L. (1995). *System identification toolbox: user's guide*. Citeseer.
- Meaburn, A. and Hughes, F. (1993). Resonance characteristics of distributed solar collector fields. *Solar Energy*, volume 51(3), 215–221.
- Philibert, C. (2010). *Technology roadmap: concentrating solar power*. OECD/IEA.
- Pickhardt, R. (1998). Application of adaptive controllers to a solar power plant using a multi-model description. In *Proceedings of the American Control Conference*, volume 5, 2895–2899. IEEE.
- Rato, L., Borrelli, D., Mosca, E., Lemos, J., and Balsa, P. (1997). Musmar based switching control of a solar collector field. In *Proceedings of the European Control Conference*, volume 5, 991–996. IEEE.
- Rossiter, J.A. (2003). *Model-based predictive control: a practical approach*. CRC press.
- Rugh, W.J. and Shamma, J.S. (2000). Research on gain scheduling. *Automatica*, volume 36(10), 1401–1425.
- Stirrup, R., Loebis, D., Chipperfield, A., Tang, K., Kwong, S., and Man, K. (2001). Gain-scheduled control of a solar power plant using a hierarchical moga-tuned

- fuzzy pi-controller. In *Proceedings of the IEEE International Symposium on Industrial Electronics*, volume 1, 25–29. IEEE.
- Van Overschee, P. and De Moor, B. (2012). *Subspace identification for linear systems: Theory-Implementation-Applications*. Springer Science & Business Media.
- Zhu, Y. (2001). *Multivariable system identification for process control*. Elsevier.

Appendix E

**TOWARDS AN IMPROVED GAIN  
SCHEDULING PREDICTIVE  
CONTROL STRATEGY FOR A SOLAR  
THERMAL POWER PLANT**

**Adham Alsharkawi and J. Anthony Rossiter**

This paper has been accepted for publication in:  
IET Control Theory & Applications.

*The layout has been revised.*

### ***Abstract***

This paper improves a recently proposed gain scheduling predictive control strategy for the ACUREX distributed solar collector field at the Plataforma Solar de Almería, in south-east Spain. Measured disturbances are an integral part of the plant and while simple classical, series and parallel, feedforward approaches have been proposed and used extensively in the literature, the proposed approach incorporates a feedforward systematically into the predictive control strategy by including the effects of the measured disturbances of the ACUREX plant into the predictions of future outputs. Models of the measured disturbances are estimated around a family of operating points directly from input-output data and using a subspace identification method while taking into account the frequency response of the plant. Input-output data are obtained from a validated nonlinear simulation model of the plant rather than the plant itself. The nonlinear simulation model is validated here against measured data obtained from the ACUREX plant and the effectiveness of the proposed control approach is evaluated in the same nonlinear simulation environment. The paper also considers related issues like the significance of sufficient modelling of the measured disturbances of the ACUREX plant and the impact of incorporating the expected future behaviour of a measured disturbance along a given prediction horizon, a theme which has received little attention in the literature.

### ***E.1 Introduction***

ACUREX is a parabolic trough-based solar thermal power plant. It is one of the research facilities at the Plataforma Solar de Almería (PSA) owned and operated by the Spanish research centre for energy, environmental studies and technology (CIEMAT). ACUREX is mainly composed of a distributed solar collector field, a thermal storage tank and a power unit. The distributed solar collector field consists of 480 east-west single axis collectors arranged in 10 parallel loops with 48 collectors in each loop.

Collectors are parabolic in shape and concentrate the incident solar radiation onto a receiver tube that is placed at its focal line. A heat transfer fluid (HTF) is heated as it flows through the receiver tube and circulates through the distributed solar collector field. The heated HTF then passes through a series of heat exchangers to produce steam which in turn is used to drive a steam turbine to generate electricity. The control problem at the ACUREX plant is to maintain the field outlet temperature at a desired level despite changes, mainly in solar radiation and the field inlet temperature, by efficiently manipulating the volumetric flow rate of the HTF. For a detailed description of the plant, see Camacho et al. (2012).

#### *E.1.1 The use of feedforward with ACUREX*

Solar radiation and the field inlet temperature act as measured disturbances to the plant and hence it is not surprising that many feedforward approaches have been proposed over the years to compensate for their effects.

One of the early approaches can be traced back to the early nineties of the last century when two simple alternatives, series and parallel feedforward compensation, were proposed (Camacho et al., 1992). Both alternatives are derived from a nonlinear lumped parameter model of the ACUREX plant at steady-state conditions. Experimental data were used to determine some unknown parameters. A similar approach is proposed in Meaburn and Hughes (1997) to compensate for changes in solar radiation. A static version of a nonlinear model of the plant is used and two unknown parameters had to be found experimentally while the plant was in equilibrium using standard optimization techniques. Changes in the field inlet temperature are compensated for dynamically by simple transfer functions. Series and parallel feedforward compensation were assessed and it was found that in contrast to the series feedforward compensation, the parallel feedforward compensation resulted in poor set point tracking. In Silva et al. (1997), measurements of solar radiation and the field inlet temperature were used in an adaptive predictive control strategy. Measurements of solar radiation pass through a filter in an attempt to mitigate the fast

changes in solar radiation. The parallel feedforward compensation in Camacho et al. (1992) is used in Cardoso et al. (1999) for the design of a dynamic compensation of the field inlet temperature and a simple proportional compensation of solar radiation. The dynamic compensator includes a low pass filter and a delay term and the proportional compensator is based on the deviation of the measured solar radiation from an estimated value.

By the beginning of a new century, a static version of a model that describes the internal energy of the plant is used to compensate for changes in solar radiation and the field inlet temperature (Johansen and Storaa, 2002). A few years later, a feedforward based on steady-state energy balance was proposed in Cirre et al. (2009); the feedforward compensates for changes in solar radiation and the field inlet temperature and includes a field inlet-outlet temperature time delay. The time delay depends on the flow rate of the HTF and the length of the receiver tube. It is claimed that taking explicit account of the field inlet-outlet temperature time delay improves the feedforward capabilities in terms of compensating for changes in the field inlet temperature. In Álvarez et al. (2009) and after performing some simplifications and Taylor series expansions to a nonlinear distributed parameter model of the plant, transfer functions relating the dynamics of solar radiation and the field inlet temperature to the field outlet temperature are obtained. The transfer functions are used for the design of a classical parallel feedforward compensation. However, the use of the obtained transfer functions was not straightforward since they have exponential expressions that had to be simplified using a first order Padé approximation and, due to the noncausal nature of the obtained feedforward compensators, a causal version of the resulting compensators had to be implemented. More recently, changes in solar radiation are considered in Beschi et al. (2014) as a load disturbance and incorporated into a first order plus dead-time model of the plant. The effect of solar radiation is modelled as a gain times the variation of the current incident solar radiation with respect to an initial value of the incident solar radiation.

In Meaburn and Hughes (1993), it was argued that the ACUREX distributed

solar collector field possesses resonance characteristics, namely resonant modes that lie well within the desired control bandwidth and the resonance phenomena arise due to the relatively slow flow rate of the HTF and the length of the receiver tube involved. It was also found that these phenomena have a significant impact on the control performance and hence modelling the resonant modes sufficiently accurately is crucial to ensure high control performance with adequate robustness. More importantly however, it was noticed (using experimental data) that the dynamics relating the field outlet temperature to changes in solar radiation are similar to the dynamics relating the field outlet temperature to changes in the volumetric flow rate of the HTF and yet, none of the feedforward earlier approaches have explicitly appreciated this fact and utilised its potential for control implications.

#### *E.1.2 Paper contribution*

This paper aims to confirm the experimental findings in Meaburn and Hughes (1993) and then builds on this to show that also fast and abrupt changes in the field inlet temperature can excite the resonance dynamics of the plant. The paper also demonstrates that incorporating sufficient dynamic models of solar radiation and the field inlet temperature, that take explicit account of the resonance phenomena of the plant, can significantly improve the control performance during the transient phase, set point tracking and disturbance rejection. Finally, focus is given to an area that has received little or no attention in the literature by considering the impact of incorporating the *expected* future behaviour of a measured disturbance along a given prediction horizon.

In summary and taking into account the resonance characteristics of the ACUREX plant, the main contribution of this paper, is to improve a gain scheduling (GS) predictive control strategy proposed in Alsharkawi and Rossiter (2016b) by incorporating a systematic feedforward design to compensate for the measured disturbances, solar radiation and the field inlet temperature. The remainder of this paper is organised as follows: Nonlinear dynamic models of the plant are described

in Section E.2. Section E.3 is devoted to system identification and models of the measured disturbances. Section E.4 outlines the proposed model-based predictive control (MPC) design. Section E.5 shows some simulation results and discusses the main findings. Finally, concluding remarks are given in Section E.6.

## ***E.2 Nonlinear Dynamic Models of ACUREX***

This section presents a brief description of a nonlinear distributed parameter model which is used to construct a nonlinear simulation model of the ACUREX plant, followed by a simpler nonlinear lumped parameter model which is used to construct, at a given operating point, a local model of the measured disturbances, solar radiation and the field inlet temperature.

### *E.2.1 Nonlinear distributed parameter model*

The dynamic behaviour of the plant can be described by the following set of energy balance partial differential equations (PDEs):

$$\rho_m C_m A_m \frac{\partial T_m}{\partial t} = n_o G I - D_o \pi H_l (T_m - T_a) - D_i \pi H_t (T_m - T_f), \quad (\text{E.1a})$$

$$\rho_f C_f A_f \frac{\partial T_f}{\partial t} + \rho_f C_f q \frac{\partial T_f}{\partial x} = D_i \pi H_t (T_m - T_f), \quad (\text{E.1b})$$

where the subindex  $m$  refers to the metal of the receiver tube and  $f$  to the HTF (Carmona, 1985; Camacho et al., 2012). Table E.1 gives a description of all the variables and parameters and lists their SI units.

**Remark E.1.** *Issues related to modelling the thermal storage tank of the ACUREX plant are outside the scope of this paper, however, to gain understanding of how the storage component interacts with the other components of a solar thermal power plant, see Powell and Edgar (2012).*

Table E.1: Variables and Parameters

Symbol	Description	SI unit
$\rho$	Density	kg/m <sup>3</sup>
$C$	Specific heat capacity	J/kg°C
$A$	Cross-sectional area	m <sup>2</sup>
$T$	Temperature	°C
$t$	Time	s
$I$	Solar radiation	W/m <sup>2</sup>
$n_o$	Mirror optical efficiency	–
$G$	Mirror optical aperture	m
$D_o$	Outer diameter of the receiver tube	m
$H_l$	Global coefficient of thermal losses	W/m°C
$T_a$	Ambient temperature	°C
$D_i$	Inner diameter of the receiver tube	m
$H_t$	Metal-fluid heat transfer coefficient	W/m <sup>2</sup> °C
$q$	HTF volumetric flow rate	m <sup>3</sup> /s
$x$	Space	m

*Construction of a nonlinear simulation model*

A nonlinear simulation model of the plant was constructed in Alsharkawi and Rossiter (2016a) by dividing the receiver tube into  $N$  segments each of length  $\Delta x$  and hence the nonlinear distributed parameter model in (E.1) is approximated, for  $n = 1, \dots, N$ , by the following set of ordinary differential equations (ODEs) with the boundary condition  $T_{f,0} = T_{f,inlet}$  (field inlet temperature) and  $H_l, H_t, \rho_f$  and  $C_f$  being time-varying.

$$\rho_m C_m A_m \frac{dT_{m,n}}{dt} = n_o G I - D_o \pi H_l (T_{m,n} - T_a) - D_i \pi H_t (T_{m,n} - T_{f,n}), \quad (\text{E.2a})$$

$$\rho_f C_f A_f \frac{dT_{f,n}}{dt} + \rho_f C_f q \frac{T_{f,n} - T_{f,n-1}}{\Delta x} = D_i \pi H_t (T_{m,n} - T_{f,n}). \quad (\text{E.2b})$$

It was shown in Alsharkawi and Rossiter (2016a) that dividing the receiver tube into 7 segments gives a reasonable trade-off between prediction accuracy and computational burden while adequate enough to capture the resonant modes of the plant. For a detailed modelling analysis, see Alsharkawi and Rossiter (2017).

**Remark E.2.** *The set of ODEs in (E.2) is implemented and solved using the MATLAB<sup>®</sup> solver ODE45 (an explicit Runge-Kutta method) where the temperature distribution in the receiver tube and HTF can be accessed at any point in time and for any segment  $n$ . The number of ODEs solved at each sample time  $k$  for  $N$  segments is  $2 \times N$ .*

#### *Validation of the nonlinear simulation model*

The nonlinear simulation model proposed in (E.2) is validated in this paper against measured data obtained from the ACUREX plant which was collected on 15 July 2003 after a series of step changes in the volumetric flow rate of the HTF. During the data collection, the number of active loops was 9 and mirror optical efficiency ( $n_o$ ) was 56%.

Fig. E.1 shows the measured inputs (measured disturbances and manipulated variable) of the ACUREX plant and Fig. E.2 shows the measured output against model output. One can notice that the measured disturbances have experienced significant changes during the early stage of the flow rate changes and yet, the model output, as shown in Fig. E.2, is still able to capture the main dynamics with slight deviation from the measured output. Once the measured disturbances have almost settled, the model output can be clearly seen converging smoothly to the measured output. In summary, the nonlinear simulation model described by the system in (E.2) is accurate enough for simulation and analysis purposes.

**Remark E.3.** *It is worth noting that the field outlet temperature at the ACUREX plant is measured far away from the distributed solar collector field at the end of*

a return tube which implies slight changes to the dynamics at the distributed solar collector field and more importantly a variable dead-time. Hence, as the nonlinear simulation model represents the outlet temperature at the distributed solar collector field and for a fair comparison, the model output is validated against the outlet temperature of collector loop 5 which is located at the middle of the solar collector field and has the maximum temperature of the ten collector loops. More information about the variable dead-time problem can be found in Gálvez-Carrillo et al. (2009) along with other supplementary dynamics of the plant.

### E.2.2 Nonlinear lumped parameter model

The dynamic behaviour of the ACUREX plant can also be approximately described by a simple nonlinear lumped parameter model. Variation in the internal energy of the fluid can be described by:

$$C \frac{dT_f}{dt} = n_o S I - Q P_{cp} (T_f - T_{f,inlet}) - H_l (T_{mean} - T_a), \quad (E.3)$$

where  $S$  is the solar field effective surface,  $Q$  is the HTF volumetric flow rate,  $P_{cp}$  is a factor that takes into account some geometrical and thermal properties and  $T_{mean}$  is the mean of  $T_f$  and  $T_{f,inlet}$  (Carmona, 1985; Camacho et al., 2012).

**Remark E.4.** *At a given operating point, a local model of the measured disturbances of the ACUREX plant can be derived from first principles using the nonlinear lumped parameter model in (E.3). Under the assumptions that the volumetric flow rate of the HTF ( $q$ ) is no longer a variable (assuming steady-state condition) and with proper adjustment of the factor  $P_{cp}$  to compensate for the heat losses ( $H_l(T_{mean} - T_a)$ ), the variation of the internal energy of the fluid can be given as:*

$$\frac{dT_f}{dt} = C_1 T_f + C_2 I + C_3 T_{f,inlet}, \quad (E.4)$$

where  $C_1 = \frac{-Q P_{cp}}{C}$ ,  $C_2 = \frac{n_o S}{C}$  and  $C_3 = \frac{Q P_{cp}}{C}$ . The dynamic model in (E.4) is a typical first-order ordinary differential equation (ODE) with multiple inputs ( $I$  and  $T_{f,inlet}$ ) and single output ( $T_f$ ) which can be easily represented in a discrete-time state space form.

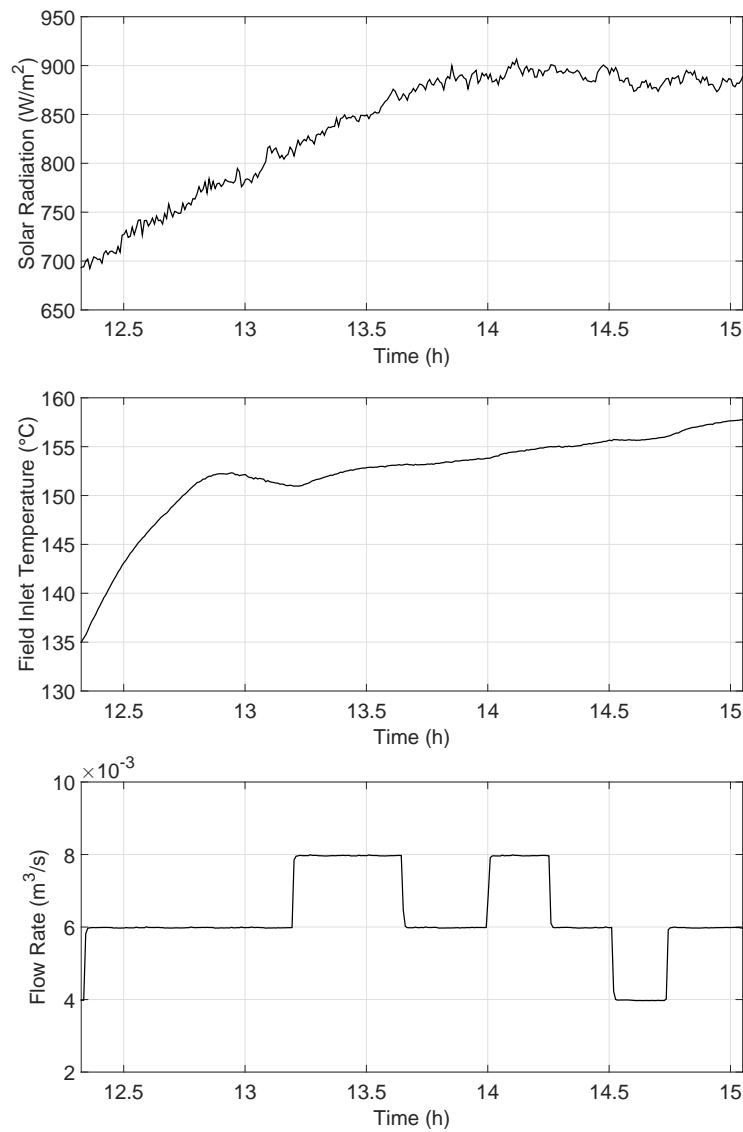


Figure E.1: Measured inputs to the ACUREX plant.

### ***E.3 System Identification and Models of the Measured Disturbances***

It was discussed in Section E.1 that the dynamics of the measured disturbances of the ACUREX plant have been underestimated in the literature. More specifically, the link between the resonant modes of the plant and the dynamics of the measured disturbances has not been fully appreciated. Hence, in this section, an effective mod-

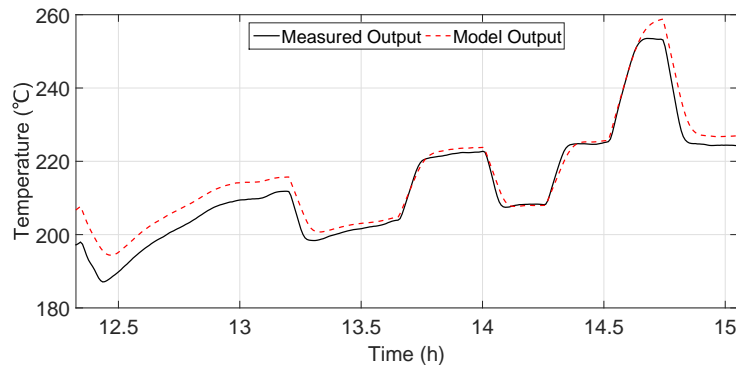


Figure E.2: Measured output against model output.

elling approach for the measured disturbances of the ACUREX plant is proposed. The proposed approach makes use of system identification and takes into account the frequency response of the plant.

### *E.3.1 System identification*

Due to the nonlinearity of the ACUREX plant, local LTI state space models relating the volumetric flow rate of the HTF ( $q$ ) to the field outlet temperature ( $T_f$ ) were estimated in Alsharkawi and Rossiter (2016b) directly from input-output data around the operating points  $q = 0.004, 0.006, 0.008$  and  $0.010 \text{ m}^3/\text{s}$ . Predictions of these models are improved here by estimating models of solar radiation ( $I$ ) and the field inlet temperature ( $T_{f,inlet}$ ) around the same operating points.

The nonlinear simulation model of the plant described by the system in (E.2) was excited with a set of full-length PRBS signals with a clock period equal to the process sampling time 39s (the process time constant is around 6 min). The identification process was carried out separately for solar radiation and the field inlet temperature and a data set of 1100 samples was used for each of the nominal operating points.

### E.3.2 Models of the measured disturbances

Compact local LTI state space models of solar radiation and the field inlet temperature were identified around the four nominal operating points using the subspace identification method N4SID (Van Overschee and De Moor, 1996). The general form of a discrete-time LTI state space model is given as:

$$\begin{aligned}x_{k+1} &= Ax_k + Bu_k + \xi_k, \\y_k &= Cx_k + Du_k + \eta_k,\end{aligned}\tag{E.5}$$

where  $x_k \in \mathbb{R}^{n \times 1}$ ,  $u_k \in \mathbb{R}^{m \times 1}$ ,  $y_k \in \mathbb{R}^{l \times 1}$ ,  $\xi_k \in \mathbb{R}^{n \times 1}$  and  $\eta_k \in \mathbb{R}^{l \times 1}$  are the state vector, input vector, output vector, process noise and measurement noise respectively at sampling instant  $k$ .  $A, B, C$  and  $D$  are the coefficient matrices of appropriate dimensions.

Models of solar radiation and the field inlet temperature were estimated under the assumptions that there is no direct feedthrough from the input to the output ( $D = 0$ ) and the system is deterministic ( $\xi_k = \eta_k = 0$ ). Model order was selected by inspecting the singular values of a covariance matrix constructed from the observed data.

Model order and best fit criterion are shown in Table E.2 for solar radiation and in Table E.3 for the field inlet temperature. Models 1, 2, 3, and 4 refer to the nominal operating points  $q = 0.004, 0.006, 0.008$  and  $0.010 \text{ m}^3/\text{s}$  respectively. The best fit criterion reflects the ability of an estimated model to reproduce the main dynamics of the plant at a given operating point and time horizon. The ability of an estimated model to capture the resonance dynamics of the plant is validated by inspecting the frequency response at a given operating point. Bode plots of the estimated models are shown in Fig. E.3 for solar radiation and in Fig. E.4 for the field inlet temperature and one can clearly identify the resonant modes of the plant and observe the dependence of their frequencies on the flow rate of the HTF.

As expected the dependence of the dynamics of the field outlet temperature on solar radiation is very similar to the dependence of the dynamics of the field outlet

temperature on the volumetric flow rate of the HTF and indeed fast and abrupt changes in the field inlet temperature can excite the resonance dynamics of the plant, especially at low flow rates.

Table E.2: Model Order and Best Fit Criterion ( $I$ )

Model	q (m <sup>3</sup> /s)	Model order	Best fit criterion (%)
1	0.004	4 <sup>th</sup>	97.97
2	0.006	4 <sup>th</sup>	98.51
3	0.008	5 <sup>th</sup>	98.77
4	0.010	5 <sup>th</sup>	98.91

Table E.3: Model Order and Best Fit Criterion ( $T_{f,inlet}$ )

Model	q (m <sup>3</sup> /s)	Model order	Best fit criterion (%)
1	0.004	5 <sup>th</sup>	96.56
2	0.006	7 <sup>th</sup>	97.48
3	0.008	7 <sup>th</sup>	97.91
4	0.010	7 <sup>th</sup>	98.16

### *E.3.3 An insight into the resonant modes*

One of the aims of this paper is to confirm the experimental findings in Meaburn and Hughes (1993) and show that the dynamics relating the field outlet temperature to changes in solar radiation are adequately captured using the system identification approach. Fig. E.5 shows the normalised frequency responses of the field outlet temperature for changes in the volumetric flow rate of the HTF (Model  $\alpha$ ) and solar radiation (Model  $\beta$ ) around the operating point 0.006 m<sup>3</sup>/s and one can clearly see that both responses are almost identical within the Nyquist bandwidth. This

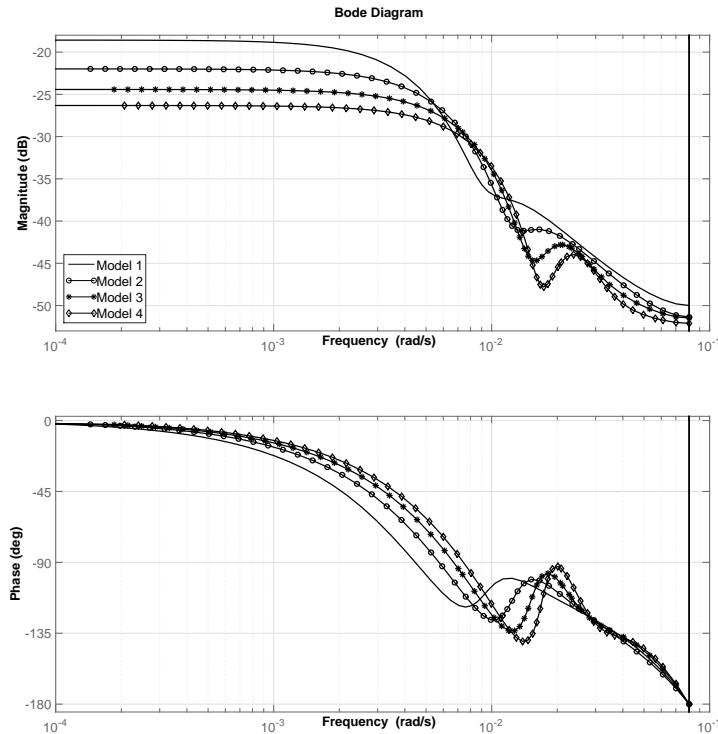


Figure E.3: Bode plot: Estimated models of solar radiation.

confirms the experimental findings in Meaburn and Hughes (1993) and shows that indeed the resonant modes have been adequately captured by the estimated model of solar radiation.

Estimated models of solar radiation and the field inlet temperature around a given operating point, can also be used to demonstrate that the dynamics of the measured disturbances have been underestimated in the literature and simple models derived from first principles and based on steady-state condition are not adequate enough to capture the actual dynamics of these measured disturbances. Fig. E.6 shows the frequency responses of the field outlet temperature for changes in solar radiation and the field inlet temperature around the operating point  $0.006 \text{ m}^3/\text{s}$ . Model  $\gamma$  is a discrete-time state space representation of the dynamic model in (E.4) and Model  $\omega$  is an augmented model of solar radiation and the field inlet temperature

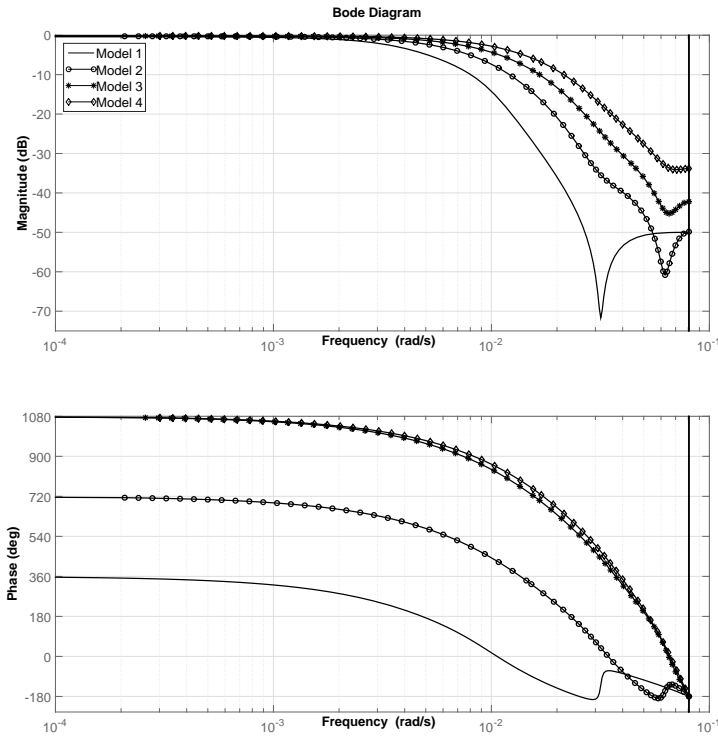


Figure E.4: Bode plot: Estimated models of the field inlet temperature.

obtained through system identification. The simplistic dynamics of Model  $\gamma$  are quite apparent and the impact of this on the control performance will be illustrated in a later section.

#### E.4 Control Design

A predictive control strategy, namely dual mode MPC is proposed in Rossiter (2003) for the deterministic state space case and used in Alsharkawi and Rossiter (2016b) within a gain scheduling framework. The term dual mode refers to a separation in the model predictions into transient (mode 1) and asymptotic (mode 2) predictions. The separation gives a handle on the predictions over an infinite horizon, where a simple linear feedback law can be implemented, thus allowing a reduction in the

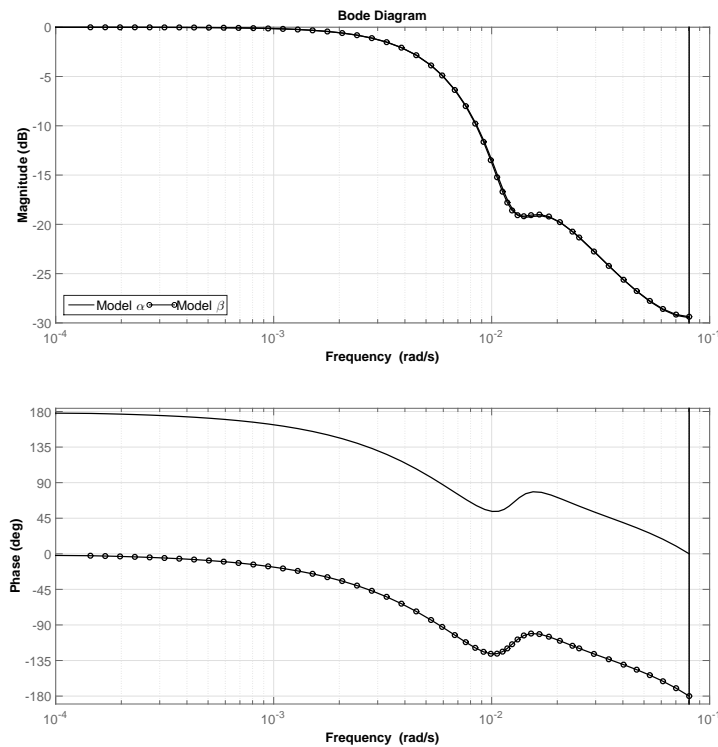


Figure E.5: Frequency responses of the field outlet temperature for changes in the volumetric flow rate of the HTF (Model  $\alpha$ ) and solar radiation (Model  $\beta$ ) around a given operating point.

number of degrees of freedom (or optimisation variables) and constraints (Rossiter, 2003). In this section, the dual mode MPC is extended to include the effects of the measured disturbances of the ACUREX plant.

#### E.4.1 Dual mode MPC

As mentioned earlier, the main contribution of this paper is to improve the GS predictive control strategy proposed in Alsharkawi and Rossiter (2016b), where local dual mode MPC controllers were designed around the nominal operating points  $q = 0.004, 0.006, 0.008$  and  $0.010 \text{ m}^3/\text{s}$ .

Having a scheduling variable to switch among the local linear dual mode MPC

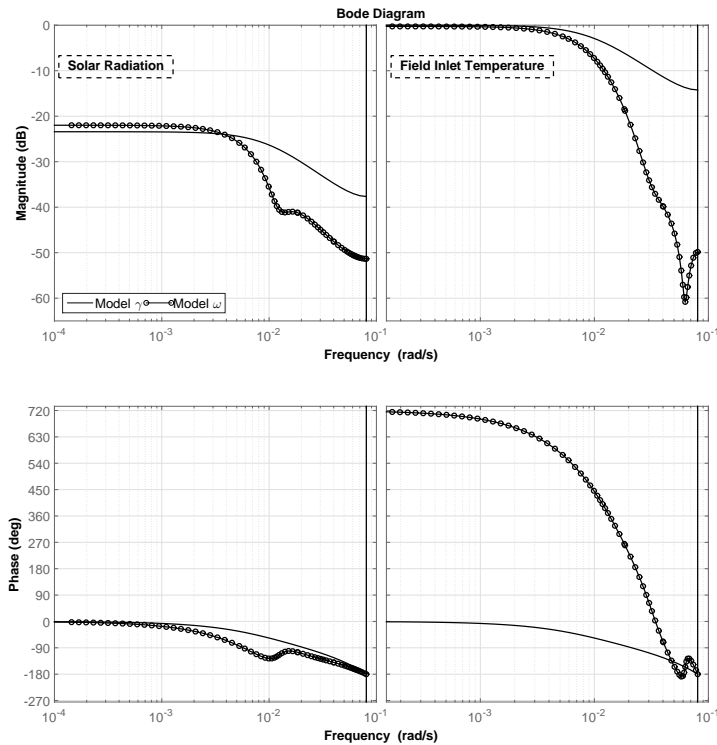


Figure E.6: Frequency responses of the field outlet temperature for changes in solar radiation and the field inlet temperature obtained through two different approaches around a given operating point.

controllers as the plant dynamics change with time or operating conditions is an intrinsic part of the GS predictive control strategy in Alsharkawi and Rossiter (2016b). Since the plant dynamics are mainly characterised by the volumetric flow rate of the HTF (Camacho et al., 2012) and given the lumped nonlinear dynamic model in (E.3), the scheduling variable, under certain assumptions, takes the following form:

$$Q = \frac{n_o SI}{P_{cp}(T_{ref} - T_{f,inlet})}, \quad (E.6)$$

where  $Q$  here is an approximate representation of the volumetric flow rate (control signal)  $q$  and  $T_{ref}$  is the desired reference temperature. For further details on this, see Alsharkawi and Rossiter (2016b). The design steps of each of the local controllers

can be summarised as follows <sup>1</sup>:

- For a deterministic version of the system in (E.5) and assuming no direct feedthrough from the input to the output, the deviations  $\bar{x}_k, \bar{y}_k, \bar{u}_k$  from some an estimated steady-state values  $x_{ss}, u_{ss}$  and  $y_{ss}$  can be expressed as:

$$\bar{x}_{k+1} = A\bar{x}_k + B\bar{u}_k, \quad \bar{y}_k = C\bar{x}_k. \quad (\text{E.7})$$

- Hence, a standard dual mode cost function (online performance measure)  $J$  is given as (Rossiter, 2003):

$$J = \sum_{i=0}^{n_c-1} [\bar{x}_{k+1+i}^T \delta \bar{x}_{k+1+i} + \bar{u}_{k+i}^T \lambda \bar{u}_{k+i}] + \bar{x}_{k+n_c}^T P \bar{x}_{k+n_c}, \quad (\text{E.8})$$

where  $n_c$  is the number of free d.o.f.,  $\delta$  and  $\lambda$  are weighting matrices of appropriate dimensions and  $P$  is the terminal weight obtained from an appropriate Lyapunov equation.

- Optimisation of the cost function in (E.8) subject to system predictions meeting constraints can be simplified (details omitted as standard in the literature) to take the form of a quadratic programming problem and solved online as:

$$\min_{\substack{\bar{u} \\ \rightarrow}} \bar{u}_{\rightarrow k-1}^T S \bar{u}_{\rightarrow k-1} + \bar{u}_{\rightarrow k-1}^T L \bar{x}_k, \quad \text{s.t.} \quad \beta \bar{u}_{\rightarrow} \leq \gamma, \quad (\text{E.9})$$

where  $\bar{u}_{\rightarrow k-1}$  is the vector of control moves:

$$\begin{bmatrix} \bar{u}_k \\ \bar{u}_{k+1} \\ \vdots \\ \bar{u}_{k+n_c-1} \end{bmatrix}, \quad (\text{E.10})$$

$S$  and  $L$  depend upon the matrices  $A, B, \delta, \lambda$  and  $P, \beta$  is time-invariant and  $\gamma$  depends upon the system past input-output information.

---

<sup>1</sup>Detailed treatment of dual mode MPC, variable definitions and parameters can be found in Rossiter (2003).

The design steps can be summarised by the following LMPC algorithm. Note that the LMPC can be easily modified to cover a wide range of operation through gain scheduling (Alsharkawi and Rossiter, 2016b), and hence we can also define the GSMPC algorithm.

---

Local dual mode MPC (LMPC)

---

- 1: Given an operating point and the local process model in (E.7), define the parameters in (E.9).
  - 2: At each sampling instant, perform the optimization in (E.9).
  - 3: Solve for the first element of  $\bar{u}_{\rightarrow}$  and implement on process.
- 

---

GS dual mode MPC (GSMPC)

---

- 1: For each of the nominal operating points and given the local process model in (E.7), define the parameters in (E.9)
  - 2: For a selected local controller and at each sampling instant, perform the optimization in (E.9).
  - 3: Solve for the first element of  $\bar{u}_{\rightarrow}$  and implement on process.
- 

The LMPC and GSMPC algorithms are improved next by including the dynamics of the measured disturbances.

*E.4.2 Feedforward dual mode MPC*

Slight but essential modifications are required to include the dynamics of the measured disturbances in the local process model (E.7).

**Remark E.5.** *The local process model in (E.7) can be augmented to include the*

disturbance dynamics as follows:

$$\underbrace{\begin{bmatrix} \bar{x}_{k+1} \\ \bar{x}_{k+1}^{d_1} \\ \bar{x}_{k+1}^{d_2} \end{bmatrix}}_{\bar{z}_{k+1}} = \underbrace{\begin{bmatrix} A & 0 & 0 \\ 0 & A^{d_1} & 0 \\ 0 & 0 & A^{d_2} \end{bmatrix}}_{\bar{A}} \underbrace{\begin{bmatrix} \bar{x}_k \\ \bar{x}_k^{d_1} \\ \bar{x}_k^{d_2} \end{bmatrix}}_{\bar{z}_k} + \underbrace{\begin{bmatrix} B & 0 & 0 \\ 0 & B^{d_1} & 0 \\ 0 & 0 & B^{d_2} \end{bmatrix}}_{\bar{B}} \begin{bmatrix} \bar{u}_k \\ \bar{d}_{1k} \\ \bar{d}_{2k} \end{bmatrix}, \quad (\text{E.11})$$

$$\bar{\psi}_k = \underbrace{\begin{bmatrix} C & C^{d_1} & C^{d_2} \end{bmatrix}}_{\bar{C}} \underbrace{\begin{bmatrix} \bar{x}_k \\ \bar{x}_k^{d_1} \\ \bar{x}_k^{d_2} \end{bmatrix}}_{\bar{z}_k},$$

where the subindices  $d_1$  and  $d_2$  indicate that the system has two measured disturbances.  $\bar{d}_1$  and  $\bar{d}_2$  at sample time  $k$  are the deviations of the measured disturbances  $d_1$  and  $d_2$  from some an estimated steady-state values  $d_{1ss}$  and  $d_{2ss}$  respectively.

Appropriate modifications to the dual mode cost function in (E.8) and consequently the optimisation in (E.9) depend upon the assumptions made about the future of the measured disturbances.

**Theorem E.1.** *If the expected future behaviour of the measured disturbances  $d_1$  and  $d_2$  along a given prediction horizon is considered and given the augmented local process model in (E.11), then the optimisation in (E.9) is extended as follows:*

$$\min_{\bar{u}} \quad \bar{u}_{\rightarrow k-1}^T S \bar{u}_{\rightarrow k-1} + \bar{u}_{\rightarrow k-1}^T L \bar{z}_k + \bar{u}_{\rightarrow k-1}^T M \bar{d}_{1\rightarrow k-1} + \bar{u}_{\rightarrow k-1}^T N \bar{d}_{2\rightarrow k-1}, \quad \text{s.t.} \quad \beta \bar{u}_{\rightarrow} \leq \gamma, \quad (\text{E.12})$$

where  $S$  and  $L$  in this case depend upon the matrices  $\bar{A}$ ,  $B$ ,  $\delta$ ,  $\lambda$  and  $P$ ,  $M$  depends upon the matrices  $\bar{A}$ ,  $B$ ,  $B^{d_1}$ ,  $\delta$  and  $P$ , and similarly  $N$  depends upon the matrices  $\bar{A}$ ,  $B$ ,  $B^{d_2}$ ,  $\delta$  and  $P$ .

*Proof.* Under the assumption that the first  $n_c$  control moves are free and that the

remaining moves are given by a fixed feedback law, let the predictions be:

$$\begin{aligned}
 z_{k+i} &= \bar{A}z_{k+i-1} + Bu_{k+i-1} + B^{d_1}d_{1k+i-1} \\
 &+ B^{d_2}d_{2k+i-1}, \quad u_{k+i-1} \text{ are d.o.f.}, \quad i = 1, \dots, n_c, \\
 z_{k+i} &= [\bar{A} - BK]z_{k+i-1} + B^{d_1}d_{1k+i-1} \\
 &+ B^{d_2}d_{2k+i-1}, \quad u_{k+i-1} = -Kz_{k+i-1}, \quad i > n_c.
 \end{aligned} \tag{E.13}$$

Now given some steady-state estimates  $z_{ss}$ ,  $u_{ss}$ ,  $d_{1ss}$  and  $d_{2ss}$  and under the assumption that  $d_{1k+i-1} = d_{1ss}$  and  $d_{2k+i-1} = d_{2ss}$ ,  $\forall i > n_c$ , then the deviation of  $z_{k+i}$ ,  $\forall i$  can be expressed as:

$$\begin{aligned}
 \bar{z}_{k+i} &= \bar{A}\bar{z}_{k+i-1} + B\bar{u}_{k+i-1} + B^{d_1}\bar{d}_{1k+i-1} \\
 &+ B^{d_2}\bar{d}_{2k+i-1}, \quad i = 1, \dots, n_c, \\
 \bar{z}_{k+i} &= [\bar{A} - BK]\bar{z}_{k+i-1}, \quad i > n_c,
 \end{aligned} \tag{E.14}$$

and hence, it is convenient to separate the cost:

$$J = \sum_{i=0}^{\infty} \bar{z}_{k+1+i}^T \delta \bar{z}_{k+1+i} + \bar{u}_{k+i}^T \lambda \bar{u}_{k+i}, \tag{E.15}$$

into two parts as follows:

$$\begin{aligned}
 J &= J_1 + J_2; \\
 J_1 &= \sum_{i=0}^{n_c-1} \bar{z}_{k+1+i}^T \delta \bar{z}_{k+1+i} \\
 &+ \bar{u}_{k+i}^T \lambda \bar{u}_{k+i}, \\
 J_2 &= \sum_{i=0}^{\infty} \bar{z}_{k+n_c+1+i}^T \delta \bar{z}_{k+n_c+1+i} \\
 &+ \bar{u}_{k+n_c+i}^T \lambda \bar{u}_{k+n_c+i}.
 \end{aligned} \tag{E.16}$$

Note that one can form the whole vector of future predictions up to a horizon  $n_c$  as follows:

$$\underbrace{\begin{bmatrix} \bar{z}_{k+1} \\ \bar{z}_{k+2} \\ \vdots \\ \bar{z}_{k+n_c} \end{bmatrix}}_{\bar{z}_{\rightarrow k}} = \underbrace{\begin{bmatrix} \bar{A} \\ \bar{A}^2 \\ \vdots \\ \bar{A}^{n_c} \end{bmatrix}}_{W_x} \bar{z}_k + \underbrace{\begin{bmatrix} B & 0 & \dots \\ \bar{A}B & B & \dots \\ \vdots & \vdots & \vdots \\ \bar{A}^{n_c-1}B & \bar{A}^{n_c-2}B & \dots \end{bmatrix}}_{H_x} \tag{E.17}$$

$$\begin{aligned}
& \underbrace{\begin{bmatrix} \bar{u}_k \\ \bar{u}_{k+1} \\ \vdots \\ \bar{u}_{k+n_c-1} \end{bmatrix}}_{\bar{u}_{\rightarrow k-1}} + \underbrace{\begin{bmatrix} B^{d_1} & 0 & \cdots \\ \bar{A}B^{d_1} & B^{d_1} & \cdots \\ \vdots & \vdots & \vdots \\ \bar{A}^{n_c-1}B^{d_1} & \bar{A}^{n_c-2}B^{d_1} & \cdots \end{bmatrix}}_{F_x} \\
& \underbrace{\begin{bmatrix} \bar{d}_{1k} \\ \bar{d}_{1k+1} \\ \vdots \\ \bar{d}_{1k+n_c-1} \end{bmatrix}}_{\bar{d}_1_{\rightarrow k-1}} + \underbrace{\begin{bmatrix} B^{d_2} & 0 & \cdots \\ \bar{A}B^{d_2} & B^{d_2} & \cdots \\ \vdots & \vdots & \vdots \\ \bar{A}^{n_c-1}B^{d_2} & \bar{A}^{n_c-2}B^{d_2} & \cdots \end{bmatrix}}_{G_x} \underbrace{\begin{bmatrix} \bar{d}_{2k} \\ \bar{d}_{2k+1} \\ \vdots \\ \bar{d}_{2k+n_c-1} \end{bmatrix}}_{\bar{d}_2_{\rightarrow k-1}}.
\end{aligned}$$

Hence, substituting (E.17) into  $J_1$  in (E.16) gives:

$$\begin{aligned}
J_1 &= [W_x \bar{z}_k + H_x \bar{u}_{\rightarrow k-1} + F_x \bar{d}_1_{\rightarrow k-1} + G_x \bar{d}_2_{\rightarrow k-1}]^T \\
& \text{diag}(\delta) [W_x \bar{z}_k + H_x \bar{u}_{\rightarrow k-1} + F_x \bar{d}_1_{\rightarrow k-1} + G_x \bar{d}_2_{\rightarrow k-1}] \\
& + \bar{u}_{\rightarrow k-1}^T \text{diag}(\lambda) \bar{u}_{\rightarrow k-1},
\end{aligned} \tag{E.18}$$

and according to Rossiter (2003):

$$\begin{aligned}
J_2 &= [W_{nc} \bar{z}_k + H_{nc} \bar{u}_{\rightarrow k-1} + F_{nc} \bar{d}_1_{\rightarrow k-1} + G_{nc} \bar{d}_2_{\rightarrow k-1}]^T \\
& P [W_{nc} \bar{z}_k + H_{nc} \bar{u}_{\rightarrow k-1} + F_{nc} \bar{d}_1_{\rightarrow k-1} + G_{nc} \bar{d}_2_{\rightarrow k-1}],
\end{aligned} \tag{E.19}$$

where  $W_{nc}$ ,  $H_{nc}$ ,  $F_{nc}$  and  $G_{nc}$  are the  $nc^{th}$  block rows of  $W_x$ ,  $H_x$ ,  $F_x$  and  $G_x$  respectively. Finally one can combine  $J_1$  and  $J_2$  from (E.18) and (E.19) to give:

$$\begin{aligned}
J &= [W_x \bar{z}_k + H_x \bar{u}_{\rightarrow k-1} + F_x \bar{d}_1_{\rightarrow k-1} + G_x \bar{d}_2_{\rightarrow k-1}]^T \text{diag}(\delta) \\
& [W_x \bar{z}_k + H_x \bar{u}_{\rightarrow k-1} + F_x \bar{d}_1_{\rightarrow k-1} + G_x \bar{d}_2_{\rightarrow k-1}] + \bar{u}_{\rightarrow k-1}^T \\
& \text{diag}(\lambda) \bar{u}_{\rightarrow k-1} + [W_{nc} \bar{z}_k + H_{nc} \bar{u}_{\rightarrow k-1} + F_{nc} \bar{d}_1_{\rightarrow k-1} \\
& + G_{nc} \bar{d}_2_{\rightarrow k-1}]^T P [W_{nc} \bar{z}_k + H_{nc} \bar{u}_{\rightarrow k-1} + F_{nc} \bar{d}_1_{\rightarrow k-1} \\
& + G_{nc} \bar{d}_2_{\rightarrow k-1}],
\end{aligned} \tag{E.20}$$

which can be simplified to:

$$\begin{aligned}
 J = & \underbrace{\bar{u}_{\rightarrow k-1}^T [H_x^T \text{diag}(\delta) H_x + \text{diag}(\lambda) + H_{nc}^T P H_{nc}] \bar{u}_{\rightarrow k-1}}_S \\
 & + \underbrace{\bar{u}_{\rightarrow k-1}^T 2[H_x^T \text{diag}(\delta) W_x + H_{nc}^T P W_{nc}] \bar{z}_k}_L \\
 & + \underbrace{\bar{u}_{\rightarrow k-1}^T 2[H_x^T \text{diag}(\delta) F_x + H_{nc}^T P F_{nc}] \bar{d}_1}_{M \rightarrow k-1} \\
 & + \underbrace{\bar{u}_{\rightarrow k-1}^T 2[H_x^T \text{diag}(\delta) G_x + H_{nc}^T P G_{nc}] \bar{d}_2}_{N \rightarrow k-1} + \alpha,
 \end{aligned} \tag{E.21}$$

where  $\alpha$  does not depend on  $\bar{u}_{\rightarrow k-1}$ . ■

**Remark E.6.** *The optimisation in (E.12) implies the availability of  $n_a$ -step ahead predictions of a measured disturbance  $d$ , however, this may not always be the case.*

**Corollary E.1.** *Given a set of  $n_a$ -step ahead predictions of  $d_1$  and the current estimate of  $d_2$  ( $d_{2k} = d_{2k+1} = \dots = d_{2_{ss}}$ ), then the optimization required will take the form:*

$$\min_{\bar{u}_{\rightarrow}} \quad \bar{u}_{\rightarrow k-1}^T S \bar{u}_{\rightarrow k-1} + \bar{u}_{\rightarrow k-1}^T L \bar{z}_k + \bar{u}_{\rightarrow k-1}^T M \bar{d}_1, \quad \text{s.t.} \quad \beta \bar{u}_{\rightarrow} \leq \gamma. \tag{E.22}$$

*Proof.* This falls out directly from the optimisation in (E.12). The assumption  $d_{2k} = d_{2k+1} = \dots = d_{2_{ss}}$  implies  $\bar{d}_2 = 0$ . ■

---

Local feedforward dual mode MPC 1- $n_a$ -step ahead (LFFMPC1- $n_a$ -step ahead)

---

- 1: Given an operating point and the local process model in (E.11), define the parameters in (E.22).
  - 2: At each sampling instant, perform the optimization in (E.22).
  - 3: Solve for the first element of  $\bar{u}_{\rightarrow}$  and implement on process.
- 

Note that the current estimate of  $d_2$  at sample time  $k$  is handled implicitly by the optimisation in (E.22). Note also that the optimisation in (E.22) suggests that an assumption needs to be made regarding the estimation of the steady-state value  $d_{1_{ss}}$  in order to ensure a systematic inclusion of integral action.

**Remark E.7.** For a set of  $n_a$ -step ahead predictions of a measured disturbance  $d$ , the estimated steady-state value  $d_{ss}$  is assumed<sup>2</sup> to be equal to  $d$  at sample time  $k + n_a$ .

**Remark E.8.** A set of  $n_a$ -step ahead predictions of a measured disturbance  $d$  is considered by the optimisation in (E.22) if and only if  $n_a \leq n_c$ .

**Corollary E.2.** Given the current estimates of  $d_1$  and  $d_2$  ( $d_{1k} = d_{1k+1} = \dots = d_{1ss}$  and  $d_{2k} = d_{2k+1} = \dots = d_{2ss}$ ), then the optimisation required will take the form:

$$\min_{\vec{\bar{u}}} \quad \vec{\bar{u}}_{\rightarrow k-1}^T S \vec{\bar{u}}_{\rightarrow k-1} + \vec{\bar{u}}_{\rightarrow k-1}^T L \vec{z}_k, \quad \text{s.t.} \quad \beta \vec{\bar{u}}_{\rightarrow} \leq \gamma. \quad (\text{E.23})$$

It is clear from the optimisation in (E.23) that  $\vec{\bar{d}}_1_{\rightarrow k-1} = \vec{\bar{d}}_2_{\rightarrow k-1} = 0$  which implies that the current estimates of  $d_1$  and  $d_2$  at sample time  $k$  are dealt with implicitly.

---

#### Local feedforward dual mode MPC 1 (LFFMPC1)

---

- 1: Given an operating point and the local process model in (E.11), define the parameters in (E.23).
  - 2: At each sampling instant, perform the optimization in (E.23).
  - 3: Solve for the first element of  $\vec{\bar{u}}_{\rightarrow}$  and implement on process.
- 

Similar to the LMPC, the LFFMPC1 can also be easily modified to cover a wide range of operation through gain scheduling.

---

#### GS feedforward dual mode MPC (GSFFMPC)

---

- 1: For each of the nominal operating points and given the local process model in (E.11), define the parameters in (E.23).
  - 2: For a selected local controller and at each sampling instant, perform the optimization in (E.23).
  - 3: Solve for the first element of  $\vec{\bar{u}}_{\rightarrow}$  and implement on process.
- 

---

<sup>2</sup>This is validated in the next section through simulation.

### *E.4.3 Alternative formulations of LFFMPC1*

Alternative formulations of LFFMPC1 can be obtained by making different assumptions about the models of the measured disturbances and the number of the measured disturbances available. So far, it has been assumed that the models of the measured disturbances are obtained through system identification as discussed in the previous section, however, as it has been pointed out in Section E.2, the measured disturbances can also be modelled from first principles and based on steady-state condition, and hence an equivalent algorithm to LFFMPC1 can be developed as follows.

---

#### Local feedforward dual mode MPC 2 (LFFMPC2)

---

- 1: For a given operating point, represent the dynamic model in (E.4) in a discrete-time state space form using a sampling time of 39 s (process sampling time).
  - 2: Given the local process model in (E.11), define the parameters in (E.23).
  - 3: At each sampling instant, perform the optimization in (E.23).
  - 4: Solve for the first element of  $\bar{u}_{\rightarrow}$  and implement on process.
- 

Another alternative of LFFMPC1 can be obtained by making an assumption that only a single measured disturbance is available.

---

#### Local feedforward dual mode MPC 3 (LFFMPC3)

---

- 1: Given an operating point and the local process model in (E.11) and assuming a single measured disturbance ( $\bar{x}_k^{d_2} = \bar{d}_{2k} = 0$ ), define the parameters in (E.23).
  - 2: At each sampling instant, perform the optimization in (E.23).
  - 3: Solve for the first element of  $\bar{u}_{\rightarrow}$  and implement on process.
- 

### *E.4.4 Summary*

This section has introduced a number of variants of dual mode MPC tailored to the application at hand. While the main contribution is the proposed GSFFMPC,

the other proposed algorithms are equally important to highlight issues like the significance of sufficient modelling of the measured disturbances of the plant and the impact of considering the expected future behaviour of a measured disturbance along a given prediction horizon. For a better insight into the different dual mode MPC algorithms and before moving to the next section, Table E.4 lists all the discussed algorithms and shows their distinct features.

### ***E.5 Simulation Results***

By way of some simulation scenarios, this section aims to:

- Show the efficacy of the proposed GSFFMPC with respect to the GSMPC during the transient phase, set point tracking and disturbance rejection.
- Emphasise the significance of sufficient modelling of the measured disturbances of the plant and the approach to this is by evaluating the control performance of LMPC, LFFMPC1, LFFMPC2 and LFFMPC3.
- Draw attention to the impact of considering the expected future behaviour of solar radiation along a given prediction horizon. This is achieved by comparing LFFMPC1- $n_a$ -step ahead with LFFMPC1.

**Remark E.9.** *There is no attempt at any point in this section to compare a gain scheduling algorithm with a local algorithm as this has already been discussed in Alsharkawi and Rossiter (2016b) and the benefits of a well designed gain scheduling predictive control strategy over locally designed predictive control strategy have been clearly illustrated.*

Remark E.9 emphasises the point that, while LMPC has been improved in Alsharkawi and Rossiter (2016b) by the design of GSMPC, here GSMPC is further improved by the design of GSFFMPC where local process models take direct and

Table E.4: Dual Mode MPC Algorithms

Algorithm	Feedforward	Gain scheduling	Comments
LMPC	No feedforward action	No gain scheduling	Proposed in Rossiter (2003) and the model used is obtained through system identification
GSMPC	No feedforward action	Includes gain scheduling	Proposed in Alsharkawi and Rossiter (2016b) and the models used are obtained through system identification
LFFMPC1- $n_a$ -step ahead	Takes into account $n_a$ -step ahead of $d_1$ and the current measurement of $d_2$	No gain scheduling	Models of the measured disturbances are obtained through system identification
LFFMPC1	Takes into account the current measurement of $d_1$ and $d_2$	No gain scheduling	Models of the measured disturbances are obtained through system identification
GSFFMPC	Takes into account the current measurement of $d_1$ and $d_2$	Includes gain scheduling	Models of the measured disturbances are obtained through system identification
LFFMPC2	Takes into account the current measurement of $d_1$ and $d_2$	No gain scheduling	Model of the measured disturbances is derived from first principles and based on steady-state condition
LFFMPC3	Takes into account the current measurement of $d_1$ and not of $d_2$	No gain scheduling	Model of the single measured disturbance is obtained through system identification

explicit account of the dynamics of the measured disturbances. However, one can notice that local algorithms, which have no gain scheduling, have also been considered in order to meet the last two aims of this section to:

- Demonstrate the pure impact of the various modelling aspects discussed earlier without the influence of gain scheduling and thus show that the extension of LFFMPC1 to GSFFMPC is reasonable.
- Explore the efficacy of LFFMPC1- $n_a$ -step ahead, given the expected future behaviour of solar radiation, over LFFMPC1 and see whether LFFMPC1- $n_a$ -step ahead is worthy of extension to the gain scheduling case.

Various simulation scenarios have been designed in order to meet the main aims of this section, but before proceeding any further with these scenarios, some preliminaries are discussed first.

### *E.5.1 Preliminaries*

The plant is represented by the nonlinear simulation model described by the system in (E.2) with a slight increase to thermal losses in order to make the scenarios more realistic. Field inlet temperature ( $T_{f,inlet}$ ) and ambient temperature ( $T_a$ ) are kept fixed at 189°C and 28°C respectively. Even though this may not be the case in the normal operation of the plant, this is still a reasonable assumption during the steady-state phase. The HTF is assumed to be the synthetic oil Therminol® 55 and constrained to the range 0.002–0.012 m<sup>3</sup>/s, where the minimum limit is normally for a safety reason. Exceeding a temperature of 305°C puts the synthetic oil at the risk of being decomposed. The difference between the field inlet-outlet temperature is constrained not to exceed 80°C to avoid the risk of oil leakage (Camacho et al., 2012); this has been taken care of implicitly when the nominal operating points and the desired reference temperature were selected. The HTF flow rate constraints are considered explicitly in the control design process as demonstrated in the following scenarios.

### *E.5.2 Gain scheduled feedforward control*

The following scenario shows the efficacy of the proposed GSFFMPC compared to the previously proposed GSMPC (Alsharkawi and Rossiter, 2016b), that is, it demonstrates the benefits of utilising feedforward information where available. The scenario shown in Fig. E.7 starts with a clear day and slowly time-varying solar radiation. During the transient phase (9–9.15 h) and while the GSFFMPC is performing very well with fast transients and no overshoot, the GSMPC has somewhat poorer performance with a large overshoot around 13 °C and an oscillatory control signal. As the day goes by a sudden drop in solar radiation occurs at 13.15 h due to a passing and persistent cloud. As can be clearly seen in Fig. E.7, the GSFFMPC performs better than the GSMPC with much less deviation from the desired reference temperature and a faster recovery time. Here again, the control signal of the GSMPC is slightly oscillatory.

Set point tracking performance is evaluated for both algorithms over a short period of time during steady-state; Table E.5 shows the numerical set point tracking performance of both algorithms over a period of 42 min (11.16–11.58 h). GSFFMPC achieves lower root mean square error (RMSE) with a reduction of approximately 13%.

Both algorithms, GSMPC and GSFFMPC, have nearly matching switching performance. This is illustrated at the bottom of Fig. E.7 where the switching from one local controller to another as the plant dynamics change with time and operating conditions is clearly seen. Local controllers 1, 2, 3, and 4 refer to the nominal operating points  $q = 0.004, 0.006, 0.008$  and  $0.010 \text{ m}^3/\text{s}$  respectively.

**Remark E.10.** *Despite the apparent benefits of GSFFMPC, it is fair to say that the control signal in general has experienced some large changes in response to the relatively large set point changes which could result in undesired wear in the actuator. Reference governor control strategies similar to the ones reported in Cirre et al. (2009) could potentially be a solution to this problem as the desired reference*

Table E.5: Set Point Tracking Performance (GS Case)

Algorithm	RMSE ( $^{\circ}\text{C}$ )
GSMPC	0.0271
GSFFMPC	0.0237

*temperature is more smoothly generated while taking into account the plant safety constraints.*

### E.5.3 Local feedforward control

The scenario in Fig. E.8 demonstrates locally the importance of sufficient modelling of solar radiation and the field inlet temperature. In particular, it highlights the superiority of the LFFMPC1 over the LMPC, LFFMPC2 and LFFMPC3.

Controllers are designed around the nominal operating point  $0.006 \text{ m}^3/\text{s}$  and similar to the scenario in Fig. E.7, the scenario in Fig. E.8 starts with a clear day and slowly time-varying solar radiation. During the transient phase (9–9.26 h), LMPC, which has no feedforward action, has the worst control performance with significant overshoot around  $17^{\circ}\text{C}$  and a substantial oscillatory control signal. LFFMPC2 has better performance than LMPC with a noticeable improvement in the overshoot (around  $9.5^{\circ}\text{C}$ ) and slight improvement in the control signal. The model of the measured disturbances for the LFFMPC2 is derived from first principles and based on steady-state condition. Best control performance is exhibited by LFFMPC1 with no overshoot and a relatively smooth control signal.

Note that LFFMPC3 is designed based on the dynamics of the volumetric flow rate of the HTF and solar radiation. In other words, dynamics of the field inlet temperature are not considered in the control design process. The impact of not considering the dynamics of the field inlet temperature on the transient phase is fairly obvious. One would expect a large overshoot and oscillatory control signal.

Fig. E.8 also shows the behaviour of the four controllers during a sudden drop in solar radiation across the period 12.45–13.15 h. While the impact of the passing cloud on LFFMPC1 is barely noticed, LMPC gives notably poorer performance. LFFMPC2 makes less effective use of the feedforward information and gives a seriously poor control signal whereas, as expected, LFFMPC3 shows a similar response to LFFMPC1. Table E.6 gives numerical comparison of set point tracking performance during steady-state (10.37–11.42 h). Clearly, LFFMPC1 and LFFMPC3 give the lowest RMSE. Note that the set point tracking performance of LFFMPC2 is still better than LMPC.

Table E.6: Set Point Tracking Performance (Local Case)

Algorithm	RMSE (°C)
LMPC	0.0413
LFFMPC1	0.0130
LFFMPC2	0.0207
LFFMPC3	0.0130

In summary and for a given operating point, LFFMPC1 has demonstrated that incorporating sufficient dynamic models of solar radiation and the field inlet temperature, that take explicit account of the resonance phenomena of the plant, can significantly improve the control performance during the transient phase, set point tracking and disturbance rejection. Hence, the extension of LFFMPC1 to GSFFMPC to cover more operating points is reasonable.

#### *E.5.4 Measured disturbances along a given prediction horizon*

This part of the section investigates the impact of incorporating the expected future behaviour of solar radiation along a given prediction horizon. The performance of LFFMPC1 for the current incident solar radiation is compared to the performance

of LFFMPC1 when the solar radiation is forecasted 23-step ahead (around 15 min); see Chu and Coimbra (2017) for short-term forecasts of direct normal irradiance. The scenario here is quite extreme. Fig. E.9 shows drastic changes in solar radiation due to thick and scattered passing clouds.

Just before 12.15 h, the performance of LFFMPC1 is fairly similar to the performance of LFFMPC1-23-step ahead. After 12.15 h and due to the strong disturbances, some differences started to emerge, yet, the impact of the forecast capabilities is not quite clear. Hence, set point tracking performance and online performance measure have been assessed for both algorithms. During the time of the strong disturbances, it has been found that LFFMPC1-23-step ahead has a lower RMSE and cost of regulation than LFFMPC1 by about 11.7% and 22% respectively. Note that, however, the choice of 23-step ahead here is not optimal for the control design and needs further investigation.

As a final remark here, the steady-state value of a measured disturbance  $d$  was defined earlier as  $d$  at sample time  $k + n_a$  and in order to validate this assumption, a typical daily cycle of solar radiation on a clear day is simulated. The cycle has a mean value of  $800 \text{ W/m}^2$  and covers a range of 5 h 27 min and 36 s. Fig. E.10 shows the deviation of solar radiation after applying LFFMPC1-23-step ahead for a desired reference temperature of  $237^\circ\text{C}$ . The deviation can be clearly seen converging to zero across the whole range of operation.

## ***E.6 Conclusion***

This paper has discussed the main feedforward approaches that have been proposed over the years for the ACUREX distributed solar collector field as well as the need for the development of a new feedforward approaches. Moreover, the paper has shown that the dynamics of the field outlet temperature due to changes in solar radiation are very similar to the dynamics of the field outlet temperature due to changes in the volumetric flow rate of the HTF, which is consistent with the experimental findings in Meaburn and Hughes (1993) and the analysis in Meaburn and Hughes (1997). This

paper has also taken the analysis of the measured disturbances of the ACUREX plant a step further by investigating the dynamics of the field inlet temperature and showing that indeed fast and abrupt changes in the field inlet temperature can excite the resonance dynamics of the plant.

The GS predictive control strategy proposed in Alsharkawi and Rossiter (2016b) is improved in this paper by including the effects of the measured disturbances of the ACUREX plant in the predictions of future outputs (systematic feedforward design). Using a validated nonlinear simulation model of the ACUREX plant, models of the measured disturbances are estimated around a family of operating points directly from input-output data using the subspace identification method N4SID while taking into account the frequency response of the plant.

Simulation results have shown that incorporating sufficient dynamic models of the measured disturbances can significantly improve the control performance during the transient phase, set point tracking and disturbance rejection. The results have also shown that deriving a dynamic model of the measured disturbances from first principles and based on steady-state condition is an underestimation of their actual dynamics, which thus can result in a poor control performance during disturbance rejection.

Changes in the field inlet temperature are mostly noticed during the transient phase of the plant (start-up phase) (Camacho et al., 2012), and since the simulation scenarios have assumed that the plant is operating at the steady state phase, the field inlet temperature had to be kept fixed at a certain value. Yet, the impact of not considering the dynamics of the field inlet temperature in the control design for a particular local feedforward controller (LFFMPC3) has been investigated. It has been found that the transient is affected the most with large overshoot and quite oscillatory control signal.

Finally, the paper has attempted to draw attention to the impact of considering the expected future behaviour of solar radiation along a given prediction horizon. Even though the results were positive, one might argue that the improvements over

that current incident solar radiation are not that significant. It is worth noting that questions like: *How far ahead should one predict?* and accordingly *How significant can the improvements be?* still need to be answered.

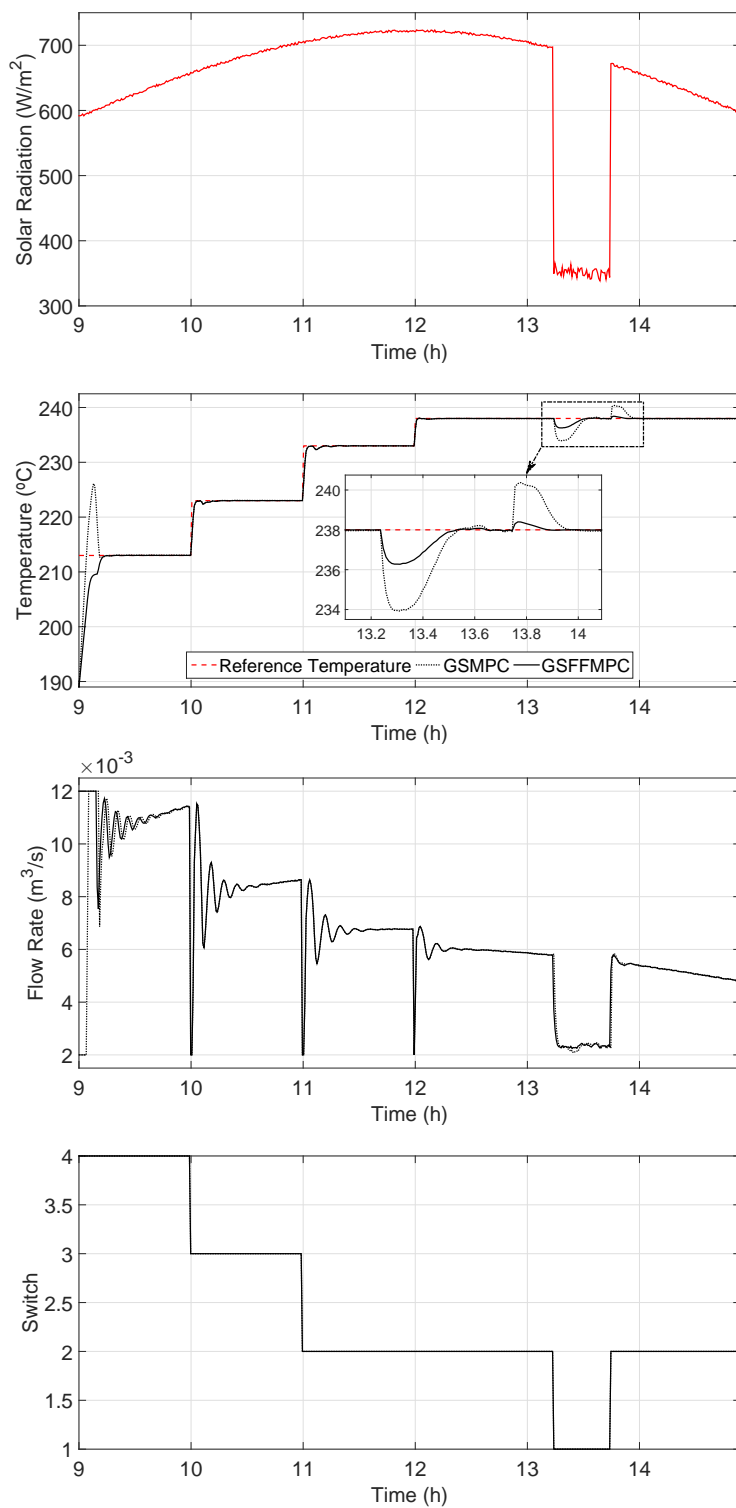


Figure E.7: A performance comparison: GSMPC against GSFFMPC.

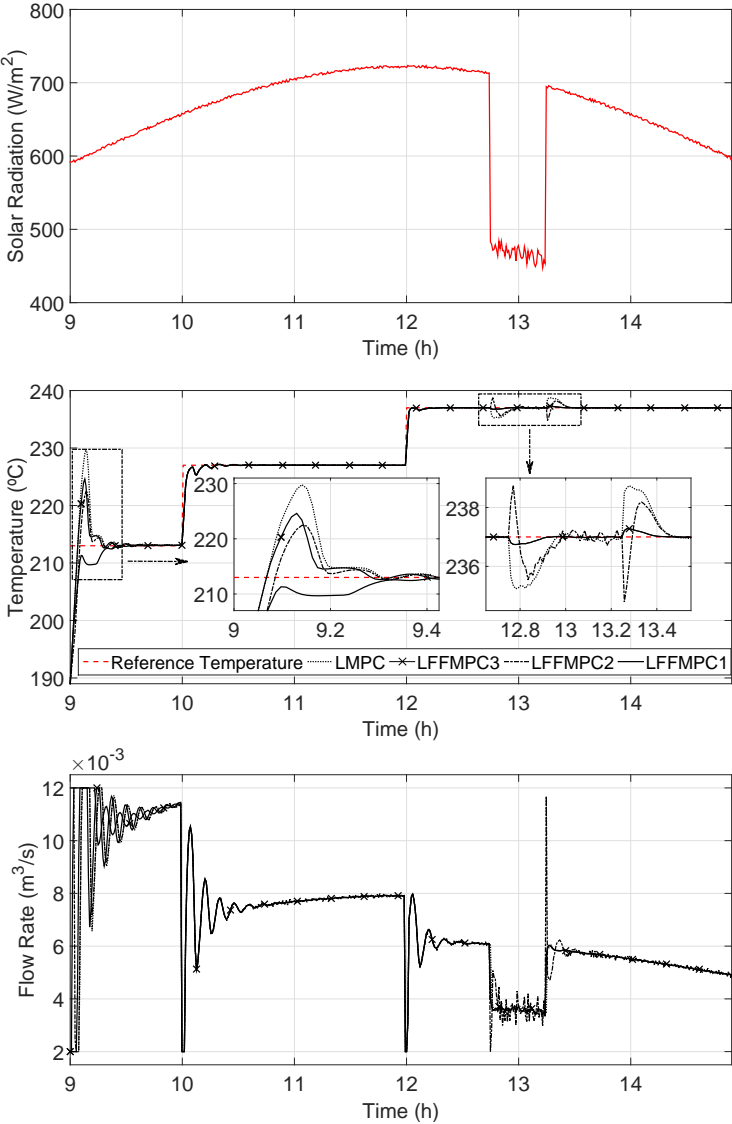


Figure E.8: A local performance comparison.

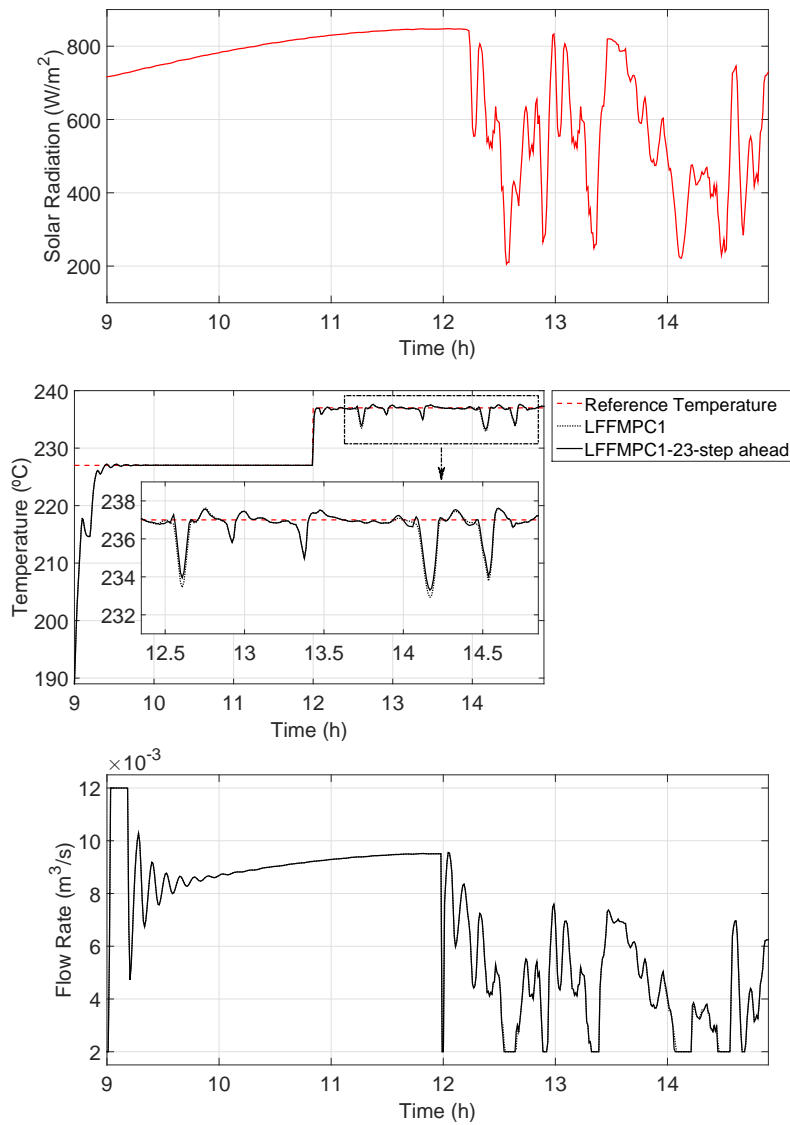


Figure E.9: A performance comparison: LFFMPC1 against LFFMPC1-23-step ahead.

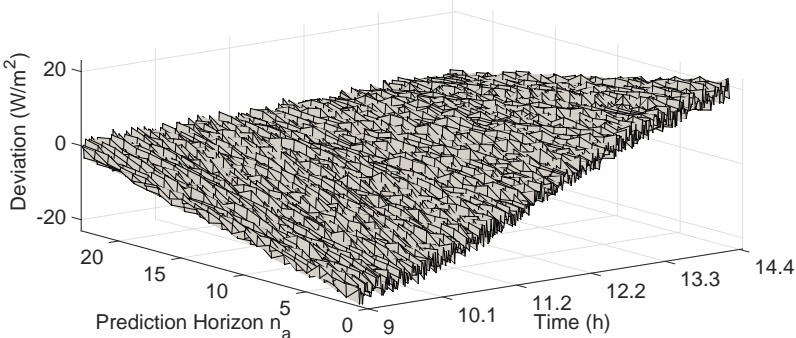


Figure E.10: Deviation of solar radiation from an estimated steady-state value.

# BIBLIOGRAPHY

- Alsharkawi, A. and Rossiter, J.A. (2017). Modelling analysis of a solar thermal power plant. In *Proceedings of the 6th International Conference on Clean Electrical Power, Liguria, Italy*.
- Alsharkawi, A. and Rossiter, J.A. (2016a). Dual mode MPC for a concentrated solar thermal power plant. In *Proceedings of the 11th IFAC Symposium on Dynamics and Control of Process Systems, including Biosystems, Trondheim, Norway*, volume 49(7), 260–265. Elsevier.
- Alsharkawi, A. and Rossiter, J.A. (2016b). Gain scheduling dual mode MPC for a solar thermal power plant. In *Proceedings of the 10th IFAC Symposium on Nonlinear Control Systems, California, USA*, volume 49(18), 128–133. Elsevier.
- Álvarez, J., Yebra, L., and Berenguel, M. (2009). Adaptive repetitive control for resonance cancellation of a distributed solar collector field. *International Journal of Adaptive Control and Signal Processing*, volume 23(4), 331–352.
- Beschi, M., Dormido, S., Sanchez, J., Visioli, A., and Yebra, L.J. (2014). Event-based pi plus feedforward control strategies for a distributed solar collector field. *IEEE Transactions on Control Systems Technology*, volume 22(4), 1615–1622.
- Camacho, E.F., Berenguel, M., Rubio, F.R., and Martínez, D. (2012). *Control of solar energy systems*. Springer-Verlag.
- Camacho, E., Rubio, F., and Hughes, F. (1992). Self-tuning control of a solar power plant with a distributed collector field. *IEEE control Systems*, volume 12(2), 72–78.

- Cardoso, A., Henriques, J., and Dourado, A. (1999). Fuzzy supervisor and feedforward control of a solar power plant using accessible disturbances. In *Proceedings of the European Control Conference*, 1711–1716. IEEE.
- Carmona, R. (1985). *Analysis, modeling and control of a distributed solar collector field with a one-axis tracking system*. Ph.D. thesis. University of Seville, Spain.
- Chu, Y. and Coimbra, C.F. (2017). Short-term probabilistic forecasts for direct normal irradiance. *Renewable Energy*, volume 101, 526–536.
- Cirre, C.M., Berenguel, M., Valenzuela, L., and Klempous, R. (2009). Reference governor optimization and control of a distributed solar collector field. *European Journal of Operational Research*, volume 193(3), 709–717.
- Gálvez-Carrillo, M., De Keyser, R., and Ionescu, C. (2009). Nonlinear predictive control with dead-time compensator: Application to a solar power plant. *Solar Energy*, volume 83(5), 743–752.
- Johansen, T.A. and Storaa, C. (2002). Energy-based control of a distributed solar collector field. *Automatica*, volume 38(7), 1191–1199.
- Meaburn, A. and Hughes, F. (1993). Resonance characteristics of distributed solar collector fields. *Solar Energy*, volume 51(3), 215–221.
- Meaburn, A. and Hughes, F. (1997). Feedforward control of solar thermal power plants. *Journal of Solar Energy Engineering*, volume 119(1), 52–60.
- Powell, K.M. and Edgar, T.F. (2012). Modeling and control of a solar thermal power plant with thermal energy storage. *Chemical Engineering Science*, volume 71, 138–145.
- Rossiter, J.A. (2003). *Model-based predictive control: a practical approach*. CRC press.

Silva, R., Rato, L., Lemos, J., and Coito, F. (1997). Cascade control of a distributed collector solar field. *Journal of Process Control*, volume 7(2), 111–117.

Van Overschee, P. and De Moor, B. (1996). *Subspace identification for linear systems: Theory-Implementation-Applications*. Springer Science & Business Media.

Appendix F

**HIERARCHICAL CONTROL  
STRATEGY FOR A SOLAR THERMAL  
POWER PLANT:  
A PRAGMATIC APPROACH**

**Adham Alsharkawi and J. Anthony Rossiter**

This paper has been submitted to:  
Journal of Process Control.

*The layout has been revised.*

### ***Abstract***

This paper proposes a novel design for a two-layer hierarchical control strategy applied to a solar thermal power plant. Taking into account the status of the measured disturbances, an adequate reachable reference temperature (set point) is generated conceptually from an upper layer while satisfying the plant safety constraints. The approach of generating the reference temperature makes use of system identification and takes into account the frequency response of the plant. Due to the nature of hierarchy, a nonlinear predictive control strategy is adopted in a lower layer for set point tracking and coping with the plant nonlinear dynamics. The efficacy of the proposed two-layer hierarchical control strategy is illustrated by way of some simulation scenarios and measured data from the plant.

### ***Keywords***

Solar thermal power plant; Hierarchical control; System identification; Nonlinear control.

## ***F.1 Introduction***

### ***F.1.1 Background***

Global energy consumption has grown rapidly during the second half of the last century due to the relatively cheap fossil fuels and high rates of industrialisation, mainly in North America, Europe and Japan. Moreover, energy consumption is expected to continue to increase over the next 50 years, for example due to China's and India's rapid development. Given this, the expected exhaustion of oil reserves in the near future and the impact of fossil fuels on climate change (Goswami et al., 2015), there is an urgent need to develop clean and sustainable energy resources.

Solar energy technologies are one of the promising and clean sustainable energy resources. In 2011, the International Energy Agency (IEA) stated that *The develop-*

*ment of affordable, inexhaustible and clean solar energy technologies will have huge longer-term benefits. It will increase countries energy security through reliance on an indigenous, inexhaustible and mostly import-independent resource, enhance sustainability, reduce pollution, lower the costs of mitigating climate change, and keep fossil fuel prices lower than otherwise. These advantages are global. (IEA, 2011).*

Solar energy is converted into electrical energy by two main technologies, photovoltaic and thermal technology. While the current commercial efficiency of photovoltaic technology has reached more than 20 %, thermal technology has achieved efficiencies of 40-60 %. Also, a significant advantage of thermal technology is that thermal energy can be stored efficiently. This is an essential condition to ensure a continuous operation of a solar thermal power plant (Goswami et al., 2015).

This paper looks into the design of a control strategy for ACUREX, a parabolic trough-based solar thermal power plant (Camacho et al., 2012). Despite the huge longer-term benefits mentioned earlier, decisions about investing in solar energy technologies are rarely based on these benefits (Goswami et al., 2015). Hence, the aim of the proposed control strategy is to make solar thermal applications similar to ACUREX more appealing for governments and investors by improving their current economic state, more specifically, by decreasing their operation and maintenance costs.

### *F.1.2 Hierarchical control: an overview on the literature*

The proposed control strategy has a hierarchical structure. The idea of hierarchical control involves all aspects of automation of the decision making process (measurement, control, optimisation and logistics) and is believed to be an effective way of responding to a dynamic and unpredictable marketplace conditions with minimal capital investment (Prett and Garcia, 1988). The application of hierarchical control to the solar thermal power plant ACUREX was first discussed in Berenguel et al. (2005) and later on a two-layer hierarchical control strategy was first implemented (Cirre et al., 2009). This was followed by the design of a three-layer hierarchical

control strategy (Camacho and Gallego, 2013). However, apart from these control strategies (Cirre et al., 2009; Camacho and Gallego, 2013), this area has received little attention in the literature.

The main argument in Cirre et al. (2009); Camacho and Gallego (2013) is that the ACUREX plant is constantly subject to changes in solar radiation and the field inlet temperature (measured disturbances) and hence the plant requires the full attention of an experienced plant operator, whose job is to set an adequate reachable reference temperature that takes into account the status of the measured disturbances and the plant safety constraints. Moreover, the narrow temperature operating range of the plant steam turbine has to be maintained. In parallel, the operator must choose between potentially ambitious and perhaps unreachable targets and safer targets. Ambitious targets can lead to actuator saturation and safer targets imply electricity production losses.

This paper proposes an effective hierarchical control strategy that can handle this dilemma without any help from the plant operator and without adding cost. The technicalities of both Cirre et al. (2009) and Camacho and Gallego (2013) will be discussed as appropriate to highlight the novelty by comparison with the proposed hierarchical control strategy.

### *F.1.3 Paper contribution and organisation*

This paper proposes a pragmatic approach to drive the plant near optimal operating conditions by generating a reference temperature that is adequate, reachable and smoothly adapted to changes in solar radiation and the field inlet temperature while at the same time satisfying the plant safety constraints. Under the normal operating conditions of the plant, the generated reference temperature also satisfies the narrow operating range of the plant steam turbine. Conceptually, a two-layer hierarchical control structure is proposed, an upper layer for generating a reference temperature (set point) and a lower layer for set point tracking and coping with the plant nonlinear dynamics. The proposed approach to generate the reference temperature is quite

simple and intuitive. Compact linear time-invariant (LTI) state space models of solar radiation and the field inlet temperature are estimated from measured data while taking into account the frequency response of the plant. The estimated models establish clear, direct and dynamic relationships with the field outlet temperature (reference temperature).

The remainder of this paper is organised as follows. Section F.2 gives a brief description of the ACUREX plant and highlights an intrinsic phenomena of the plant. Section F.3 gives an overview of the nonlinear dynamic models of the ACUREX plant, Section F.4 introduces the proposed two-layer hierarchical control structure, Section F.5 illustrates the efficacy of the proposed structure in various scenarios and finally conclusions are given in Section F.6.

## ***F.2 Plant Description and the Phenomena of Resonant Modes***

ACUREX is one of the research facilities at the Plataforma Solar de Almería (PSA) in south-east Spain and has served as a benchmark for many researchers across academia and industry. Control problem and key features of the plant are given next, followed by an outline of an intrinsic phenomena of the plant.

### *F.2.1 ACUREX: control problem and key features*

Collectors of the ACUREX plant are parabolic in shape and concentrate the incident solar radiation onto a receiver tube that is placed at its focal line; see Fig. F.1. A heat transfer fluid (HTF) is heated as it flows through the receiver tube and circulates through a distributed solar collector field. The heated HTF then passes through a series of heat exchangers to produce steam which in turn is used to drive a steam turbine to generate electricity. One of the biggest challenges of such a plant, from a control point of view, is to maintain the field outlet temperature at a desired level despite changes, mainly in solar radiation and the field inlet temperature. This can be handled efficiently by manipulating the volumetric flow rate of the HTF. However, during the normal operation of the plant, the volumetric flow rate of the HTF should

not exceed a certain range.



Figure F.1: ACUREX distributed solar collector field.

The HTF of the ACUREX plant is the synthetic oil Therminol<sup>®</sup> 55 and during the normal operation of the plant, the volumetric flow rate should be within the range  $0.002\text{-}0.012\text{ m}^3/\text{s}$ . The minimum limit helps to maintain the field outlet temperature below  $305\text{ }^\circ\text{C}$ . Exceeding this temperature puts the synthetic oil at the risk of being decomposed. Another important restriction is to keep the difference between the field inlet and outlet temperature less than  $80\text{ }^\circ\text{C}$ . Exceeding a temperature difference of  $100\text{ }^\circ\text{C}$  gives a significant risk of oil leakage due to high oil pressure in the piping system. For a detailed description of the plant, readers are referred to Camacho et al. (2012).

### *F.2.2 Resonant modes*

In Meaburn and Hughes (1993) it was argued that the ACUREX distributed solar collector field possesses resonance characteristics, namely resonant modes that lie well within the desired control bandwidth and the resonance phenomena arise due

to the relatively slow flow rate of the HTF and the length of the receiver tube. It was also found that the phenomena have a significant impact on the control performance and hence, modelling the resonant modes sufficiently accurately is crucial to ensure high control performance with adequate robustness.

More importantly however, the dynamics relating the field outlet temperature to changes in solar radiation are very similar to the dynamics relating the field outlet temperature to changes in the volumetric flow rate of the HTF. Indeed a dynamic analysis of the measured disturbances in Alsharkawi and Rossiter (2017) found that fast and abrupt changes in the field inlet temperature can also excite the resonance dynamics of the plant.

In summary, modelling solar radiation and the field inlet temperature while taking into account the frequency response of the plant is essential to ensure high prediction accuracy. While this issue was ignored in Cirre et al. (2009); Camacho and Gallego (2013), it is given special attention in this paper.

### ***F.3 Nonlinear Dynamic Models of the Plant***

The ACUREX plant is represented in this paper by a nonlinear simulation model. The model was constructed based on a nonlinear distributed parameter model of the plant. This is discussed next. This section also discusses briefly a simple nonlinear lumped parameter model of the plant that is used for the control design at the lower layer.

#### *F.3.1 Nonlinear distributed parameter model*

The dominant dynamics of the ACUREX plant are captured by the following set of energy balance partial differential equations (PDEs):

$$\begin{aligned} \rho_m C_m A_m \frac{\partial T_m}{\partial t} &= n_o G I - D_o \pi H_l (T_m - T_a) - D_i \pi H_t (T_m - T_f), \\ \rho_f C_f A_f \frac{\partial T_f}{\partial t} + \rho_f C_f q \frac{\partial T_f}{\partial x} &= D_i \pi H_t (T_m - T_f), \end{aligned} \quad (\text{F.1})$$

where the subindex  $m$  refers to the metal of the receiver tube and  $f$  to the HTF (Carmona, 1985; Camacho et al., 2012). Table F.1 gives a description of all the

variables and parameters and lists their SI units.

Table F.1: Variables and Parameters.

Symbol	Description	SI unit
$\rho$	Density	kg/m <sup>3</sup>
$C$	Specific heat capacity	J/kg°C
$A$	Cross-sectional area	m <sup>2</sup>
$T$	Temperature	°C
$t$	Time	s
$I$	Solar radiation	W/m <sup>2</sup>
$n_o$	Mirror optical efficiency	–
$G$	Mirror optical aperture	m
$D_o$	Outer diameter of the receiver tube	m
$H_l$	Global coefficient of thermal losses	W/m°C
$T_a$	Ambient temperature	°C
$D_i$	Inner diameter of the receiver tube	m
$H_t$	Metal-fluid heat transfer coefficient	W/m <sup>2</sup> °C
$q$	HTF volumetric flow rate	m <sup>3</sup> /s
$x$	Space	m

A nonlinear simulation model of the plant has been constructed in Alsharkawi and Rossiter (2016a) by dividing the receiver tube into  $N$  segments each of length  $\Delta x$  and hence the nonlinear distributed parameter model in (F.1) has been approximated by the following set of ordinary differential equations (ODEs):

$$\begin{aligned} \rho_m C_m A_m \frac{dT_{m,n}}{dt} &= n_o G I - D_o \pi H_l (T_{m,n} - T_a) - D_i \pi H_t (T_{m,n} - T_{f,n}), \quad n = 1, \dots, N, \\ \rho_f C_f A_f \frac{dT_{f,n}}{dt} + \rho_f C_f q \frac{T_{f,n} - T_{f,n-1}}{\Delta x} &= D_i \pi H_t (T_{m,n} - T_{f,n}) \end{aligned} \quad (\text{F.2})$$

with the boundary condition  $T_{f,0} = T_{f,inlet}$  (field inlet temperature) and  $H_l, H_t, \rho_f$  and  $C_f$  being time-varying.

It has been shown in Alsharkawi and Rossiter (2016a) that dividing the receiver tube into 7 segments ( $N = 7$ ) is a reasonable trade-off between the prediction accuracy and computational burden while still adequate enough to capture the resonant modes of the plant.

**Remark F.1.** *The set of ODEs (F.2) is implemented and solved using the MATLAB<sup>®</sup> solver ODE45 (an explicit Runge-Kutta method) where the temperature distribution in the receiver tube and HTF can be accessed at any point in time and for any segment  $n$ . The number of ODEs solved at each sample time  $k$  for  $N$  segments is  $2 \times N$ .*

In summary, the ACUREX plant is represented in this paper by the nonlinear simulation model described by the system in (F.2).

### F.3.2 Nonlinear lumped parameter model

The dynamic behaviour of the ACUREX plant can also be approximately described by a simple nonlinear lumped parameter model. Variation in the internal energy of the fluid can be described by:

$$C \frac{dT_f}{dt} = n_o S I - Q P_{cp} (T_f - T_{f,inlet}) - H_l (T_{mean} - T_a), \quad (\text{F.3})$$

where  $S$  is the solar field effective surface,  $Q$  is the HTF volumetric flow rate,  $P_{cp}$  is a factor that takes into account some geometrical and thermal properties and  $T_{mean}$  is the mean of  $T_f$  and  $T_{f,inlet}$  (Camacho et al., 2012).

In summary, the nonlinear lumped parameter model in (F.3) is used under certain assumptions for the control design at the lower layer. Further discussion of this will be given in a later section.

## F.4 Two-Layer Hierarchical Control Structure

This section discusses the proposed two-layer hierarchical control structure, an upper layer for generating a reference temperature (set point) and a lower layer for set point

tracking and coping with the plant nonlinear dynamics. The proposed structure operates the ACUREX plant automatically without any help from the plant operator.

This area has received little attention in the literature. More specifically, a fuzzy logic approach was proposed in Cirre et al. (2009) along with an optimisation-based approach performed in steady state. To overcome some shortcomings of that approach by taking into account the nonlinear dynamic behaviour of the plant, a different optimisation-based approach was proposed in Camacho and Gallego (2013).

The fuzzy logic approach is somewhat ad hoc and requires years of experience in operating the plant, while the optimisation-based approaches are complicated and, at some point, even unrealistic. Hence the approach proposed in this paper requires little knowledge of the plant (process time constant) and drives the plant near optimal operating conditions rather than solving a direct nonlinear optimisation problem. More importantly however, the proposed approach here takes explicit account of the resonant modes of the plant; these were ignored in Cirre et al. (2009); Camacho and Gallego (2013).

The upper and lower layer designs are discussed next followed by a summary to give insight into the overall design.

#### *F.4.1 Upper layer*

In this layer a reference temperature is generated for the lower layer taking into account the status of the measured disturbances and the plant safety constraints. Under normal operating conditions, the generated reference temperature also meets the desired narrow temperature range of the plant steam turbine.

The proposed approach to generate a reference temperature is intuitive and makes use of system identification. The following subsections summarise key steps, the identification signal, the identification method, model order selection, best fit criterion and the phenomena of resonant modes. The estimated LTI state space models of solar radiation and the field inlet temperature form the core of the proposed two-layer hierarchical control structure.

*Overview*

Given the process time constant and taking into account the frequency response of the plant, LTI state space models of solar radiation and the field inlet temperature are estimated around a number of operating points across the whole range of operation (flow rates 0.002-0.012 m<sup>3</sup>/s). The estimated models establish a clear, direct and dynamic relationships with the field outlet temperature (reference temperature). In particular, at each operating point, a complete one-step ahead prediction model predicts the *best* reference temperature given the measurements of solar radiation and the field inlet temperature. Due to the nonlinear dynamic behaviour of the plant, a mean value of the generated reference temperatures is considered.

**Remark F.2.** *The mean reference temperature ensures that the reference temperature is within a reachable limit at all times and it corresponds to a medium flow rate (around 0.006 m<sup>3</sup>/s). Hence, the risk of saturation is reduced.*

*System identification: the whole story*

Next, the process of estimating the LTI state space models of solar radiation and the field inlet temperature is discussed thoroughly. Dynamics of the ACUREX plant are mainly characterised by the flow rate of the HTF (Camacho et al., 2012) and hence a one-step ahead prediction model of the reference temperature is developed around five different operating points across the whole range of operation,  $q = 0.003, 0.005, 0.007, 0.009$  and  $0.011$  m<sup>3</sup>/s.

The nonlinear simulation model of the plant described by the system in (F.2) was excited by a set of full-length Pseudo-Random Binary Sequence (PRBS) signals with a clock period equal to the process sampling time 39 s (the process time constant is around 6 min). The identification process assumed steady-state operating conditions and was carried out separately for solar radiation and the field inlet temperature. A data set of 1100 samples was used to estimate each of the nominal LTI state space models.

Compact LTI state space models of solar radiation and the field inlet temperature were estimated directly from input-output data and using the noniterative subspace identification method N4SID (Van Overschee and De Moor, 1996). The general form of a discrete-time LTI state space model is given as:

$$\begin{aligned}x_{k+1} &= Ax_k + Bu_k + \xi_k, \\y_k &= Cx_k + Du_k + \eta_k,\end{aligned}\tag{F.4}$$

where  $x_k \in \mathbb{R}^{n \times 1}$ ,  $u_k \in \mathbb{R}^{m \times 1}$ ,  $y_k \in \mathbb{R}^{l \times 1}$ ,  $\xi_k \in \mathbb{R}^{n \times 1}$  and  $\eta_k \in \mathbb{R}^{l \times 1}$  are the state vector, input vector, output vector, process noise and measurement noise respectively at discrete time instant  $k$ .  $A, B, C$  and  $D$  are the coefficient matrices of appropriate dimensions.

Models of solar radiation and the field inlet temperature were estimated under the assumptions that there is no direct feedthrough from the input to the output ( $D = 0$ ) and the system is deterministic ( $\xi_k = \eta_k = 0$ ). This gives:

$$\begin{aligned}x_{k+1} &= Ax_k + Bu_k, \\y_k &= Cx_k.\end{aligned}\tag{F.5}$$

Model order was selected by inspecting the singular values of a covariance matrix constructed from the observed data. Model order and best fit criterion are shown in Table F.2 for solar radiation and in Table F.3 for the field inlet temperature. Models 1, 2, 3, 4 and 5 refer to the nominal operating points  $q = 0.003, 0.005, 0.007, 0.009$  and  $0.011 \text{ m}^3/\text{s}$  respectively.

The best fit criterion (Ljung, 2015) reflects the ability of the estimated models to reproduce the main dynamics of the plant at a given operating point and time horizon. Meanwhile, the ability of the estimated models to capture the resonance dynamics of the plant is validated by inspecting their frequency response. Fig. F.2 and Fig. F.3 show Bode plots of the estimated models and one can clearly identify the resonant modes of the plant and observe the dependence of their frequencies on the flow rate of the HTF.

Table F.2: Model Order and Best Fit Criterion ( $I$ )

Model	Model order	Best fit criterion (%)
1	4 <sup>th</sup>	97.37
2	4 <sup>th</sup>	98.03
3	5 <sup>th</sup>	98.66
4	5 <sup>th</sup>	98.85
5	6 <sup>th</sup>	98.96

Table F.3: Model Order and Best Fit Criterion ( $T_{f,inlet}$ )

Model	Model order	Best fit criterion (%)
1	6 <sup>th</sup>	95.56
2	7 <sup>th</sup>	97.12
3	7 <sup>th</sup>	97.73
4	7 <sup>th</sup>	98.05
5	7 <sup>th</sup>	98.24

#### *One-step ahead prediction model*

The development of a complete one-step ahead prediction model of the reference temperature is discussed next. The reader is reminded that LTI state space models of solar radiation and the field inlet temperature are estimated separately at each of the nominal operating points.

**Proposition F.1.** *Estimated LTI state space models of solar radiation and the field inlet temperature at a given operating point can be augmented to form a complete one-step ahead prediction model of the reference temperature  $T_{ref}^i$ , for  $i \in \{1, 2, 3, 4, 5\}$ , as follows:*

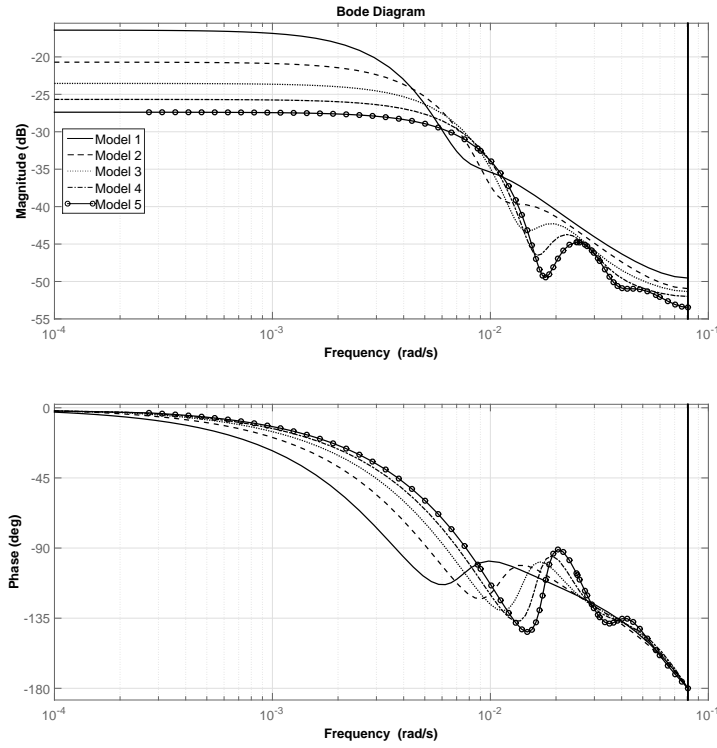


Figure F.2: Bode plot: Estimated models of solar radiation.

$$\underbrace{\begin{bmatrix} x_{k+1}^I \\ x_{k+1}^{T_f, \text{inlet}} \end{bmatrix}}_{x_{k+1}^i} = \underbrace{\begin{bmatrix} A^I & 0 \\ 0 & A^{T_f, \text{inlet}} \end{bmatrix}}_{A^i} \underbrace{\begin{bmatrix} x_k^I \\ x_k^{T_f, \text{inlet}} \end{bmatrix}}_{x_k^i} + \underbrace{\begin{bmatrix} B^I & 0 \\ 0 & B^{T_f, \text{inlet}} \end{bmatrix}}_{B^i} \underbrace{\begin{bmatrix} I_k \\ T_{f, \text{inlet}, k} \end{bmatrix}}_{u_k}, \quad (\text{F.6})$$

$$T_{ref, k}^i = \underbrace{\begin{bmatrix} C^I & C^{T_f, \text{inlet}} \end{bmatrix}}_{C^i} \underbrace{\begin{bmatrix} x_k^I \\ x_k^{T_f, \text{inlet}} \end{bmatrix}}_{x_k^i}.$$

*Proof.* This is straightforward given the model structure in (F.5). ■

**Remark F.3.** The mean reference temperature  $T_{ref}$  ( $\frac{T_{ref}^1 + T_{ref}^2 + T_{ref}^3 + T_{ref}^4 + T_{ref}^5}{5}$ ) is considered for the lower layer. This works indirectly as feedforward to the lower layer, hence enables better feedback control performance. This is obvious from (F.6) and given the basic understanding of process control.

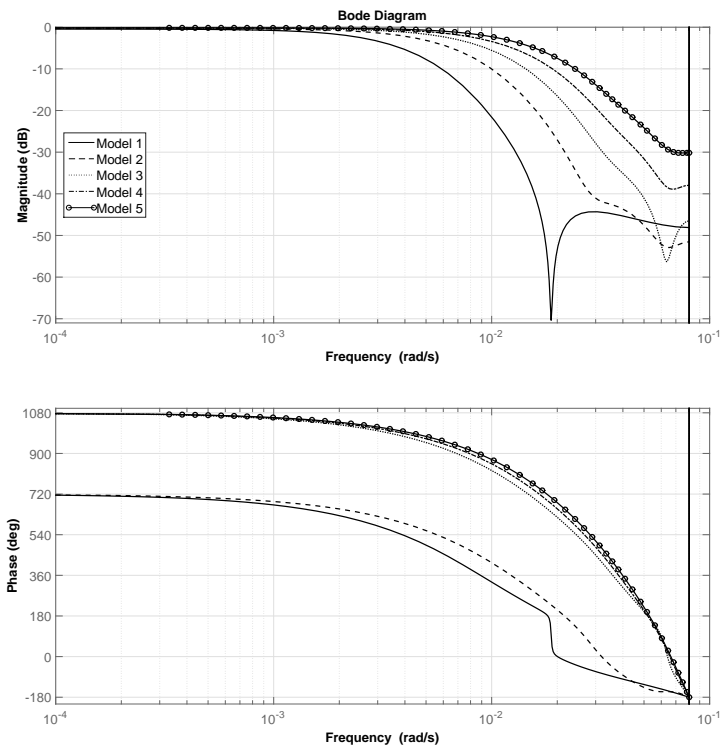


Figure F.3: Bode plot: Estimated models of the field inlet temperature.

Remark F.3 implies the necessity of an effective modelling of solar radiation and the field inlet temperature not just for a better prediction accuracy of the reference temperature, but also for a better feedback control reaction. Otherwise, the feedback control at the lower layer would end up dealing with unnecessary unmodelled dynamics of the measured disturbances.

#### *F.4.2 Lower layer*

The gain scheduling (GS) model-based predictive control (MPC) strategy proposed in Alsharkawi and Rossiter (2016b) is used here for the lower layer for tracking the desired reference temperature generated from the upper layer and coping with the plant nonlinear dynamics.

*Overview*

A GS control strategy is adopted for the lower layer because it is a widely accepted nonlinear control design strategy. It has found applications in many fields, from aerospace to process control (Leith and Leithead, 2000), and is usually seen as a way of thinking rather than a fixed design process and hence allows a flexible and tailored control design. It is also well-known for applying powerful linear design tools to a challenging nonlinear dynamic problems (Rugh and Shamma, 2000). In fact, in terms of MPC, applying a linear MPC within a GS framework to a nonlinear system overcomes the major computational drawback of a direct nonlinear MPC which is the non-convexity of the associated nonlinear optimization problem (Chisci et al., 2003).

*GS control strategy in highlight*

The design workflow of the nonlinear GS control strategy in Alsharkawi and Rossiter (2016b) involved designing and tuning a nominal linear MPC controller around medium operating condition ( $0.006 \text{ m}^3/\text{s}$ ) and then simulations were used to determine the operating conditions at which the nominal controller losses robustness. Local LTI state space models of the HTF were estimated around three new operating conditions and corresponding local linear MPC controllers were designed.

Having a scheduling variable to select an appropriate local linear MPC controller as the plant dynamics change with time or operating conditions is an essential step of the GS control design process. Given the nonlinear lumped parameter model in (F.3) and under certain assumptions, the scheduling variable in Alsharkawi and Rossiter (2016b) takes the form:

$$Q = \frac{n_o SI}{P_{cp}(T_{ref} - T_{f,inlet})}, \quad (\text{F.7})$$

where  $Q$  here is an approximate representation of the flow rate (control signal)  $q$ .

**Remark F.4.** *It is clear from (F.7) that the scheduling variable  $Q$  is mainly affected by solar radiation, the field inlet temperature and the generated reference temperature.*

Remark F.4 draws attention to the point that the control design at the lower layer is consistent with the reference temperature design at the upper layer, i.e. as the generated reference temperature is being smoothly adapted to changes in solar radiation and the field inlet temperature at the upper layer, the scheduling variable at the lower layer is simultaneously being adapted to changes in solar radiation and the field inlet temperature, as well as the generated reference temperature. Note that this is not the case in Cirre et al. (2009); Camacho and Gallego (2013) as two simple, yet different forms of proportional-integral-derivative (PID), were used for control at the lower layer.

#### F.4.3 Summary

This section has discussed the design of the upper layer and the lower layer of the proposed two-layer hierarchical control structure. Fig. F.4 gives an insight into the overall design.

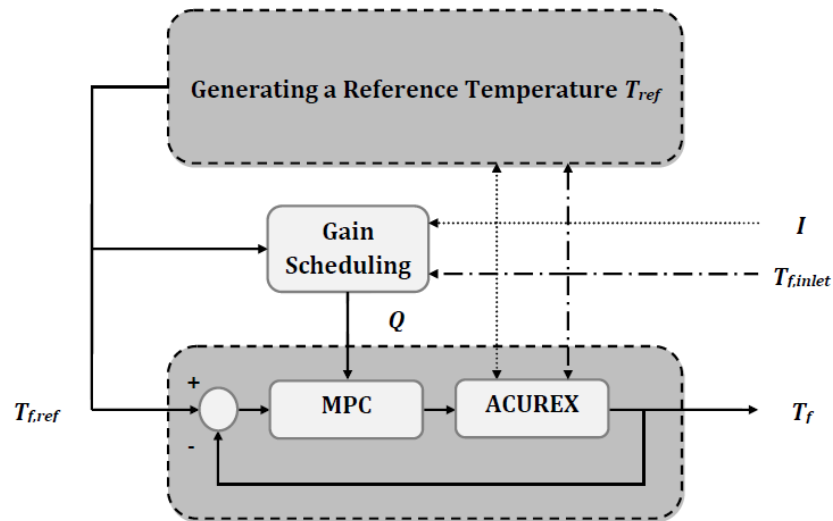


Figure F.4: Two-layer hierarchical control structure.

## ***F.5 Simulation Scenarios***

In this section the efficacy of the proposed two-layer hierarchical control strategy is illustrated by way of some simulation scenarios. More specifically:

- The first scenario illustrates, under normal operating conditions, that a reference temperature can be generated not only taking into account the status of the measured disturbances and the plant safety constraints, but also the narrow operating range of the plant steam turbine.
- The second scenario illustrates, using some measured data from the ACUREX plant, that the generated reference temperature is close enough to a measured field outlet temperature obtained in an open-loop fashion.
- Using some measured data from the ACUREX plant, the third and fourth scenarios illustrate how the generated reference temperature can adapt elegantly to changes in solar radiation and the field inlet temperature respectively while taking into account the plant safety constraints.

In summary, the first scenario demonstrates an ideal operation of the plant, the second scenario validates the prediction accuracy of the generated reference temperature and the third and fourth scenarios cover all the typical changes in solar radiation and the field inlet temperature.

### *F.5.1 First scenario*

ACUREX generates a peak power of 1.2 MW with a solar radiation ( $I$ ) of 900 W/m<sup>2</sup> (Johansen et al., 2000) and has a normal working field inlet temperature ( $T_{f,inlet}$ ) of 212°C (Camacho et al., 1993). Due to dust and dirt, the mirror optical efficiency  $n_o$  varies over time. For example, it varied from 52 % to 62 % for the year 1992 (Meaburn and Hughes, 1997). A value of 57 % is considered here and bringing all these aspects

together, the scenario in Fig. F.5 illustrates the generation of a reference temperature  $T_{ref}$  and corresponding behaviours of other core signals.

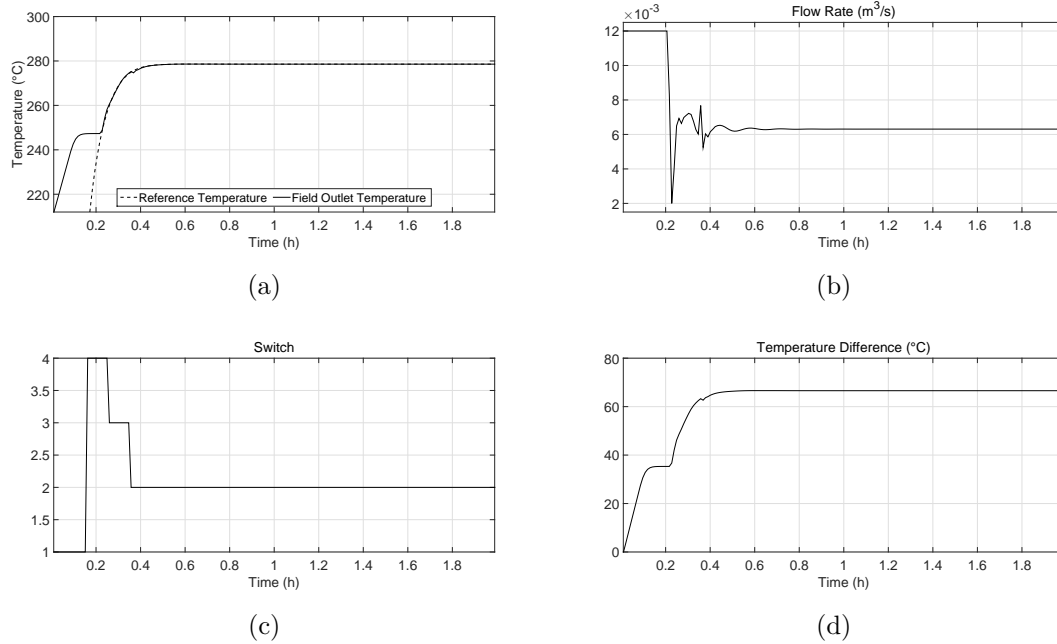


Figure F.5: First scenario: Reference temperature at normal operating conditions.

While taking into account the status of the measured disturbances, it can be clearly seen from Fig. F.5 (a) that the generated reference temperature settles at  $278.6^{\circ}\text{C}$  and maintains a temperature difference between the field inlet and outlet temperature around  $70^{\circ}\text{C}$  as required, namely  $66.6^{\circ}\text{C}$ ; see Fig. F.5 (d). Note that the generated reference temperature indeed meets the narrow operating range of the plant steam turbine  $277\text{--}292^{\circ}\text{C}$ .

On the other hand, it is worth noting that the GS predictive control strategy is coping very well with the nonlinear dynamics of the plant as illustrated in Fig. F.5 (c) by the switching from one local controller to another during the transient and showing a fine set point tracking performance by maintaining the flow rate of the HTF at around  $0.006\text{ m}^3/\text{s}$  as expected; see Fig. F.5 (b).

It is worth noting that the scenario here has not been illustrated before elsewhere in the literature, namely Cirre et al. (2009); Camacho and Gallego (2013).

### F.5.2 Second scenario

Measured data from the ACUREX plant were collected on 15 July 2003 for a series of step changes in the volumetric flow rate of the HTF.

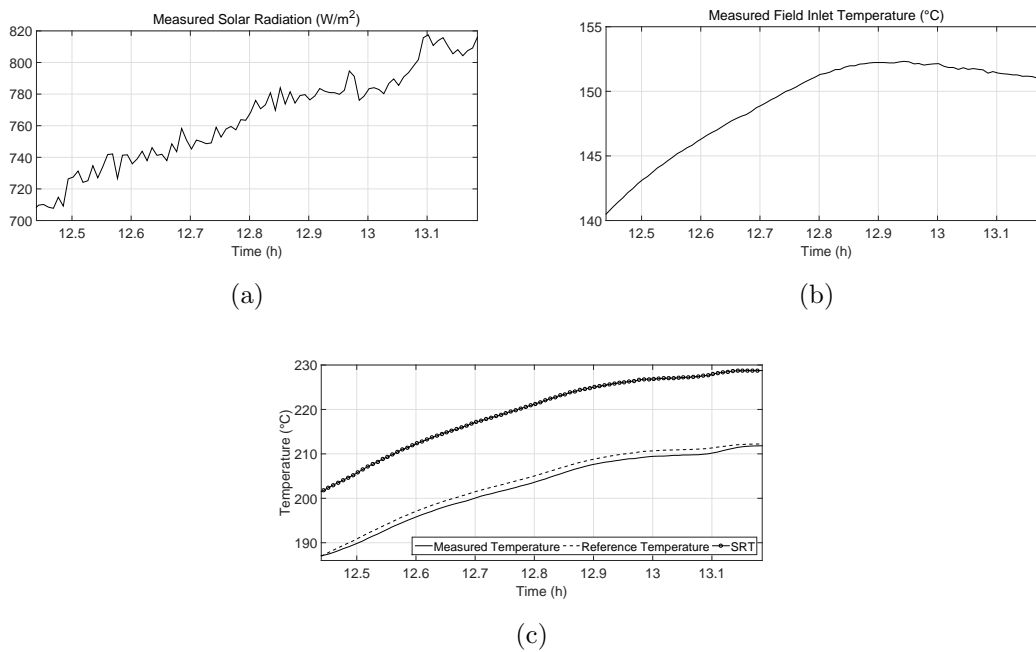


Figure F.6: Second scenario: Reference temperature against a measured field outlet temperature.

Using the same measurements of solar radiation and the field inlet temperature at the time of collecting the field outlet temperature, in addition to other operating conditions, Fig. F.6 (c) shows the generated reference temperature against the measured field outlet temperature around a medium flow rate of 0.006 m<sup>3</sup>/s. It is clear that the generated reference temperature is close enough to the measured field outlet temperature.

Note that Fig. F.6 (c) also shows a simplified reference temperature (SRT), which

refers to the reference temperature being generated based on simplified LTI state space models of solar radiation and the field inlet temperature. In other words, the estimated models of solar radiation and the field inlet temperature do not adequately take into account the resonance characteristics of the ACUREX plant and the relative inaccuracy of this is quite apparent. This, in fact, makes one question the prediction accuracy of the desired reference temperature in Cirre et al. (2009); Camacho and Gallego (2013) as the resonance characteristics did not receive any attention.

### *F.5.3 Third scenario*

Solar radiation is the main source of energy to the ACUREX plant, however, it is constantly subject to changes due to the daily cycle of radiation and quite commonly passing clouds. The measured solar radiation shown in Fig. F.7 (d) is a fine example of both the daily cycle of radiation and passing clouds. The measured cycle of radiation here is lower than a typical daily cycle of radiation and yet, a reference temperature as shown in Fig. F.7 (a) has been generated while being elegantly adapted not just to these conditions but also to the transient of the measured field inlet temperature shown in Fig. F.7 (e).

### *F.5.4 Fourth scenario*

It has been mentioned earlier that the field inlet temperature is subject to changes due to the stratified tank technology used for storing the thermal energy of the plant. The measured field inlet temperature shown in Fig. F.8 (c) demonstrates a classical transient and significant changes about midday. It can be clearly seen that the generated reference temperature shown in Fig. F.8 (a) is coping smoothly with these changes and more importantly maintaining a temperature difference between the field inlet and outlet temperature within the safety limit; see Fig. F.8 (f). One can also notice the impact of the daily cycle of radiation on the generated reference temperature once the measured field inlet temperature is settled down.

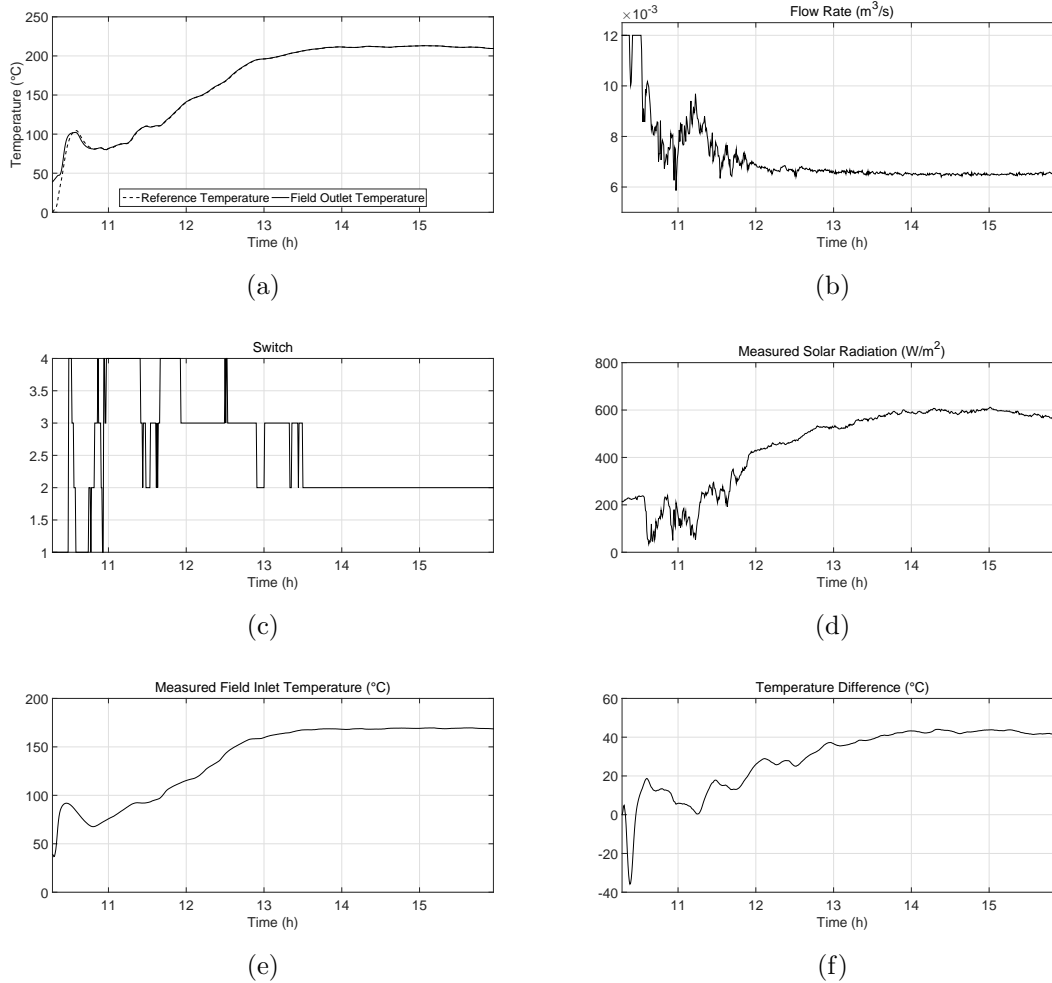


Figure F.7: Third scenario: Generation of a reference temperature using measurements from the ACUREX plant collected on 18 July 2003.

## F.6 Conclusions

This paper has proposed a novel pragmatic approach to automatically operate ACUREX, a parabolic trough-based solar thermal power plant. Namely, a two-layer hierarchical control structure is proposed, an upper layer for generating a reference temperature during the normal operation of the plant and a lower layer for tracking

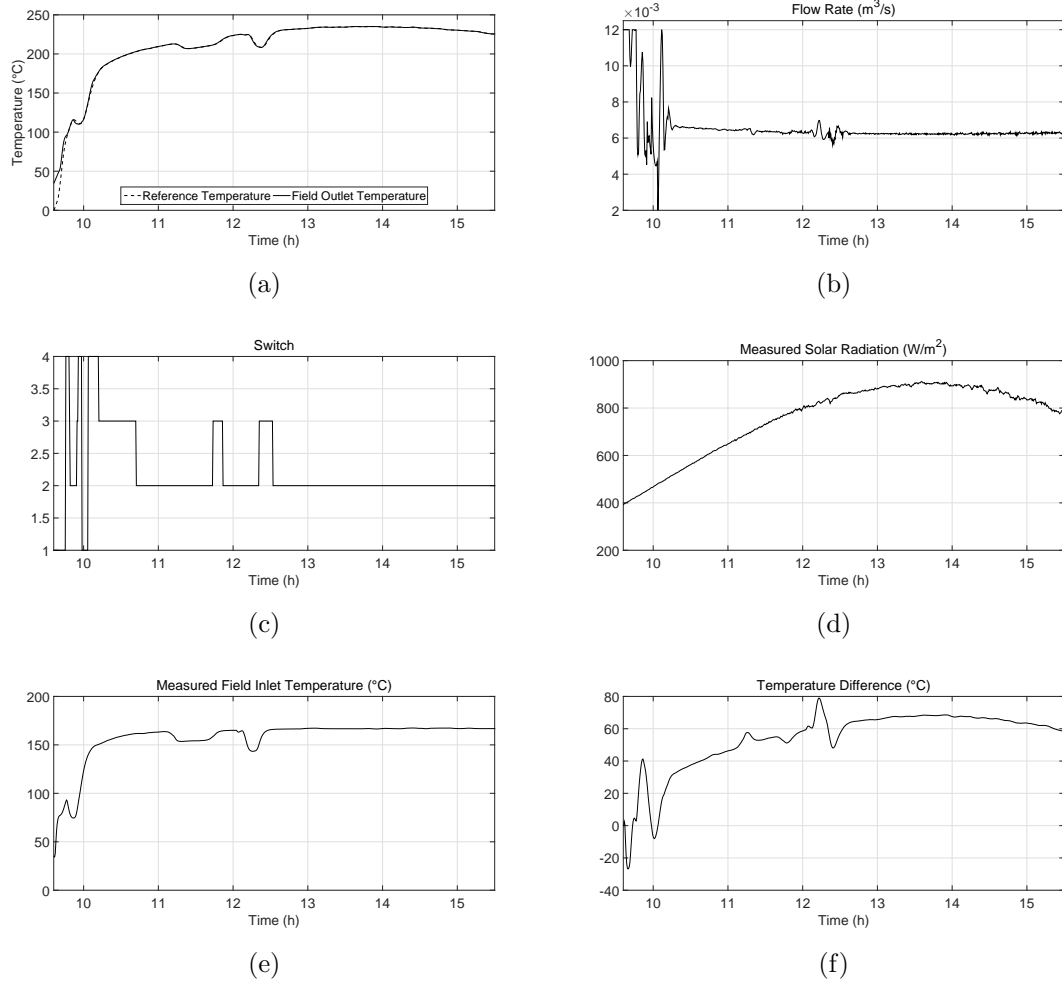


Figure F.8: Fourth scenario: Generation of a reference temperature using measurements from the ACUREX plant collected on 28 July 2003.

and coping with the plant nonlinear dynamics. The novelty of the proposed approach is its apparent simplicity, while it does not require any help from the plant operator and is easy to implement. A notable contribution is the design of the upper layer where complete one-step ahead prediction models of the reference temperature are developed using estimated LTI state space models of solar radiation and the field inlet temperature. Estimated models of solar radiation and the field inlet temperature

take an explicit account of the resonance phenomena of the ACUREX plant.

By way of simulation scenarios and measured data from the ACUREX plant, it has been illustrated that the generated reference temperature is adequate, reachable and smoothly adapts to changes in solar radiation and the field inlet temperature while at the same time satisfying the plant safety constraints. Under normal operating conditions of the plant, it has been also illustrated that the generated reference temperature satisfies the narrow operating range of the plant steam turbine.

Unlike the fuzzy logic approach in Cirre et al. (2009), the proposed approach requires little knowledge of the plant and overcomes the downside of the optimisation-based approaches in Cirre et al. (2009); Camacho and Gallego (2013) by driving the plant near optimal operating conditions rather than solving a direct nonlinear optimisation problem. The proposed approach in this paper has the potential benefits of: (i) maximising electricity production; (ii) reducing the risk of actuator saturation; (iii) extending the life span of various elements of the plant (e.g. synthetic oil, pump and valves) and (iv) limiting the role of the plant operator. Despite these benefits, it is fair to say that an improved version of the proposed approach could include: (i) compact prediction models of electricity market and (ii) systematic account of the temperature difference.

## BIBLIOGRAPHY

- Alsharkawi, A. and Rossiter, J.A. (2017). Towards an improved gain scheduling predictive control strategy for a solar thermal power plant. *IET Control Theory & Applications*, DOI: 10.1049/iet-cta.2016.1319.
- Alsharkawi, A. and Rossiter, J.A. (2016a). Dual mode MPC for a concentrated solar thermal power plant. In *Proceedings of the 11th IFAC Symposium on Dynamics and Control of Process Systems, including Biosystems, Trondheim, Norway*, volume 49(7), 260–265. Elsevier.
- Alsharkawi, A. and Rossiter, J.A. (2016b). Gain scheduling dual mode MPC for a solar thermal power plant. In *Proceedings of the 10th IFAC Symposium on Nonlinear Control Systems, California, USA*, volume 49(18), 128–133. Elsevier.
- Berenguel, M., Cirre, C.M., Klempous, R., Maciejewski, H., Nikodem, M., Nikodem, J., Rudas, I., and Valenzuela, L. (2005). Hierarchical control of a distributed solar collector field. In *Proceedings of the International Conference on Computer Aided Systems Theory*, volume 3643, 614–620. Springer.
- Camacho, E.F., Berenguel, M., Rubio, F.R., and Martínez, D. (2012). *Control of solar energy systems*. Springer-Verlag.
- Camacho, E., Berenguel, M., and Rubio, F. (1993). Simulation software package of the acurex field. *Sevilla: ESI of Sevilla, Internal Report*.
- Camacho, E. and Gallego, A. (2013). Optimal operation in solar trough plants: A case study. *Solar Energy*, volume 95, 106–117.
- Carmona, R. (1985). *Analysis, modeling and control of a distributed solar collector field with a one-axis tracking system*. Ph.D. thesis. University of Seville, Spain.

- Chisci, L., Falugi, P., and Zappa, G. (2003). Gain-scheduling MPC of nonlinear systems. *International Journal of Robust and Nonlinear Control*, volume 13(3-4), 295–308.
- Cirre, C.M., Berenguel, M., Valenzuela, L., and Klempous, R. (2009). Reference governor optimization and control of a distributed solar collector field. *European Journal of Operational Research*, volume 193(3), 709–717.
- Goswami, D.Y., Kreith, F., and Kreider, J.F. (2015). *Principles of solar engineering*. CRC Press.
- IEA (2011). *Solar energy perspectives*. International Energy Agency.
- Johansen, T.A., Hunt, K.J., and Petersen, I. (2000). Gain-scheduled control of a solar power plant. *Control Engineering Practice*, volume 8(9), 1011–1022.
- Leith, D.J. and Leithead, W.E. (2000). Survey of gain-scheduling analysis and design. *International journal of control*, volume 73(11), 1001–1025.
- Ljung, L. (2015). *MATLAB: System Identification Toolbox: User's Guide Version 9.3*. The Mathworks.
- Meaburn, A. and Hughes, F. (1993). Resonance characteristics of distributed solar collector fields. *Solar Energy*, volume 51(3), 215–221.
- Meaburn, A. and Hughes, F. (1997). Feedforward control of solar thermal power plants. *Journal of Solar Energy Engineering*, volume 119(1), 52–60.
- Prett, D. and Garcia, C. (1988). *Fundamental Process Control*. Butterworths.
- Rugh, W.J. and Shamma, J.S. (2000). Research on gain scheduling. *Automatica*, volume 36(10), 1401–1425.
- Van Overschee, P. and De Moor, B. (1996). *Subspace identification for linear systems: Theory-Implementation-Applications*. Springer Science & Business Media.

Appendix G

**TOWARDS AN IMPROVED  
HIERARCHICAL CONTROL  
STRATEGY FOR A SOLAR THERMAL  
POWER PLANT**

**Adham Alsharkawi and J. Anthony Rossiter**

This paper is to be submitted.

### ***Abstract***

This paper improves a recently proposed two-layer hierarchical control strategy for the ACUREX plant at the Plataforma Solar de Almería. Improvements target the lower layer of the two-layer hierarchical control strategy and this paper proposes/evaluates two alternative systematic approaches to utilising the the measured disturbances. Improvements are illustrated by way of some simulation scenarios and measured data from the ACUREX plant.

#### ***G.1 Introduction***

ACUREX is a parabolic trough-based solar thermal power plant. It is one of the research facilities at the Plataforma Solar de Almería (PSA) owned and operated by the Spanish research centre for energy, environmental studies and technology (CIEMAT). The PSA is located in south-east Spain and is considered the largest research centre in Europe for concentrating solar technologies.

ACUREX has served as a benchmark for many researchers across academia and industry working in process modelling and control. The plant is mainly composed of a distributed solar collector field, a thermal storage tank and a power unit; solar radiation is the main source of energy, however, ironically it acts as a disturbance to the plant due to the daily cycle of radiation and passing clouds. Due to the stratified tank technology used for storing the thermal energy of the plant, the field inlet temperature is also a dominant disturbance to the plant. Hence, designing an effective control strategy that can handle the constant changes in solar radiation and the field inlet temperature while maintaining the field outlet temperature at a desired level will enable longer plant operating hours and cost reductions (Camacho et al., 2012).

Recent work proposed, an effective two-layer hierarchical control strategy (Alsharkawi and Rossiter, 2017a) to automatically operate the ACUREX plant without intervention from the plant operator and without adding cost. Taking into account

the status of solar radiation and the field inlet temperature (measured disturbances), an adequate reachable reference temperature (set point) is generated from an upper layer while satisfying the plant safety constraints. Due to the nature of hierarchy, a gain scheduling (GS) predictive control strategy is adopted in a lower layer. It was shown (Alsharkawi and Rossiter, 2017a) that the generated reference temperature works indirectly as feedforward to the lower layer and hence the role of the GS predictive control strategy at the lower layer was merely for set point tracking and coping with the plant nonlinear dynamics. Therefore, the main objective of this paper is to improve the feedback control performance at the lower layer by taking explicit account of the measured disturbances. This is achieved here through two alternative approaches:

- The first approach utilises a recently proposed GS feedforward predictive control strategy (Alsharkawi and Rossiter, 2017c) that assumes the availability of the current measurements of solar radiation and the field inlet temperature.
- The second approach utilises a variant of the GS feedforward predictive control strategy that assumes the availability of the expected future behaviour of solar radiation and the field inlet temperature. This approach is developed here as such an assumption has received little attention in the literature.

Apart from the proposed strategies in Cirre et al. (2009); Camacho and Gallego (2013), hierarchical control for the ACUREX plant has received little attention. While no feedforward to account for the measured disturbances has been reported in Camacho and Gallego (2013) and a rather simple classical parallel feedforward has been designed for the lower layer in Cirre et al. (2009) based on steady state energy balance, the two approaches proposed here for the lower layer incorporate feedforward more systematically into a predictive control strategy by including the dynamic effects of the measured disturbances of the ACUREX plant into the predictions of future outputs.

The efficacy of both approaches within a two-layer hierarchical control structure will be illustrated by way of some simulation scenarios and measured data from the ACUREX plant. The plant description is outlined in Section G.2, Section G.3 discusses briefly a nonlinear simulation model of the Plant, Section G.4 gives an overview of the to be improved two-layer hierarchical control strategy. Section G.5 introduces the proposed approaches to improve the two-layer hierarchical control strategy given in Section G.4. Section G.6 illustrates the efficacy of both approaches within a two-layer hierarchical control structure for two common scenarios and finally conclusions are given in section G.7.

## ***G.2 Plant Description***

Collectors of the ACUREX plant are parabolic in shape and concentrate the incident solar radiation onto a receiver tube that is placed at its focal line; see Fig. G.1. The distributed solar collector field consists of 480 east-west single axis collectors arranged in 10 parallel loops with 48 collectors in each loop. Electricity is generated through the following process. A heat transfer fluid (HTF) is heated as it flows through the receiver tube and circulates through the distributed solar collector field. The heated HTF then passes through a series of heat exchangers to produce steam which in turn is used to drive a steam turbine to generate electricity.

The control problem at the ACUREX plant is to maintain the field outlet temperature at a desired level despite changes, mainly in solar radiation and the field inlet temperature. The approach to this is by efficiently manipulating the volumetric flow rate of the HTF within a certain range (0.002-0.012 m<sup>3</sup>/s). For a detailed description of the plant, see Camacho et al. (2012).

## ***G.3 Nonlinear Simulation Model of the Plant***

The ACUREX plant is represented in this paper by a nonlinear simulation model. The model is constructed based on a nonlinear distributed parameter model of the



Figure G.1: ACUREX distributed solar collector field.

plant and has been recently validated in Alsharkawi and Rossiter (2017c). The dominant dynamics of the ACUREX plant are captured by the following set of energy balance partial differential equations (PDEs):

$$\begin{aligned} \rho_m C_m A_m \frac{\partial T_m}{\partial t} &= n_o G I - D_o \pi H_l (T_m - T_a) - D_i \pi H_t (T_m - T_f), \\ \rho_f C_f A_f \frac{\partial T_f}{\partial t} + \rho_f C_f q \frac{\partial T_f}{\partial x} &= D_i \pi H_t (T_m - T_f), \end{aligned} \quad (\text{G.1})$$

where the subindex  $m$  refers to the metal of the receiver tube and  $f$  to the HTF (Carmona, 1985; Camacho et al., 2012). Table G.1 gives a description of all the variables and parameters and lists their SI units.

A nonlinear simulation model of the plant has been constructed in Alsharkawi and Rossiter (2016a) by dividing the receiver tube into  $N$  segments each of length  $\Delta x$  and hence the nonlinear distributed parameter model in (G.1) has been approximated by the following set of ordinary differential equations (ODEs):

$$\begin{aligned} \rho_m C_m A_m \frac{dT_{m,n}}{dt} &= n_o G I - D_o \pi H_l (T_{m,n} - T_a) - D_i \pi H_t (T_{m,n} - T_{f,n}), \\ \rho_f C_f A_f \frac{dT_{f,n}}{dt} + \rho_f C_f q \frac{T_{f,n} - T_{f,n-1}}{\Delta x} &= D_i \pi H_t (T_{m,n} - T_{f,n}) \end{aligned}, \quad n = 1, \dots, N, \quad (\text{G.2})$$

Table G.1: Variables and Parameters.

Symbol	Description	SI unit
$\rho$	Density	kg/m <sup>3</sup>
$C$	Specific heat capacity	J/kg°C
$A$	Cross-sectional area	m <sup>2</sup>
$T$	Temperature	°C
$t$	Time	s
$I$	Solar radiation	W/m <sup>2</sup>
$n_o$	Mirror optical efficiency	–
$G$	Mirror optical aperture	m
$D_o$	Outer diameter of the receiver tube	m
$H_l$	Global coefficient of thermal losses	W/m°C
$T_a$	Ambient temperature	°C
$D_i$	Inner diameter of the receiver tube	m
$H_t$	Metal-fluid heat transfer coefficient	W/m <sup>2</sup> °C
$q$	HTF volumetric flow rate	m <sup>3</sup> /s
$x$	Space	m

with the boundary condition  $T_{f,0} = T_{f,inlet}$  (field inlet temperature) and  $H_l, H_t, \rho_f$  and  $C_f$  being time-varying.

It has been shown (Alsharkawi and Rossiter, 2016a) that dividing the receiver tube into 7 segments ( $N = 7$ ) is a reasonable trade-off between the prediction accuracy and computational burden while still adequate enough to capture the resonant modes of the plant. This was validated against some measured data from the ACUREX plant in Alsharkawi and Rossiter (2017c) and a detailed modelling analysis Alsharkawi and Rossiter (2017b).

**Remark G.1.** *The set of ODEs (G.2) is implemented and solved using the*

MATLAB<sup>®</sup> solver *ODE45* (an explicit Runge-Kutta method) where the temperature distribution in the receiver tube and HTF can be accessed at any point in time and for any segment  $n$ . The number of ODEs solved at each sample time  $k$  for  $N$  segments is  $2 \times N$ .

In summary, the ACUREX plant is represented in this paper by the nonlinear simulation model described in (G.2).

#### **G.4 Two-Layer Hierarchical Control Structure**

The main objective of this paper is to improve the feedback control performance at the lower layer of the recently proposed two-layer hierarchical control strategy (Alsharkawi and Rossiter, 2017a). More specifically, the aim is to take systematic account of the measured disturbances at the lower layer. Before establishing how this aim is achieved, readers need to be familiar with the basic concepts of this two-layer hierarchical control strategy.

##### *G.4.1 Overview*

A novel pragmatic approach was proposed in Alsharkawi and Rossiter (2017a) to drive the plant near optimal operating conditions by generating a reference temperature that is adequate, reachable and smoothly adapted to changes in solar radiation and the field inlet temperature while also satisfying the plant safety constraints. Conceptually, the approach has a hierarchical structure, namely upper and lower layers.

##### *G.4.2 Upper layer*

The approach to generate the reference temperature at the upper layer is intuitive and makes use of system identification. Given the process time constant and taking into account the frequency response of the plant, LTI state space models of solar radiation and the field inlet temperature are estimated around five nominal

operating points across the whole range of the flow rate (0.002-0.012 m<sup>3</sup>/s). The estimated models establish a clear, direct and dynamic relationships with the field outlet temperature (reference temperature). Each LTI state space model takes the form:

$$x_{k+1} = Ax_k + Bu_k, \quad y_k = Cx_k, \tag{G.3}$$

where  $x_k \in \mathbb{R}^{n \times 1}$ ,  $u_k \in \mathbb{R}^{m \times 1}$  and  $y_k \in \mathbb{R}^{l \times 1}$  are the state vector, input vector and output vector at sample  $k$ .  $A, B$  and  $C$  are matrices of appropriate dimensions.

In particular, at each operating point, a complete one-step ahead prediction model predicts the *best* reference temperature, given the measurements of solar radiation and the field inlet temperature, as follows:

$$\underbrace{\begin{bmatrix} x_{k+1}^I \\ x_{k+1}^{T_{f,inlet}} \end{bmatrix}}_{x_{k+1}^i} = \underbrace{\begin{bmatrix} A^I & 0 \\ 0 & A^{T_{f,inlet}} \end{bmatrix}}_{A^i} \underbrace{\begin{bmatrix} x_k^I \\ x_k^{T_{f,inlet}} \end{bmatrix}}_{x_k^i} + \underbrace{\begin{bmatrix} B^I & 0 \\ 0 & B^{T_{f,inlet}} \end{bmatrix}}_{B^i} \underbrace{\begin{bmatrix} I_k \\ T_{f,inlet_k} \end{bmatrix}}_{u_k}, \tag{G.4}$$

$$T_{ref_k}^i = \underbrace{\begin{bmatrix} C^I & C^{T_{f,inlet}} \end{bmatrix}}_{C^i} \underbrace{\begin{bmatrix} x_k^I \\ x_k^{T_{f,inlet}} \end{bmatrix}}_{x_k^i},$$

where  $i \in \{1, 2, 3, 4, 5\}$  and  $T_{ref}$  is the reference temperature. Due to the nonlinear dynamic behaviour of the plant, a mean value of the generated reference temperatures is considered for the lower layer. It is obvious from (G.4) how the reference temperature works indirectly as feedforward for the lower layer.

#### G.4.3 Lower layer

A GS predictive control strategy has been adopted at the lower layer for set point tracking and coping with the plant nonlinear dynamics. The GS predictive control strategy has been proposed in Alsharkawi and Rossiter (2016b) and tailored to the ACUREX plant. A notable feature of the control strategy is the design of the scheduling variable. Given a nonlinear lumped parameter model of ACUREX plant reported in Camacho et al. (2012) and under certain assumptions, the scheduling

variable takes the form:

$$Q = \frac{n_o SI}{P_{cp}(T_{ref} - T_{f,inlet})}, \quad (\text{G.5})$$

where  $Q$  here is an approximate representation of the flow rate (control signal)  $q$ ,  $S$  is the solar field effective surface and  $P_{cp}$  is a factor that takes into account some geometrical and thermal properties.

This draws attention to the point that the control design at the lower layer is consistent with the reference temperature design at the upper layer, i.e. as the generated reference temperature is being smoothly adapted to changes in solar radiation and the field inlet temperature at the upper layer, the scheduling variable at the lower layer is simultaneously being adapted to changes in solar radiation and the field inlet temperature, as well as the generated reference temperature.

The scheduling variable  $Q$  switches on-line among four local linear model-based predictive controllers as the plant dynamics change with time or operating conditions. For a selected local controller and at each sample time  $k$ , an optimisation is performed seeking a future sequence of control moves. Nevertheless, the optimisation takes no direct account of the measured disturbances.

### ***G.5 Proposals for Improved Algorithms***

The feedback control performance at the lower layer of the two-layer hierarchical control strategy (Alsharkawi and Rossiter, 2017a) is improved here to take explicit and systematic account of the measured disturbances of the ACUREX plant. Two approaches are considered based on two different assumptions. As will be shown later, incorporating a feedforward into the lower layer has the potential benefits of both improving the actuator dynamics and reducing the risk of actuator saturation.

The first approach utilises a recently proposed GS feedforward predictive control strategy (Alsharkawi and Rossiter, 2017c) that assumes the availability of current measurements of solar radiation and field inlet temperature. The second approach utilises a variant of the GS feedforward predictive control strategy that assumes availability of the expected future behaviour of solar radiation and the field inlet

temperature for a given prediction horizon. The second approach is developed here and its efficacy with respect to the first approach is evaluated in a later section. An essential step to ensure that measured disturbances are accounted for by both approaches at the lower layer is to ensure that, at a given operating point, the local process model includes the disturbance dynamics. This is discussed next.

*G.5.1 Local process model with measured disturbances*

Due to the nonlinearity of the ACUREX plant, local LTI state space models relating the volumetric flow rate of the HTF ( $q$ ) to the field outlet temperature ( $T_f$ ) were estimated in Alsharkawi and Rossiter (2016b) directly from input-output data around four nominal operating points. Each LTI state space model takes the form of (G.3). Predictions of these models were improved in Alsharkawi and Rossiter (2017c) by estimating dynamic LTI state space models of solar radiation ( $I$ ) and the field inlet temperature ( $T_{f,inlet}$ ) around the same nominal operating points. Hence, at a given operating point, a local process model can be augmented to include the disturbance dynamics, for  $j \in \{1, 2, 3, 4\}$ , as follows:

$$\underbrace{\begin{bmatrix} x_{k+1}^q \\ x_{k+1}^I \\ x_{k+1}^{T_{f,inlet}} \end{bmatrix}}_{x_{k+1}^j} = \underbrace{\begin{bmatrix} A^q & 0 & 0 \\ 0 & A^I & 0 \\ 0 & 0 & A^{T_{f,inlet}} \end{bmatrix}}_{A^j} \underbrace{\begin{bmatrix} x_k^q \\ x_k^I \\ x_k^{T_{f,inlet}} \end{bmatrix}}_{x_k^j} + \underbrace{\begin{bmatrix} B^q & 0 & 0 \\ 0 & B^I & 0 \\ 0 & 0 & B^{T_{f,inlet}} \end{bmatrix}}_{B^j} \begin{bmatrix} q_k \\ I_k \\ T_{f,inlet_k} \end{bmatrix},$$

$$y_k^j = \underbrace{\begin{bmatrix} C^q & C^I & C^{T_{f,inlet}} \end{bmatrix}}_{C^j} \underbrace{\begin{bmatrix} x_k^q \\ x_k^I \\ x_k^{T_{f,inlet}} \end{bmatrix}}_{x_k^j}.$$

(G.6)

**Remark G.2.** *Regardless of the assumptions made about the future of the measured disturbances, the local process model in (G.6) is a core component of both GS feedforward predictive control strategies discussed next.*

### G.5.2 First approach

This first approach is a GS feedforward model-based predictive control (MPC) and has been proposed in Alsharkawi and Rossiter (2017c). This approach assumes the following:

- The availability of the current measurements of solar radiation  $I$  and the field inlet temperature  $T_{f,inlet}$  at sample time  $k$ .
- $I_k = I_{k+1} = \dots = I_{ss}$  and similarly  $T_{f,inlet_k} = T_{f,inlet_{k+1}} = \dots = T_{f,inlet_{ss}}$ , where  $I_{ss}$  and  $T_{f,inlet_{ss}}$  are steady-state estimates of solar radiation and the field inlet temperature respectively.

Given these assumptions and the local process model in (G.6), the optimisation required to find the future sequence of control moves, at a given operating point, takes the form:

$$\min_{\substack{\bar{q} \\ \rightarrow}} \bar{q}_{\rightarrow k-1}^T S \bar{q}_{\rightarrow k-1} + \bar{q}_{\rightarrow k-1}^T L \bar{x}_k, \quad \text{s.t.} \quad \beta \bar{q}_{\rightarrow} \leq \gamma, \quad (\text{G.7})$$

where  $\bar{q}_{\rightarrow k-1} = [\bar{q}_k^T \quad \bar{q}_{k+1}^T \quad \dots \quad \bar{q}_{k+n_c-1}^T]^T$  and  $n_c$  is the number of control moves.  $S$  and  $L$  depend upon the matrices  $A$ ,  $B^q$ , weighting matrices of appropriate dimensions  $\delta$  and  $\lambda$  and terminal weight  $P$  obtained from an appropriate Lyapunov equation.  $\beta$  is time-invariant and  $\gamma$  depends upon the system past input-output information. Note that  $\bar{q}$  and  $\bar{x}$  are the deviation from estimated steady-state values  $q_{ss}$  and  $x_{ss}$  respectively. For detailed treatment of this and full definitions of the various variables and parameters see Alsharkawi and Rossiter (2017c).

### G.5.3 Second approach

A notable contribution of this paper is the development of this second approach. It is a variant of the GS feedforward MPC (Alsharkawi and Rossiter, 2017c) and assumes the following:

---

**Algorithm 1**

---

- 1: For each of the nominal operating points and given the local process model in (G.6), define the parameters in (G.7).
  - 2: For a selected local controller and at each sampling instant, perform the optimization in (G.7).
  - 3: Solve for the first element of  $\bar{q}$  and implement on process.
- 

- The availability of  $n_a$ -step ahead predictions of solar radiation  $I$  and the field inlet temperature  $T_{f,inlet}$  at sample time  $k$ .
- $I_k \neq I_{k+1} \neq \dots \neq I_{ss}$  and similarly  $T_{f,inlet_k} \neq T_{f,inlet_{k+1}} \neq \dots \neq T_{f,inlet_{ss}}$ , where  $I_{ss}$  and  $T_{f,inlet_{ss}}$  in this case are  $I_{k+n_a}$  and  $T_{f,inlet_{k+n_a}}$  respectively.

**Remark G.3.** *To keep a neat and compact algorithm, the prediction horizon of solar radiation and the field inlet temperature are assumed to be the same.*

This second approach builds on the control design in Alsharkawi and Rossiter (2017c), where a single local feedforward MPC was designed around a given operating point with  $n_a$ -step ahead predictions of solar radiation. More specifically and within a gain scheduling framework, it extends the control design to cover the whole range of operation and considers  $n_a$ -step ahead predictions of both solar radiation and the field inlet temperature. Hence, given the above assumptions and the local process model (G.6), the optimisation required to find the future sequence of control moves, at a given operating point, takes the form:

$$\min_{\bar{q}} \quad \bar{q}_{\rightarrow k-1}^T S \bar{q}_{\rightarrow k-1} + \bar{q}_{\rightarrow k-1}^T L \bar{x}_k + \bar{q}_{\rightarrow k-1}^T M \bar{I}_{\rightarrow k-1} + \bar{q}_{\rightarrow k-1}^T N \bar{T}_{f,inlet,\rightarrow k-1}, \quad \text{s.t.} \quad \beta \bar{q}_{\rightarrow} \leq \gamma, \quad (\text{G.8})$$

where  $M$  depends upon  $A$ ,  $B^q$ ,  $B^I$ ,  $\delta$  and  $P$ , and similarly  $N$  depends upon  $A$ ,  $B^q$ ,  $B^{T_{f,inlet}}$ ,  $\delta$  and  $P$ . For detailed definitions of these variables and parameters see Alsharkawi and Rossiter (2017c).

---

**Algorithm 2**


---

- 1: For each of the nominal operating points and given the local process model in (G.6), define the parameters in (G.8).
  - 2: For a selected local controller and at each sampling instant, perform the optimization in (G.8).
  - 3: Solve for the first element of  $\bar{q}$  and implement on process.  
 $\rightarrow$
- 

**Remark G.4.** *Given  $n_a$ -step ahead predictions of solar radiation and the field inlet temperature and with slight modifications to the one-step ahead prediction model in (G.4), one can in fact obtain  $n_a$ -step ahead predictions of the reference temperature. It has been shown in Dughman and Rossiter (2017) that an effective use of advance information on set point changes within an optimum predictive control law can be advantageous and beneficial and yet this has been little studied in the context of solar plant.*

#### G.5.4 Summary

This section has proposed two algorithms to improve the feedback control performance at the lower layer of a two-layer hierarchical control strategy (Alsharkawi and Rossiter, 2017a). The two algorithms both make explicit use of the measured disturbances, but based on two different assumptions. The schematic diagram in Fig. G.2 gives an insight into the overall control design and information flow. To put it succinctly, a notable improvement to the two-layer hierarchical control strategy (Alsharkawi and Rossiter, 2017a) is achieved by systematic incorporation of feedforward action into the predictive control strategy represented in Fig. G.2.

## G.6 Evaluation

In this section the efficacy of Algorithm 1 and Algorithm 2 at the lower layer of a two-layer hierarchical control strategy is illustrated by way of some simulation

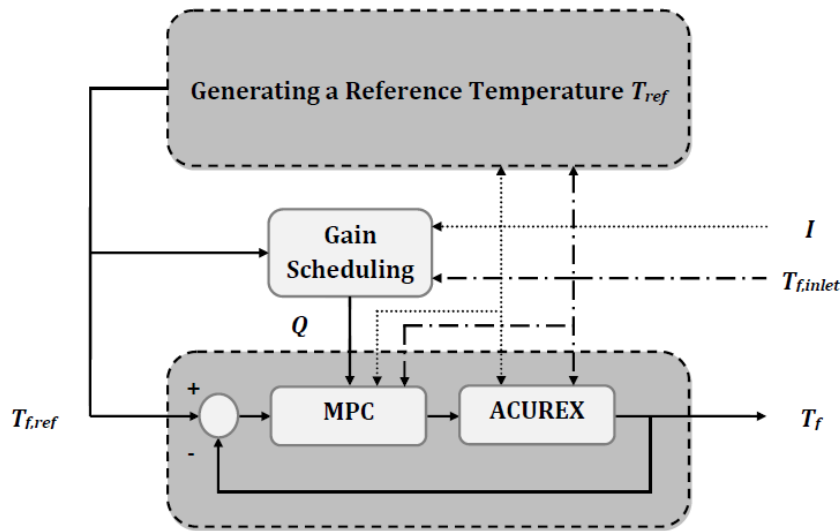


Figure G.2: Two-layer hierarchical control structure.

scenarios and, at some point, some measured data from the ACUREX plant. More specifically:

- Using some measured data from the ACUREX plant, the first scenario illustrates that incorporating Algorithm 1 at the lower layer of the two-layer hierarchical control strategy (Alsharkawi and Rossiter, 2017a) improves the feedback control action. This is illustrated by comparison with the original algorithm, that is, a standard gain scheduling model-based predictive control (GSMPC) strategy.
- The second scenario illustrates by way of comparison between Algorithm 1 and Algorithm 2 the behaviour during drastic changes in solar radiation due to thick and scattered passing clouds. While the field inlet temperature is at steady-state, Algorithm 2 shows a better set point tracking performance and lower cost of regulation provided that the prediction horizon is sufficiently large.

### *G.6.1 First scenario*

This scenario compares the feedback control performance of Algorithm 1 with the feedback control performance of the GSMPC algorithm originally used at the lower layer in Alsharkawi and Rossiter (2017a). The reference temperature shown in Fig. G.3 (c) is generated using measurements of solar radiation and the field inlet temperature shown in Fig. G.3 (a) and Fig. G.3 (b) respectively. These measurements were collected from the ACUREX plant on 15 July 2003.

One can notice from Fig. G.3 (c) that both algorithms show very similar set point tracking performance, which is not a surprise because the reference temperature, as mentioned before, is already working indirectly as feedforward for the lower layer. Hence, any improvement is due to the explicit use of the measured disturbance information by Algorithm 1 and this should be apparent in the feedback control action.

The solar radiation is constantly subject to changes due to its daily cycle and passing clouds. The measured solar radiation shown in Fig. G.3 (a) is a fine example of both. Yet and despite the transient behaviour of the measured field inlet temperature shown in Fig. G.3 (b), it is fairly obvious from the actuator dynamics in Fig. G.3 (d), before 12.5 h for transients and after 12.5 h for steady-state, that Algorithm 1 is coping very well with these conditions when compared with the GSMPC algorithm. Fig. G.3 (e) shows the switching from one local predictive controller to another across the whole range of operation and one can clearly see that both algorithms have a matching switching performance.

### *G.6.2 Second scenario*

The scenario here compares the feedback control performance of Algorithm 1 with the feedback control performance of Algorithm 2 at the lower layer of a two-layer hierarchical control strategy. The scenario is quite extreme. While the field inlet temperature as shown in Fig. G.4 (b) is at steady-state, solar radiation as shown in

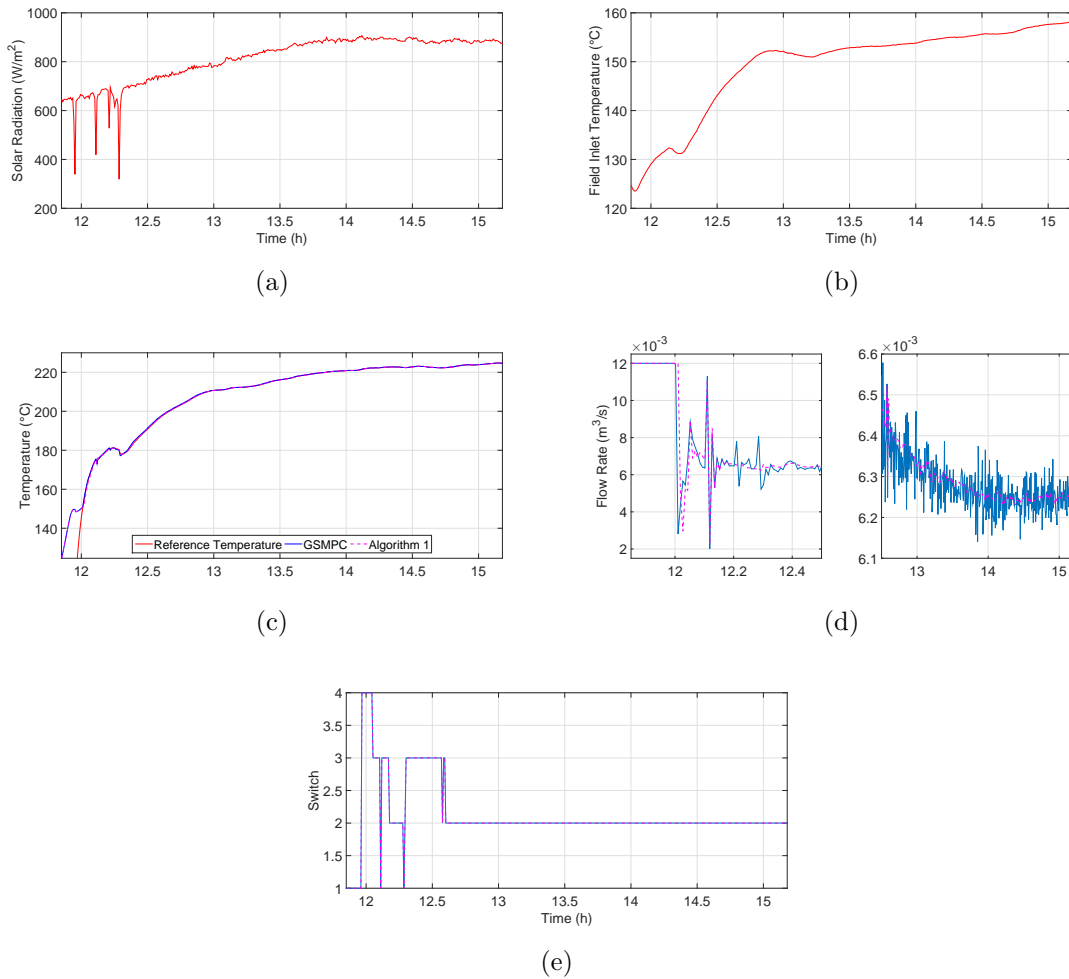


Figure G.3: First scenario: Control performance of GSMPC against Algorithm 1.

Fig. G.4 (a) is experiencing some drastic changes due to thick and passing clouds.

Just before 12.15 h, the control performance of Algorithm 1 is quite similar to the control performance of Algorithm 2 as shown in Fig. G.4 (d). Note that Algorithm 2 has a prediction horizon of 32.5 min.

After 12.15 h and due to the strong changes in solar radiation, some differences in the control performance start to emerge. As a general perception and while both algorithms have a matching switching performance as shown in Fig. G.4 (e), one

can notice that the sudden, sharp changes in the control actions are more obvious in Algorithm 1, which hence has a higher risk of actuator saturation.

To be more precise, the set point tracking performance has been assessed for both algorithms as well as the cost of regulation during the large changes in solar radiation. It has been found that Algorithm 2 has a lower root mean square error (RMSE) and cost of regulation than Algorithm 1 by about 9.2% and 2.6% respectively.

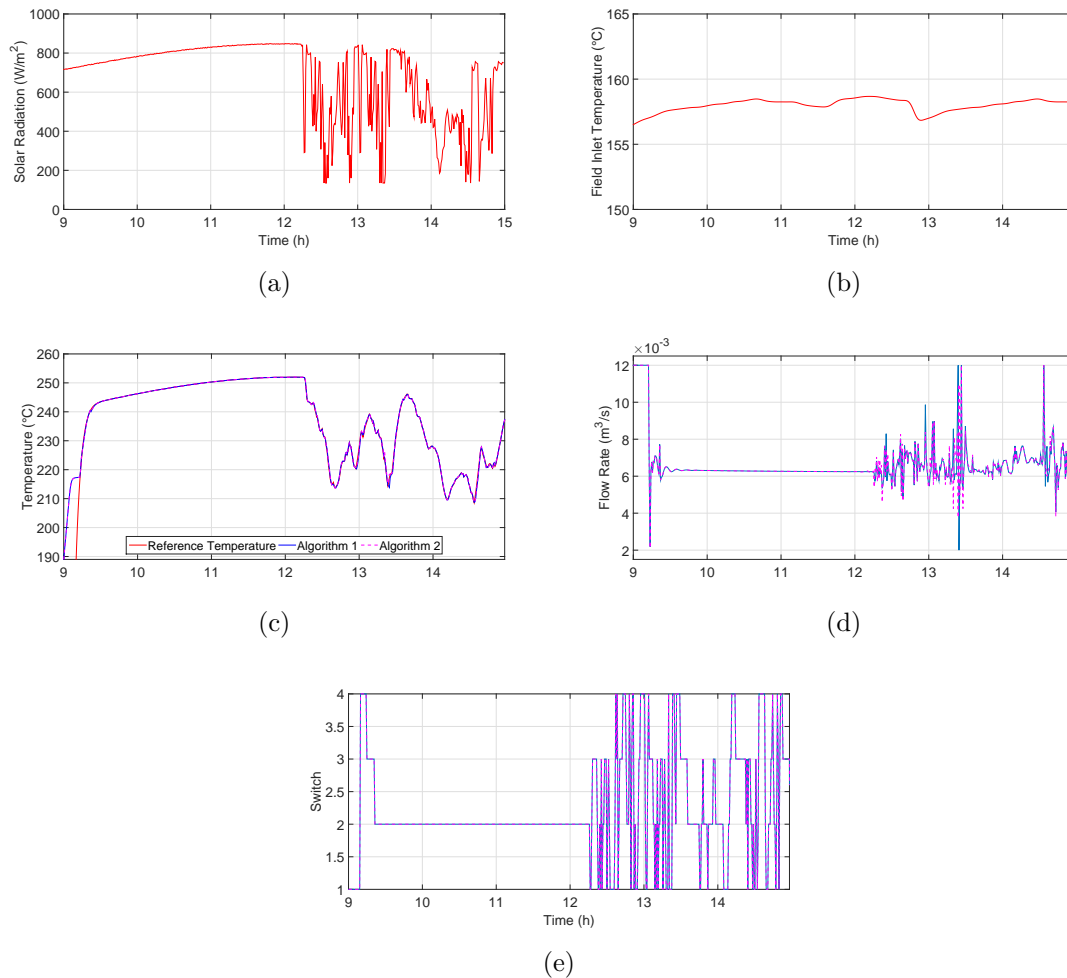


Figure G.4: Second scenario: Control performance of Algorithm 1 against Algorithm 2.

## G.7 Conclusions

This paper has improved a recently proposed two-layer hierarchical control strategy for the ACUREX plant. Improvements targeted the lower layer of the two-layer hierarchical control strategy by taking an explicit account of the measured disturbances systematically through two main approaches and based on two different assumptions.

The first approach assumes the availability of the current measurements of solar radiation and the field inlet temperature and when compared to the algorithm that was originally used in Alsharkawi and Rossiter (2017a), it has shown by way of a simulation scenario and measured data from the ACUREX plant that an improvement to the actuator dynamics can indeed be achieved.

A notable contribution of this paper is the development of the second approach that assumes the availability of the expected future behaviour of solar radiation and the field inlet temperature along a given prediction horizon. When compared with the first approach, it has shown slight improvements to the set point tracking performance and cost of regulation at the presence of strong disturbances. However, it is worth noting that the choice of the prediction horizon was not optimal and hence questions like: *How far ahead should one predict?* and accordingly *How significant can the improvements be?* still need to be answered.

# BIBLIOGRAPHY

- Alsharkawi, A. and Rossiter, J.A. (2017a). Hierarchical control strategy for a solar thermal power plant: A pragmatic approach. *Submitted to Journal of Process Control*.
- Alsharkawi, A. and Rossiter, J.A. (2017b). Modelling analysis of a solar thermal power plant. In *Proceedings of the 6th International Conference on Clean Electrical Power, Liguria, Italy*.
- Alsharkawi, A. and Rossiter, J.A. (2017c). Towards an improved gain scheduling predictive control strategy for a solar thermal power plant. *IET Control Theory & Applications*, DOI: 10.1049/iet-cta.2016.1319.
- Alsharkawi, A. and Rossiter, J.A. (2016a). Dual mode MPC for a concentrated solar thermal power plant. In *Proceedings of the 11th IFAC Symposium on Dynamics and Control of Process Systems, including Biosystems, Trondheim, Norway*, volume 49(7), 260–265. Elsevier.
- Alsharkawi, A. and Rossiter, J.A. (2016b). Gain scheduling dual mode MPC for a solar thermal power plant. In *Proceedings of the 10th IFAC Symposium on Nonlinear Control Systems, California, USA*, volume 49(18), 128–133. Elsevier.
- Camacho, E.F., Berenguel, M., Rubio, F.R., and Martínez, D. (2012). *Control of solar energy systems*. Springer-Verlag.
- Camacho, E. and Gallego, A. (2013). Optimal operation in solar trough plants: A case study. *Solar Energy*, volume 95, 106–117.
- Carmona, R. (1985). *Analysis, modeling and control of a distributed solar collector field with a one-axis tracking system*. Ph.D. thesis. University of Seville, Spain.

- Cirre, C.M., Berenguel, M., Valenzuela, L., and Klempous, R. (2009). Reference governor optimization and control of a distributed solar collector field. *European Journal of Operational Research*, volume 193(3), 709–717.
- Dughman, S. and Rossiter, J. (2017). Systematic and effective embedding of feed-forward of target information into MPC. *International Journal of Control*, 1–15.